

FACILITY FORM 802

N 65-21466

(ACCESSION NUMBER)

210

(PAGES)

CR 62182

(NASA CR OR TMX OR AD NUMBER)

(THRU)

(CODE)

14

(CATEGORY)

9G9-11

# APPROACHES TO ON-BOARD GRIDGING OF APT PICTURES

EDITED BY  
ROBERT P. BARTLETT

ARACON GEOPHYSICS COMPANY  
VIRGINIA ROAD  
CONCORD, MASSACHUSETTS

GPO PRICE \$

OTS PRICE(S) \$

Hard copy (HC)

Microfiche (MF)

\$6.00  
\$1.25

15 JANUARY 1965

FINAL REPORT  
PHASE I  
(QUARTERLY REPORT NO. 1)

UNDER

CONTRACT NO. NAS 5-9012

NATIONAL AERONAUTICS AND SPACE ADMINISTRATION

GOODARD SPACE FLIGHT CENTER

AERONAUTICS AND METEOROLOGY DIVISION

GREENBELT, MARYLAND

# APPROACHES TO ON-BOARD GRIDDING OF APT PICTURES

EDITED BY  
ROBERT P. BARTLETT

ARACON GEOPHYSICS COMPANY  
VIRGINIA ROAD  
CONCORD, MASSACHUSETTS

15 JANUARY 1965

FINAL REPORT  
PHASE I  
(QUARTERLY REPORT NO. 1)

UNDER

CONTRACT NO. NAS 5-9012

NATIONAL AERONAUTICS AND SPACE ADMINISTRATION  
GODDARD SPACE FLIGHT CENTER  
AERONOMY AND METEOROLOGY DIVISION  
GREENBELT, MARYLAND

## ABSTRACT

21466

Cloud-cover pictures taken with the Automatic Picture Transmission system designed for the Nimbus satellite and experimentally tested on a TIROS satellite, do not pass through a central processing station. These pictures are received directly by the ultimate user from the satellite. Any geographic referencing of the data in the pictures (latitude-longitude grid) must be accomplished by the receiver (user) of the data or must be added to the video picture in the satellite. This report contains the results of a study of the various methods by which the latitude-longitude grid can be added to the video picture on board the satellite. Both analog and digital approaches to onboard gridding were considered. Several digital approaches were found feasible. These approaches call for computer computation of the picture grids on the ground, transmission of the grid line data to the satellite for storage, and logic circuitry to withdraw the data from memory and electronically mix grid line marks into the video during the picture scan. The approaches judged feasible are: (1) straight-line method where the curved grid lines are approximated with straight line segments whose slope, length and initial coordinates are transmitted to the satellite, (2) coordinate method where the individual image plane coordinates of each mark are transmitted, (3) slope-coordinate method where starting coordinates and a slope range are specified to reduce the information necessary to obtain the image plane coordinates of each mark. On the basis of preliminary designs, the flight system weight and power requirement is approximately 7-8 pounds and less than 2 watts respectively.

*Heath*

## TABLE OF CONTENTS

	<u>Page</u>
ABSTRACT	ii
LIST OF FIGURES	viii
LIST OF TABLES	xi
ACKNOWLEDGMENT	xii
SECTION 1: <u>INTRODUCTION</u>	1-1
1.1       GENERAL	1-1
1.2       SYSTEM REQUIREMENTS	1-3
1.3       APPROACHES CONSIDERED	1-4
1.4       SCOPE OF EFFORT	1-7
1.5       REPORT TERMINOLOGY	1-7
1.6       SUMMARY AND RECOMMENDATIONS	1-8
SECTION 2: <u>GRIDDING REQUIREMENTS</u>	2-1
2.1       GRID LINE SPACING	2-1
2.2       GRID LINE REFERENCING	2-3
SECTION 3: <u>DIGITAL APPROACHES TO ON-BOARD GRIDDING</u>	3-1
3.1       STRAIGHT LINE METHOD	3-1
3.1.1 <u>General</u>	3-1
3.1.2 <u>Approaches to the Straight Line Method</u>	3-5
3.1.3 <u>Logical Implementation of SL-2</u>	3-15
3.2       COORDINATE METHODS	3-16
3.2.1 <u>General</u>	3-16
3.2.2 <u>Run-length Coding</u>	3-22
3.2.3 <u>Mark Plotting through a Combination of Slope and                   Coordinate Specification</u>	3-27
3.2.4 <u>Coordinate System Designs</u>	3-30
3.2.4.1   Full X-Address System CM-1A	3-32
3.2.4.2   Run-length System CM-1R	3-33
3.2.4.3   Combined Slope-Coordinate System CM-2	3-33
3.3       THE ELLIPSE METHOD	3-50
3.3.1 <u>Description</u>	3-50
3.3.2 <u>Parameters of the Ellipse</u>	3-51



	<u>Page</u>
3.3.3 <u>Storage Requirements</u>	3-52
3.3.4 <u>Logical Requirements</u>	3-52
3.3.5 <u>Evaluation</u>	3-53
3.4 ANCILIARY FUNCTIONS	3-53
3.4.1 <u>Numeral Generation</u>	3-53
3.4.1.1 Introduction	3-53
3.4.1.2 Numeral Generator, CM-1A; Marks Along Every Sweep	3-55
3.4.1.3 Numeral Generator, CM-1A; Marks Along Every Fourth Sweep	3-55
3.4.1.4 Numeral Generator, CM-1A; Marks on Non-Mesh Sweeps Only	3-56
3.4.1.5 Numeral Generator, Straight-Line Method	3-56
3.4.1.6 Numeral Generation Every Sweep; Straight-Line Method	3-56
3.4.1.7 Numeral Generation; CM-2	3-58
3.4.2 <u>Satellite Orientation Corrections</u>	3-58
3.4.2.1 Coordinate Methods, Orientation Correction	3-58
3.4.2.2 Straight Line Orientation Corrections	3-60
3.5 SYNCHRONIZATION AND ERROR DETECTION	3-61
3.5.1 <u>Udata Transmission System</u>	3-61
3.5.1.1 Modulation Form	3-61
3.5.1.2 New Commands	3-61
3.5.1.3 Udata Error Rate Due to Thermal Noise	3-63
3.5.2 <u>Demodulation and Bit Synchronization</u>	3-63
3.5.3 <u>On-Board Word Synchronizing and Error Detection System for CM-1A</u>	3-66
3.5.3.1 System Outline	3-66
3.5.3.2 Logical Description of Word Synchronizer	3-66
3.5.3.3 General Synchronization Techniques	3-68
3.5.4 <u>The Effects of the Single Bit Errors on the Gridding System</u>	3-69
3.5.4.1 Full X-Address, CM-1A	3-69
3.5.4.2 Run-Length System, CM-1R	3-70
3.5.4.3 Straight Line Method	3-70
3.5.4.4 Slope-Coordinate Systems	3-71

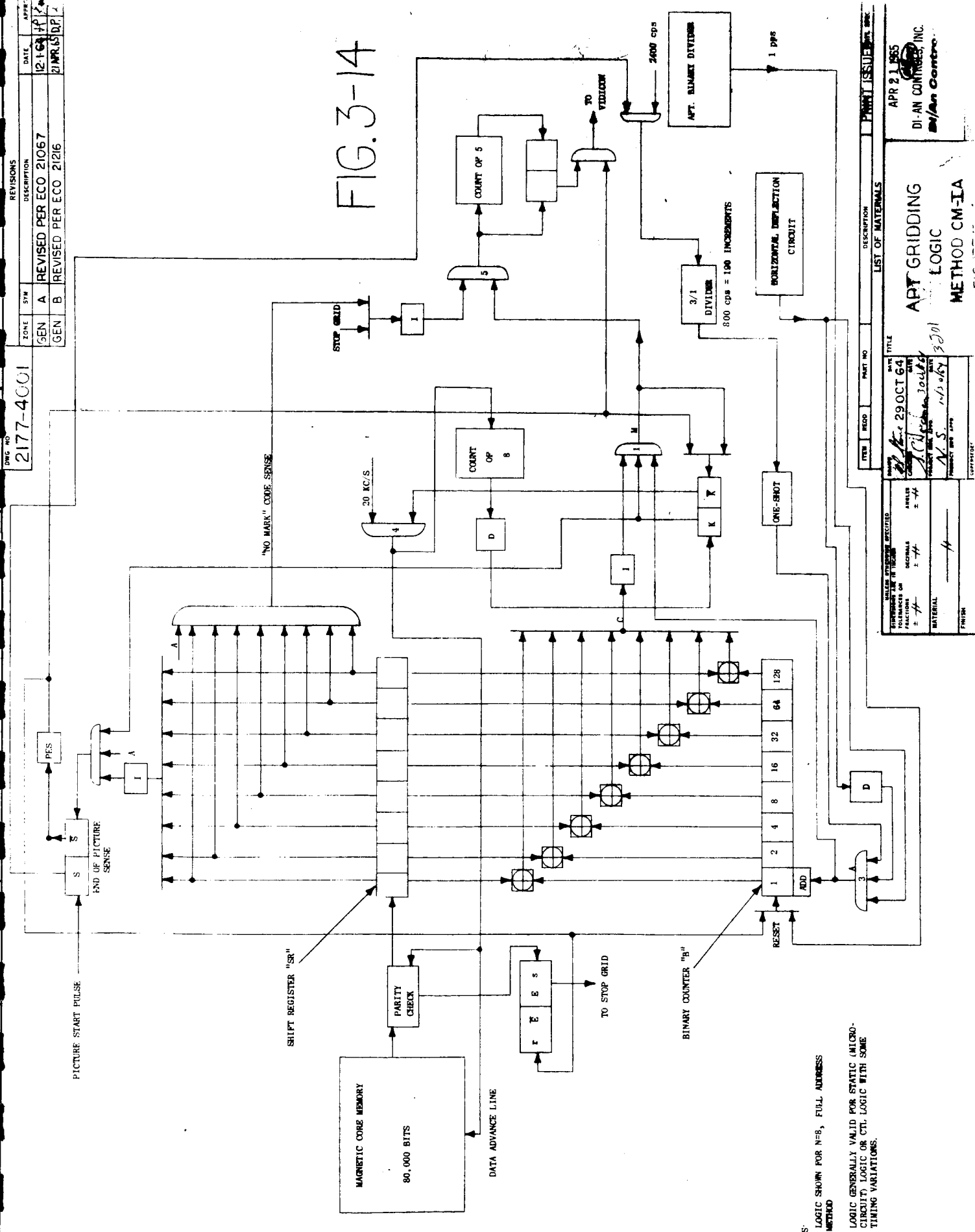


FIG. 3-14

1. LOGIC SHOWN FOR N=8, FULL ADDRESS METHOD

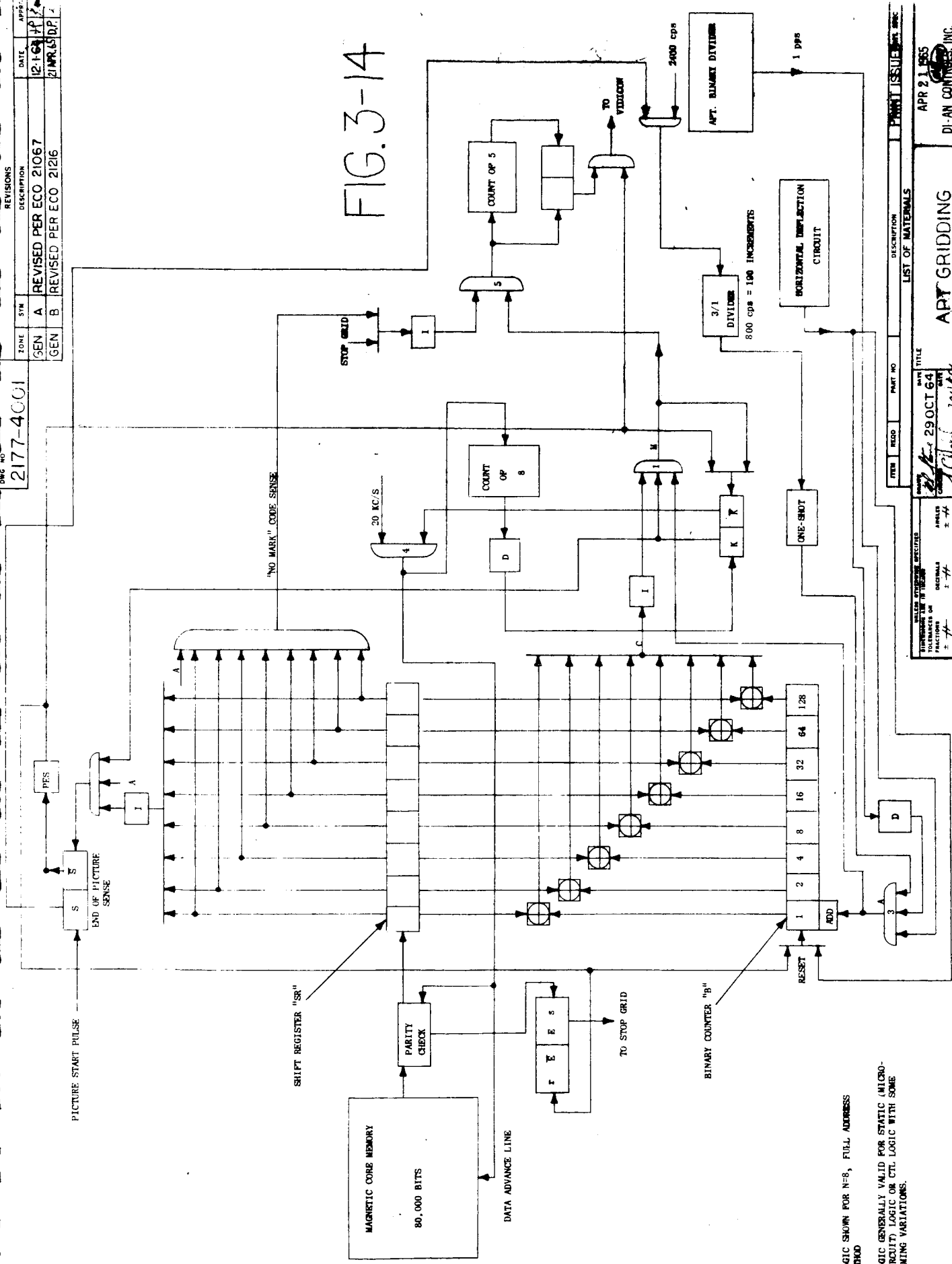
2. LOGIC GENERALLY VALID FOR STATIC (MICRO-CIRCUIT) LOGIC OR CTL LOGIC WITH SOME TIMING VARIATIONS.

[illegible]

REVISIONS		DATE	APPROVAL
ZONE	SYM		
GEN A		12-1-64	HP
GEN B		21 APR 65	DP

2177-4001

FIG. 3-14



YES  
1. LOGIC SHOWN FOR N=8, FULL ADDRESS METHOD

2. LOGIC GENERALLY VALID FOR STATIC (MICRO-CIRCUIT) LOGIC OR CTL LOGIC WITH SOME TIMING VARIATIONS.

LIST OF MATERIALS		DESCRIPTION	PART NO.	QTY.
ITEM	RECD			
<p>APR 21 1965 DI-AN CONTROLS, INC. DI/An Centre</p> <p>ART GRID LOGIC METHOD CM-1A</p> <p>DATE: 29 OCT 64 BY: [Signature] CHECKED BY: [Signature] MATERIAL: [Blank] FINISH: [Blank]</p>				

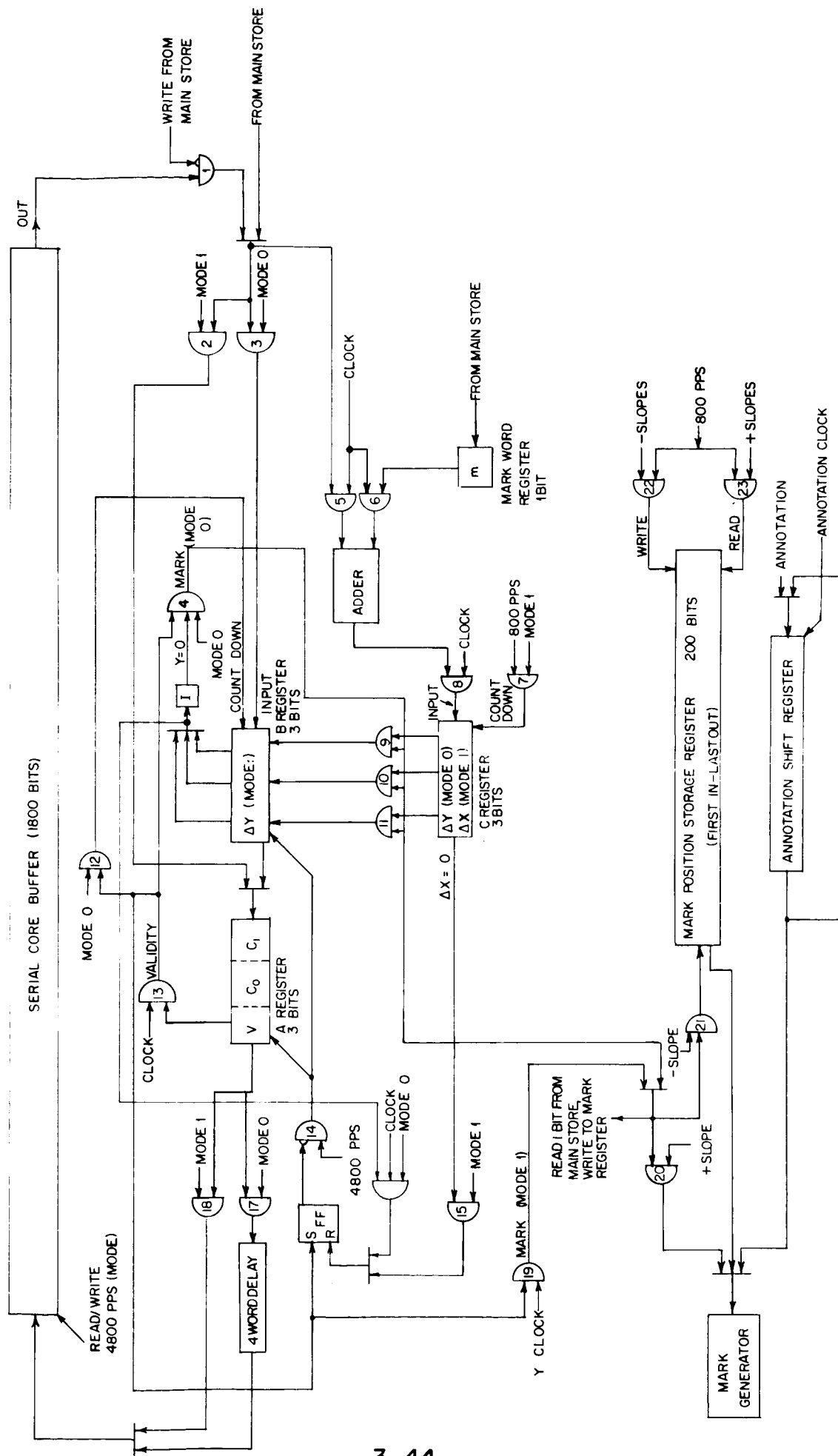


FIG. 3-22 GRID AND ANNOTATION CALCULATION LOGIC—CMII LA

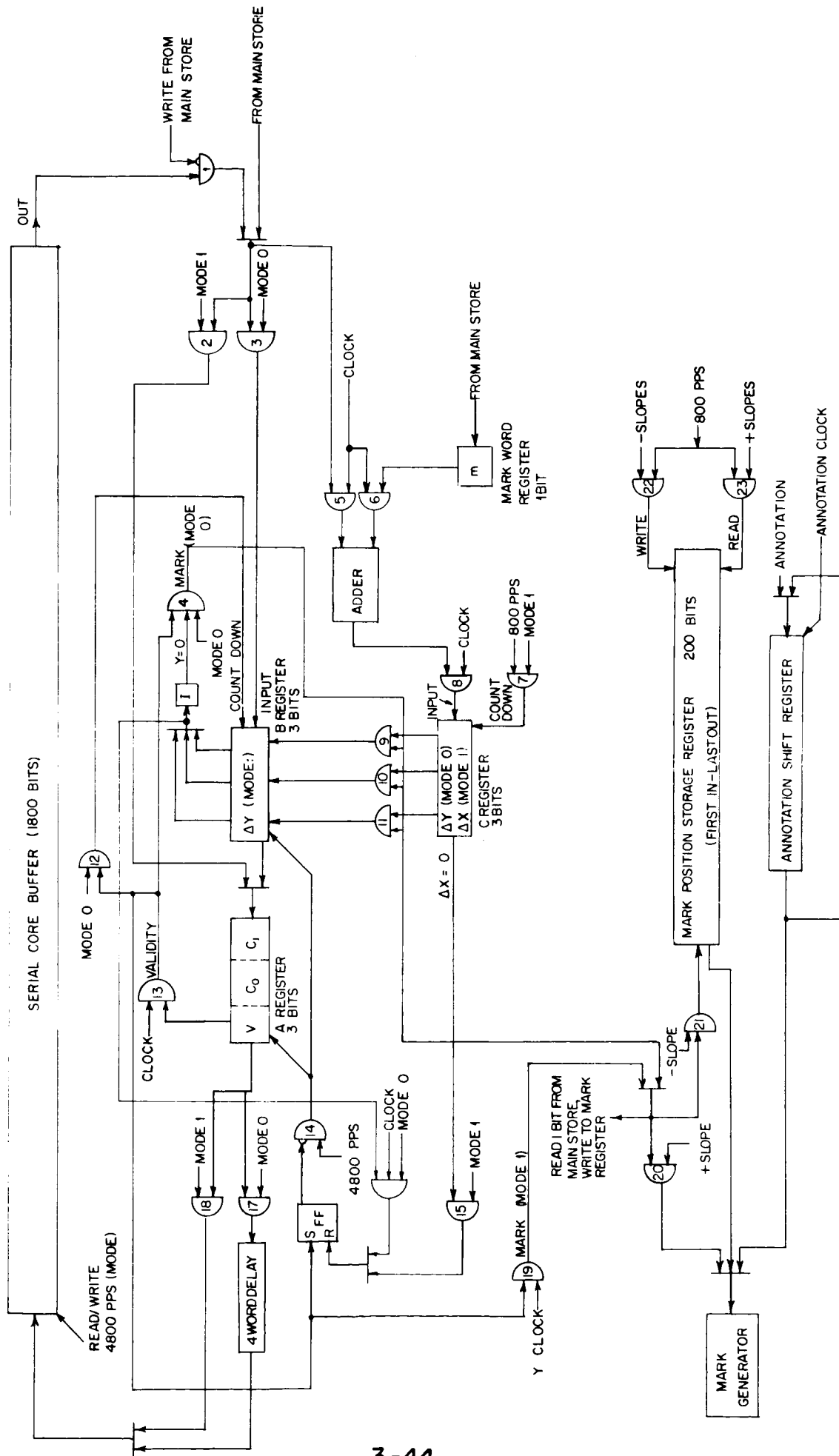


FIG. 3-22 GRID AND ANNOTATION CALCULATION LOGIC—CMII LA

	<u>Page</u>
3.5.5 <u>Methods of Error Compensation</u>	3-72
3.5.5.1 Introduction	3-72
3.5.5.2 Coordinate Method, CM-1R	3-72
3.5.5.3 Coordinate Method, CM-1A	3-73
3.5.5.4 Straight-Line Methods	3-75
3.5.5.5 Slope-Coordinate Method	3-75
3.6 ELECTRICAL AND PHYSICAL PARAMETERS	3-78
3.6.1 <u>Subsystem Parameters</u>	3-78
3.6.2 <u>Module Parameters</u>	3-85
3.6.3 <u>Reliability of APT On-Board Gridding System</u>	3-85
SECTION 4: <u>ANALOG APPROACHES TO ON-BOARD GRIDGING</u>	4-1
4.1 GENERAL	4-1
4.2 GRID STORAGE ON A FLAT MEDIUM	4-2
4.3 GRID STORAGE ON A CYLINDER	4-10
4.4 GRID STORAGE ON A SPHERE	4-11
4.5 FEASIBILITY OF ANALOG APPROACHES	4-13
SECTION 5: <u>GROUND COMPUTATION OF THE PICTURE GRID</u>	5-1
5.1 GENERAL	5-1
5.2 APPROXIMATION OF GEOGRAPHICAL GRIDS BY STRAIGHT LINES	5-1
5.2.1 <u>General Approach</u>	5-1
5.2.2 <u>Lines of Constant Latitude</u>	5-1
5.2.3 <u>Lines of Constant Longitude</u>	5-3
5.2.4 <u>Error Analysis</u>	5-4
5.2.5 <u>Grid Construction</u>	5-6
5.2.6 <u>Satellite-Earth Geometry</u>	5-6
5.3 CALCULATION OF LATITUDE-LONGITUDE ELLIPSES	5-8
5.3.1 <u>Introduction</u>	5-8
5.3.2 <u>Constant Latitude Equations</u>	5-9
5.3.3 <u>Constant Longitude Equations</u>	5-10
5.3.4 <u>Calculation of Terminal Points of Ellipses</u>	5-11
5.3.5 <u>General Approach to Generation of Transmitted Data</u>	5-16
5.3.6 <u>Specific Methods of Generating Transmitted Data</u>	5-20
5.3.6.1 Method GM-1A	5-20
5.3.6.2 Method CM-1R	5-24
5.3.6.3 Sector Coding Method CM-2L <sub>B</sub>	5-24

	<u>Page</u>
5.4 APPROACHES TO SIMULATION	5-36
5.4.1 <u>The Simulation Problem</u>	5-36
5.4.2 <u>Existing Programs</u>	5-36
5.4.3 <u>Programming Requirements for Simulation</u>	5-37
5.4.3.1 Ellipse Technique	5-37
5.4.3.2 Straight Line Techniques	5-37
5.4.3.3 Coordinate Methods	5-38
5.5 OPERATIONAL PROGRAM	5-39
SECTION 6: <u>COMPARISON OF APPROACHES TO ON-BOARD GRIDGING</u>	6-1
6.1 INTRODUCTION	6-1
6.2 APPEARANCE OF THE PICTURE GRID	6-1
6.3 SUSCEPTIBILITY TO ERROR	6-3
6.4 CONCLUSIONS	6-5
APPENDIX A: <u>ELLIPSE CHARACTERISTICS OF LATITUDE-LONGITUDE LINES</u>	A-1
A.1 CONSTANT LATITUDE LINES	A-1
A.2 MERIDIAN LINES	A-6
APPENDIX B: <u>ANTENNA PROGRAMMING</u>	B-1
APPENDIX C: <u>MEMORY CONSIDERATIONS</u>	C-1
C.1 MAIN DATA MEMORIES	C-1
C.1.1 <u>Magnetic Core Storage</u>	C-1
C.1.1.1 Background	C-1
C.1.1.2 Operating Modes	C-1
C.1.1.3 Power and Weight Estimates	C-1
C.1.1.4 Design Details	C-2
C.1.2 <u>Magnetic Thin Film Memories</u>	C-3
C.2 ACTIVE COMPUTATIONAL MEMORY	C-5
C.2.1 <u>Magnetorestrictive Delay Lines</u>	C-5
C.2.1.1 Delay Line Survey	C-5
C.2.1.2 SL-2 Requirements	C-5
C.2.1.3 Engineering Details	C-5
C.2.2 <u>Solid State Storage Elements</u>	C-7

	<u>Page</u>
APPENDIX D: <u>CHOICE OF LOGIC ELEMENTS FOR SYSTEM MECHANIZATIONS</u>	D-1
D.1 GENERAL	D-1
D.2 AVAILABLE INTEGRATED CIRCUITS	D-1
D.2.1 <u>Texas Instruments Series 51</u>	D-2
D.2.2 <u>CBS Laboratories Micropower Circuits</u>	D-2
D.2.3 <u>Complementary Multichip Circuits</u>	D-2
D.2.4 <u>Fairchild Milliwatt Micrologic</u>	D-2
D.3 CORE-TRANSISTOR LOGIC(CTL)	D-3
APPENDIX E: <u>RELIABILITY ESTIMATION</u>	E-1
E.1 INTRODUCTION	E-1
E.2 CTL - MAGNETIC LOGIC	E-1
E.2.1 <u>Life Tests</u>	E-1
E.2.2 <u>Radiation Tests</u>	E-2
E.3 FAIRCHILD INTEGRATED MICROLOGIC	E-3
E.3.1 <u>Introduction</u>	E-3
E.3.2 <u>Life Test Data</u>	E-3
E.3.3 <u>Radiation Data</u>	E-4



## LIST OF FIGURES

<u>Figure No.</u>		<u>Page</u>
1-1	Block Diagram - On-Board Grid System	1-6
1-2	Simulated Grid K = 8	1-10
2-1	Grid with 2° Spacing for 800 NM Orbit	2-2
2-2	OEC Map with Proposed 5° Grid	2-4
2-3	OEC Map Coverage as a Function of Satellite Height	2-5
2-4	Suggested Locations of Fixed North Arrows for Grid Line Referencing	2-7
3-1	Slope Specification	3-2
3-2	Locations of Grid Marks SL-1	3-4
3-3	SL-1 Block Diagram	3-6
3-4	Allowable Locations of Grid Mark SL-2	3-10
3-5	Calculation Logic Method SL-2	3-15a
3-6	Memory and Control Logic Method SL-2	3-15b
3-7	Appearance of Grid Lines n = 4 K = 8	3-18
3-8	Appearance of Grid Lines n = 8 K = 8	3-19
3-9	Appearance of Grid Lines n = 4 K = 16	3-20
3-10	Appearance of Grid Lines n = 8 K = 16	3-21
3-11	Equator Picture from 800 NM with 5° Grid	3-23
3-12	Potential Locations of New Marks	3-28
3-13	Line Marking from Combined Slope - Coordinate Specification	3-29
3-14	APT Gridding Logic Method CM-IA	3-32a
3-15	Method CM-1R Typical Magnetic Logic Implementation	3-33a
3-16	Word Composition CM II H	3-34
3-17	General Block Diagram - CM II Method	3-36
3-18	Sector Codes K = 16	3-38
3-19	Contents of Buffer Memory at Start of Sweep CM II L <sub>A</sub>	3-39
3-20	Timing Diagram CM II L <sub>A</sub>	3-41
3-21	Main Storage-Logic Interface CM II L <sub>A</sub>	3-42
3-22	Grid and Annotation Calculation Logic - CM II L <sub>A</sub>	3-44
3-23	Sector Codes K = 8	3-46
3-24	Memory-Logic Interface	3-47

<u>Figure No.</u>	-	<u>Page</u>
3-25	CM-II $L_B$ Logic for Cycles 3 and 4	3-48
3-26	CM-II $L_B$ Cycle 2	3-49
3-27	Numeral Appearance	3-54
3-28	Annotation Storage Logic Method CM-1A	3-57
3-29	Appearance of Annotation Characters for CM-II $L_A$	3-59
3-30	Error Rate vs. $\frac{\text{Energy Per Bit}}{\text{Noise Density}}$	3-62
3-31	Demodulator and Bit Synchronizer	3-64
3-32	Method CM-1A Typical Bit Sequence in Up Data	3-65
3-33	Synchronizer and Error Detector Full Address Method CM-1A	3-67
3-34	Run Length Error Detection Coordinate Method	3-74
3-35	Full Address Error Detection Coordinate Method	3-76
3-36	Error Detection Block Diagram CM-II	3-77
4-1	Location Error (After Scaling Correction) for A Height Error of $\pm 50$ nm	4-3
4-2	Grid Projection on a Plane	4-5
4-3	Analog System Using Plane Projections	4-5
4-4	Subpoint Track on the Planes of the Film Strips	4-6
4-5	Sample Subpoint Track on an OEC Map	4-9
4-6	Error Arising from Cylinder Approximation to Sphere	4-12
5-1	Geometry of Constant Latitude Lines	5-2
5-2	Permitted Arc Length for Straight-Line Approximation	5-5
5-3	Satellite-Earth Geometry	5-7
5-4	Intersections of Ellipses with Image Screen Edges	5-12
5-5	Block Diagrams for Intersections at $Y = -H$	5-14
5-6	Block Diagrams for Intersections at $X = H$	5-15
5-7	Generation of Segment End Point Pairs	5-17
5-8	General Program for Generating Ellipse Data to Transmit to a Satellite	5-18
5-9	Computation of Point Coordinates for Methods CM-1R	5-21
5-10	Calculation of $X$ and $dx/dy$	5-22
5-11	Generation of Transmitted Data-Method CM-1A ADJ Routine	5-23
5-12	Generation of Transmitted Data-Method CM-1R ADJ Routine	5-25

<u>Figure No.</u>		<u>Page</u>
5-13	Outline of Computations for Method CM-2L <sub>B</sub>	5-27
5-14	Generation of CT, A, C Coefficients	5-28
5-15	Flow Diagram for Generating Sector Data for Individual Grid Lines	5-28
5-16	Typical CT Circuit CT = 3	5-29
5-17	Comments on CT Circuit	5-30
5-18	Block Diagram for Mixing Sector Data for Different Grid Lines	5-31
5-19	Computation of $\Delta Y$ and $\Delta X$	5-32
6-1	Simulated Grid SL-2	6-2
6-2	Simulated Grid K = 8	6-6
6-3	Simulated Grid K = 12	6-7
6-4	Simulated Grid K = 16	6-8
6-5	Simulated Grid K = 8	6-9
6-6	Simulated Grid K = 12	6-10
6-7	Simulated Grid K = 16	6-11
6-8	Simulated Grid K = 8	6-12
6-9	Simulated Grid K = 12	6-13
6-10	Simulated Grid K = 16	6-14
A-1	Geometrical Relationships for Constant Latitude Lines	A-2
A-2	Image Plane Relationships for Constant Latitude Lines	A-4
A-3	Geometrical Relationships for Meridian Lines	A-7
A-4	Image Plane Coordinate Axes for Meridian Lines	A-9

## LIST OF TABLES

<u>Table</u>	<u>Page</u>
3-1 Number of Straight-line Segments Per Orbit Required for Picture Grid	3-3
3-2 SL-1 Word Structure	3-8
3-3 Word Structure Method SL-2	3-11
3-4 Mode 0 Calculation Logic	3-12
3-5 Mode 1 Calculation Logic	3-13
3-6 Number of Pictures as a Function of Satellite Altitude	3-26
3-7 CM-II Storage Requirements	3-31
3-8 CM-1 CTL Logic Implementation Per Unit Parameter Estimates	3-79
3-9 CM-1 Integrated Logic Implementation Per Unit Parameter Estimates	3-80
3-10 CM-1 Hybrid Logic Implementation Per Unit Parameter Estimates	3-81
3-11 SL-2 (CM-2H) Integrated Logic Implementation Per Unit Parameter Estimates	3-82
3-12 CM-2L Integrated Logic Implementation Per Unit Parameter Estimates	3-83
3-13 Estimate of Design Parameters for APT Gridding Subsystem	3-84
3-14 Per Module Parameters	3-86
3-15 Reliability Estimates	3-86
3-16 CM-1, CTL Reliability Estimate	3-87
3-17 CM-1 Integrated Circuits Reliability Estimate	3-87
3-18 CM-1 Hybrid Reliability Estimate	3-88
3-19 SL-2 Integrated Ckt. Reliability Estimate	3-88
5-1 Screen Edge Intersection Data	5-13
5-2 Input Data- Methods CM-1R and CM-1A	5-19
5-3 Intermediate Data - Methods CM-1A and CM-1R	5-20
5-4 Input Data - Method CM-2L <sub>B</sub>	5-33
5-5 First Intermediate Data Table - Method CM-2L <sub>B</sub>	5-34
5-6 Second Intermediate Data Table - Method CM-2L <sub>B</sub>	5-35
5-7 Output Data - Method CM-2L <sub>B</sub>	5-35
6-1 Comparison of Digital Approaches to On-Board Gridding	6-4
C-1 DI/AN Core Memory Estimate	C-2
C-2 Present Status of Thin Film Memories	C-4
C-3 Engineering Estimates of Thin Film Memories in 1966	C-4

## ACKNOWLEDGMENT

This report contains contributions from several individuals and companies. Contributors to the report are listed below:

ARACON Geophysics Company

Dr. Arnold H. Glaser  
Mr. Robert P. Bartlett  
Mr. Robert F. Smiley  
Mr. James R. Greaves

DI/AN Controls, Inc.

Mr. Samuel Goldman  
Mr. Nathan Sokal  
Mr. S. Sidney Guterman

ADCOM, Inc.

Dr. Steven Sussman

## SECTION 1

### INTRODUCTION

#### 1.1 GENERAL

Geographic referencing of pictorial data in pictures taken with "conventional" TIROS and Nimbus AVCS cameras is accomplished by superposition of latitude-longitude grid before the pictures or nephanalyses are transmitted from command and data acquisition stations. Since APT pictures do not pass through any central processing station, any grid to be applied to the pictures must be included in the picture video signal, if "manual" modes of gridding are to be avoided at the various APT receiving stations.

Manual gridding and antenna tracking procedures currently in use for APT were developed by ARACON. In use, they have proved to be effective and fairly accurate. However, significant errors (as large as 100 miles) can occur due to (1) the error in the map projection (necessary to reduce the number of maps to a manageable figure), (2) difficulties in obtaining an accurate picture time, (3) the inability of station operators to cope with attitude variations as effectively as a CDA computer-operation.

Additionally, a significant amount of operator time is required to plot the satellite track, derive the antenna program, determine satellite subpoint at picture time, determine picture azimuth, find and superpose the proper overlay on the picture, adjust for apparent yaw error, and finally trace the grid. While we have not conducted time and motion studies, it would appear that the operator has time for little besides a cup of coffee between passes so that for a 3-pass day he may be tied up for some 250 minutes or over four hours.

If the operator can be released for other weather station duties during this period, a significant manpower economy is possible. Multiplied by the potential number of APT stations in the world, which we will conservatively take at 200, a two hour saving becomes 400 hours per day. At U.S. direct labor rates, this approaches \$500,000 annually. More importantly, it may make the difference establishing the economic feasibility of APT in marginal situations. A modicum of further automation in antenna control could then reduce the requirement for operator intercession to an attractive minimum.

If DRIR is added to the APT capability, an on-board gridding system would more than double the labor saving mentioned above. Manual IR gridding has proved to be extremely laborious, largely because of the nature of the projection arising from the circular scan of the HRIR instrument. A fixed IR grid can be used with the resulting projection only if the recipients of the data are willing to accept a completely arbitrary set of values for the geographic grid lines. This would considerably complicate the task of cross-referencing the IR data with video data and earth geography.

There are other reasons to supplant manual methods of gridding at the receiving station. The APT stations are not able to receive telemetry data from the satellites. As a result they are unable to correct for the effects of attitude error in the geographic referencing of the picture data. An on-board gridding system can make corrections in the picture grid for roll and pitch errors determined from attitude sensor outputs at the time of picture taking. Further, the ground operator seldom has a good fix on picture time.

Although at present a station operator must carefully set antenna drive controls as a function of time, the satellite tracking procedure can be considerably simplified. Indeed, the capability for line drawing and annotation of an on-board gridding system in itself offers a method of simplifying the tracking procedures. Tracking data for tomorrow's orbits can be included in today's APT pictures (see Appendix B). The combination of an on-board gridding system and simplified tracking procedures will make the automatic picture transmission system a truly "automatic" system. This would be especially beneficial to military users or commercial users of the APT data who have little or no knowledge of satellite tracking and data reduction procedures.

If the APT system is to take its proper place in the weather station as an operational tool providing weather data with as little attention required of the man in the station as demanded by the weather facsimile devices, the manual procedures now mandatory must be eliminated. An onboard gridding system will eliminate the greater percentage of time consuming and error inherent procedures now demanded to make use of APT data.

A variety of methods can be potentially applied to the task of on-board gridding; this report is a design study of advantages and disadvantages of each method.

## 1.2 SYSTEM REQUIREMENTS

The on-board gridding system, if practical, will be flown on a future Nimbus satellite. However, such a system is potentially useful on board any cloud cover observing satellite. In studying the possible approaches to on-board gridding, all constraints common to any of the meteorological satellites now in use or in planning were considered. The range of height for the meteorological satellites was fixed between 400 and 800 nautical miles. Although it is presumed that the satellite orbits will be circular, consideration was given to the effects of elliptical orbits. The study assumed the use of the present APT camera system, the  $107^\circ$  diagonal angular aperture forming the primary constraint for this system. The following APT system parameters were assumed.

1. Pictures per orbit	10 to 15, dependent on height
2. Field of view	$107^\circ$ diagonal
3. Number of lines per frame	800
4. Number of elements per line	784
5. Frame rate	208 seconds
6. Frame scanning time	200 seconds
7. Line rate	250 milliseconds/line
8. Exposure time	40 milliseconds

The latitude-longitude lines may be represented by discontinuous grid marks. Maximum spacing between grid marks called for in the original specification is one percent of the side dimension in either X or Y displacement on the picture plane. The shape of the grid marks was specified as two black followed by three white picture elements, one line thick. Some form of annotation is to be included in the picture to allow the data user to readily identify the grid lines. The grid spacing as initially specified is as follows:

### Latitude spacing on picture

- a.  $2^\circ$  from  $0-70^\circ$  latitude north and south.
- b.  $4^\circ$  from  $>70^\circ$  latitude north and south.

### Longitude spacing on picture

- a.  $2^\circ$  from  $0-40^\circ$  latitude north and south.
- b.  $4^\circ$  from  $40-70^\circ$  latitude north and south.
- c.  $8^\circ$  from  $70-82^\circ$  latitude north and south.
- d.  $40^\circ$  from  $>82^\circ$  latitude north and south.



The maximum error of grid marks is to be no greater than one percent. The error is defined:

$$e = \frac{P_t - P_a}{s} \quad (100)$$

where

- e - percent error
- $P_t$  - true grid point
- $P_a$  - actual grid mark
- s - side dimension of picture

It is assumed that the time of picture taking is known in advance. It is also assumed that the approximate satellite attitude for the time of picture taking will be known. In particular for Nimbus, which is actively controlled in all three of its axes, the attitude should be constant. However, the remaining error may be sufficient to cause error in APT picture location. Consequently, an on-board gridding system should be capable of including the possibility of grid corrections from onboard attitude sensors.

CDC 924 computers are available in the ground stations for computation of the picture grids. However, an important constraint is that the computational time be short to avoid interfering with the station operations normally assigned to these computers.

Since a possibility of using the existing command channel of the Nimbus satellite exists, the capabilities of the command channel form a part of the specifications. Command receiver specifications are:

Frequency	149 Mc
Bandwidth	40 kc, i. f.
S/N ratio	17 dB at 20 kc bandwidth of receiver output, worst case

Finally, the cost on an on-board gridding system is a constraint in that it must be compatible with the advantages gained from manual procedures at the receiving station.

### 1.3 APPROACHES CONSIDERED

A number of analog schemes were studied. These included systems which optically add the grid to the video picture and systems in which the grid, stored

on board the satellite, is scanned and mixed with the signal during transmission. Some of the forms of grid storage considered were:

1. Storage of the picture grid on continuously advancing film strips.
2. Storage of the picture grid on a cylinder.
3. Storage of the picture grid on a sphere.

The analog approaches are contained in Section 4 of this report.

Digital approaches to on-board gridding are:

1. Ellipse Method - In the ellipse method the coefficients of the ellipses can be transmitted and stored in the satellite. At the time of transmission of the picture, the coordinates of the ellipse section can be computed from the stored coefficient and mixed with the picture.

2. Straight Line Method - In the ground station computer the latitude-longitude lines can be fitted with straight line segments restricted to the specified maximum error. The picture plane can be represented by 800 Y coordinates representing the scan lines and 800 X coordinates representing the elements of the scan lines. The initial coordinates and the slope of the line segments are then transmitted and stored. The information for a particular section is then extracted from the main memory and compared with the scanning of the picture to mix in grid marks at the proper locations as the picture is scanned for transmission. The  $\Delta X$  of the slope is added to the previous mark coordinate to locate the next mark. The initial Y coordinate of the following line segment can be used to terminate the previous line segment. This method will allow many coordinates to be plotted with only moderate memory since the initial coordinates plus the slope will only take as much memory as two sets of coordinates but may plot out many points.

3. Coordinate Method - All the coordinates of the points of the grid lines can be transmitted and stored. On picture transmission the points are mixed with the picture. Storing all the points would take a rather large memory; however, by reducing the number of possible coordinates, within the restriction of the given maximum error, the memory may be reduced to a feasible size while not degrading the grid lines excessively.

A block diagram showing the basic elements common to all the digital approaches appears in Figure 1-1.



#### 1.4 SCOPE OF EFFORT

At the beginning of the study, all of the approaches listed above were briefly analyzed to permit dropping those approaches which were obviously impractical. Rough designs were done for those approaches which showed any promise. Two of the digital approaches, the straight line method and the coordinate method, appeared to be practical. Fairly detailed system designs were completed for each of these methods to allow the determination of the following parameters.

- a. Storage requirements.
- b. Error tolerance and system reliability.
- c. Instantaneous and average power requirements.
- d. Weight and volume.
- e. Interface requirements.
- f. Communications channel requirements.
- g. CDA station computer requirements.

#### 1.5 REPORT TERMINOLOGY

Some of the nomenclature used in this report is often ambiguous; e. g. , line is commonly used for a television sweep and is easily confused with grid line. Hence, the following terms are defined as they will be used in this report.

1. Coordinate - refers to the location of an element on the 800 x 800 element picture.

2. Mesh - the set of points of a particular defined coordinate subsystem. More specifically, a set of points lying on an array of perpendicular equally spaced lines. The horizontal lines of the mesh are parallel to the APT horizontal sweeps. The mesh line spacing is specified by  $n$ , which is the number of picture elements between mesh lines.

3. Picture element - conventional definition in common use for television. For the APT system there are 800 x 800 picture elements in a single picture.

4. Sweep - as in conventional television terminology.

5. Grid - the set of meridian and parallels to be superimposed on a particular APT picture.

6. Mark (grid mark) - a pattern consisting of five coded adjacent elements on a single sweep, specified to be three black followed by two white picture elements, one line thick.

7. Line - a set of marks approximating a meridian, parallel, arrow, or alphanumeric character in the APT pictures.

8. K - the number of picture elements between successive marks of a mode 0 line or the number of sweeps separating marks of a mode 1 line.

9. Mode 0 line - a grid line which makes an intersection angle  $\theta$  with a sweep such that  $0^\circ \leq \theta < 45^\circ$ .

10. Mode 1 line - a grid line which makes an intersection angle  $\theta$  with a sweep such that  $45^\circ \leq \theta \leq 90^\circ$ .

11. Mesh interval - a distance along a mesh line of  $n$  picture elements. The mesh intervals are a set of allowable mark locations.

12. Zone - an equalized group of contiguous horizontal sweeps in a picture which divides the picture for purposes of frequent resynchronization in case of errors.

## 1.6 SUMMARY AND RECOMMENDATIONS

None of the analog approaches to on-board gridding are considered practical relative to the digital approaches for the following reasons.

1. A flexible analog system contains most of the elements of any of the digital systems - data channel (demodulator, synchronizer, error detection circuitry), memory (storage of data for correction of orbit and picture parameter errors), and logic circuitry to compensate for attitude, orbit and APT parameter errors. The additional equipment needed for the analog systems - lens or scanner, grid storage medium, servo controls - places the analog system at a severe weight disadvantage when compared to the digital approaches.

2. The reliability of the electromechanical analog approaches is inherently lower.

3. The spacecraft on which an on-board gridding system is useful (Nimbus-TIROS) are sensitive to internal motions. The motion compensation required complicates design and produces further weight penalties.

4. Optical mixing approaches require modification of the mechanical (and preferably the optical) portions of the APT system. The extremely wide angular coverage of the APT lens ( $107^\circ$ ) complicates the optical design for introducing the picture grid into the camera focal plane.

5. Annotation (for grid line referencing) is difficult to accomplish unless an annotated grid of the entire earth is stored. Digital approaches which draw grid lines can produce alphanumeric characters with relative ease.

Consideration was given to the use of the Nimbus PCM recorder (stored-A) for the storage of the grid data. This would permit a substantial savings in weight. However, this approach was dropped due to the nature of the interface and the loss of the ability to produce a "standard package" useful on any meteorological satellite.

Several approaches to on-board gridding appear promising. These are the straight line method, the coordinate method and a modification of the coordinate method which utilizes slope prediction and storage to reduce the amount of data necessary to specify the locations of the individual grid marks.

All of the approaches judged promising can be accomplished with a flight system weight in the 6.5 to 9 lb range and an average power requirement of less than 2 watts. These estimates were obtained by preparing fairly detailed preliminary designs for each method. The final choice of the system design is dependent on grid-appearance and anticipated updata communications channel errors as summarized in Section 6. A simulated grid, characteristic of the coordinate method, appears in Figure 1-2.

The digital methods require that picture times be predictable. Although timing problems have been experienced with TIROS satellites in the past, this problem will certainly not persist as there are no fundamental obstacles to obtaining predictable shutter times. As a safeguard, the individual picture grids, stored in the satellite memory, could very well be tagged with the times for which they were computed. These times could be compared to an external or grid-system-contained clock to insure that a grid is superimposed on a picture only if the shutter is tripped at the predicted time.

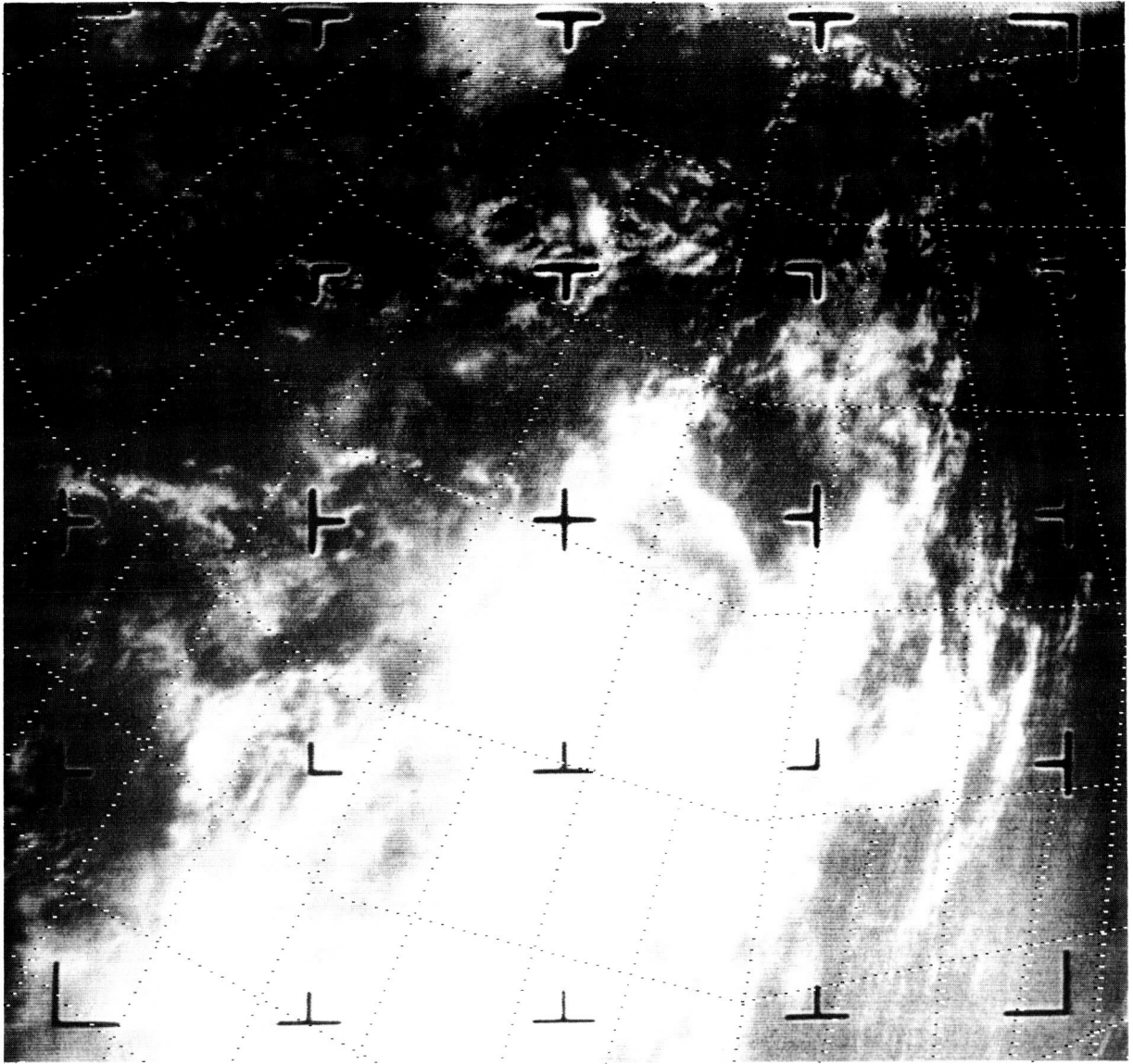


Fig. 6-1 Simulated Grid SL-2

## SECTION 2

### GRIDDING REQUIREMENTS

#### 2.1 GRID LINE SPACING

The initial specification for grid line spacing is as follows:

##### Latitude spacing on picture

- a.  $2^{\circ}$  from  $0-70^{\circ}$  latitude, north and south
- b.  $4^{\circ}$  from  $>70^{\circ}$  north and south

##### Longitude spacing on picture

- a.  $2^{\circ}$  from  $0-40^{\circ}$  latitude, north and south
- b.  $4^{\circ}$  from  $40-70^{\circ}$  latitude, north and south
- c.  $8^{\circ}$  from  $70-82^{\circ}$  latitude, north and south
- d.  $40^{\circ}$  from  $>82^{\circ}$  latitude, north and south.

If this spacing were maintained for the complete height range of the satellites (400-800 nm.), pictures taken at the higher altitudes would be virtually obscured by the grid lines. Figure 2-1 shows a picture grid with a basic  $2^{\circ}$  interval as suggested above for a height of 800 nm. It is obvious that the grid line spacing must be either a function of altitude or if it is to remain constant, it must be made larger than specified above.

The problem of grid line spacing has been previously examined in some detail. Picture data from the APT system will often be manually transferred to a base map. Widger and Glaser have shown that these base maps are almost universally graduated in  $5^{\circ}$  intervals, \* making the transfer from a  $2^{\circ}$  gridded picture to a standard map extremely laborious. For these reasons we suggest the following grid spacing:

Latitude:  $5^{\circ}$  throughout

Longitude:  $5^{\circ}$  - equator to  $60^{\circ}$  latitude  
 $10^{\circ}$  -  $60^{\circ}$  to  $75^{\circ}$  latitude

---

\* Widger, W.K., Jr., and A.H. Glaser, 1963: A Rationale for Geographic Referencing of Meteorological Satellite Data, Technical Report No. 1, Contract No. NAS 5-1204, ARACON Geophysics Company.



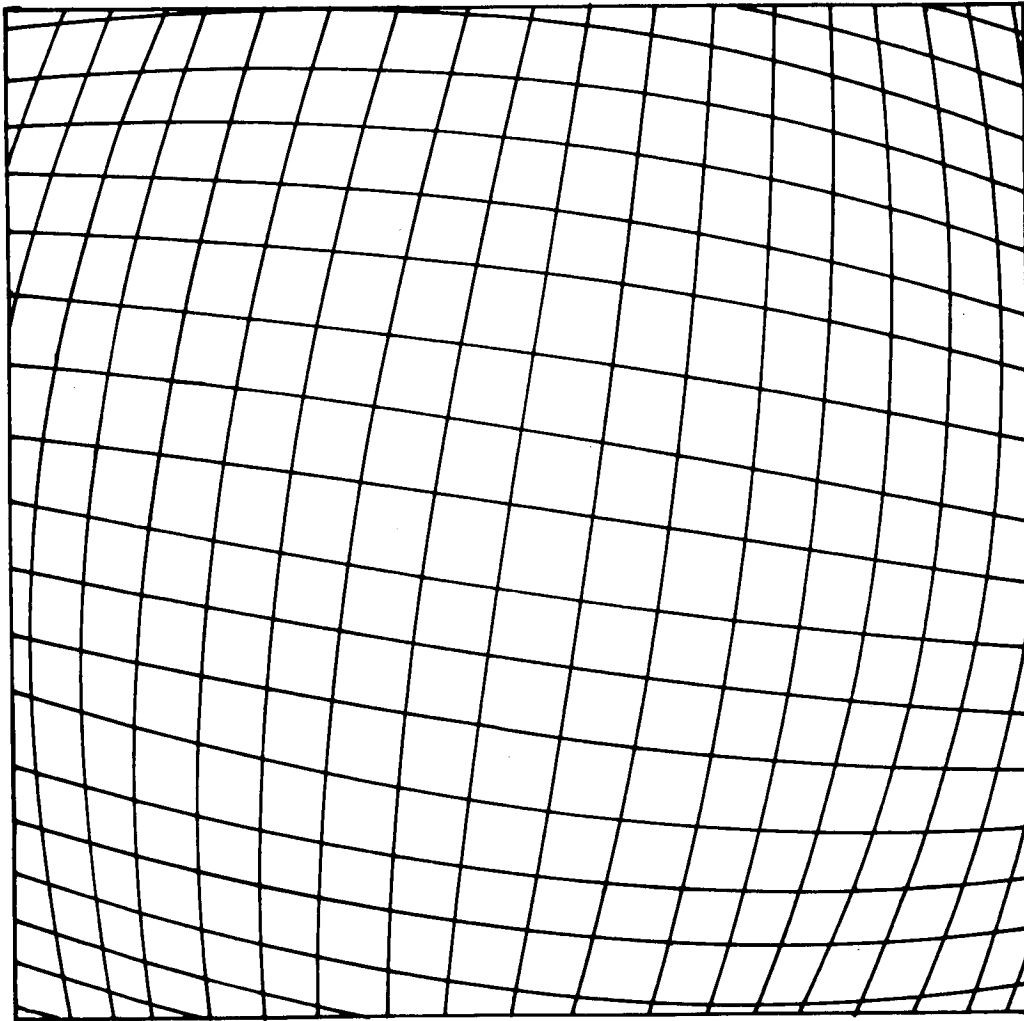


Fig. 2-1 Grid With  $2^{\circ}$  Spacing for 800 NM Orbit

20° - 75° to 85° latitude  
40° - 85° latitude to pole.

This has the additional advantage of maintaining a uniform spacing throughout the vast majority of the habitable regions of the world.

An appreciation for the appearance of the grid lines as they would appear in the pictures as a function of altitude can be attained by superimposing the camera apertures shown in Figure 2-3 onto the OEC map of Figure 2-2. (The apertures are contained in the pocket attached to the rear of this report.)

It is our recommendation that the 5° grid be universally used regardless of altitude. Should strong objections to the 5° grid interval occur for pictures taken at low altitudes, we would recommend that the basic 5° grid be maintained but that 2 1/2° lines, identifiable as such, be added between 5° lines in the picture. This will still permit correlation of the grid and base map lines to be obtained easily. If the 2 1/2° grid is used, it is recommended that it be reserved for altitudes of <500 nm.

## 2.2 GRID LINE REFERENCING

The grid lines appearing in the picture must be somehow referenced to enable the latitude and longitude identification of the lines. In the past, it has been common to place a north arrow at one of the grid line intersections whose latitude, longitude coordinates are sent with the picture. It would certainly be desirable to maintain this method of grid line referencing for the on-board system. Alphanumeric characters must be superimposed upon the pictures along with the grid lines to identify the coordinates of the north arrow. With the basic 5° grid proposed, at least two latitude or longitude lines are visible in the pictures even at an altitude of 400 nm. Thus, the north arrow could always be placed at a latitude or longitude line which is an integral multiple of 10°. This enables the lines to be identified with four alphanumeric characters. N or S (+ or -) and one decimal character will suffice to identify the latitude of the north arrow and two decimal characters will identify the east or west longitude of the north arrow.

The ease with which the alphanumeric characters can be generated in an on-board gridding system is highly dependent upon the type of system chosen. For this reason, a second alternate scheme of grid line referencing is proposed. North arrows can be placed at fixed latitude and longitude intersections. At least one north arrow must be visible in any picture which might be taken. The arrangement of the north arrows on a global map must be such that a data analyst cannot confuse two sections

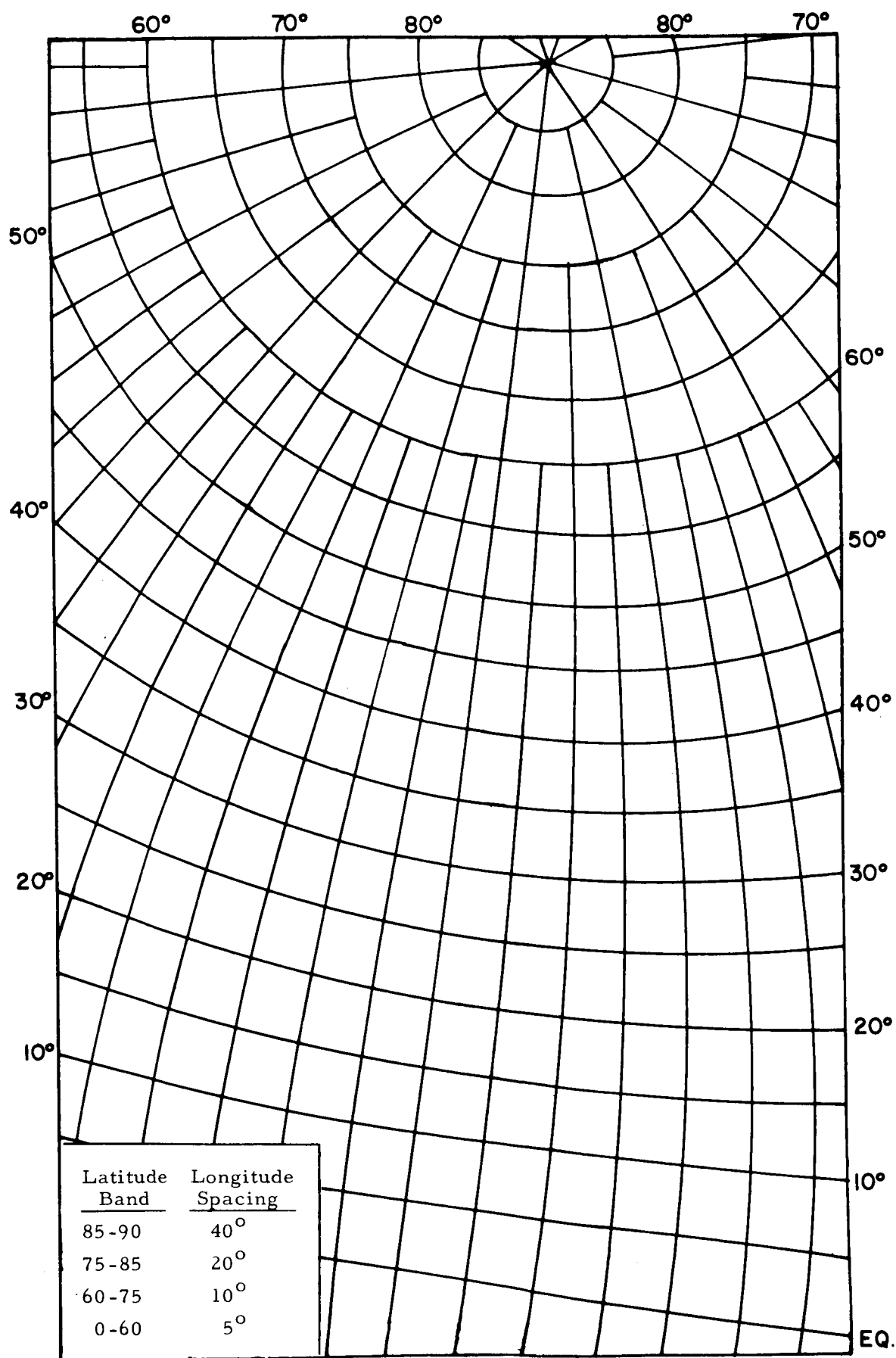


Fig. 2-2 OEC Map With Proposed 5° Grid

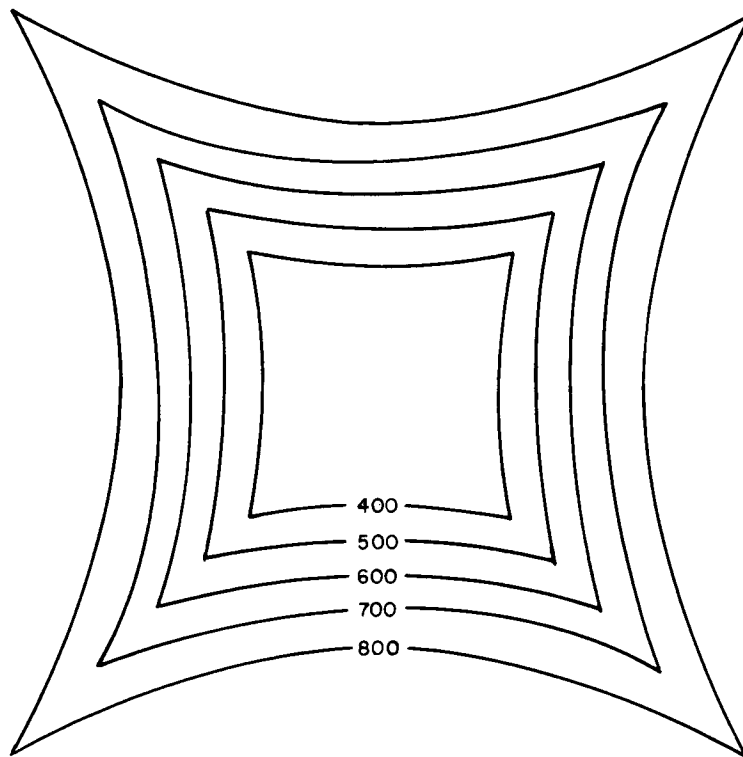


Fig. 2-3 OEC Map Coverage as a Function of  
Satellite Height

of the globe over a wide enough band of latitude and longitude to preclude error. Preferably a single fixed catalog of arrows would be employed for all altitudes. A suggested arrangement of north arrows is shown in Figure 2-4. With the arrangement of arrows depicted in Figure 2-4 an analyst must make an error of  $10^{\circ}$  in both latitude and longitude or  $20^{\circ}$  in one of the coordinates in order to incorrectly identify the lines. Since any receiver of the APT data must have a fairly accurate estimate of the satellite orbit in order to operate the ground station (track the satellite) it is extremely unlikely that he can make this large an error. His most likely error is an incorrect latitude guess. Latitude of the pictures is primarily a function of time. To make a  $10^{\circ}$  error in latitude, the estimate of picture time must be almost three minutes in error. Since it is unlikely that this large an error in picture time will be made, the fixed catalog of north arrows shown in Figure 2-4 should suffice to enable error-free grid-line identification.

The identification of grid lines through superimposed alphanumeric annotation is certainly superior to identification of grid lines through a fixed catalog of north arrows. The alphanumeric picture annotation provides a permanent record of the grid line coordinates. However it may be useful to compare the cost of the two approaches.

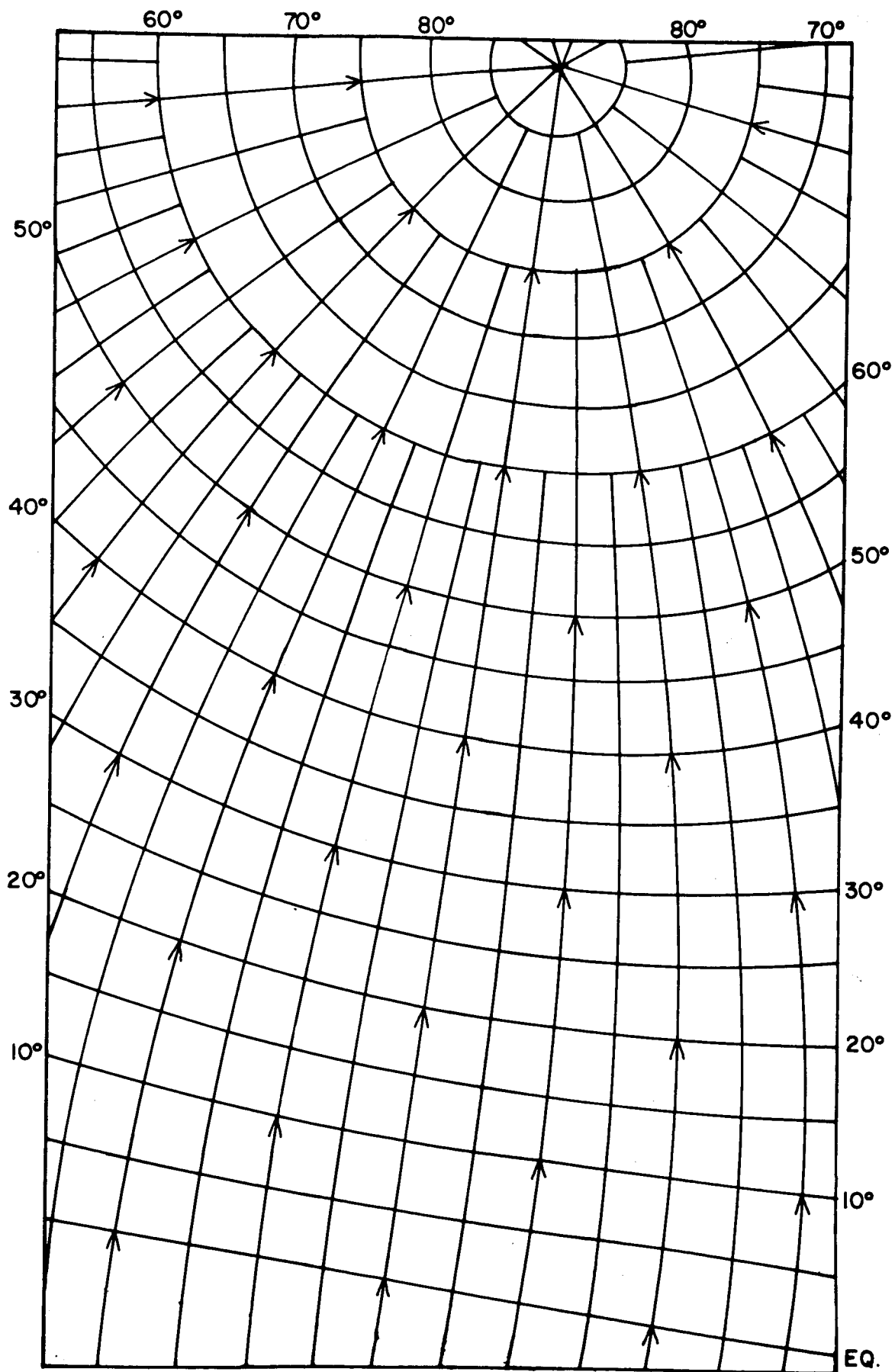


Fig.2-4 Suggested Locations of Fixed North Arrows  
for Grid Line Referencing

## SECTION 3

### DIGITAL APPROACHES TO ON-BOARD GRIDGING

#### 3.1 STRAIGHT LINE METHOD

##### 3.1.1 General

The straight line methods approximate the curved lines of the geographic grid by a sequence of straight lines. In general the line segments should be made as long as possible, subject to the limitation of a maximum one percent error, to minimize the number of line segments and hence the required data transmission to the satellite. Each line segment can be characterized by its initial starting coordinates and a slope. If we are to have the longest possible line segments, the tolerable one percent error should represent primarily the deviation of the curved true grid line from the straight line. To obtain this condition the initial coordinates and slope of the line should be represented with the highest precision with which it is possible to plot the points in the picture. A single picture element is considered to be the smallest resolvable distance in the APT picture. Thus the initial X, Y coordinates for the start of a line segment are specified with ten bit precision. If the slope of a line were characterized by the number of picture elements along a sweep ( $\Delta X$ ), the range of slope encountered would be  $\frac{1}{800}$  (nearly horizontal line) to 800 (nearly vertical line). In a fixed point notation system, a total of 20 bits would be required to achieve this range of slope. An alternate manner of specifying slope is depicted in Figure 3-1. Lines which make an intersection with the TV sweep of  $<45^\circ$  (mode 0) are characterized by the increment in Y for  $\Delta X = K$  (mark spacing). Lines which make an angle of intersection with the TV sweep which is  $>45^\circ$  (mode 1) are characterized by the  $\Delta X$  corresponding to a  $\Delta Y$  of K sweeps. If we ignore the perfect  $45^\circ$  line, the slope of any line can then be specified with a total of 12 bits, one for the mode, one for the slope (positive sloping lines have a  $\Delta X$  component in the sweep direction for increasing Y), and 10 for the  $\Delta X$  or  $\Delta Y$ .

A line segment once started, can be terminated in several different ways. If these segments are stored in an addressable location in the satellite memory, a line segment can be terminated by writing a new segment or a termination command into the segment location. However a better way of terminating a line which is independent of the type of memory employed, is to include in the segment specification the length of the line. The segment length should be specified in terms of the largest available

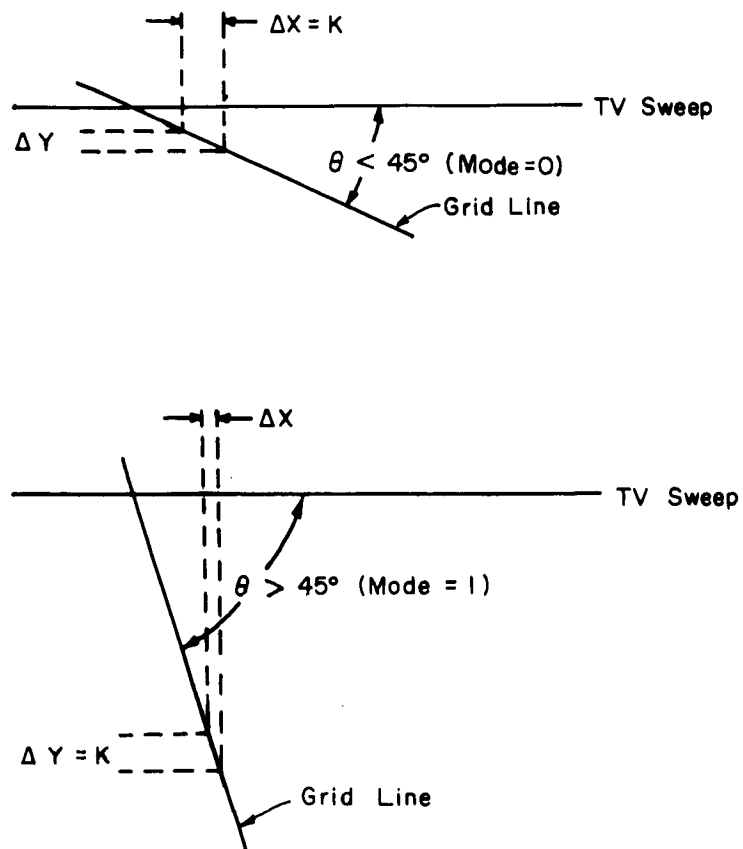


Fig. 3-1 Slope Specification



quantity to minimize the number of bits for the length specification. The largest integral quantity which can be used for this purpose is the number of marks to be layed down for the line segment. Thus the number of bits to specify segment length will depend on the mark spacing. For a mark spacing,  $K = 8$ , a maximum of 100 marks will be layed down along any line. (This assumes that marks are spaced such that the distance along a line between marks is  $K$  picture elements for mode 0 lines, or  $K$  sweeps for mode 1 lines.) Thus, a line segment is specified by its starting coordinates  $X, Y$ , (20 bits), slope (12 bits), and line length  $L$  (7 bits).

One of the important design parameters is the number of straight-line segments which the system would be required to handle to grid the pictures of a complete orbit. To obtain this figure, a number of grids were drawn for an 800 nm. polar orbit on the CDC 160-A computer at Point Mugu. (The 800 nm. orbit, showing the greatest earth coverage, requires the highest density grid for an individual picture.) The number of straight line segments required to grid this orbit was determined by manually fitting straight lines to the curved latitude/longitude lines with a maximum estimated error of one percent.

Table 3-1 shows the number of straight line segments needed to grid the pictures of an orbit as a function of satellite height. From the table, we see that the maximum number of segments is 372, if the  $2\ 1/2^\circ$  grid is employed only for orbits of 500 miles or lower. An additional 30 line segments are needed to include north arrows in a 15 picture orbit. This brings the maximum segment total to approximately 400.

Table 3-1  
Number of Straight-line Segments Per Orbit  
Required for Picture Grid

$5^\circ$ GRID INTERVAL		
<u>Satellite Height (nm.)</u>	<u>Number of Pictures</u>	<u>Number of segments</u>
800	10	360
400	14	150
$2.5$ GRID INTERVAL		
500	15	372
400	14	288

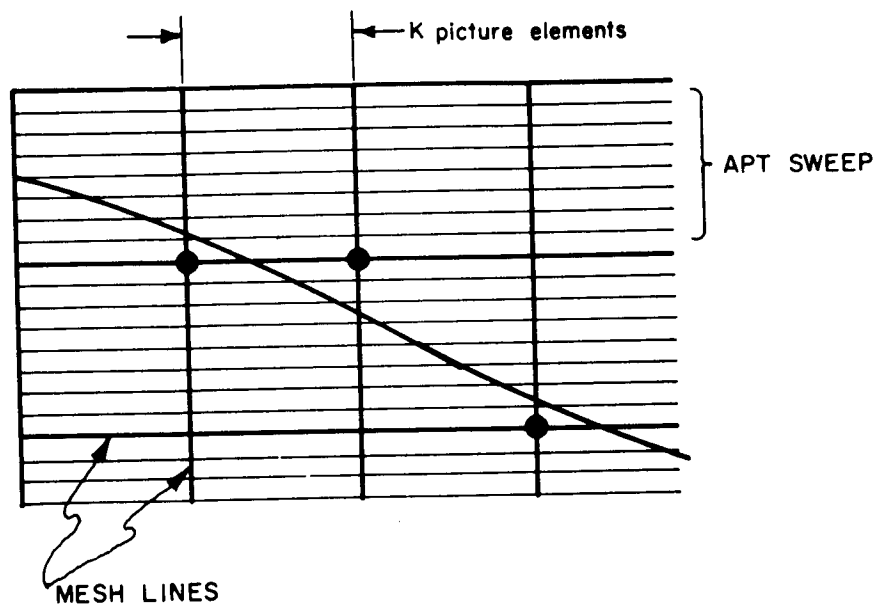


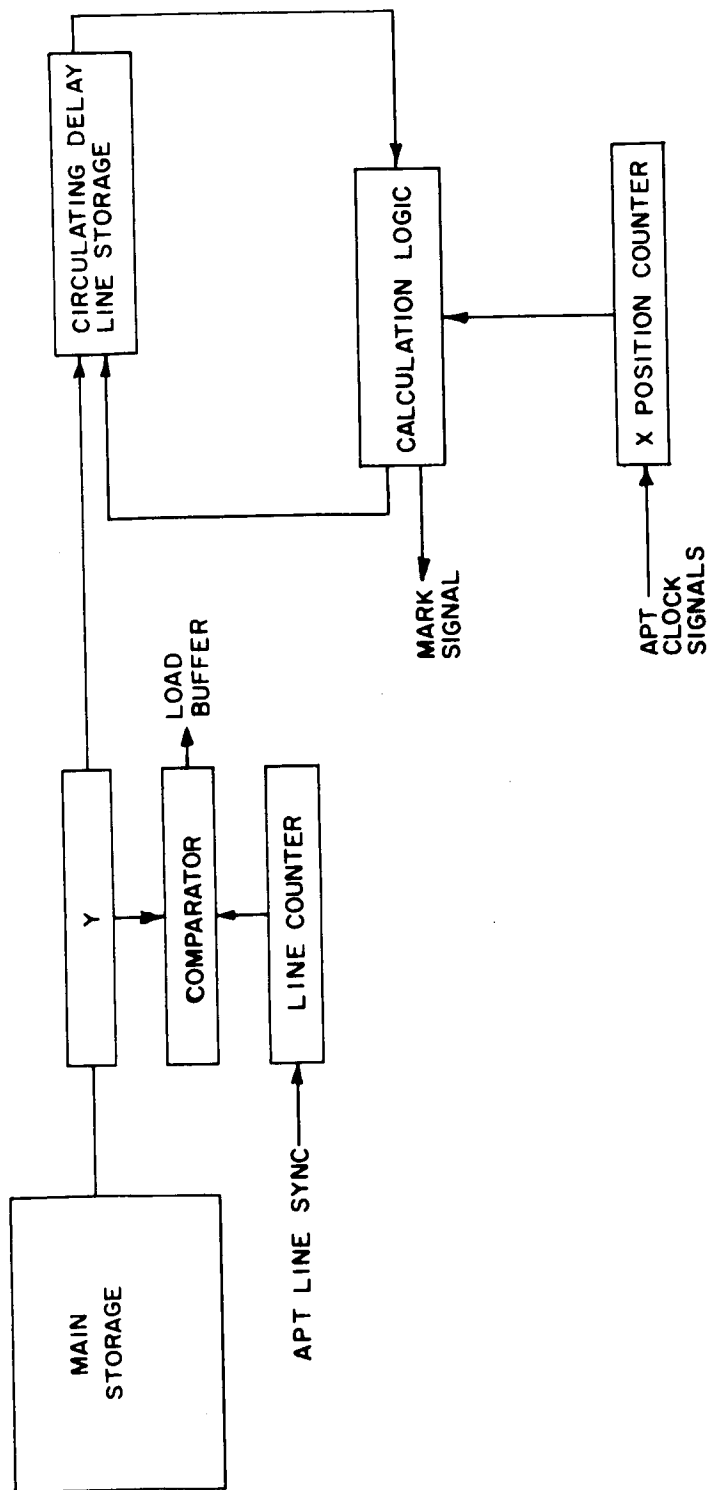
Fig. 3-2 Locations of Grid Marks SL-1

To reduce the amount of data which must be transmitted to the satellite, an investigation was made of the possibility of treating a grid line as a total entity rather than a number of line segments. The data for the line would consist of its initial starting coordinates, the slope of the initial segment, and a constant slope change for the additional segments of the line. Due to the nature of the slope changes, it was found that a constant slope change could be applied only to a single segment, i.e., each new segment would usually require a different slope change. The very small savings in information transmission are offset by the increased complexity of the on-board logic, so this approach was dropped.

Assuming that each line segment required 39 bits for its specification, a total of approximately 15,600 bits must be transmitted to the satellite to produce the picture grid. An additional 2,000-10,000 bits will be needed for annotation, depending on how annotation is accomplished.

### 3.1.2 Approaches to the Straight Line Method

Two different approaches to generating grid lines through sequences of straight line segments were investigated. In the first approach, all line segment data for grid lines in process is presented to the calculation logic in a time interval which is less than the time required for the vidicon electron beam to move between two consecutive positions at which a mark is allowed. If marks are to be plotted with a position accuracy corresponding to a picture element, the grid line data in a buffer memory must be completely cycled to the calculation logic in 310 microseconds. An attempt was made to take advantage of the fact that marks on any given line segment are spaced  $K$  picture elements apart. Thus the calculation logic should only be required to cycle in a time interval corresponding to the  $K$  picture elements. Figure 3-2 shows a fictitious array of perpendicular lines (mesh) spaced  $K$  picture elements apart superimposed on an APT picture ( $m = K$  for this case). Grid marks may only be located at the intersections of these lines. The maximum error in plotting a point of the straight line segment is then  $\pm \frac{K}{2}$  picture elements. If  $K = 8$ , the error in plotting the straight line is four picture elements, and the condition that marks be spaced either horizontally or vertically every  $K$  picture elements is satisfied. It should be noted that the error of  $\pm \frac{K}{2}$  elements must be subtracted from the tolerable one percent error that the marks can deviate from the true grid line. This will tend to raise the number of straight line segments required since the length of the straight line segments must drop, to satisfy the reduced error tolerance. A block diagram of



the SL-1 system appears in Figure 3-3. The grid line data transmitted from the CDA station is stored in a thin film or magnetic core memory. When the picture taking sequence is initiated, the Y portion of the word for the first line segment is compared to a line counter. When the APT sweep reaches the value of the Y-coordinate of the starting point of the line segment, the word is transferred from the main storage to a circulating delay line storage. The delay line storage will contain all the line segment data in process at any given time. The delay line cycles at a rate sufficient to present all the line segment words to the calculation logic in the time interval which corresponds to the distance between mesh lines. Each line segment word is examined by the calculation logic to determine if a mark should be made before each new mesh intersection is reached.

Table 3-2 shows the structure of the line segment words in the buffer memory which are delivered to the calculation logic for mark determinations every  $K^{\text{th}}$  sweep. (From Figure 3-2 we see that marks are only allowed every K lines.) When a word reaches the calculation logic its X value is examined to determine if a mark should be made. If the value contained in the X position counter matches that of the X coordinate in the segment word, a pulse is sent to the mark generator and new mark coordinates are computed using the slope data. For a mode 0 line  $\Delta Y$  is added to the Y portion of the segment word and the word is returned to memory. The value of Y for each line segment word is decremented by one during the picture retrace interval for each new mesh line. Thus when Y becomes less than one a new mark will be made and the slope will again be added to Y. Each time the slope is added to Y the X value is changed by one mesh interval in the direction dependent on the slope sign.

After the initial mark of the line is plotted (mode 1) the  $\Delta X$  of the slope is added to the X position value, and the word is returned to the calculation logic. The value of Y is ignored for mode 1 lines, since marks are made every K sweeps for all mode 1 lines.

The maximum number of line segments which must be handled by the buffer at any one time (number of line segments intersected by a single sweep) is 17 for the most dense grid corresponding to an 800 nm. altitude. If we include the possibility of north arrow annotation, this number is increased to 23. This results in a storage requirement for the delay line of approximately 900 bits, to be cycled every  $2 \frac{1}{2}$  milliseconds for  $K = 8$ . This figure is entirely practical for present day aerospace qualified delay lines. However, a mesh whose lines are separated K picture elements, requires a large increase in the number of straight line segments needed to fit the curved gridlines. A satisfactory mesh spacing from the point of view of storage

Table 3-2

## SL-1 Word Structure

Number of Bits	1	1	20-2B	10-B	1	10-B	1	10-B	1
Content	I	H	X	Y	M	$\Delta X$ or $\Delta Y$	S	L	P

used in  
buffer only

$$2^B = K \text{ (Mark spacing)}$$

- I      Index. Indicates absence or presence of data in each delay line storage location.
- H      Hold. Used to end plotting of points of a given line segment on any given sweep. H is reset to zero for each new mesh line.
- X, Y    Initial coordinates of a line segment in updata. X position and residue and Y residue in delay line.
- M      Mode.
- S      Slope sign.
- $\Delta X$  or  $\Delta Y$      $\Delta X$  is the number of mesh intervals between successive marks of a mode 1 line.  $\Delta Y$  is the number of mesh intervals between successive marks of a mode 0 line.
- L      Line length (number of marks).
- P      Parity bit.

requirements (minimum number of segments) has its lines spaced apart two picture elements. This forces the delay line operating speed up to two megacycles. As a result, further work on this method was dropped in favor of the system described in the following paragraphs.

The second approach to be investigated (SL-2), employs two separate fixed meshes, one for each line mode. For mode 0 lines the vertical lines of the mesh are spaced apart K picture elements. The horizontal lines of the mesh are spaced apart a single picture element (sweep). See Figure 3-4a. The horizontal mesh spacing permits the mode 0 line segment words to be cycled through the calculation logic in a time interval corresponding to K picture elements. Points for mode 1 lines (see Figure 3-4b) are plotted on a mesh whose vertical lines are spaced apart a single picture element, and whose horizontal lines are spaced apart K sweeps. The use of these fixed meshes for plotting allows any line to be marked at intervals of K picture elements. The direction in which the mark spacing (horizontal or vertical) equals K is determined by the mode. The use of these meshes also permit marks to be plotted with single picture element precision as can be seen from examining the marks for the grid lines of Figure 3-4.

The word structure for SL-2 is shown in Table 3-3. In order to cycle the mode 1 line segment words through the calculation logic once every K picture elements, and still retain the ability to make a mark at any of the 800 mesh intervals along a sweep, the following logic is employed. The portion of the X position data which indicates the mesh interval number of the next mark for a line segment is compared to the corresponding bits of the X beam-position counter. When the difference between these two values is less than one mesh interval, the difference (in terms of picture elements) is stored in a register. This difference is then decremented by one for each horizontal advance of a picture element and a mark is made when the difference becomes 0. In the meantime, the data for the segment will have been returned to the buffer memory. The calculation logic which is applied to each of the modes is shown in Tables 3-4 and 3-5.

In general the block diagram for the SL-2 system looks quite similar to that for SL-1, shown in Figure 3-3. Only those line segments currently in process are contained in the buffer memory. Line segment data is withdrawn from the main memory and stored in the buffer when the sweep count for the APT picture equals the initial Y coordinate for the line segment. Since the data in the buffer storage (delay line) is cycled through the calculation logic in a time interval corresponding to K picture elements, the required clock rate remains relatively low (approximately 410 kc),

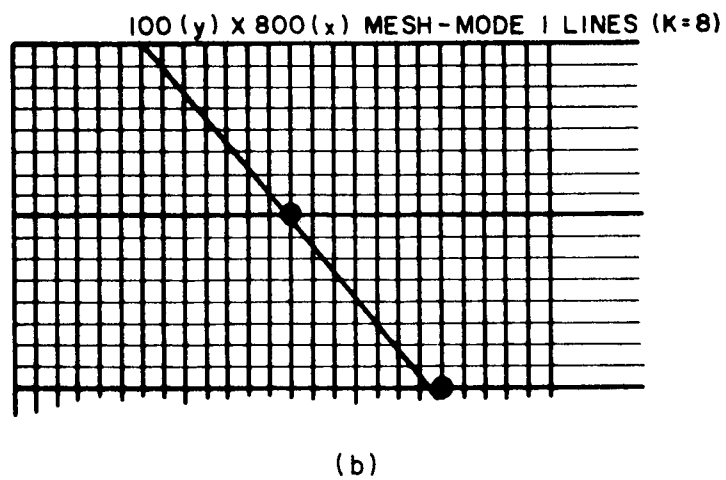
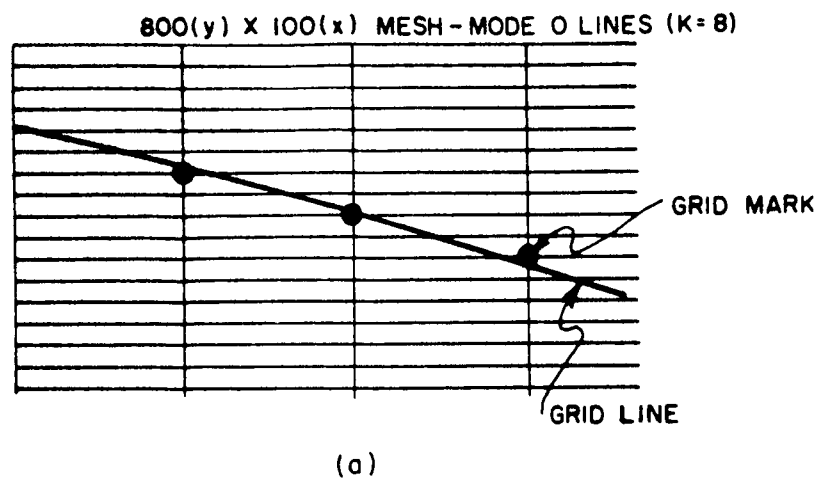


Fig. 3-4 Allowable Locations of Grid Mark SL-2



Table 3-3

## Word Structure Method SL-2

SL-2 Bit Sequence in Delay Lines

Bit Name	S <sub>p</sub>	P	L	S	W	X <sub>m</sub>	R <sub>m</sub>	R <sub>L</sub>	M	H	I
Number of Bits	1	1	7	10	1	7	3	7	1	1	1

(40 bits to TCL)

- I = Index Bit. Indicates vacancy of address in delay line.
- H = Hold Bit. Inhibits further marking on particular sweep for this word.
- M = Mode Bit.
- R<sub>L</sub> = Least significant bits of residue (fractional part of X or Y in terms of picture elements).
- R<sub>m</sub> = Most significant bits of residue in Mode 0. (Sweeps before next mark.)  
Least significant bits of X address in Mode 1. (Integral number of picture elements between mark and preceding mesh line.)
- X<sub>m</sub> = Most significant bits of X address. (Integral number of mesh intervals to mark position.)
- W = Sign of slope.
- S = Slope in Mode 0. (Slope is  $\Delta Y$  for Mode 0.)  
Inverse slope in Mode 1. (Slope is  $\Delta X$  for Mode 1.)
- L = Number of Marks to be made in this segment.
- P = Parity Bit.
- S<sub>p</sub> = Spare Bit.

Table 3-4

## Mode 0 Calculation Logic

L (Line Length)	S (Slope $\Delta X$ )	W (Slope sign)	M (Mode)	$X_M$ (Mesh Interval Number)	$R_M^*$	$R_L^{**}$	H Hold	I (Index)
-----------------------	-----------------------------	----------------------	-------------	------------------------------------	---------	------------	-----------	--------------

## Mode 0 Segment Word

\* Integral number of sweeps before next mark.

\*\* Fractional number of sweeps before next mark.

1. If H (Hold bit) is ZERO,

- A. Compare  $X_M$  to corresponding bits of X vidicon beam position counter.
- B. When  $X_M$  = beam position, test  $R_M$ .
- C. If  $R_M = 0$ , mark; set H to ONE; add to or subtract from  $X_m$  the quantity 1, as determined from slope sign; add slope ( $\Delta Y$ ) to  $R_M + R_L$ , decrement L.
- D. If  $L = 0$ , set I to ZERO.
- E. If  $R_M \neq 0$ , reset H to ZERO.
- F. Return word to buffer.

2. If H is ONE,

- A. Mark; Add to or subtract from  $X_M$  the quantity 1 as determined by slope sign, add slope ( $\Delta Y$ ) to  $R_M + R_L$ , decrement L.
- B. If  $R_M \neq 0$ , reset H to ZERO.
- C. If  $L = 0$ , set I to ZERO.
- D. Return to memory.

Table 3-5

## Mode 1 Calculation Logic

L (Line Length)	S (Slope-- $\Delta X$ )	W (Slope Sign)	M (Mode)	$X_M$ Mesh Interval Number	$R_M^*$	$R_L^{**}$	H
-----------------------	-------------------------------	----------------------	-------------	----------------------------------	---------	------------	---

## Mode 1 Segment Word

\* Integral number of picture elements between mesh line  $X_M$  and next mark.

\*\* Fractional number of picture elements between mesh line  $X_M$  and next mark.

- A. Compare  $X_M$  to corresponding bits of X vidicon beam position counter. Mode 1 words are examined every  $K^{\text{th}}$  sweep only.
- B. If H is ZERO and  $X_M - X$  beam position  $\leq$  mesh interval, store the difference (number of picture elements) in a register, decrement L.
- C. Set H to ONE; add to or subtract from  $R_M + R_L + X_M$  the slope ( $\Delta X$ ) as determined by sign bit W.
- D. Return to buffer.
- E. Decrement  $X_M - X$  beam position for each horizontal advance of one picture element.
- F. When  $X_M - X$  beam position = 0, mark.
- G. Reset H for mode 1 lines at end of each sweep.

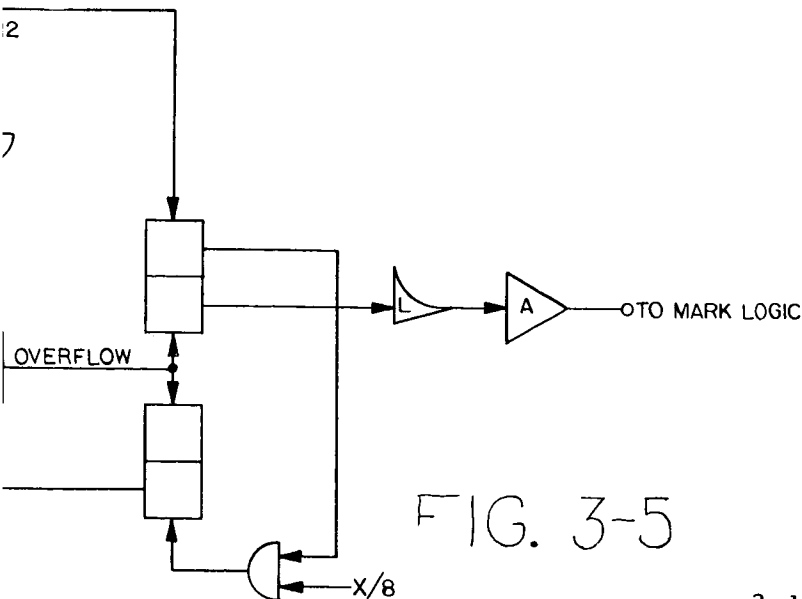
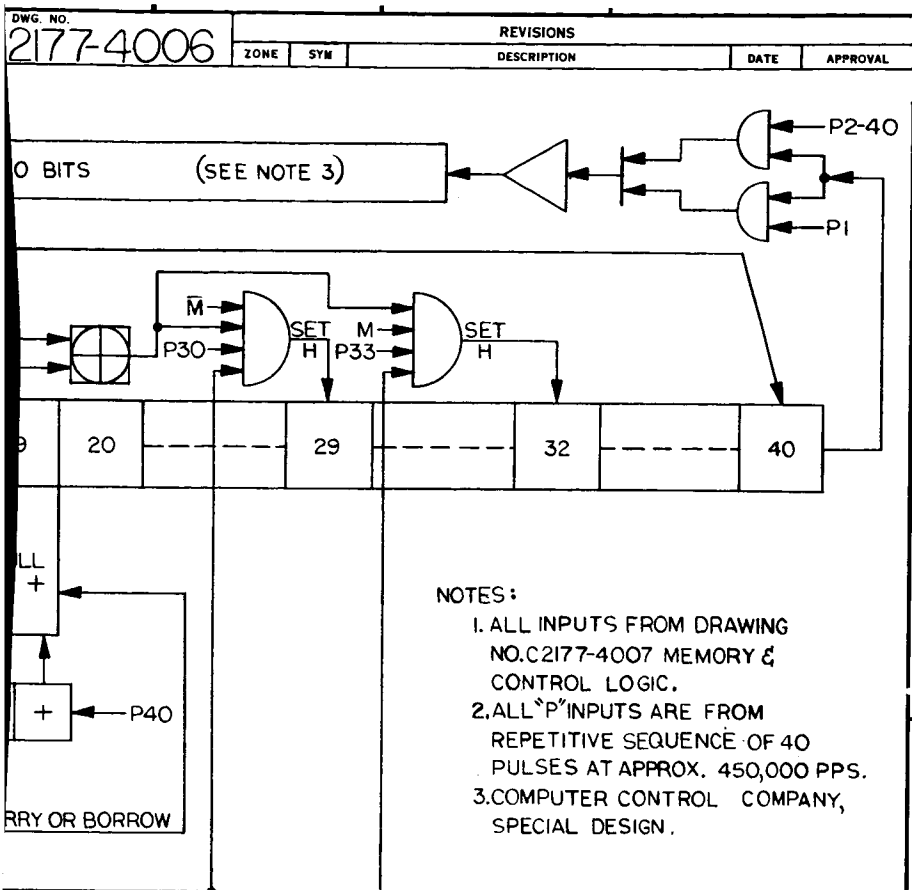
while the point plotting accuracy is maximum. Certain other advantages accrue from the SL-2 approach, including similar operations at similar bit positions of the buffer word in the calculation logic.

When a negative slope of less than  $1/K$  occurs, the normal addition of the slope to the Y coordinate yields scan coordinates which have already been passed by the vidicon beam. In the SL-2 system, these lines can be very easily handled in the following manner. The initial X coordinate of the line is reduced by the number of points to be marked on the first line. After the first mark is made, the slope addition (increment of Y) is made to Y and X is decremented by 1 in the normal manner for the SL-2 system. In addition H is set to ONE. For each additional cycle of the delay line, during the sweep, a mark command is generated until the upper three bits of Y ( $R_m$ ) are no longer zero at which time, H is reset to ZERO. This condition occurs when the accumulated increments of Y add up to one line. Note that when H is ONE, the test on X (comparison of X-scan and X-line values) is not a part of the mark decision. Only after H is reset to ZERO is the X comparison again made a part of the mark decision. This ignoring of the line segment X-coordinate is possible in SL-2, since marks for mode 0 lines are generated at fixed intervals of horizontal advance. Each time a mark is made the line segment X-coordinate is decremented by one in a bit position that actually corresponds to a horizontal displacement of K elements with the result that at the end of a mark sequence for a given line, we have the correct initial position for the first mark of the line segment on the next line. A maximum error of one picture element is made in plotting lines of negative slope  $< \frac{1}{K}$  with the above technique.

The maximum number of straight line segments in this method which will be stored concurrently in the buffer is 23. The mechanization developed further assumes that every word is in the calculation logic for one word time; therefore, a total path cycle time is 24 words. On this basis, the minimum clock rate is 388 kc. However, it must be remembered that every K coordinate intervals the X counter changes its value and during this changing time, no computation can be performed. This raises the clock rate to at least 410 kc for  $K = 8$ . Because of the advantages of the SL-2 method cited above, a detailed mechanization of this method was performed.



2



3-15a

ITEM	REQD	PART NO.	DESCRIPTION	MATL	MATL SPEC.
LIST OF MATERIALS					
<p>DATE 25 NOV 64</p> <p>BY <i>[Signature]</i></p> <p>PROJECT ENG. APPD. <i>[Signature]</i></p> <p>PRODUCT ENG. APPD. <i>[Signature]</i></p> <p>SUPERSEDES</p> <p>REFERENCE</p>			<p>TITLE</p> <p>CALCULATION LOGIC</p> <p>METHOD SL-2</p> <p>FIGURE 3-5</p>		
<p>SCALE</p> <p>WEIGHT</p>			<p>SIZE C</p> <p>DWG. NO. 2177-4006</p> <p>REV. —</p> <p>CODE 06900</p> <p>SHEET 1 OF 1</p>		

DiAn Controls, Inc. BOSTON, MASS.



2

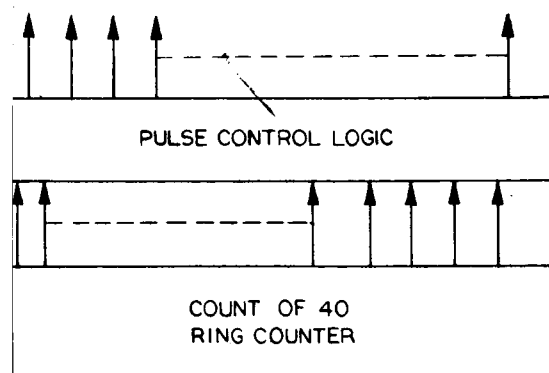
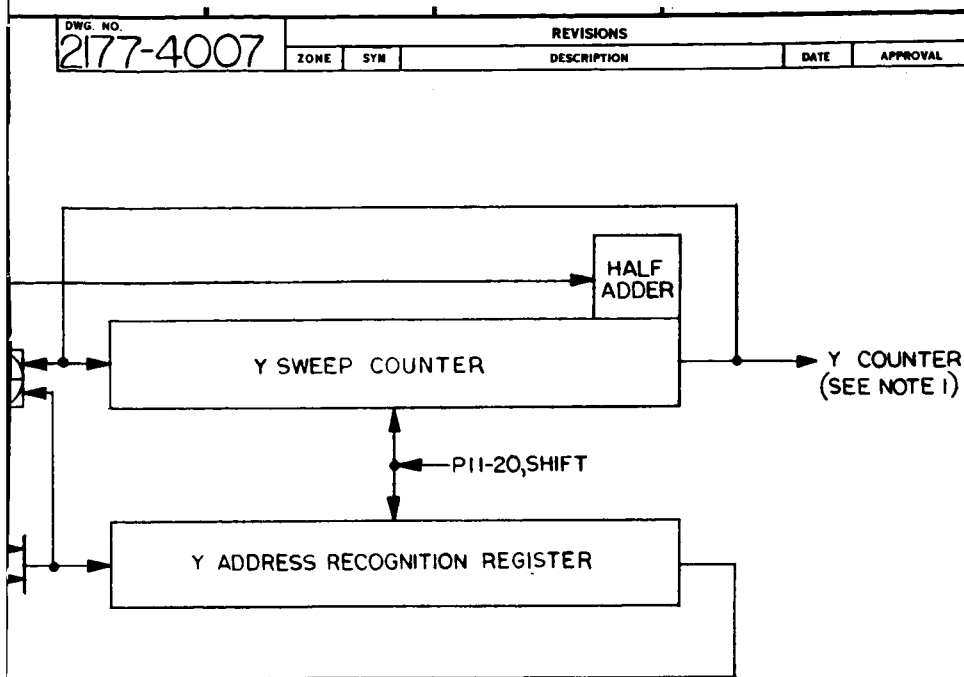


FIG. 3-6

3-15b

ITEM	REQD	PART NO.	DESCRIPTION	MATL	MATL SPEC
<b>LIST OF MATERIALS</b>					
DRAWN <i>D. Page</i> DATE 27 NOV. 64 CHECKED <i>J. C. [Signature]</i> DATE 4 Dec. 64 PROJECT ENG. APP. <i>[Signature]</i> DATE 4 Dec. 64 PRODUCT ENG. APP. <i>[Signature]</i>			<b>MEMORY &amp; CONTROL LOGIC</b> <b>METHOD SL-2</b> <b>FIGURE 3-6</b>		
SUPERSEDES REFERENCE					
SCALE <i>1/8"</i> WEIGHT <i>1/8"</i>			<div style="text-align: center;">   <b>Di/An Controls, Inc.</b>            BOSTON, MASS.         </div>		
SIZE <b>C</b> DWG. NO. <b>2177-4007</b> REV <b>—</b>			CODE 06900 SHEET 1 OF 1		



### 3.1.3 Logical Implementation of SL-2

A complete calculation and timing logic implementation was done for method SL-2. The system used the internal bit sequence shown in Table 3-3. The complete logic is shown in two separate diagrams. Figure 3-5 gives the calculation and delay line control logic along with the output logic. Figure 3-6 shows the timing and memory control logic, the pulse gate logic and the beam position counters. The entire logic operates at a minimum frequency of 430 kc/s.

The basic serial clock is derived from the APT logic, is applied to a ring counter of 40. The ring counter and associated timing circuits drive the calculation logic. All the computations are performed serially in a 40 stage shift register which is controlled by a network of switches and gates. In order to aid the study of these diagrams, the following definitions are listed:

- a. Symbols  $F$  and  $\bar{F}$  refer to the vidicon sweep and retrace periods respectively. These signals are obtained directly from the APT subsystem.
- b. The  $p$  pulses are pulses of numerical sequence from 1 to 40 from the ring counter.
- c. The main control flip-flops are identified by letters and defined as follows:
  - E - The error flip-flop E is in the ONE state when the word being viewed is not to be sent to the calculation logic. In the  $\bar{E}$  state, the shift register calculation logic is enabled.
  - I - When the Index flip-flop equals ONE, a segment word of 40 bits, in the delay line contains an active line segment. When the flip-flop is in the  $\bar{I}$  state, the delay line at that address is empty or contains a word which has been fully marked.
  - M - The mode flip-flop M designates whether mode 1 or mode 0 describes the word entering the shift register. This flip-flop enables and switches the proper logic so that the calculation is correct for that mode.
  - S - The segment flip-flop S when in the ONE state will admit new data from the memory into the Y register and into the shift register. In addition, the flip-flop activates a gate which sets  $I = 1$  in the delay line address being entered.

+/- The  $\pm$  flip-flop determines whether the incremental slope shall be subtracted from or added to the slope residue. The flip-flop is controlled by the W (sign) bit in the segment word.

A&B - The A & B flip-flops control the mark logic depending on whether mode 0 or mode 1 lines are being described.

The mark logic is not shown; however, it is essentially the same as that given in Figure 3-14 for the coordinate method.

## 3.2 COORDINATE METHODS

### 3.2.1 General

The coordinate method requires new information for each mark plotted to approximate a grid line. Consequently, the coordinate approach is not economical of storage. However, it can offer sufficient decrease in logic complexity for mark calculation to offset the increased storage requirement.

The number of marks needed to produce the grid lines in the APT pictures is dependent on the mark spacing, the method of picture annotation, and the spacing of the latitude longitude lines. We will assume that the  $5^\circ$  grid spacing recommended for the straight line system is adopted for the coordinate method. In drawing the grid lines for the  $5^\circ$  grid for an 800 nm., 10 picture orbit, the equivalent of 156 straight horizontal or vertical lines, completely crossing the picture, is produced. The equivalent of two more complete lines is required to produce the north arrows in the picture. If we assume that the mark density of the north arrow lines is twice that of the grid lines, the equivalent of four additional complete lines is required, for a total of 160 lines.

With a horizontal or vertical spacing of eight picture elements, 100 marks are needed to produce a full line across the picture. The total number of marks required to plot the grid lines and a single north arrow per picture is approximately 16,000 for the 800 mile orbit. A complete X, Y specification of the coordinates with single picture element precision would require a total of 256,000 bits. As a first step toward reducing the required storage, let us consider how much of a reduction in the precision of mark location specifications can be tolerated. The accuracy specification of one percent error of the picture height or width permits marks to be laid down at the intersections of a mesh whose lines are spaced 16 picture elements apart ( $n = 8$ ) if no other factors contribute to position error. However, the appearance

of a line composed of marks placed at the intersections of such a grid is quite displeasing. Figures 3-7 and 3-8 show the appearance of lines drawn using fixed meshes specified by  $n = 4$  and  $n = 8$  respectively, with marks spaced 8 elements apart ( $K = 8$ ). Each mark is three picture elements long by one element wide to simulate the white portion of the desired grid mark. A necessarily subjective evaluation of the lines depicted in Figures 3-7 and 3-8 has resulted in our eliminating any further consideration of drawing lines using the  $n = 8$  mesh as long as the mark spacing remains 8 elements. The use of  $n = 4$  mesh allows us to specify points on a line with a precision of 4 parts in 800, or 8 bits per axis.

A second possibility for reducing the storage requirement is a reduction in the mark density. The initial specification called for a maximum mark spacing of one percent of the side dimension in either X or Y displacement on the picture plane. This would result in a mark density which is significantly larger than the density of the grid-line marks appearing in the recent Nimbus AVCS photos. It is our opinion that a mark spacing of 16 horizontal or vertical elements produces an adequate grid and results in less occlusion of the pictorial data. Figures 3-9 and 3-10 show the appearance of lines drawn with 4 and 8 element meshes with a mark spacing of 16 elements. It is suggested that the lines drawn with the 4 element mesh and 16 element mark spacing represent a reasonable compromise between the storage reduction and appearance requirements.\* Increasing the mark spacing to 16 elements reduces the maximum number of marks required to produce the grid for an orbit to 8,000. A full coordinate specification of each mark with 8 bit precision for each axis brings the total storage requirement down to 128,000 bits.

The Y portion of the mark location coordinate set can be eliminated by inserting line "markers" between sets of X coordinates for the marks of a single line. Thus the word length for a mark is reduced to the eight elements of the X position. A line "marker" is simply an illegal X code. Since the 4 element mark gives us in essence a 200 line picture, 2,000 "marker" words must be added to the storage requirement (200 lines x 10 pictures for the 800 nm. orbit). The bit total is then

---

\* If a mark spacing of 8 picture elements must be adapted, the ratio of mark spacing to mesh separation  $\frac{K}{n}$  should equal that of Figure 3-9 to maintain a pleasing appearance of the grid lines. This requires a mesh specified by  $n = 2$  for  $K = 8$ . The X, Y coordinates would then be specified with 9-bit precision for each axis.

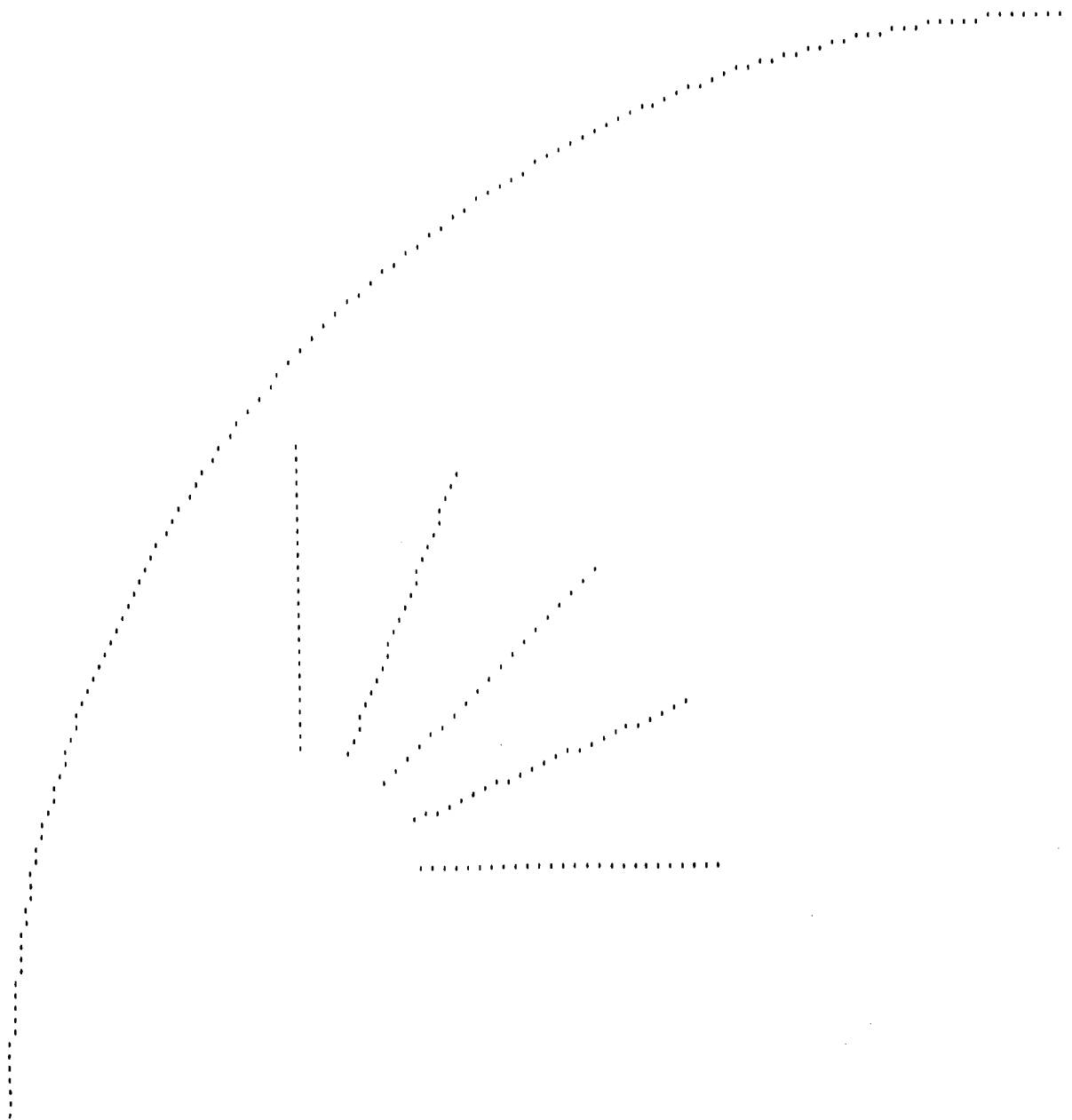


Fig.3-7 Appearance of Grid Lines  $n = 4$   $K = 8$

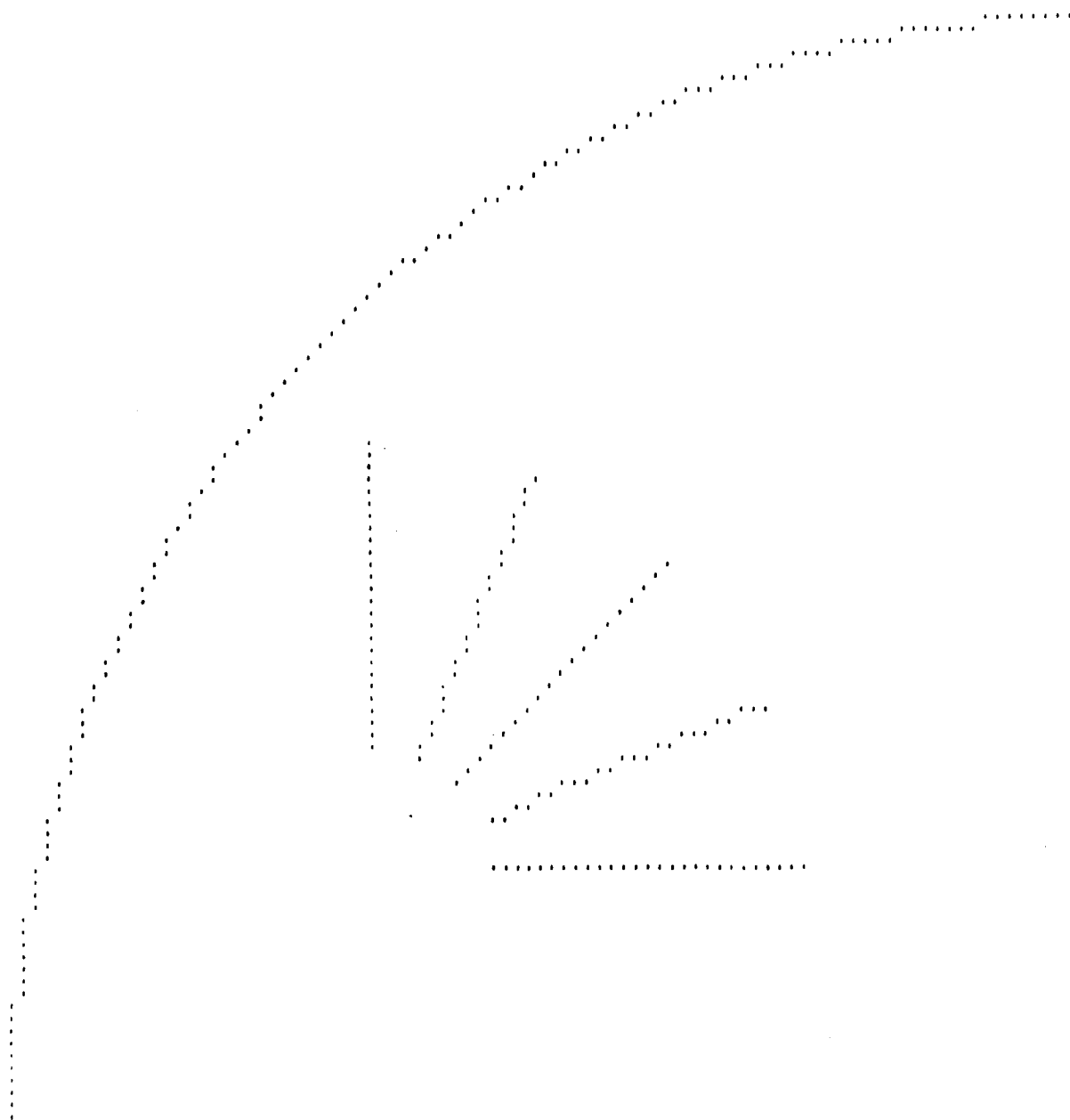


Fig.3-8 Appearance of Grid Lines  $n = 8$   $K = 8$

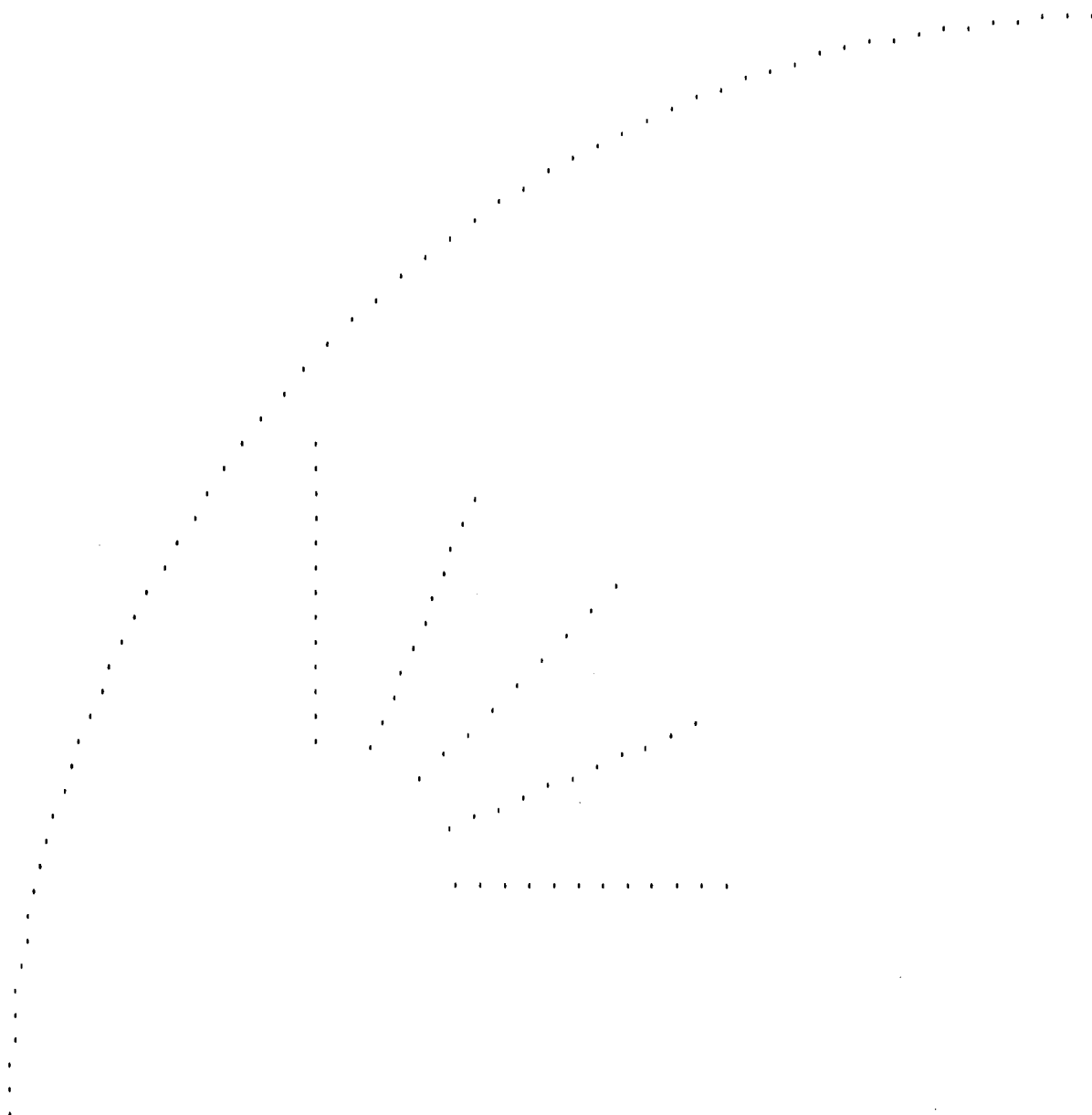


Fig.3-9 Appearance of Grid Lines  $n = 4$   $K = 16$

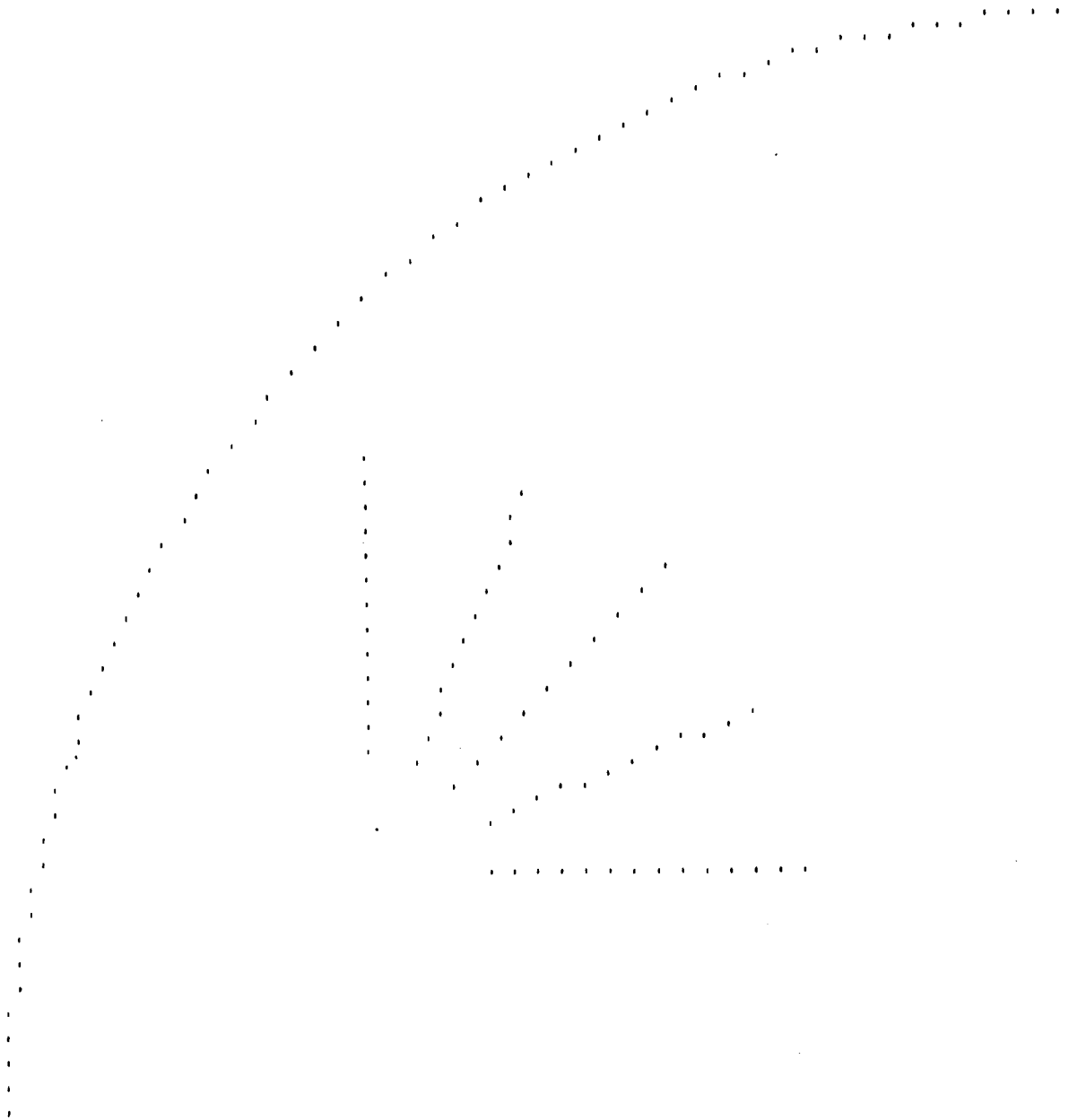


Fig.3-10 Appearance of Grid Lines  $n = 8$   $K = 16$

reduced to 80,000. Line markers can be largely eliminated by employing logic which detects a decrease in the value of the X coordinate of a word relative to the previous word in a sequence. The X coordinate for each mark along a mesh sweep will increase monotonically until a mark word for a new mesh sweep appears. For those mesh sweeps during which no marks are plotted, or for which the X coordinate of the mark is greater than that of the last X coordinate of the previous sweep marked, two alternatives are available: 1) a line marker can be employed; 2) extra marks located at the end of a sweep (or in the retrace interval) can be added. This technique permits a reduction in the bit total to approximately 70,000 bits to produce the grid lines.

A system employing a full X address for each mark is described in Section 3.2.4.2.

### 3.2.2 Run-length Coding

Assuming that the coordinates of the marks can be efficiently represented through a run-length coding approach, the distances between marks must be accurately determined. Grid marks are only allowed on the intersections of a mesh. Using a mesh,  $n = 4$ , only 200 sweeps per picture will be used for production of the picture grid. The average number of grid line marks per allowable sweep or mesh line is 4 marks per mesh line. Thus the average distance between marks on a mesh line is equal to 50 mesh intervals. However the distribution of distances between marks varies widely, as a function of satellite altitude, orbit inclination, and yaw. Consider the grid depicted in Figure 3-11. There are approximately 7 meridians running up and down the picture. If the marks of each meridian appear on every fourth mesh line (16 picture element spacing) the average spacing between the meridian marks is around 28 mesh intervals. Three out of every four mesh lines would not bear any meridian marks.

There are roughly six parallels running across the picture. The six parallels would be represented by about 300 marks, and for the orientation of the grid shown in the figure, about 90% of the mesh lines would have at least one mark belonging to a parallel. The result is that about one quarter of the mesh lines would have distances between marks clustered around 33 mesh intervals, 7-8% of the mesh lines would have no marks and the remainder of the mesh lines would have distances between marks averaging roughly 130 mesh intervals.



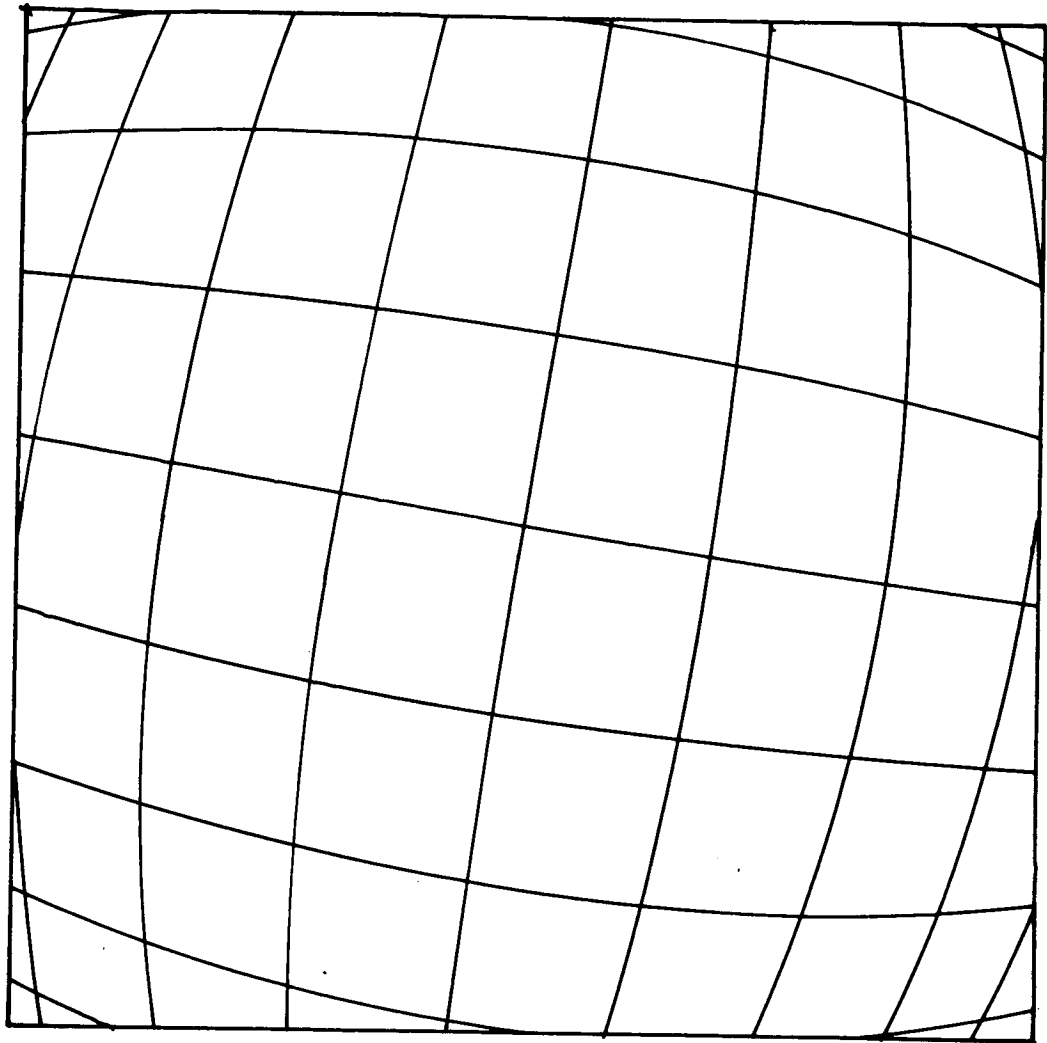


Fig.3-11 Equator Picture from 800 NM with 5° Grid

Next we can consider the mark distances (along a mesh line) if the vehicle is yawed through an angle compensating the orbit inclination ( $9^\circ$  for the grid of Fig. 3-11), which results in the Equator appearing as a horizontal line. Our meridian marks are spaced in much the same manner as they were in the case described above. Three quarters of the mesh lines contain no meridian marks. However, now approximately 60% of the mesh lines have no marks belonging to parallels. Of the 40% which do contain parallel marks, the average spacing between the marks for the parallel is about 50 mesh intervals, but the spacings are widely distributed about the average. For the Equatorial line, the spacing between marks is 4 mesh intervals ( $K = 16$ ). Moving toward the higher latitudes, the number of parallel marks per line decreases and the mark spacing increases all the way up to a full line width (196 mesh intervals). Thus we are faced with a distribution of distances between marks which is a function of the orbit parameters, and which covers a range of 4 - 600+ mesh elements (extending the count over more than one line).

The distribution will show some very pronounced peaks. Certainly the distance of 4 mesh intervals (the mark spacing) will be encountered quite often for sections of grid lines slightly inclined to the sweep lines. Another peak in the distribution will occur around the average meridian spacing and will be dependent on the satellite altitude. The peak will flatten as the orbit inclination approaches  $45^\circ$ . The peaked nature of the spacing distribution curve suggests the application of efficient coding techniques. However, the formulation of the appropriate mathematical model which would permit the spacing distribution to be determined as a function of orbit parameters is considered to be beyond the scope of this study, in which all possible approaches are to be considered.

Some valid generalizations can be drawn from the above analysis. The distances corresponding to the meridian mark spacings (half the marks in the picture) are clustered around 28 mesh intervals and would not exceed 60 mesh intervals for any orientation of the picture. These distances could be specified by fixed length words of 6 bits. Approximately 50% of the distances between parallel marks on the same sweep could also be represented by a 6 bit word. The remaining 25% of the marks can be represented by a sequence of two or more words. Suppose we reserve several of the six bit codes to represent the distances between true marks and false marks. (A false mark would not appear in the picture.) Four codes are immediately available, since the mesh interval distances of 0, 1, 2 and 3 never occur. If we make the code of 0 (decimal) correspond to a distance of 63, distances between 64 and 126 can be represented by two consecutive words. The first word causes an advance of

63, but no mark. The second word causes an advance and a mark. The weighting of the additional false mark codes might be graduated in binary fashion, (126, 252, 504) requiring about 2.5 words per mark for those mark distances which exceed 63. This procedure would result in an average of 1.4 words per mark. The total storage for the 8,000 grid marks would then be in the order of 65,000 bits.

So far, we have only considered the highest (800 nm.) orbit to be encountered. This orbit represents a worst case from the viewpoint of the number of total marks, since the greatest number of grid lines appears in the picture at the highest altitude. However, it is possible that the largest storage requirement exists for a lower altitude. The number of pictures taken per orbit increases from 10 at 800 nm. to 15 at 500 nm.

The number of lines visible in the picture is roughly proportional to the ratios of the side-to-side dimensions of the coverages on the earth. The number of pictures which can be taken as a function of altitude is shown in Table 3-6. (The 208 second expose-scan cycle is the factor which limits the number of possible pictures.) The adjacent column in the table lists the number of pictures which would be required at each altitude to obtain continuous earth coverage with no picture overlap. The second to last column lists the number of pictures which might reasonably be taken without getting into excessive picture overlap for the higher altitudes. In the last column, the product of earth coverage and the estimated number of pictures per orbit is listed. This factor determines the relative number of lines and hence grid marks visible in the pictures as a function of satellite height. The numbers indicate that the number of marks will be relatively constant for the 500 to 800 nm. altitude range.

Another important consideration for a run-length coding system is the spacing of the grid lines as a function of altitude. The numbers derived for the 800 nm. orbit represents distances for the highest grid line density. If we examine the grid for a 500 nm. orbit, we observe that the average distance between the meridians is in the order of 25% of the picture width. This still permits the six bit word length to be used for the meridian marks. With the decreased number of parallels in the picture, more of the mesh lines will not bear a mark, making the number of false marks needed to grid the picture somewhat larger. If the orbit inclination is on the order of  $45^{\circ}$ , the spacing can reach 33% of the picture side, in which case six bits is no longer sufficient. In light of the increased storage necessary for the 500 nm. orbit which virtually cancels any bit saving for run-length coding, it would appear that the use of the full eight bits necessary to specify the horizontal mesh element of each mark is justified to obtain a flexible system capable of handling the grid lines for any orbit.

Table 3-6

## Number of Pictures as a Function of Satellite Altitude

Satellite Altitude (nm.)	Earth * Angular Coverage (degrees)	Maximum Possible No. Pictures/Orbit	Number Pictures/Orbit No Overlap	Estimated Number Pictures/Orbit	Est. Number Pictures/Orbit	Earth Angular Coverage X
400	13.5	14.3	13.3	14	189	
500	19.2	14.9	10.5	15	288	
600	21.1	15.5	8.5	14	295	
700	25.1	16.1	7.2	12	301	
800	29.4	16.6	6.1	10	294	

\* Great circle arc through the picture principal point and bisecting the picture sides.

### 3.2.3 Mark Plotting through a Combination of Slope and Coordinate Specification

So far, we have treated each piece of mark data as almost completely independent of the previous piece. However to minimize the amount of data transmission to the satellite, we should try to send only that part of a mark coordinate specification which represents new information, and add some memory capability to the grid-drawing system so that critical parts of the data for past events can be retained. An implementation of this approach might consist in having the data for the marks on a new TV line consist only of the changes in the coordinates of the grid lines currently being mixed into the pictures. Consider the potential points at which a mark of a grid line can be placed relative to the last mark for the grid line. For a mark spacing of 16 picture elements (horizontal or vertical -- depending on the slope) and a mesh  $n = 4$ , the potential points at which a new mark can occur are shown in Figure 3-12a. The number of allowable new positions is 16. With a four-bit code we can then specify the next mark position for the grid line if we modify the last mark coordinates in accordance with the code. If we maintain mark position registers, one for each line in process, we can then specify the changes in the mark positions from a store of 32,000 bits (8,000 marks). However, in making our choice of the next coordinate for a grid line in this manner, we have not utilized any information about the line other than the coordinates of the last mark laid down. Grid lines are quite regular and predictable. We could then, divide the grid lines into two broad categories, as shown in Figure 3-12b, and rarely would we be required to change categories in the course of drawing out the grid line on the picture. Taking advantage of the regularity of the lines has thus reduced each new mark word to 3 bits (while retaining an additional bit for each line in a buffer memory). Carrying this technique to its ultimate, we divide the 16 potential new mark positions into 16 categories or sectors of  $10^\circ$  average (Fig. 3-12c) and end up requiring a single bit for each new mark position for a grid line, since only two potential mark positions are allowed for a given sector.

A sector actually defines a slope band. The grid lines must be broken into segments, where each segment is contained in one of the slope bands. Examine the drawing at the top of Figure 3-13, and consider a line segment whose slope starts at  $0^\circ$  and ends at  $14^\circ$ . This segment will be plotted by a sequence of marks occupying position 1 (Fig. 3-13) relative to the preceding mark where the slope of the segment is zero. As the slope increases, the new mark position will oscillate between points 1 and 2, and when the segment slope approaches  $14^\circ$  the new mark positions

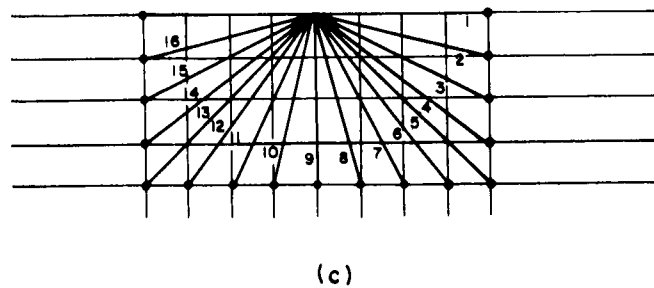
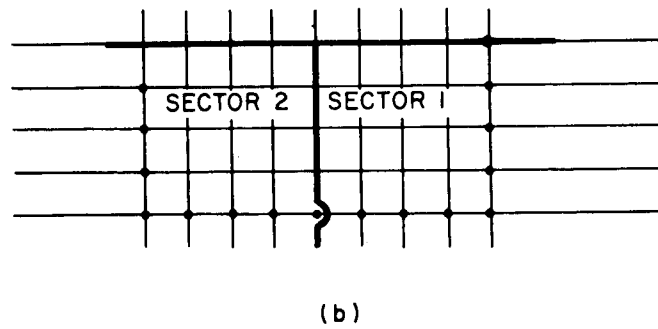
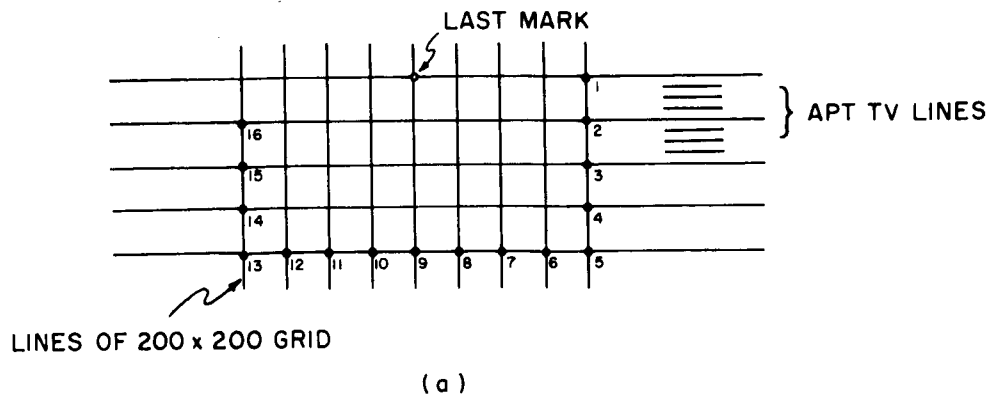
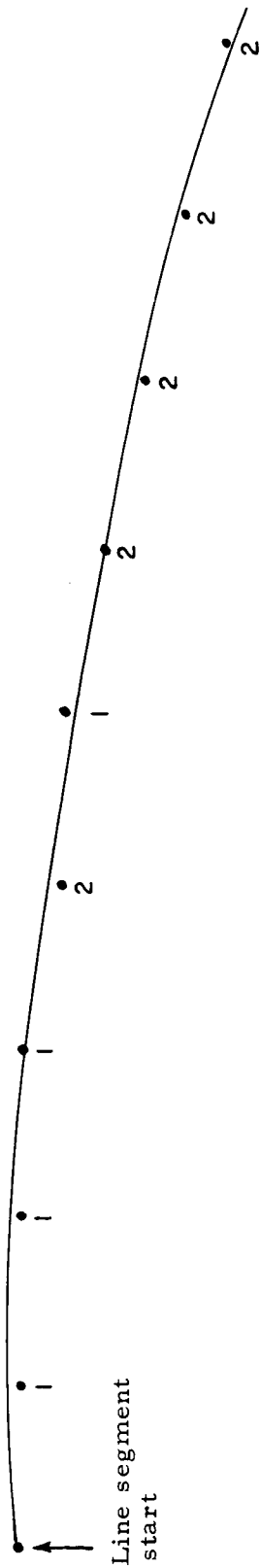


Fig. 3-12 Potential Locations of New Marks



- A. Plot initial mark when vidicon beam position equals segment starting coordinates  $X_o Y_o$ .
- B. From sector code and 1 bit mark word determine next mark position relative to first.
- C. When vidicon beam position reaches coordinates of second mark, make the mark and determine coordinates of third mark from sector code and 1 bit mark word, etc.

#### REQUIRED DATA

$Y_o$	$X_o$	Sector Code	9 Single bit mark words
-------	-------	-------------	-------------------------

8 bits    8 bits    4 bits    9 bits     $\longrightarrow$  TOTAL = 29 bits for 10 marks

Figure 3-13. Line Marking From Combined Slope - Coordinate Specification

will occur to be at point 2 relative to each preceding mark. The basic logic and the data required for this method of marking is listed in Figure 3-13. We can see that 10 marks can be plotted with a data requirement averaging 3 bits per mark.

To ascertain the practicality of this approach, the number of sector changes experienced in drawing grid lines was approximately determined for the 800 nm. orbit. For the recommended basic  $5^{\circ}$  grid interval, the number of sector changes is in the vicinity of 300. Since this figure does not appear to impose any serious limitation, we shall pursue the total storage requirement for this technique.

Note that Figure 3-12c includes point 17, even though this position cannot be marked unless computed prior to the vidicon's sweep circuits arriving at the previous mark position. A four bit sector code can be used for the marks on a line segment, in combination with the individual mark words, until the slope of the line changes enough to move the line marks into a new sector. We then have the lines divided into segments, as in the straight line system, but the line segments are not required to be straight. The initial coordinates of each segment must be specified along with the sector code. The sector code is 4 bits long and a fifth (erase) bit is needed to terminate lines in mid-picture. This yields a total of 21 bits to start or end (mid-picture) a line segment.

For an 800 nm. - 10 picture orbit, approximately 250 line starts, 54 terminations, and 278 sector changes occur for a bit total of 12,306. Adding to this the 8,000 bits for the 1 bit mark words, the total memory requirement for the grid lines is approximately 21,300 bits. The total storage requirements of the slope-coordinate method (including annotation discussed in a later section) is shown in Table 3-7.

Since the CM-2 approach appears to offer a much lower storage requirement than the previously described coordinate methods, (CM-1A and CM-1R) while producing better looking lines with simpler logic when compared to the straight-line method, several design approaches were investigated and appear in Section 3.2.4.3.

A drawback to the slope-coordinate method is the requirement for dissimilar word lengths (1 bit mark words and 21 bit segment words). This requirement will increase susceptibility to error as will be seen in a following section.

### 3.2.4 Coordinate System Designs

The various considerations of memories needed for main and buffer storage in the coordinate and straight line approaches are treated in detail in Appendix C. Appendix C contains weight and power estimates for memory units which can be used for the systems described below.



Table 3-7

CM-II Storage Requirements

K=16

Grid line starts	250	
Grid line terminations (picture interior)	54	
Sector changes	278	
Additional line starts to resync		
4 zone picture	270	
North arrow starts (15 pictures)	30	
North arrow terminations	<u>30</u>	
Total sector words		912 x 21 bits word = 19,152 bits
Grid marks	8000	
North arrow marks	200	
Annotation marks	<u>2100</u>	
Total mark words		10,300 x 1 bit word = <u>10,300</u> bits
Total storage		29,452 bits

K=8

Total sector words		912 x 23 bits word = 20,976
Grid marks	16,000	
North arrow marks	400	
Annotation marks	<u>2,100</u>	
Total mark words		18,500 x 1 bit word = <u>18,500</u>
Total storage		39,476

The preliminary designs presented here were done to provide a firm basis for the hardware estimates needed in comparing the various approaches.

#### 3.2.4.1 Full X-Address System CM-1A

For coordinate methods CM-1A and CM-1R (run-length system), the bit storage is approximately 80,000. (Approximately 10,000 bits are needed for the annotation which will be described in a later section.)

A general logical diagram of method CM-1A is shown in Figure 3-14 . The principal logical elements are:

a. S-Stage Shift Register "SR" - This register holds the mark address word from memory for comparison with the mesh interval address of the vidicon beam.

b. Counter "B" - This counter has a maximum value of 192 and keeps track of the position of the beam along a mesh sweep.

(Note: The case considered in Figure 3-14 is for  $n = 4$  in which a  $200 \times 200$  mesh is utilized.)

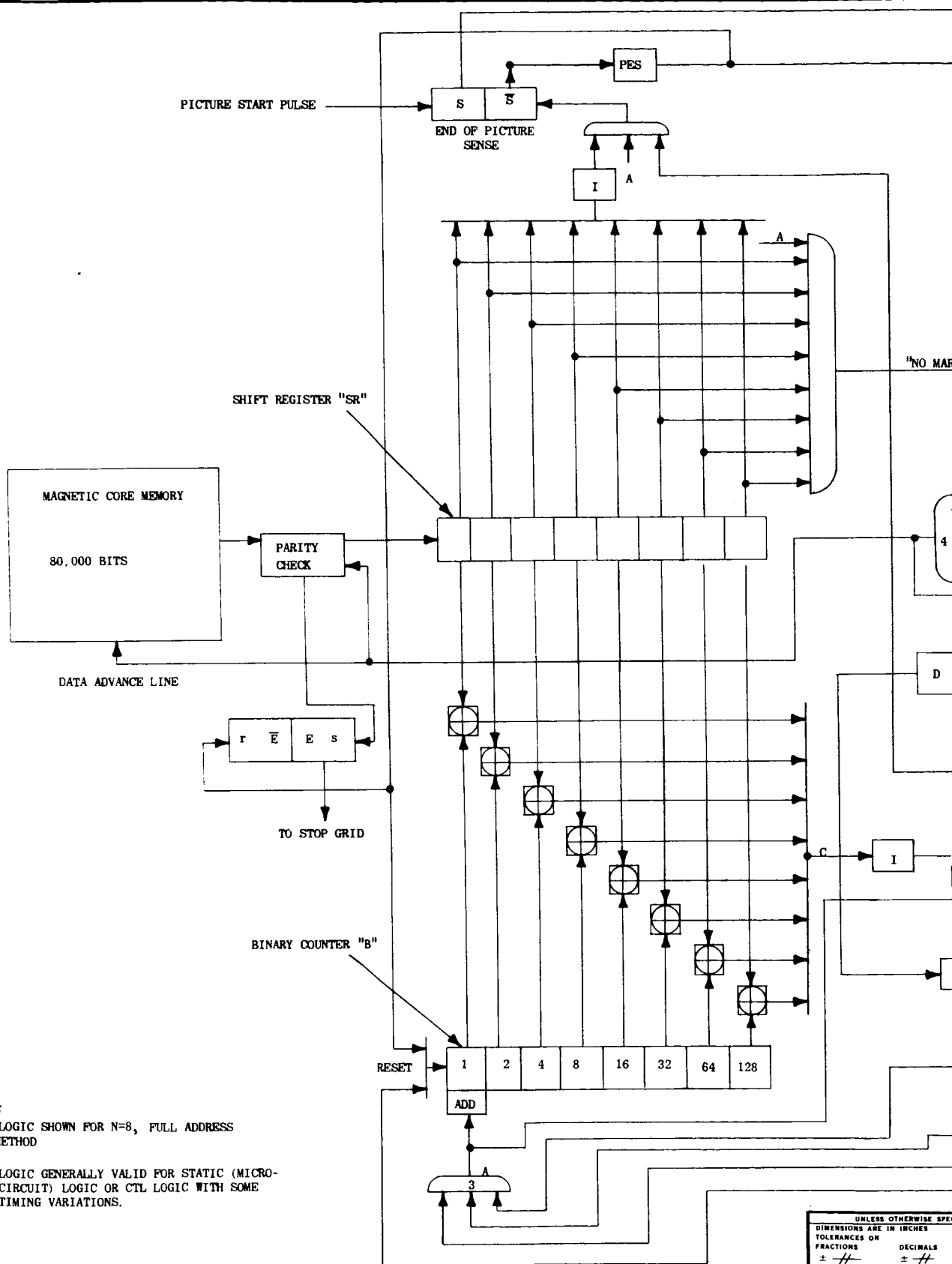
c. APT Timing Circuits - The binary divider chain and the horizontal deflection circuits in the APT subsystem provide the basic gating pulses to generate the required mesh. The mesh intervals are obtained by dividing the 2400 cps camera pluses down to 800 cps.

d. Parity Check Circuitry - The case considered in Figure 3-14 assumes that a parity bit has been stored in the memory. If a parity error occurs, the flip-flop E prevents any further marks from being sent to the video mixer.

(Note: Parity bits are not included in the memory estimate.)

e. EXCLUSIVE or Circuitry - For the implementation of Figure 3-14 , parallel comparison of the address is made in S solid state half adders. (Serial comparison can also be done here; the net system differences will be small.) The basic logical sequence for this implementation is as follows:

A word is advanced into "SR". If that word has proper parity, then it is compared to the current state of counter "B". Counter "B" is incremented once for each mesh interval.



NOTES:

1. LOGIC SHOWN FOR N=8, FULL ADDRESS METHOD
2. LOGIC GENERALLY VALID FOR STATIC (MICRO-CIRCUIT) LOGIC OR CTL LOGIC WITH SOME TIMING VARIATIONS.

UNLESS OTHERWISE SPECIFIED  
DIMENSIONS ARE IN INCHES  
TOLERANCES ON  
FRACTIONS DECIMALS  
± .01 ± .005

MATERIAL

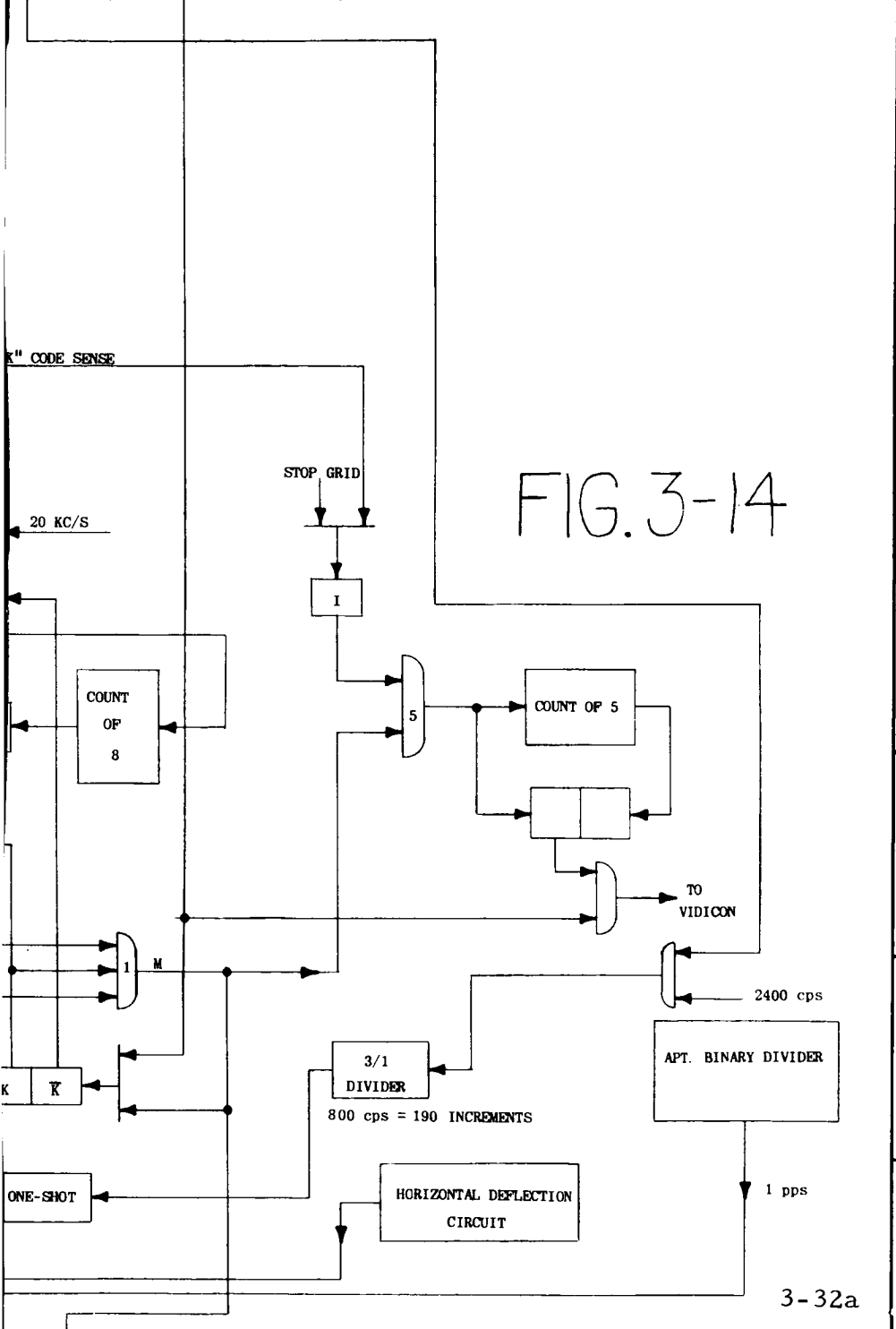
FINISH

NEXT ASSY	USED ON	NEXT ASSY	FIN ASSY
APPLICATION		QTY REQ'D	

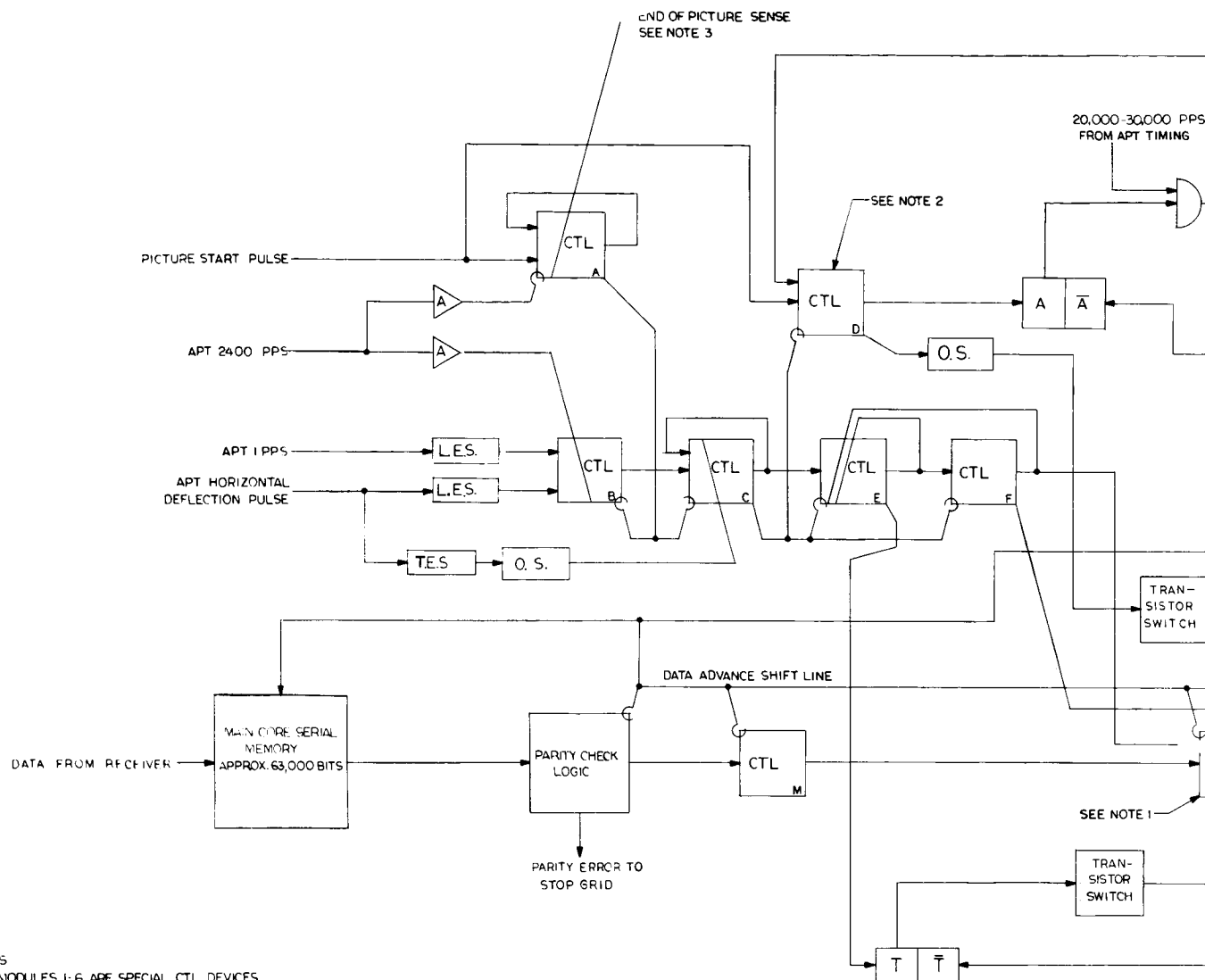
PROJECT E1550

2

DWG. NO		REVISIONS			
2177-4001		ZONE	SYM	DESCRIPTION	DATE
		GEN	A	REVISED PER ECO 21067	12-1-64
					APPROVAL

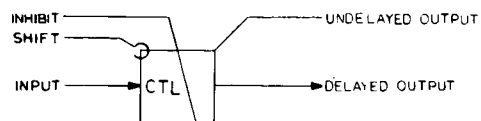


ITEM	REQD	PART NO.	DESCRIPTION	MATL	MATL SPEC
LIST OF MATERIALS					
<div style="display: flex; justify-content: space-between;"> <div> <p>APR 29 OCT 64</p> <p>CHECKED <i>S. C. [Signature]</i> 30 OCT 64</p> <p>PROJECT ENG. APPD. <i>N. S.</i> 11/30/64</p> <p>PRODUCT ENG. APPD.</p> <p>SUPERSEDES</p> <p>REFERENCE</p> </div> <div> <p>APT GRIDDING LOGIC METHOD CM-1A</p> <p>FIGURE 3-14</p> </div> <div> <p><b>di/an</b></p> <p><b>Di/An Controls, Inc.</b></p> <p>BOSTON, MASS</p> </div> </div>					
SIZE	DWG. NO.	REV			
C	2177-4001	A			
CODE	06900	SHEET	1	OF	1



#### NOTES

1. MODULES 1-6 ARE SPECIAL CTL DEVICES.
2. MODULES LABELED CTL ARE STANDARD DI/AN PKO BIT DEVICES, CONNECTED AS SHOWN BELOW.
3. LOGIC FOR SENSING END OF PICTURE CODE AND 64 COUNT CODE NOT SHOWN.



DWG NO  
2177-4002

## REVISIONS

## DISCUSSION

## DISCUSSION

100

• **RESEARCH**

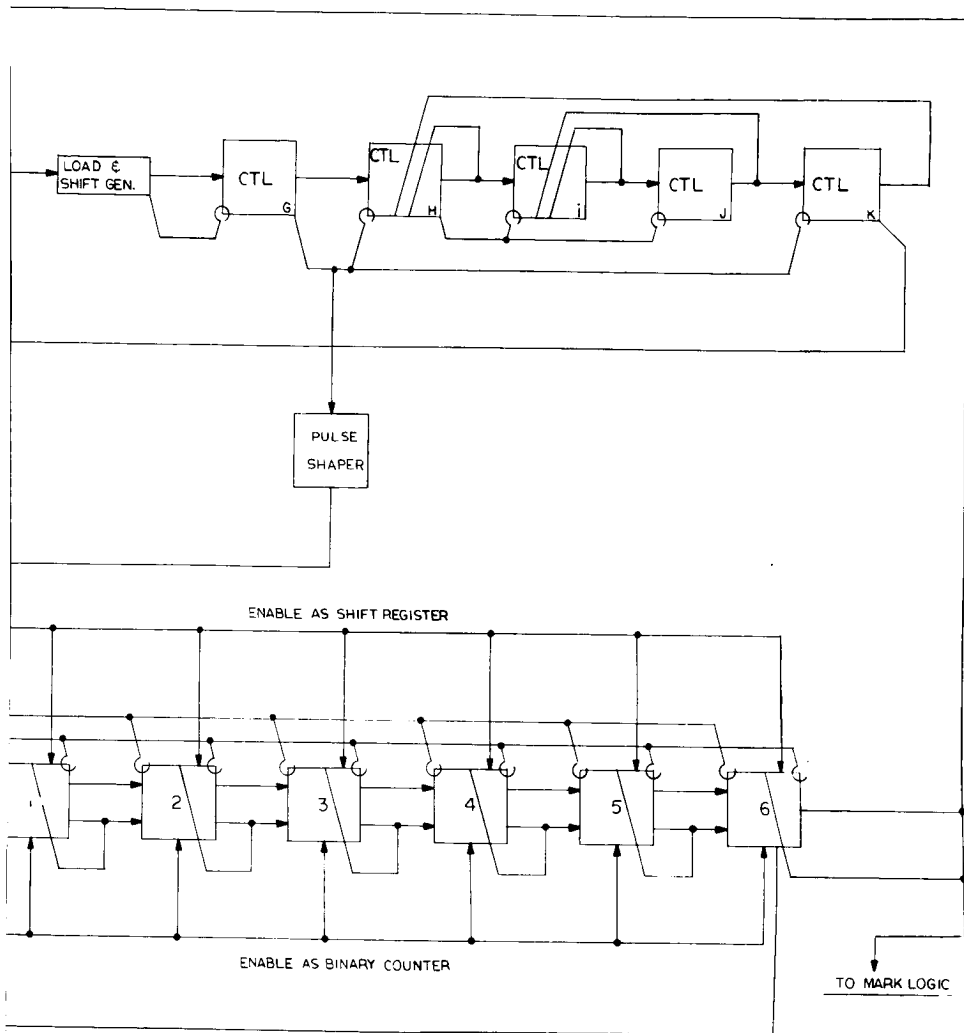



FIG. 3-15

UNLESS OTHERWISE SPECIFIED			ITEM		REQD	PART NO	DESCRIPTION		MATL	SPEC
DIMENSIONS ARE IN INCHES TOLERANCES ON FRACTIONS			DRAWING		DATE		LIST OF MATERIALS			
DECIMALS			CHECKED		DATE		METHOD CM-1R			
ANGLES			PROJECT		DATE		TYPICAL			
MATERIAL			FINISH		DATE		MAGNETIC LOGIC		 <b>Dillan Controls, Inc.</b> BOSTON, MASS.	
FINISH			APPENDICES		DATE		IMPLEMENTATION		SIZE D    DWG NO USED ON    HEAT ASSY    FIN ASSY    PROJECT E 1550	
REFERENCE			SCALE		WEIGHT		FIGURE 3-15		ID    2177-4002    REV CODE    SHEET    OF	

When  $B = SR$ , a mark pulse is sent through Gate 1 to the mark generation logic (unless a "no mark" code has been sensed). At the same time, nine 20kc/s pulses from the APT divider advance a new word from memory into SR. This is done in less than one mesh interval. The comparison circuitry is reactivated by flip-flop K.

#### 3.2.4.2 Run-length System CM-1R

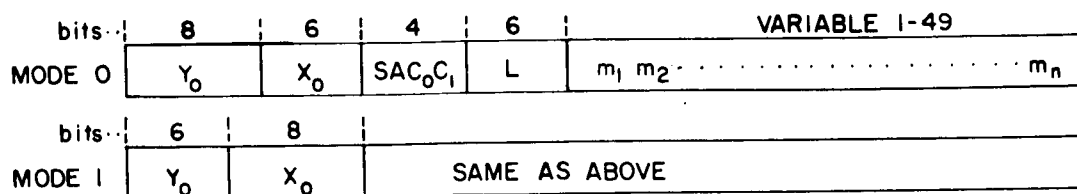
Method CM-1R utilizes a run-length code. A schematic diagram of this method implemented in CTL logic is shown in Figure 3-15. The principles of this scheme differ from CM-1A in that the 6-bit word consists of the mesh interval separations between two successive marks, rather than 8-bit mark addresses.

Implementation of this scheme is particularly simple with a modified CTL device which can be enabled as a shift register or as a binary counter. (The same function can also be performed by a shift register loop counter.) The 6-bit word stored in memory is  $M = 64 - D$  where  $D$  is the number of mesh intervals between two successive marks. The number  $M$  is first preset into a 6-stage binary counter. After  $D$  counts, the counter supplies an overflow bit which represents the occurrence of a mark at the proper mesh interval location.

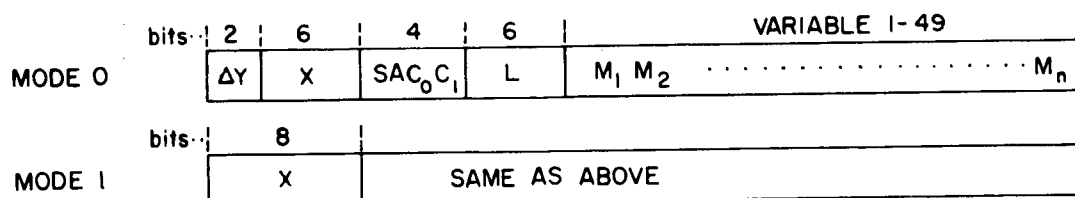
The logic in Figure 3-15 (CM-1R) shows the same functions as Figure 3-14 (CM-1A) but in this case, the functions have been mechanized.

#### 3.2.4.3 Combined Slope-Coordinate System CM-2

Three different design approaches were considered for the CM-2 method. The first, labeled CM-2H requires a higher logic speed and is very similar to SL-2. Each line segment sector code and its mark bits are combined to form a single word. See Figure 3-16. This has the advantage that all line segments are completely specified by fixed length words for transmission to the satellite. Since the number of mark words varies from segment to segment, ZEROES must be added to the Mark bits to bring the total number of bits to 73 for each segment. (A maximum of 50 marks is made on any single line segment.) Each line segment word contains the line segment length  $L$ , which eliminates the necessity to transmit line segment termination words to the satellite. Since 73 bits will be transmitted for each line segment, the total transmission for the 250 line starts and 278 sector changes is 38,500 bits.



MAIN STORE



BUFFER

$SAC_0C_1$  - SECTOR CODE

L - NUMBER OF MARKS

$m_1 m_2 \dots$  - MARK WORDS (1 BIT)

$X_0 Y_0$  - INITIAL POSITION COORDINATES

$\Delta Y$  - NUMBER OF LINES BEFORE NEXT MARK

X - HORIZONTAL COORDINATE OF NEXT MARK

NOTE :

The mode is determined by bit A of the 4-bit sector code.

Fig. 3-16 Word Composition CM II H



After receipt of the data in the satellite, the "empty" mark bit spaces in each word could be eliminated before storage, since the line length  $L$  indicates the number of mark words or bit spaces for each word. This drops the main storage requirement back to approximately 20,000 bits.

The grid mark calculation logic is very similar to SL-2. (Note a mode bit is included.) The primary difference is that the addition made to  $X$  or  $Y$  after a mark is made is not a constant slope, but a value determined by the sector code and mark bit. As each mark bit is used, the whole string of mark bits would be shifted one place to keep the bits used in each calculation in the same relative positions for each word. Since the mechanization is so similar to SL-2, no further design work was done on this approach. The principle advantage of the SL-2 type of logic used for a CM-2 system is the retention of constant word length for data transmission (hence reduced susceptibility to error). A disadvantage is the higher level of complexity associated with the SL-2 type of logic.

The two other designs considered for CM-2 operate at low clock speeds and bear the label CM-2L. A general block diagram appears in Figure 3-17. Both systems use a buffer register to hold the sector data for each of the line segments in process at one time. The buffer is a bit-sequential core memory. A word space for a sector code is available for each of the horizontal mark intervals (200 storage locations for  $n = 4$ ). The calculation logic and the buffer memory form a loop. The contents of each word location are read, word and bit-sequential, to the logic in synchronism with the  $X$  advance of the vidicon beam, and then read back to the buffer. A sector code is stored in the buffer in the word location which corresponds to the  $X$  position of the next mark to be made on the segment specified by the sector code. Most of the word locations will be empty since usually only 16 segments intersect a single sweep. The word location holding the sector code must also have space for  $\Delta Y$ , the number of mesh sweeps between marks. The basic operation performed by the calculation logic is a moving of the segment data from one word location to another, to maintain the proper  $X$  coordinates of the marks, and a determination of the  $\Delta Y$ , (number of mesh sweeps) before the next mark. Each time a mark is made, the calculation logic pulls a mark word from the main storage, and uses it in combination with the sector code to determine the new memory position and  $\Delta Y$  for the segment data for plotting of the next mark on the segment. Thus the mark words must be ordered in the sequence in which they will be required by the logic.

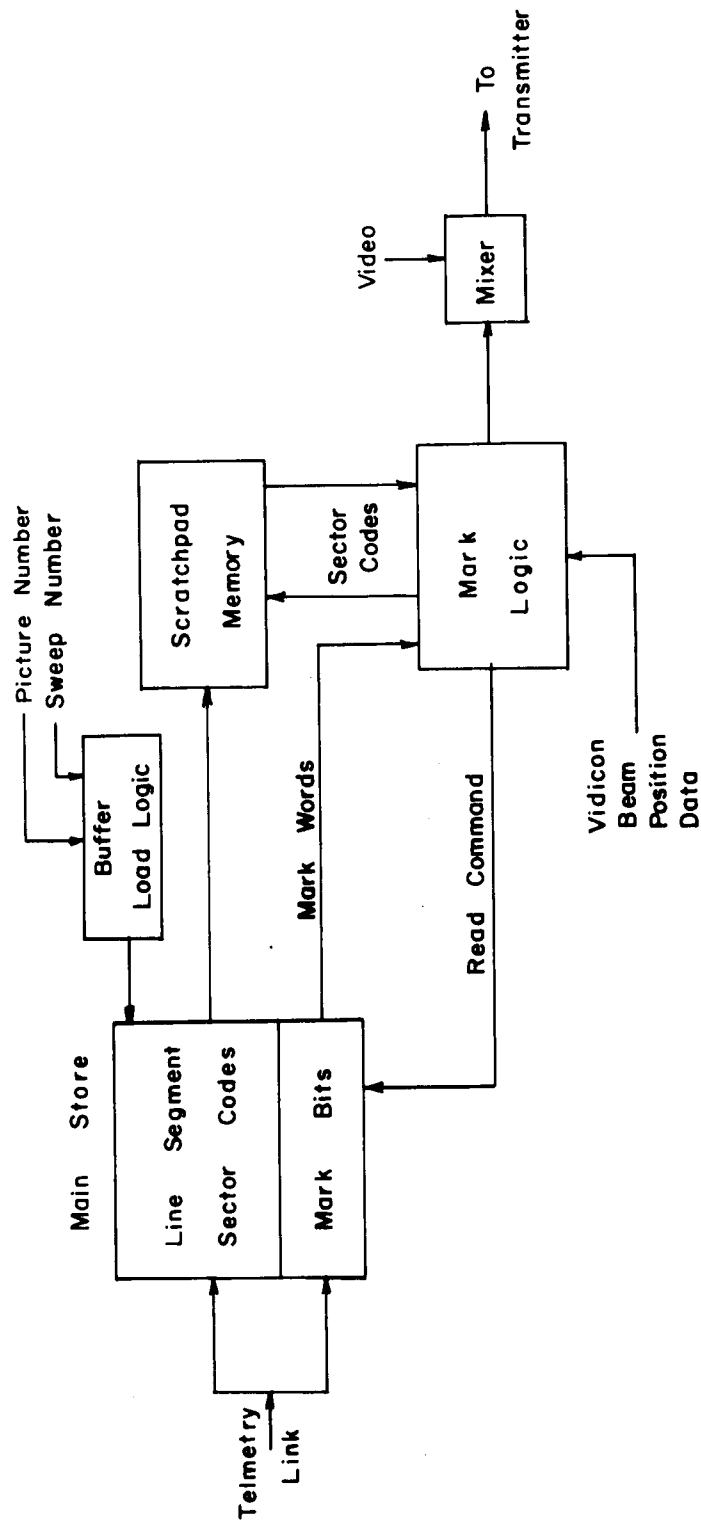


Fig.3-17 General Block Diagram - CM II Method

The most efficient storage of the 21 bit segment words and the 1 bit mark words is obtained if they are mixed, bit serial, in the order in which they should be fed to the buffer and calculation logic. The method in which the 1 and 21 bit words are separated (to be described in the following sections) is slightly different for the two approaches.

#### CM-2L<sub>A</sub>

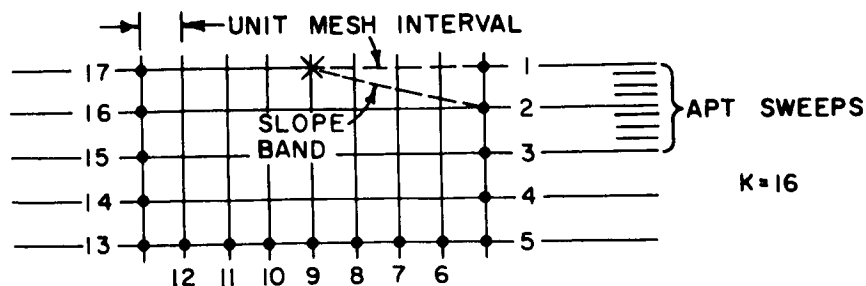
The composition of the sector codes is shown in Figure 3-18. The first bit of the code (S) indicates the sign of the slopeband. Lines which run (top to bottom) in the same direction as the APT sweep are considered positive. The second bit (A) defines the axis on which the two possible mark locations exist for a given sector, and is equivalent to the mode specification described in the straight line section. It will be convenient to retain the mode concept in describing this system. The constant (C) portion of the sector code is composed of two bits ( $C_0, C_1$ ) for  $K = 16$ . C specifies the number which is added to the value of the mark word to determine the mark location. For example, suppose the line segment lies in the  $26.5^\circ - 37^\circ$  slope band. In this band each new mark may be at position 3 or 4 (Fig. 3-18) relative to the old mark. For this sector, the change in X position is constant at 4 mesh intervals. The  $\Delta Y$  is either 1 or 2 mesh lines.  $\Delta Y$  is determined by adding the value of the mark bit to C. The position change of +4 for the sector data in the serial buffer is obtained by a delay of 4 mesh interval times in reading the data back to the buffer from the calculation logic.

For all positive sloping lines, position changes are obtained by the delayed readback. For mode 1 lines, the delay interval may be 0-4 mesh interval times, as determined by the sector code and mark word. The  $\Delta Y$  for mode 1 lines is always a fixed interval of 4 mesh lines.

There are a total of 4 APT sweeps for each of the griddable mesh lines. The CM-2L<sub>A</sub> system uses each of the sweeps for marking as follows:

- Sweep 1 - mode 0 lines of positive slope
- Sweep 2 - mode 0 lines of negative slope
- Sweep 3 - mode 1 lines of positive slope
- Sweep 4 - mode 1 lines of negative slope

For any individual sweep, the word location read from the buffer corresponds to the X position of the vidicon beam. The contents of the buffer are shown in Figure 3-19, as it appears at the beginning of a mesh line if the buffer is visualized as a shift register for purposes of illustration. For each mode 0 sweep, 50 locations



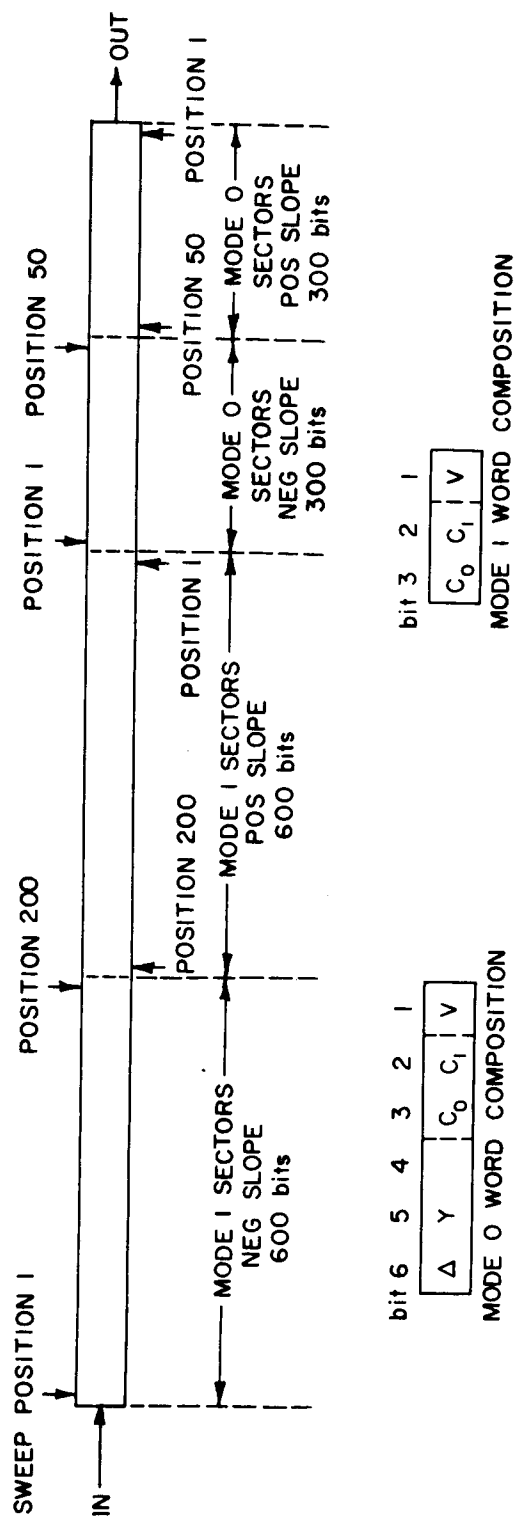
LOCATIONS 1 THROUGH 17 ARE POSSIBLE LOCATIONS OF THE NEXT MARK FOLLOWING X.

NEXT MARK	(SECTOR) SLOPE BAND	SIGN (S)	AXIS OF VARIABLE * COORDINATE (A)	CONSTANT (C)	INTERVAL ALONG FIXED AXIS
1 OR 2	0-14°	+	Y	0	$\Delta X = +4$
2 OR 3	14-26.5	+	Y	1	"
3 OR 4	26.5-37	+	Y	2	"
4 OR 5	37-45	+	Y	3	"
5 OR 6	45-53	+	X	3	$\Delta Y = +4$
6 OR 7	53-63.5	+	X	2	"
7 OR 8	63.5-76	+	X	1	"
8 OR 9	76-90	+	X	0	"
9 OR 10	90-104	-	X	0	"
10 OR 11	104-116.5	-	X	1	"
11 OR 12	116.5-127	-	X	2	"
12 OR 13	127-135	-	X	3	"
13 OR 14	135-143	-	Y	3	$\Delta X = -4$
14 OR 15	143-153.5	-	Y	2	"
15 OR 16	153.5-166.5	-	Y	1	"
16 OR 17	166.5-180	-	Y	0	"

\* EQUIVALENT TO MODE

CODE

Fig. 3-18 Sector Codes K = 16



V - VALIDITY

C<sub>0</sub>, C<sub>1</sub> - CONSTANT PORTION OF SECTOR WORD (SAC)

Fig. 3-19 Contents of Buffer Memory at Start of Sweep CM II L<sub>A</sub>

are available in the buffer since mode 0 lines are plotted at 50 mesh intervals. ( Mode 0 lines are plotted at intersections of a mesh with 200 horizontal and 50 vertical lines.) Each mode 0 word location can hold six bits, sector, validity, and  $\Delta Y$ .

The order of the corresponding sweep positions for buffer locations holding mode 0 segments of negative slope is reversed in the buffer. As a result, the word location corresponding to position 50 is read to the calculation logic when the vidicon is at position 1 on sweep 2. This enables negative sloping line segments to change position in the negative X direction through use of the same delay technique employed for lines of positive slope. The only limitation is that marks cannot be made during sweep 2 and 4 at the time the calculation logic generates a mark command. Mark decisions for negative sloping lines are stored as described below.

Mode 1 line segment word locations in the buffer are only three bits long since no  $\Delta Y$  is required. Mode 1 lines are plotted at intersections of a mesh of 50 horizontal and 200 vertical lines. Consequently mode 1 lines need be operated on by the calculation logic every 4 horizontal mesh lines (16 sweeps). Every 16<sup>th</sup> sweep, marks are made for each of the mode 1 segments. The division of the line segments by mode and slope completely eliminates the possibility of the calculation logic attempting to write two segment words into the same word space in the buffer since 2 grid lines whose slope difference is  $45^\circ$  cannot intersect. (Each of the 4 divisions represents a  $45^\circ$  slope band.) Note that the division also permits the S and A bits of the sector code to be dropped. These bits actually determine on which of the 4 sweeps associated with a mesh line the buffer is loaded. The full 10-bit Y value of the segment start determines the sweep (and hence the sign and mode) during which the buffer should be loaded and the X value of the segment start determines the load time along the sweep. (Data actually enters the buffer through the calculation logic as will be seen below.) The timing diagram shown in Figure 3-20 shows some of the required clock signals. Figure 3-21 shows the main storage-logic interface and the arrangement of segment and mark words in the main memory. The  $Y_0$ ,  $X_0$  values for the initial line segment of a picture (the first 18 bits after picture sync) are loaded into a register and compared with the X, Y vidicon beam position counters. When equality is obtained, the 2 bits of the sector code ( $C_0$ ,  $C_1$ ) are read into the calculation logic for subsequent buffer loading. The next data which appears in the memory is the  $Y_0 X_0$  for the next line segment which will be started regardless of its starting position in the picture. These data are advanced into the 18 bit register immediately following the withdrawal of the sector code of the first line segment. The next bit in

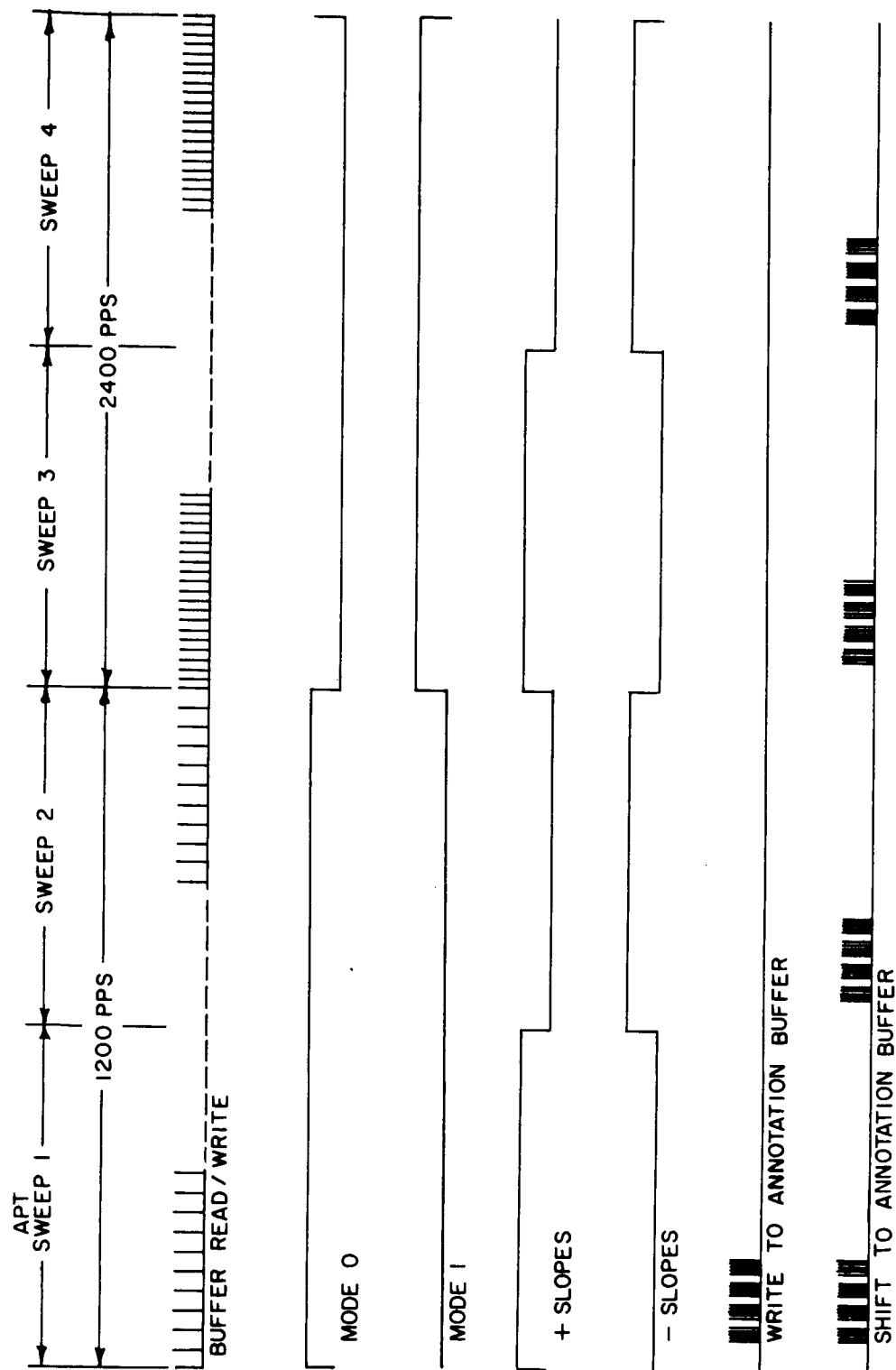


Fig. 3-20 Timing Diagram CM II L<sub>A</sub>

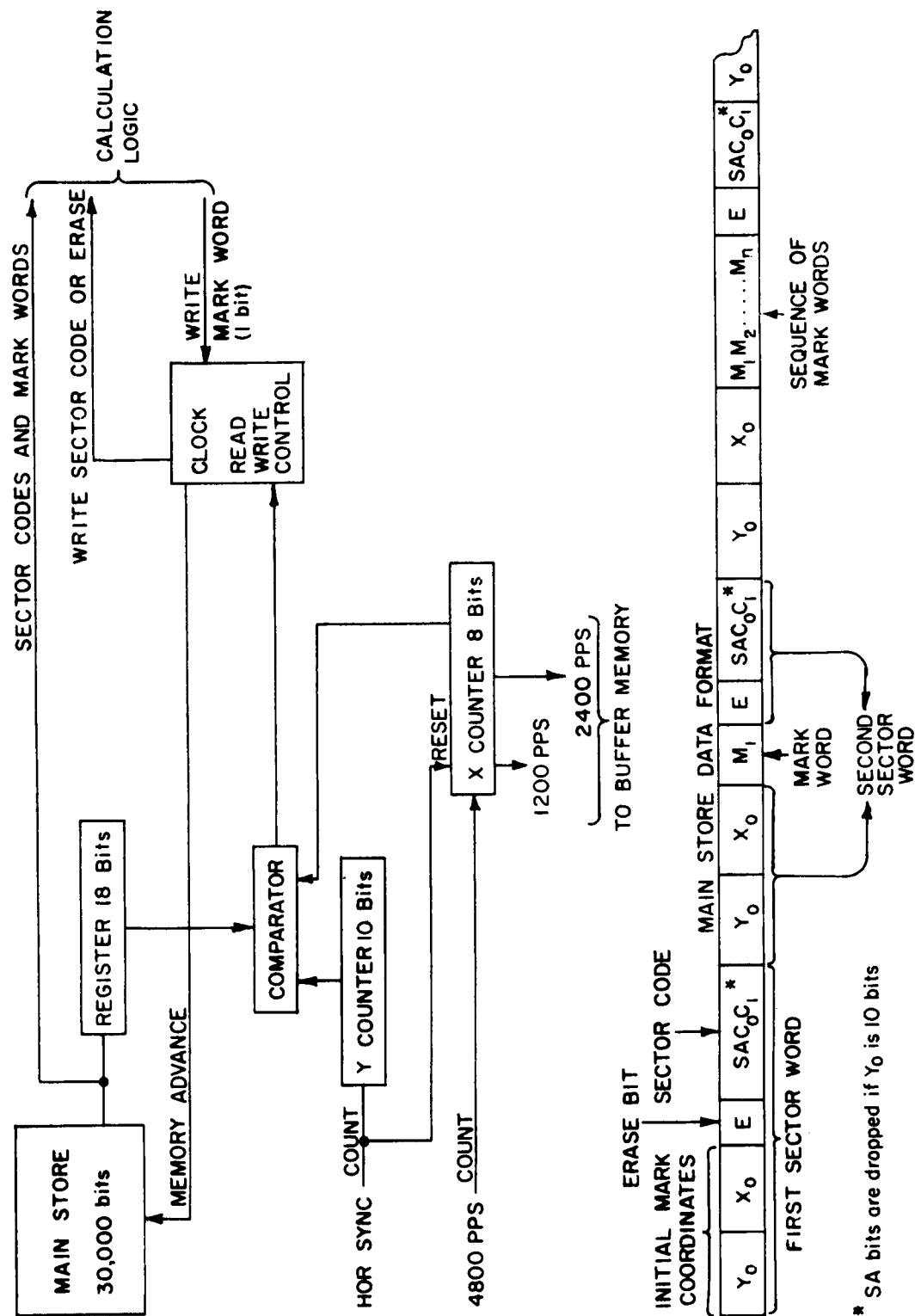


Fig. 3-21 Main Storage-Logic Interface CM II LA



memory will be a mark word associated with the first line segment. If a second line segment is to be started before the second mark of the first line is made, its sector code will come next in memory and will be withdrawn when its  $X_0 Y_0$  values, previously stored in the 18 bit register, are equal to the values in the beam position counters. The extension of this sequence is obvious. Sector codes are interlaced with the mark words in the sequence required by the calculation logic to plot the desired grid lines.

The calculation logic and buffer storage are shown in Figure 3-22. First consider the sequence of events for mode 0 words. The contents of the six bit word corresponding to a beam position are read from the core buffer (or main memory) into the A and B registers. If the word contains segment data, a clock pulse is passed by AND gate 13 to the input of AND gates 4 and 12. The output of 12 causes the  $\Delta Y$  to be decremented by one. The output of 13 will pass through 4 and generate a mark command if  $\Delta Y$  (B register) = 0. If the slope is positive, the mark command passes through gate 20 to the mark generator. If the slope is negative, the mark command is stored in a 200 bit storage register, which is read out in the reverse order to storage on the next sweep.

When the word is first read into the A and B registers, the  $C_0 C_1$  of the word is added to the next available mark word and stored in C. The output of 4 (mark command) causes the sum of  $C_0 C_1$  and the mark word to be read into the B register to form the new  $\Delta Y$ , and the word is clocked through gate 17 and a four word interval delay back to the memory. A new mark word is read from the main store only when a mark command is generated.

For mode 1 lines, gates 2 and 3 cause the B register to be bypassed and the three bit mode 1 words are read to A. Simultaneous with the loading of register A, the sum of  $C_0 C_1$  and the mark word are loaded in the C register. (Calculation is enabled for mode 1 lines every  $K^{\text{th}}$  sweep.) If presence of data is established (validity bit = ONE), the output of gate 13 sets FF1 which inhibits the clock pulses which will return the word in the A register to the buffer. The C register contains the number of word delays for the segment data in A to obtain the proper X-coordinate for the new mark. This value is decremented by one from the word clock. When it goes to zero, a pulse is delivered to the reset input of FF1, allowing the data to be returned to the buffer.

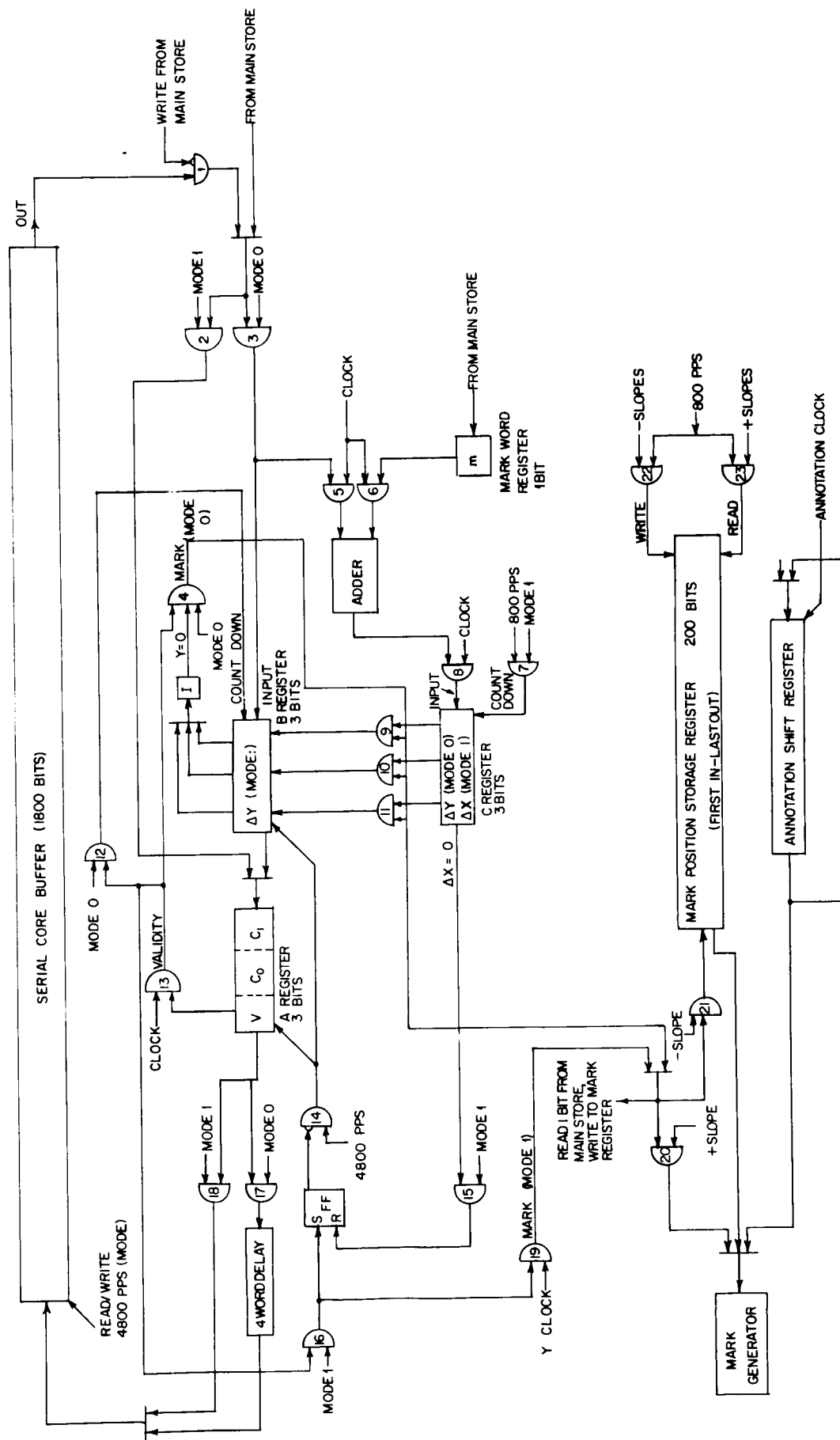


FIG. 3-22 GRID AND ANNOTATION CALCULATION LOGIC—CMII L A

### CM-2L<sub>B</sub>

The design of CM-2L<sub>B</sub> uses a buffer memory which does not separate the segment data by sign and mode. Two hundred separate word positions exist in the memory, one position for each mesh interval on a sweep.

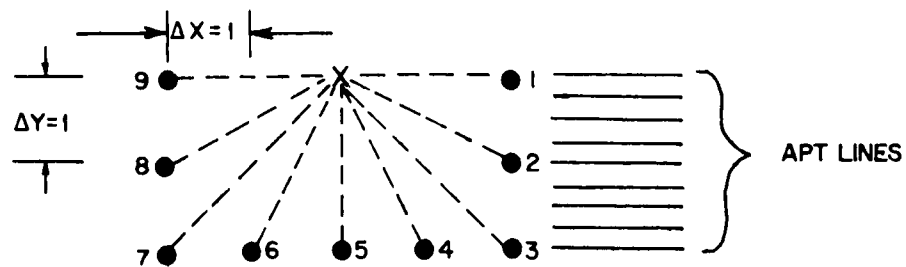
The design was accomplished for a mark spacing,  $K = 8$ . The sector codes are shown in Figure 3-23.

A four cycle operation is accomplished for each horizontal mesh line as follows:

- Sweep 1 - Load new sector data from buffer, decrement  $\Delta Y$ , mark.
- Sweep 2 - Compute next mark position for each line segment of positive slope. This is done by combining a mark word with the sector code to compute the new memory position (X coordinate) and  $\Delta Y$ .
- Sweep 3 - No grid mark operations
- Sweep 4 - Compute next mark positions for line segments of negative slope. During this cycle, the data from the buffer is read out in a sequence opposite to that of sweep 2.

Figure 3-24 shows the main memory-logic interface. The calculation logic is shown in Figures 3-25 and 3-26. Each buffer word consists of the three bit code which identifies the sector, and a three bit code which will be used to: 1) indicate the number of mesh lines between successive marks of a line segment, 2) provide validity information for the memory location. The latter function is necessary since all eight of the three bit sector codes are valid. The validity of the information in a buffer memory location is established by adding one to the Y value between successive marks. An empty buffer location is then determined by a zero-test on the three bit Y portion of the segment data. Each segment is specified by a six bit code in the buffer, for a buffer capacity of 1,200 bits.

The computation of the new X, Y values for a mark consists of a decoding of the three bit sector code and the mark bit, an encoding of the new  $\Delta Y$ , and the determination of the delay for reading back to the buffer. The accompanying drawings illustrate the operation of the system with parallel logic, although the operation can almost certainly be performed with more economy of circuitry if serial logic is employed.

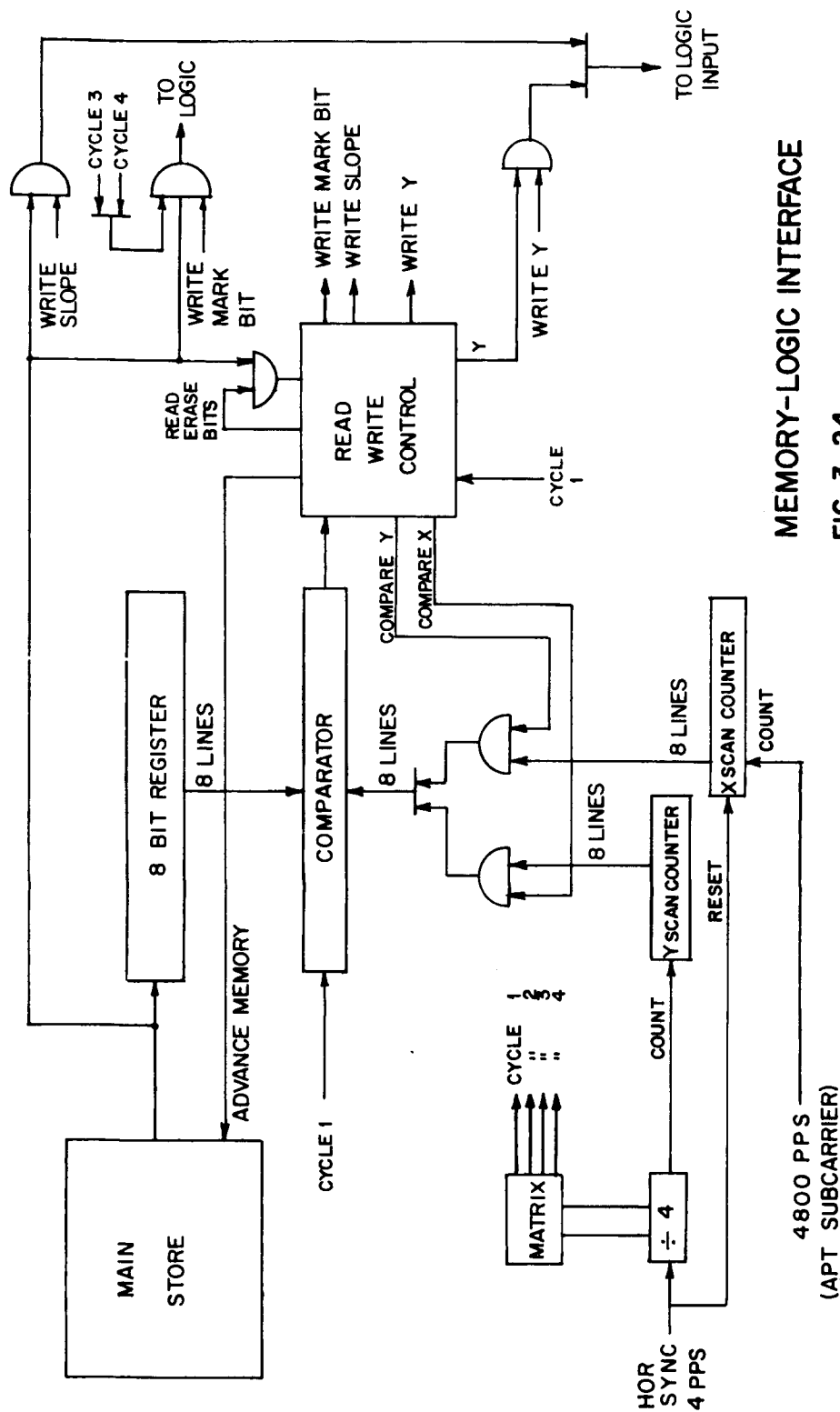


Locations 1 through 9 are possible locations of next mark relative to X .

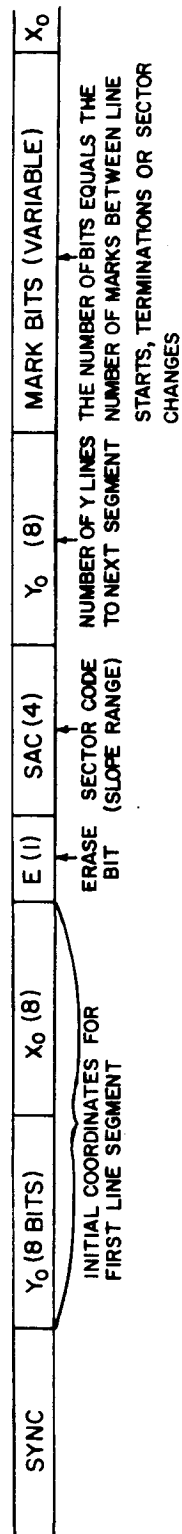
$\theta$	Next Mark	Sign (S)	Axis (A)	Constant (C)	Fixed Condition
$26.5^\circ$	1 or 2	+ (1)	Y (1)	0 (0)	$\Delta X = + 2$
$18.5^\circ$	2 or 3	+ (1)	Y (1)	1 (1)	$\Delta X = + 2$
$18.5^\circ$	3 or 4	+ (1)	X (0)	1 (1)	$\Delta Y = + 2$
$26.5^\circ$	4 or 5	+ (1)	X (0)	0 (0)	$\Delta Y = + 2$
$26.5^\circ$	5 or 6	- (0)	X (0)	0 (0)	$\Delta Y = + 2$
$26.5^\circ$	6 or 7	- (0)	X (0)	1 (1)	$\Delta Y = + 2$
$18.5^\circ$	7 or 8	- (0)	Y (1)	1 (1)	$\Delta X = - 2$
$18.5^\circ$	8 or 9	- (0)	Y (1)	0 (0)	$\Delta X = - 2$
Sector Code		( )	( )	( )	

Figure 3-23

Sector Codes K = 8



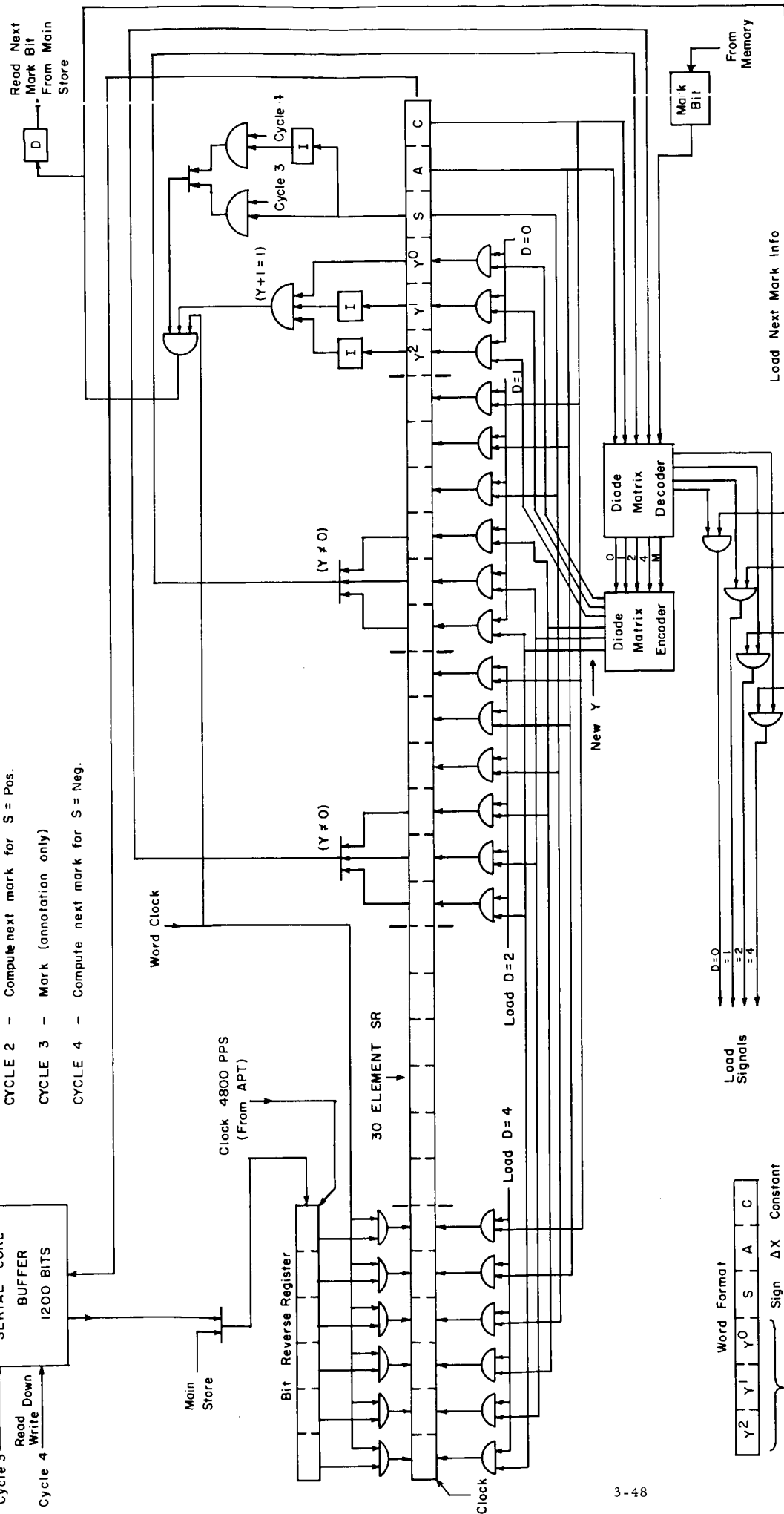
MEMORY DATA FORMAT



X CLOCK

- CYCLE 1 - Load, decrement Y, mark  
 CYCLE 2 - Compute next mark for S = Pos.  
 CYCLE 3 - Mark (annotation only)  
 CYCLE 4 - Compute next mark for S = Neg.

FIG. 3-25 CM-II L<sub>B</sub> LOGIC FOR CYCLES 3 AND 4  
 (COMPUTE NEW MARK)



Word Format

Y <sub>2</sub>	Y <sub>1</sub>	Y <sub>0</sub>	S	A	C
----------------	----------------	----------------	---	---	---

Where Y = number Slope of lines/4 to next mark

Sign ΔX or 0 or 1  
 Constant ΔY

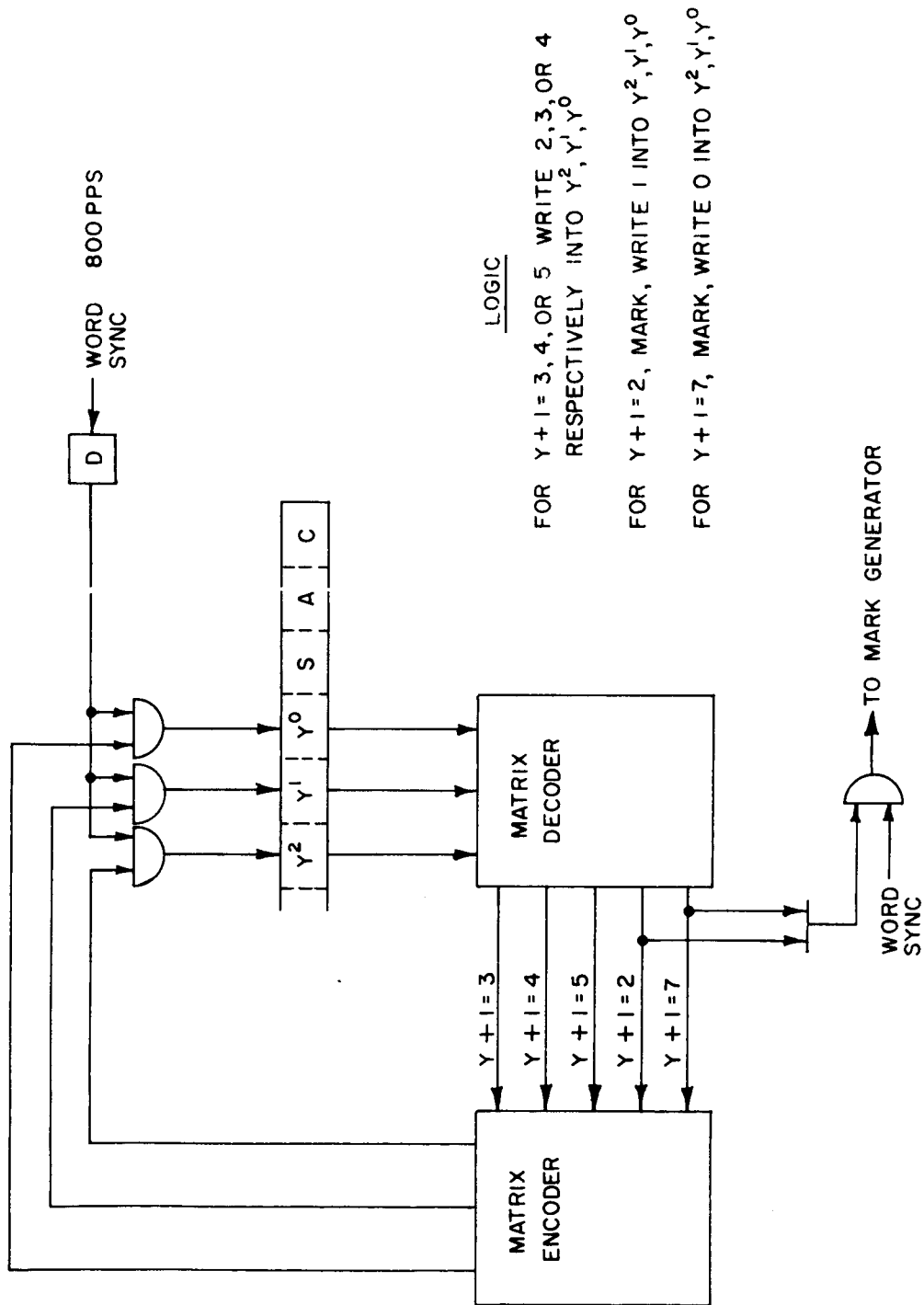


Fig. 3-26 CM-II L<sub>B</sub> Cycle 2 (Decrement Y and Mark)

Occasionally, the computation will call for the loading of the segment data into a buffer position already occupied (intersecting lines). This situation is remedied by making a test on the Y portion of the subsequent word spaces which might receive the data. (The system illustrated has five words available to the logic at one time, an unnecessary constraint in a serial system.) In the process of decoding the segment data to determine the new X coordinate, the results of the tests which indicate occupancy are included so that the new X, Y positions computed are those for  $2\Delta X$  if the values for  $1\Delta X$  results in two words occupying the same buffer position.

With the system described above, the required bit rate in the logic section is only 4.8 kc making all magnetic logic quite feasible. Operation of the buffer in both the forward and backward mode allows lines of any slope, including lines of very small negative slope, to be drawn.

On nearly horizontal lines, the segment data will move from one position to another before a mark cycle is reached, requiring a temporary storage of a mark command. This is obtained by writing an illegal code into the Y + 1 portion of the word, which is erased on the subsequent mark cycle.

### 3.3 THE ELLIPSE METHOD

#### 3.3.1 Description

Appendix A shows in some detail the fact that all latitude and longitude lines seen in an undistorted picture are ellipses or sections of ellipses. Within limits, distortion can also be accommodated by modifying the ellipses.

This geometric fact leads to a possible technique of on-board gridding, the sending of basic or composite parameters of each ellipse to the satellite, followed by expansion of the ellipse synchronously during scanning

Such a technique has been suggested, but not adopted, for ground gridding of AVCS. The ground technique was oriented to the peculiarities of the CDC 924 computer, so should not be used as more than a general guide to an on-board technique.

Expansion of the grid is achieved by inserting the Y-value (line count) into the grid expansion formula, inserting the proper parameters for each ellipse, and solving for X, the element count along the line. This is repeated for each ellipse to be gridded on a given forthcoming scan line. The latitude and longitude ellipses can be ordered on the ground, so that two ordered sets of X-coordinates are produced. One simple expedient for avoiding merging these sets is gridding latitudes only on



even lines, longitudes on odd; the penalty for this is a coarsening of slope capabilities for near-horizontal lines.

Special logical provisions must be made for:

- Grid line initiation at top of picture
- Grid line initiation at sides or within picture
- Grid line termination at sides or within picture
- Rejection of grid points falling outside picture area
- Increasing vertical density of gridding with diminishing slope
- Coping with near-horizontal lines, so that several grid marks may fall on one line

None of these logical requirements is unique to the ellipse technique. Eventual output is achieved by an equivalent to the GRIPE technique.

### 3.3.2 Parameters of the Ellipse

The general ellipse is described by a set of 5 parameters. One description of this set is:

- semi-major axis
- semi-minor axis
- orientation of semi-major axis
- X and
- Y coordinates of center of ellipse.

While we have not searched extensively, we have found no effective way of essentially reducing the set by making one or more parameters serve for all latitude or longitude lines within a picture.

In addition to the basic set, additional information is required to terminate the ellipses within the frame of the picture and to suppress those parts of the ellipses that would enter the frame from the back of the mathematically transparent earth. Still further information is required to originate and end ellipses that are wholly contained within the picture frame (polar latitudes).

The ellipse computation equations of Section 5 of this report show that the basic parameters enter into subtractions, so that somewhat greater precision is required in specifying parameters than is desired in the final results. This suggests 8 bits for each of the basic parameters, 7 bits for beginning or otherwise specifying

the character of the grid, another 7 bits for longitudes if it is desired to terminate them within the picture frame, and 1 bit for the sign of the radical to keep back-of-earth grids out of the picture and permit grids of either slope.

In counting ellipses, any ellipse that goes through zero slope is counted two, as is an ellipse that leaves the picture and enters again.

### 3.3.3 Storage Requirements

For the worst case 800-mile orbit with  $5^\circ$  grids, some 250 ellipse segments will be encountered. Leaving aside the problem of termination within the picture, 48 bits are required to specify each ellipse. Thus, the minimum tenable storage is 12,000 bits. Markers, frame syncs, etc. plus any addenda to simplify logic (see below) may double this number to about 24,000 bits.

Storage requirements are relatively small, but are similar in magnitude to other compact-storage techniques.

### 3.3.4 Logical Requirements

Expansion of the basic ellipse formula requires one square root, three multiplications, and four addition/subtractions per grid point. This is in addition to the logic required to start and stop lines and to produce a suitable density of grid marks regardless of grid slope, all of which must act essentially serially.

While the level of arithmetic and logic suggests either a stored-program computer or its equivalent in a sequential-instruction wired program, a custom computer might be able to save time by performing one multiplication while the square root is being performed, and by providing internal gating for logical options.

A characteristic  $K = 16$  picture contains 800 marks to be computed in 200 seconds or about 250 milliseconds per mark. Extensive output buffering can permit computation speeds of this order, although it may be desirable to at least quadruple this speed to permit grid points on each line with only a one or two line buffer.

In units of add time we have:

4 adds @ 1	4
3 multiplies @ 4	12
1 root @ 10	<u>10</u>
	26
logic and data shuffling	<u>24</u>
	50 add times per point

Even with quadrupled speed, this calls for an add time of 1.25 milliseconds. hardly speedy by modern standards. This low speed requirement suggests the use of delay line serial arithmetic for dodging the requirement for random access interim storage. This unfavorably changes the relation between multiply and add times, however, and may well introduce wait times. The result points to a delay line approaching a megacycle rate, plus a fair amount of busy logic.

Looking at the problem with more perspective, the ellipse technique apparently requires an on-board computer with multiply, add, square root (wired or programmed), input-output, and nearly full logical capabilities. Its speed need be only medium, and its random or serial access storage can be of the order of 1,000 bits. Such spaceborne computers are doubtlessly available.

### 3.3.5 Evaluation

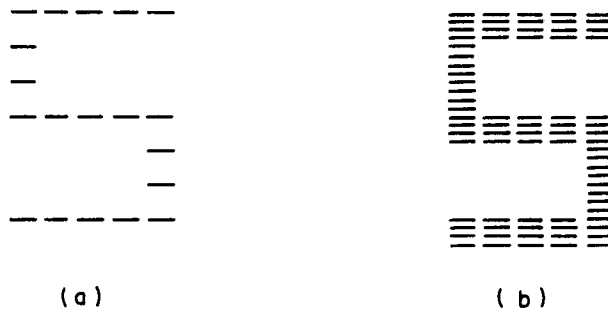
Compared to other potential techniques, the ellipse method calls for equivalent storage and nearly an entire computer, plus GRIPE. Design of an appropriate special-purpose computer has seemed unprofitable to us, and the ellipse technique has not been pursued further.

## 3.4 ANCILIARY FUNCTIONS

### 3.4.1 Numeral Generation

#### 3.4.1.1 Introduction

The generation of numerals on the picture to identify selected latitude and longitude grid lines can require the use of additional logic which is separate from the calculation logic used for generating marks for the grid lines. In the coordinate method, the annotation data are included with the grid data, but numeral marks will appear only on mesh sweeps unless more equipment is added. Extra storage is needed to make marks along the sweeps between meshes if it is desired to produce more attractive numerals. Examples of both types of numerals are given in Figure 3-27.



(a) Numeral with marks along every fourth sweep

(b) Numeral with marks along every sweep

FROM DI/AN CONTROLS, INC. DRWG 2177-4010

Fig. 3-27 Numeral Appearance

#### 3.4.1.2 Numeral Generator, CM-1A; Marks Along Every Sweep

In this case, we assume that it has been decided beforehand that numeral notation shall be made between sweeps  $Y_a$  and  $Y_b$ . This information is pre-programmed into the spacecraft so that when sweep  $Y_a$  is at hand, the numeral generator knows that the information immediately following the next sweep change is numeral information and is not intended for use in grid mark generation. The four annotation characters will take up 26 mesh intervals along the sweep and 7 mesh sweeps for  $5 \times 7$  matrix numerals with a space of 2 matrix elements between adjacent numerals. (Numerals are each 20 picture elements wide and 28 sweeps high. Spaces are 8 picture elements wide.) Following the arrival of a numeral identification code after  $Y_a$ , the numeral mark locations are fed into an integrated 26-bit (or more) recirculating shift register. This loading may be done during the retrace time. This register delivers a sequence of "mark" or "no mark" signals during 26 mesh intervals at the beginning of sweep  $Y_a$  and for the next three sweeps between mesh sweeps. These data are dumped at the next mesh sweep and are replaced by new data to be used on that mesh sweep and the three sweeps following. Seven sets of data are used for a 7-high dot matrix. Numerals as shown in Figure 3-27 will be generated. At  $Y_b$ , the auxiliary register is retired until the next picture. A code can be saved by making the numeral start coincident with a zone start. The additional storage required for annotating in this manner is about 2,700 bits.

#### 3.4.1.3 Numeral Generator, CM-1A; Marks Along Every Fourth Sweep

If the extra register is not used, the annotation marks will occur only every fourth sweep (for  $n = 4$ ). Numerals as shown in Figure 3-27a will be generated. In this case, annotation of numerals merely requires mark location data to be stored in memory exactly as for marks used in plotting grid lines. For a  $5 \times 7$  matrix of 35 possible points, each numeral will require about 12 marks. The four characters then require 48 marks per picture. For the 15 picture orbit, we then require 720 addresses (5,800 bits) in memory.

#### 3.4.1.4 Numeral Generator, CM-1A; Marks on Non-Mesh Sweeps Only

A method somewhat easier to implement than that described in 3.4.1.2 is shown in Figure 3-28 in logical form. In this method, only the non-mesh sweeps are marked with the character data. For simplicity, characters are placed on the first 28 sweeps and first 26 mesh intervals and occupy the upper left hand corner of the picture. In order to avoid the necessity of loading during retrace, the entire logic is merely operated on the sweep following the first mesh sweep ( $M + 1$ ) and after every  $K^{\text{th}}$  sweep thereafter up to sweep 28. On sweep  $M + 1$ , data is read from memory, marked, and placed in the temporary storage register. It is recirculated and re-plotted on the remaining interval sweeps, but, is erased before the next mesh sweep. In this way, numeral and grid data can overlap with no interference or extra circuitry for a load operation during retrace.

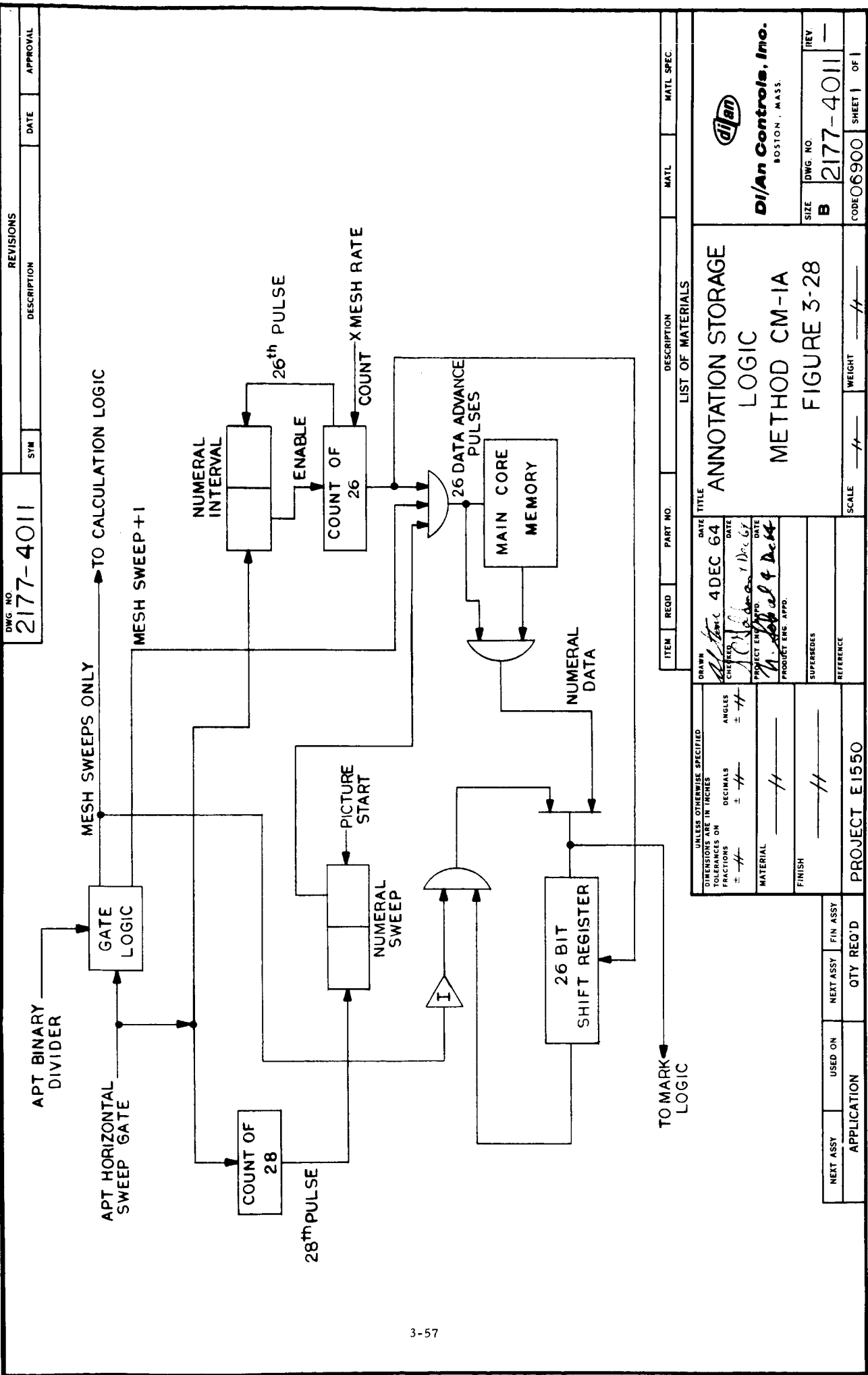
#### 3.4.1.5 Numeral Generator, Straight-Line Method

In the case of the straight-line method, an alternative to numeral generation from a dot or mark matrix is to approximate the numerals by short straight lines. The approximation of the numerals by sets of straight lines requires up to 17 extra segments per picture, and would call for a delay line with a bit rate and storage capacity about 20% higher than at present. This method also adds approximately 10,000 bits to the 16,000 needed for grid lines.

#### 3.4.1.6 Numeral Generation Every Sweep; Straight-Line Method

Although the method outlined in the previous section involves no extra logic it will not produce pleasing numerals due to the wide spacing between marks. A modification of the auxiliary storage method described in Section 3.4.1.4 for the coordinate methods can be used in the straight-line method.

As previously described, following the occurrence of a specified Y sweep, counters indicate that the next data out of the memory must be numeral data. This data is sent to the auxiliary storage register during the next retrace time. On the following sweeps the data in the auxiliary register is superimposed on the grid data from the calculation logic. This process is repeated for the required 23 sweeps of the numeral matrix. Due to the fact that extra timing is required to provide proper sequencing during retrace, the logic required to perform this annotation implementation



LIST OF MATERIALS		TITLE	
ITEM	REQD	PART NO	DESCRIPTION
		ANNOTATION STORAGE LOGIC METHOD CM-1A FIGURE 3-28	
		SCALE $\frac{1}{4}$ WEIGHT $\frac{1}{4}$	

DIMENSIONS ARE IN INCHES TOLERANCES ON FRACTIONS $\pm \frac{1}{16}$ DECIMALS $\pm .005$ ANGLES $\pm 1^\circ$		DRAWN <i>[Signature]</i> CHECKED <i>[Signature]</i> DATE 4 DEC 64
MATERIAL FINISH		PROJECT ENG APP'D <i>[Signature]</i> DATE 1 DEC 64
NEXT ASSY USED ON APPLICATION		QTY REQ'D FIN ASSY
PROJECT E1550		SHEET 1 OF 1

is estimated as 10% above that required in the coordinate method. The parameter estimates of Tables 3-11 and 3-13 have assumed the use of the technique described here.

#### 3.4.1.7 Numeral Generation; CM-2

For the CM-2L<sub>A</sub> version of the slope-coordinate method, annotation characters are generated by loading a shift register (read out every sweep) with single bit mark words from the main store. The words are automatically loaded at times corresponding to the X, Y coordinate positions reserved for annotation. The only extra circuitry required is the shift register and the modules needed to produce the proper clock pulses. Insertion of the annotation mark words in the proper place in the data stream is an extension of the logic already required for the slope-coordinate method. The appearance of the characters is shown in Figure 3-29. The additional storage requirement for annotation is approximately 2,700 bits. CM-2H annotation is the same as SL-2.

#### 3.4.2 Satellite Orientation Corrections

##### 3.4.2.1 Coordinate Methods, Orientation Correction

In either CM-1A or CM-1R, the corrections for pitch and roll are made rather easily. The detection of a roll error indicates that the location mark S along a mesh sweep are incorrect. The roll error is sampled at the time the picture is taken. In the case of the run-length coordinate method, a roll correction can be made by simply adding or subtracting a single value at the start of each run length sequence. For the case of the full address coordinate method, the correction must be added to each address word. Either method can be implemented by the insertion of a full adder just following the output of the memory. In the run-length case, the adder is activated at the start of each sequence. In the full address method, it is activated each time an address word is selected.

An alternate roll correction method is to shift the time axis by presetting (up or down) the X mesh interval counter.



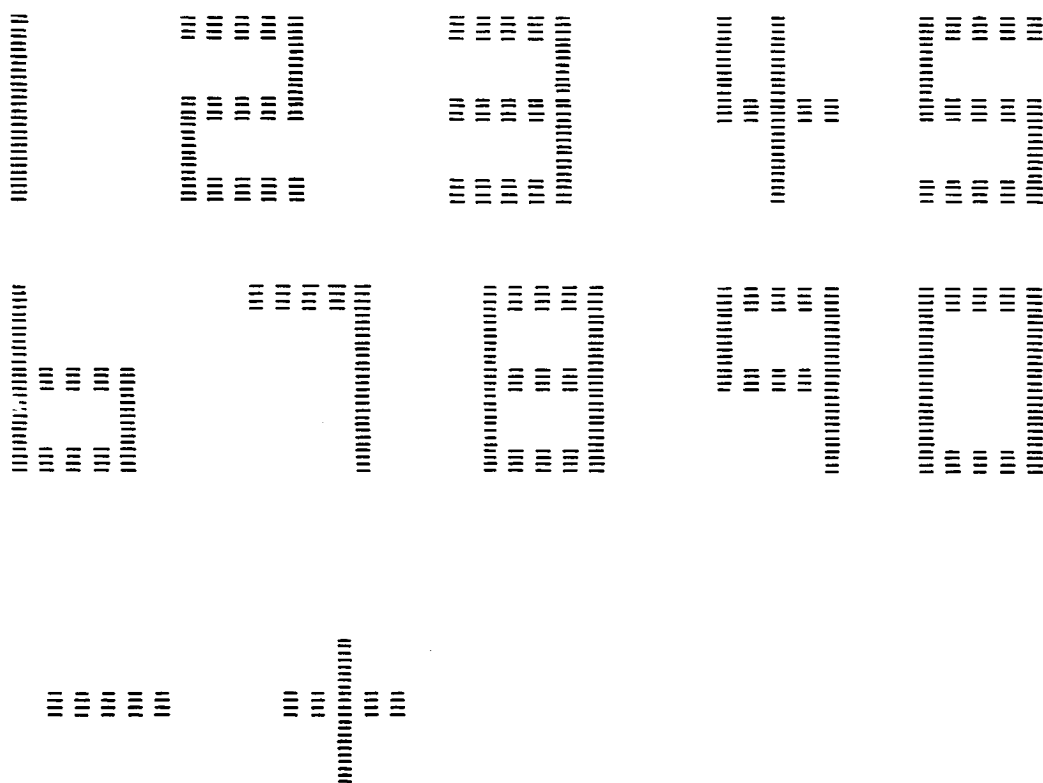


Fig. 3-29 Appearance of Annotation Characters for CM-II L<sub>A</sub>

Both methods, although in many ways easy to operate, allow a whole class of points that cannot be put on the picture to reach the calculation logic, and a comparison must be made to allow the memory to advance to the proper location as each sweep is changed.

Correction for pitch can be made similarly by delaying or advancing the count of the Y interval counter. The consequences of this situation are not as severe as that for the mesh interval roll correction as sweeps which are shifted off the picture due to a forward pitch are covered by the methods already described, that is, they are rejected. Sweeps that are shifted off the picture by backwards pitch would not be plotted since they would not leave memory until after the vertical sweep had been terminated. Sweeps that may be "left over" in the memory following a pitch corrected picture would be wiped out when the synchronizing system automatically seeks the start of the next picture.

In the slope-coordinate system, portions of line segments cannot be dropped without upsetting the operation of matching mark words to segments. This situation can be remedied by prohibiting grid line marks within 3.5% of the picture borders. For this condition, marks would not move out of the borders for a  $3^{\circ}$  roll or pitch error. The corrections for pitch can be made by adding to or subtracting from the Y counter. Roll corrections can be made by presetting the X counter for each sweep.

#### 3.4.2.2 Straight Line Orientation Corrections

The compensation technique for pitch and roll in the straight line methods is similar to the technique outlined for the CM-1 methods. However, the timing is somewhat more complicated because of the more complex word structure. With use of an adder at the memory output, pitch and roll correction can be obtained by adding fixed numbers to the origin X and Y address. ("Origin" means the point at which a straight line segment begins.)

### 3.5 SYNCHRONIZATION AND ERROR DETECTION

#### 3.5.1 Udata Transmission System

##### 3.5.1.1 Modulation Form

The data transmission system will use the basic OGO FSK /AM and Command Data Link built for the Nimbus system. The binary data are put in NRZ form and used to establish "zero" and "one" audio frequencies. Since the NRZ form does not yield positive sync, the basic bit rate is superimposed by AM on the FSK signal. The composite signal is amplitude modulated on an RF carrier and sent to the satellite. In the satellite, an FSK demodulator and an envelope detector recover data and bit sync from the signal. The APT Gridding System should use a separate FSK demodulator from the command demodulator already on board the satellite because:

a. The APT Gridding bit transmission rate is one or two orders of magnitude faster than the command data rate, and would be too fast for the narrow band FSK demodulator already on board. The FSK command demodulator would have to be modified (thus reducing the noise margin in the command link) to recover the wide band data transmission.

b. It is desirable that existing satellite systems be modified as little as possible.

##### 3.5.1.2 New Commands

"GRID DATA START" and "GRID DATA END" commands should be added to the Nimbus vocabulary. In addition, "GRID DATA HOLD" should be added if it is desired to have the capability to interrupt and later to resume grid data transmission. The FSK APT data demodulator supplies to the APT gridding subsystem the data obtained from the ground along with a bit synchronization pulse train. Word sync is contained in the data in appropriate codes and is inserted at pre-planned times.

The APT gridding demodulator would be turned on and off by the new commands described above, via the existing command decoder.

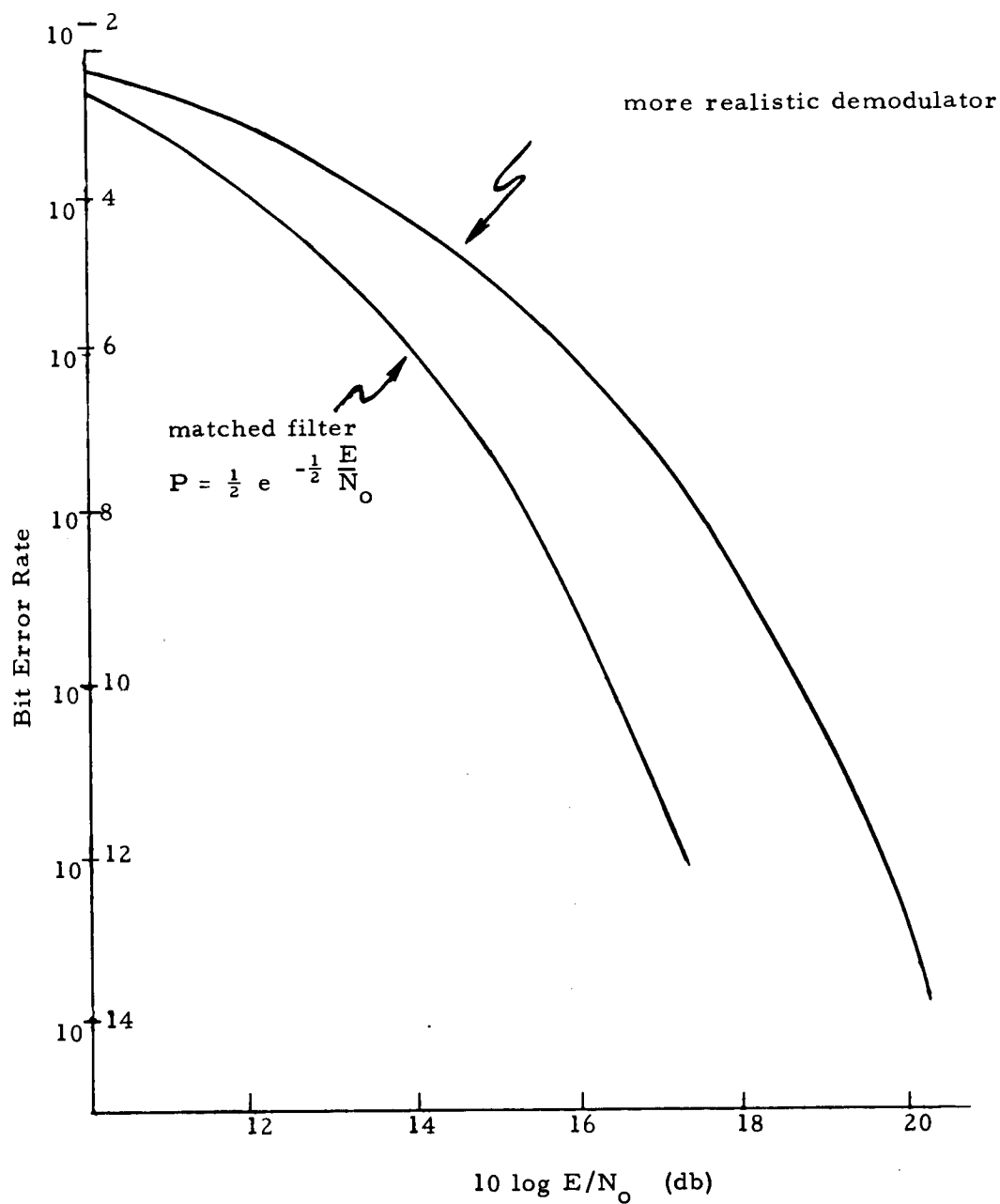


Fig. 3-30 Error Rate vs.  $\frac{\text{Energy Per Bit}}{\text{Noise Density}}$  (db at Audio)

$$\frac{E}{N_0} = \frac{\text{Audio B.M.}}{\text{Data Rate}} \times \frac{S}{N} \text{ Audio}$$

### 3.5.1.3 Udata Error Rate Due to Thermal Noise

The theoretical performance of an OGO type FSK demodulator is shown in Figure 3-30 taken from "Command System Study for the Operation and Control of Scientific Satellites" by ADCOM, Inc. The signal-energy to noise power density ratio is given by:

$$\frac{E}{N_o} = \frac{ST}{N/W} = TW \left( \frac{S}{N} \right)$$

Where  $\frac{S}{N}$  is the demodulator input signal-to-noise ratio, W is the bandwidth in which the noise power is measured, and T is the bit duration or inverse of the data rate.

We have been informed that under the worst condition of thermal noise,

$$\frac{S}{N_{\text{audio}}} = 50 \text{ (17db)}$$

Assuming the fastest available data rate of 1,600 bits/sec and Audio Bandwidth = 20,000 cps.

we find

$$\frac{E}{N} = \frac{20,000}{1,600} \times 50 = 620 \text{ (28db)}$$

The 28db point is well below the bit error rate of  $10^{-14}$  at the bottom of the graph. With respect to thermal noise disturbance, to which the 17db SNR figure presumably refers, the system is essentially error free.

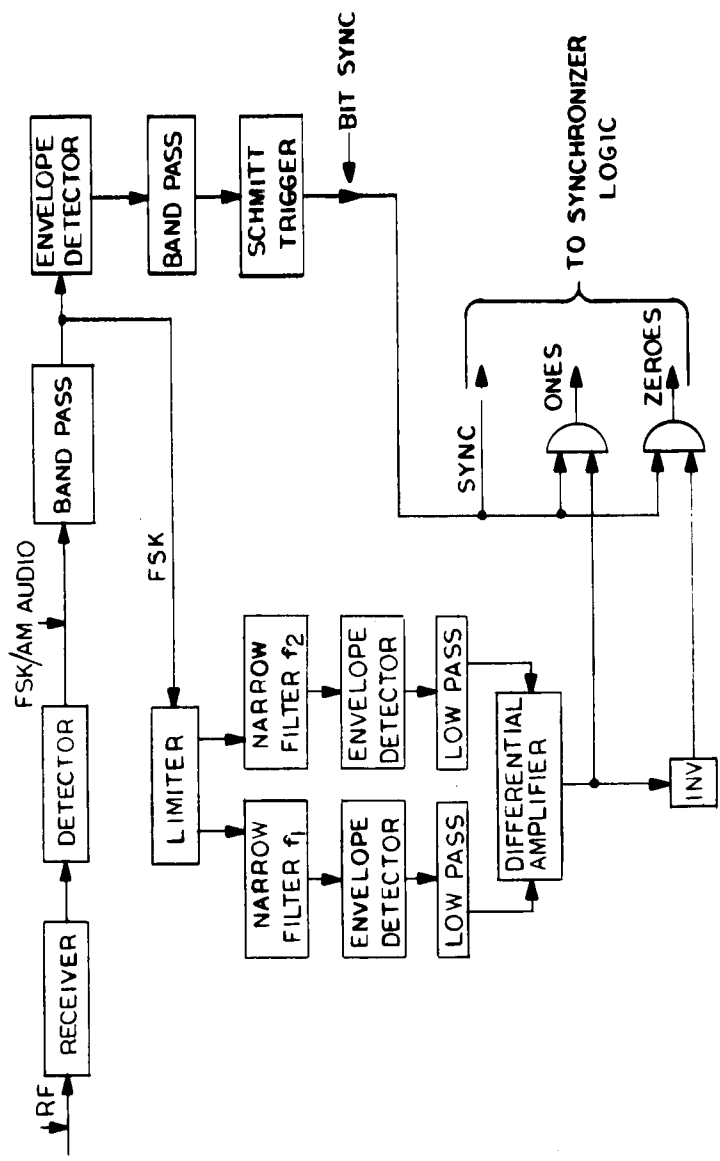
### 3.5.2 Demodulation and Bit Synchronization

The decoding of the FSK/AM audio signal from the receiver-detector to a string of "ones" and "zeros" is a standard procedure such as shown in Figure 3-31. This figure follows the logical design used by Space Technology Laboratories for their OGO satellite command demodulator. The logic shown presents "one" and "zero" pulses. The two separate detection systems supply the bit synchronization information and the decoded data. The time constant of the envelope detector in the bit synchronization decoder effectively determines the time required for positive synchronization in the absence of noise.

REVISIONS

DATE	DESCRIPTION	APPROVAL

DWG NO  
**21774058**



ITEM	REQ'D	PART NO.	DESCRIPTION	MATL	MATL SPEC.
LIST OF MATERIALS					
DEMODULATOR AND BIT SYNCHRONIZER FIGURE 3-31					
TITLE R. Nelson IDEC64 DATE 11/1/64 PROJECT NO. 10-100-10-100 PRODUCT ENG. APP.					
DIMENSIONS ARE IN INCHES TOLERANCES ON FRACTIONS DECIMALS ANGLES ± # ± # ± # MATERIAL FINISH SUPPLIERS REFERENCE					
PROJECT E-1550					
NEXT ASSY	USED ON	QTY REQ'D	FIN ASSY		
APPLICATION					
Di/An Controls, Inc. BOSTON, MASS.					
SIZE	DWG NO	REV	CODE	SHEET	OF
B	2177-4008	—	0690C	1	1



### 3.5.3 On-Board Word Synchronizing and Error Detecting System for CM-1A

#### 3.5.3.1 System Outline

The following statements will give an overall picture of the system.

- a. Data is addressed in an 8-bit code representing the mesh interval value along a mesh sweep.
- b. Along any particular mesh sweep, the address values must be monotonically increasing.
- c. Sweep sync is contained in the updata by means of a 24-bit synchronizing code that is transmitted at the start of each monotonic sequence.
- d. A parity bit will be used for checking the fully addressed code. We accept the possibility that an occasional single point may be plotted in the wrong place.
- e. The synchronizing code sent from the ground is not placed into the memory.
- f. Error detection circuitry to be outlined is included in the decoder which removes codes found to be in error through detection of an address decrease before the end of the data for a single sweep.
- g. The observation by the synchronizer logic of a decrease in the address value (after error checking and loss of sweep sync data), indicates that a sweep change (new mark line) should occur. For mark sweeps on which the above interim is not satisfied, line marker codes or extra marks at the sweep end must be used.

Once the data has been placed in memory, the operational sequence is as already outlined for the full address coordinate method

#### 3.5.3.2 Logical Description of Word Synchronizer

As shown in the timing diagram of Figure 3-32, the first word in the updata stream is a 24-bit synchronizing code. Initial conditions on the logic of Figure 3-33 are such that Gate 3 causes a sync search to be made after each bit clock pulse C. Following each clock pulse, the counter of 24 enables the 24-stage shift register and the serial synchronizing code generator and an exclusive OR circuit compares the shift register content to the fixed code. The number of errors in each 24-bit sequence of this comparison are counted. If three errors in a single search are accumulated, sync has not been obtained. Calculations of probabilities for the 24-bit Barker Code indicated that allowing two errors still yields a very high probability of correct word sync.





When the 24-bit sync code is recognized and less than three errors occur, flip-flop E will remain in the  $\bar{E}$  state at the conclusion of the search. The 24<sup>th</sup> high-speed clock-count will then load another counter of 24 (in a more sophisticated design the two counters could be consolidated) and beginning with the next C pulse, the 24-bit sync word will be replaced by data. At the conclusion of the 24 counts, flip-flop B is in the  $\bar{E}$  state, Gate 2 is enabled and memory write begins.

As successive 8-bit words appear at the input and output of the final eight stages of the shift register, a check is made to determine the monotonic increase of the signal addresses. In addition, every 8 pulses a sync search is made. This procedure continues until one of the following conditions arises:

- a. A borrow pulse is emitted from the subtractor due to a decrease in the X address, or
- b. The recognizer determines that the 24-bit synchronizing code has been received.

In case of an error causing a decrease in the X address, the system goes into sync search and will not put any data in memory until the next synchronizing code appears.

If no errors have occurred during the time between two sweep syncs, the system will automatically continue in operation. The 192 code indicates an address at the very end of the picture and its presence assures that a monotonic sequence indicating an address decrease at the end of the sweep would be noticed by the calculation logic even if bit errors had occurred.

### 3.5.3.3 General Synchronization Techniques

The logical structure of the equipment described in the previous section will not be radically different for methods other than the 8-bit fully addressed coordinate method. Of course, the search for the monotonically increasing address is unique to method CM-1A. The error detection in the case of method CM-1R would more probably rely on single or double parity bits which would not be inserted into the main memory. In the case of the straight-line method, the synchronizing problem changes slightly due to the longer word (40 bits) for a line segment. Here again the search for monotonic increases of the Y address can be done as an error detection technique, in addition to multiple parity bit insertions. In estimates of size, power

#### 3.5.4.2 Run-Length System, CM-1R

In this system, each mark is given an address relative to the previous mark. The X counter is zeroed every time a mark is plotted. The run-length sequence continues for one entire zone.

The first line below shows a set of possible codes placed in memory and intended for the  $i^{\text{th}}$  sweep. The second line shows the mesh interval values of the marks. The third line shows an error picked up due to a one-bit change in the codes.

4	41	36	39	33	-	Run Length Address
4	45	81	120	153	-	Resultant X Location
5	<u>57</u>	36	39	33	-	Incorrect Run Length Address
5	61	97	136	169	-	Resultant X Location

All points following the mark in error are plotted incorrectly. Since the run-count extends beyond one sweep, this displacement along the X axis (to the right in this case) is picked up everywhere resulting in a plausible but displaced grid structure.

A parity bit could detect the presence of this error, but even detection of the error would not help in reconstructing the correct picture. In fact, a single error necessitates scrubbing the remainder of the zone. If we add line markers to note the end of each sweep, we can shorten the run-count and limit the error to just one sweep. But, the extra line marker codes require considerable additional storage; six bits per word, 200 words, 10 pictures, = 12,000 bits, exclusive of parity or sync bits; if parity is added to this coding scheme, we add 11,000 more bits.

#### 3.5.4.3 Straight-Line Method

In both straight-line methods so far implemented, the basic line segment word is stored in serial memory and is fed as demanded by the logic into a cycling delay line. The basic word is a 40-bit sequence containing origin points, slope, and length information.

The least important error takes place when the segment length is altered by an error. The segment will be shortened or extended and no interaction with the rest of the rest of the picture takes place. If the slope, slope sign, or mode bit is in error, the resultant line segment will not connect with its subsequent segments and will yield a more-or-less obvious error.

and weight, the synchronizing system described in the previous section has been applied to all methods since there is no indication that the actual circuitry for any of the methods would involve either principles or complexities very different from the one described here.

### 3.5.4 The Effects of the Single Bit Errors on the Gridding System

#### 3.5.4.1 Full X-Address, CM-1A

In this method of gridding, an 8-bit binary number is employed to locate each mark. A mark is generated by subtracting the X-count along the sweep from the available address. So long as this number is positive, nothing happens. When the count equals the address, a mark is made. If the result is negative, the word in the test register is less than the count, indicating that it belongs to the next sweep. A constraint on the method is that the X address of the last mark on the  $i^{\text{th}}$  mesh sweep exceeds the X address of the first mark on the  $(i + 1)^{\text{st}}$  sweep. At the end of each mesh interval count (192 intervals) the counters are reset. The process continues for an entire picture until a word indicating end of a zone is read from the memory.

On any sweep, the X address monotonically increases and has values

$$A_1, A_2, \dots, A_n, \text{ where } A_{i+1} > A_i.$$

On the next sweep, each of these coordinates has increased or decreased an amount depending on the slopes of the lines which they are approximating. The new addresses are:

$$B_1, B_2, \dots, B_n.$$

Suppose that an error occurs in  $A_i$ , such that  $A_i > A_i + 1$ . A typical sweep sequence and the same sequence with an inserted one bit (128) error is:

5	47	92	165	-- correct
5	175	92	165	-- error

In the incorrect sequence, marks at 5 and 175 will be plotted. When 92 is reached in memory, the counter (having already plotted 175) will be past count 92 and a mark at 92 will be plotted on the next mesh sweep along with 165. After this the process will continue normally, but, delayed one sweep out of step.

If  $A_i - 1 < A_i < A_i + 1$  then the only picture error will be a misplaced mark at  $A_i$ . So long as the monotonic address increase remains undisturbed, this error will not affect the overall picture.

#### 3.5.4.2 Run-Length System, CM-1R

In this system, each mark is given an address relative to the previous mark. The X counter is zeroed every time a mark is plotted. The run-length sequence continues for one entire zone.

The first line below shows a set of possible codes placed in memory and intended for the  $i^{\text{th}}$  sweep. The second line shows the mesh interval values of the marks. The third line shows an error picked up due to a one-bit change in the codes.

4	41	36	39	33	-	Run Length Address
4	45	81	120	153	-	Resultant X Location
5	<u>57</u>	36	39	33	-	Incorrect Run Length Address
5	61	97	136	169	-	Resultant X Location

All points following the mark in error are plotted incorrectly. Since the run-count extends beyond one sweep, this displacement along the X axis (to the right in this case) is picked up everywhere resulting in a plausible but displaced grid structure.

A parity bit could detect the presence of this error, but even detection of the error would not help in reconstructing the correct picture. In fact, a single error necessitates scrubbing the remainder of the zone. If we add line markers to note the end of each sweep, we can shorten the run-count and limit the error to just one sweep. But, the extra line marker codes require considerable additional storage; six bits per word, 200 words, 10 pictures, = 12,000 bits, exclusive of parity or sync bits; if parity is added to this coding scheme, we add 11,000 more bits.

#### 3.5.4.3 Straight-Line Method

In both straight-line methods so far implemented, the basic line segment word is stored in serial memory and is fed as demanded by the logic into a cycling delay line. The basic word is a 40-bit sequence containing origin points, slope, and length information.

The least important error takes place when the segment length is altered by an error. The segment will be shortened or extended and no interaction with the rest of the rest of the picture takes place. If the slope, slope sign, or mode bit is in error, the resultant line segment will not connect with its subsequent segments and will yield a more-or-less obvious error.

If the error occurs in the mesh interval origin of the segment, more complex errors can develop. A horizontal displacement of the line will result, with the possibility that the line will try to go off the picture. However, it is in the Y origin (mesh sweep) address that errors can have major effects. A word is extracted from the main serial memory after the first seven (most significant) bits of the Y origin address have been found equal to the Y sweep counter  $Y_c$ . Let us consider the situation where the  $i^{\text{th}}$  word having Y origin  $Y_a(i)$  is in error and instead has origin  $Y_e(i)$ . Assume the Y sweep counter has value  $Y_c$ . Consider the two types of errors:

a.  $Y_e(i) < Y_a(i)$

The address of the  $i^{\text{th}}$  word has been reduced so that it arrives earlier in the picture than it should. This error can be detected if  $Y_e(i) < Y_a(i - 1)$ . The data for the line segment would be dumped and the logic would proceed to the next word.

If  $Y_a(i - 1) < Y_e(i) < Y_a(i + 1)$ , then the  $i^{\text{th}}$  line segment will be plotted in the wrong place but the picture will progress normally thereafter.

b.  $Y_e(i) > Y_a(i)$

This is the more serious error situation. If  $Y_e(i) > Y_a(i + 1)$  or in general,  $Y_e(i) > Y_a(i + N)$ ,  $N = 1, 2, 3, \dots, K$ , then all the line segments between  $Y_a(i - 1)$  and  $Y_a(i + K + 1)$  will be missed, with the exception of  $Y_c(i)$  which will be in the wrong place. The most severe case (caused by a 1-bit error) would occur if  $Y_1(1)$ , the first segment ( $a = 1$ ) to be introduced on the first sweep ( $i = 1$ ) had its address changed to  $Y_1(512)$  as the result of an error in the most significant bit. Nothing at all would be plotted until  $Y_c = 512$ . Thereafter, lines appearing of address less than 512 would be scrubbed. Lines of address greater than 512 would be plotted in their proper places.

#### 3.5.4.4 Slope-Coordinate Systems

Single-bit errors in the low speed versions (CM-2L<sub>A</sub> and CM-2L<sub>B</sub>) can produce disastrous effects in the grid. These systems have 21 bit segment words (sector code, initial coordinates) interspersed with single bit mark words. If the error occurs in the mark word, the immediate effect is to offset a single line segment by a mesh interval. This is the only effect in the CM-2L<sub>A</sub> system. For CM-2L<sub>B</sub>, additional errors are caused when the offset segment intersects another segment, since the mark words for the region of intersection will be applied to the wrong segments producing another mesh interval offset in each line.

A single bit error in the sector code or initial coordinates of a segment produces catastrophic results since the correct sequence of data withdrawal from the memory is destroyed.

In the high speed version of the slope-coordinate system CM-2H, the effects depend strongly on the main memory organization. For efficient storage of the data, the word length for a segment must be variable and the length of a word included in the word itself. However, constant word length can be employed in the updata transmission and error detection employed prior to storage. As a minimum safeguard, only those words whose correct length is verified on board would be stored. Assuming no errors in the main memory, the error susceptibility is then identical to that of the straight-line system.

### 3.5.5 Methods of Error Compensation

#### 3.5.5.1 Introduction

In this section coding schemes are presented which permit operation of the gridding logic in the face of possible bit errors. At the start of each of the following sections, the axioms applicable to each system are stated.

#### 3.5.5.2 Coordinate Method, CM-1R

- a. Run Length Code
- Zone and Picture Sync
- Word Parity

From standpoints of implementation, the run-length method CM-1 offers advantages over other systems. The principle source of error is not due to receiver noise and external phenomena will have a far greater effect on the error rate. In particular, on-board generated transients are the most significant error source. In this system, a parity bit (not included in memory estimates) can be included with the basic coordinate run-length code. This parity check would be performed after withdrawal of the word from memory. Since errors are interdependent, the detection of an error should call for immediate cessation of gridding. No more points are plotted until the sweep has advanced to the next of the equal zones. When an error is detected, the memory is cycled forward until a special Barker code in the

memory is decoded. These codes are sent in the updata at points following the last code of a particular sector. A flow diagram of the process is shown in Figure 3-34.

- b. Run Length
  - No Stored Parity
  - Sweep Sync by False Code
  - Error Detection by Accumulation

In the above methods, parity checking was performed after the word information had been withdrawn from the memory. However, with the addition of an unallowable code word to signify the end of a sweep and by adding some active logic, an alternate scheme for error detection can be devised. Error will be detected by progressive accumulation of the run-length values which will OK a sweep if all the points total up to 192, the length of a complete mesh increment scan.

The signal from the ground will constitute a run-length code for each point to be marked plus some false points. When all the marks for a given line have been specified and sufficient false points have been sent so that the run length totals 192, a Barker sync code is transmitted. This code and the false marks are not placed in memory. The Barker code recognition can trigger a rope memory which places an unallowable six-bit end-of-sweep code in the memory. The run length mark positions in the updata which were totaled in the accumulator are held in a 120-bit (20 marks maximum per sweep) storage register. If the mark addresses do not total 192, then the mark addresses in the register are scrubbed and only the end-of-sweep code is put into memory. As an additional check, the run-length addresses can be parity tagged, but the addition of the false bits and Barker codes add about 40,000 bits to the updata. The accumulation method is a more positive error detection than parity.

#### 3.5.5.3 Coordinate Method, CM-1A

- Full X Address
- Sweep and Picture Sync
- Word Parity

The system in which the full X address is stated (8 bits) can be handled in the same way as the run-length was handled, with the saving grace that the detection of an error does not necessitate scrubbing the entire picture grid, only the erroneous mark. Information determining a sweep change consists of an unallowed code. The





system is synchronized at the start of each picture. The parity bit is stored in memory so that this method, with parity and sweep code, requires the largest memory. A block diagram of the CM-1A error detection circuits appears in Figure 3-35.

#### 3.5.5.4 Straight-Line Methods

##### Parity Check All Words

##### Picture Sync Only

As outlined previously, the straight-line method requires error checks of a type similar to those used for the coordinate methods. A parity bit is easily kept in the word at all times. A parity check can be made after the main core memory and be included in the basic delay-line loop. Thus an error that could occur during calculation would be detected. The only practical consequence of an error detection would be to dump all the information in the delay line, although if it is assumed that sync cannot be lost, the dumping of the particular word is sufficient. The testing for parity is to be done only during the retrace period so that the word dumping sequence in use for the case of a line vacancy can be utilized.

#### 3.5.5.5 Slope-Coordinate Method

Since the low speed (CM-2L) method is especially sensitive to single bit-errors, it is recommended that the updata be sent twice, and that a matching of the two transmissions be obtained before data is stored. To minimize the amount of storage required before error detection takes place, the data can be sent in short bursts, with each burst repeated twice.

Figure 3-36 shows the general layout of an approach to CM-2L error detection. Eight bits of data enter the shift register. The next eight bits are gated (by the output stage of the counter) to the main memory write circuits provided each bit is identical to its corresponding bit contained in the shift register. Once an error is detected by the comparator, the memory loading is stopped until the next zone sync. Thus, no incorrect data is stored. A single bit error in the average will result in the loss of 1/8 of the picture grid for a four zone picture.

The same technique can be applied to CM-2H with the exception that only the segment in which the error occurs need be dropped. Synchronization can be reobtained for each new segment or groups of segments. After error detection, the non-data bits, added to the segment data for constant word length in the updata transmission,



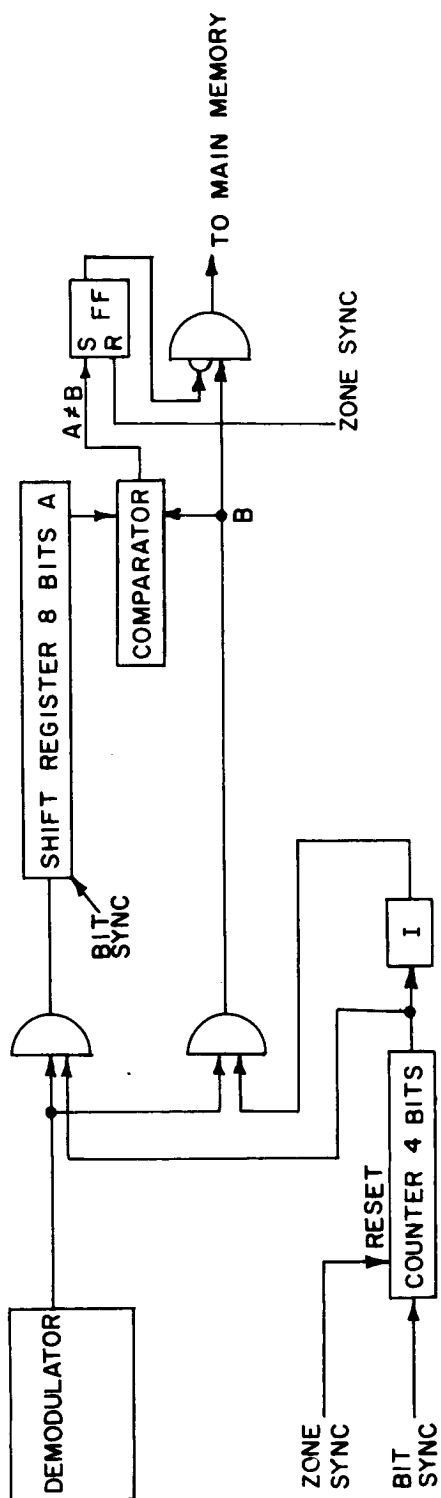


Fig. 3-36 Error Detection Block Diagram CM II

are discarded as determined by those bits of the word which indicate segment length. The segment length determines the word length for both memory write and read, so that if no bit errors occur in the memory, the variable word length should present no problem.

### 3.6 ELECTRICAL AND PHYSICAL PARAMETERS

#### 3.6.1 Subsystem Parameters

The weight and power goals for the gridding systems were informally specified to be 5 pounds and 4 watts. The study performed here kept these limitations in mind but optimum designs to minimize a weighted combination of these parameters were not evolved. Information on the memories whose weights and powers are used in this section can be found in Appendix C, "Memory Considerations". Appendix D, "Choice of Logic Elements for System Mechanizations", gives information on the logic elements whose use is assumed here.

In previous sections, the logical methods for performing the required tasks were outlined. From this information and a consideration of the number of logic elements required for each function, the following parameters were calculated for each subsystem, and are shown in Tables 3-8 through 3-12 for the various system implementations.

- a. Module Count
- b. Power: Average per Orbit and Peak
- c. Weight
- d. Volume
- e. Cost
- f. Reliability

Tables 3-8 through 3-10 show estimates for CM-1 type systems. Table 3-8 assumes the use of core transistor logic (CTL) elements, Table 3-9 integrated circuit logic elements, and Table 3-10 a combination of the two element types used to best advantage. Table 3-11 is an estimate for the straight line (SL-2) system using integrated circuitry. The module estimates of these four tables are on the designs previously described.

Table 3-8

CM-1 CTL Logic Implementation  
Per Unit Parameter Estimates

Unit	Module Power	Peak Power	Avg. Power/ Orbit	Wt(lbs.)	Vol(in <sup>3</sup> )
Calculation	35	250*	6	.63	14
Sync and Error	60	420**	7	1.1	24
Annotation	48	5*	0	.89	20.6
Roll and Pitch	43	10*	0	.76	17.5
FSK Detector, Demod.	25	250	10	.45	10
Interfaces	30	150*	60	.54	12
Memory, 100 KB	1	100*	100	3.5	140
TOTALS	242	845	183	7.9	238

\* Power drains that can occur simultaneously

\*\* Error detection power drain approximately 20% of total.

Table 3-9

## CM-1 Integrated Logic Implementation

## Per Unit Parameter Estimates

Unit	Module Power	Peak Power	Avg. Power/ Orbit	Wt(lbs.)	Vol(in <sup>3</sup> )
Calculation	60	470*	360	.63	14
Sync and Error	58	980**	17	.35	11.6
Annotation	53	600*	35	.29	10
Roll and Pitch	34	290*	215	.19	6.3
FSK Detector, Demod.	25	250	10	.45	10
Interfaces	30	150*	60	.54	12
Memory, 100 KB	1	100*	100	3.5	140
TOTALS	261	1510	797	5.95	205

\* Power drains that can occur simultaneously

\*\* Error detection power drain approximately 20% of total.

Table 3-10

CM-1 Hybrid Logic Implementation  
Per Unit Parameter Estimates

Unit	Module Power	Peak Power	Avg. Power/ Orbit	Wt(lbs.)	Vol(in <sup>3</sup> )
Calculation CTL	35	250*	6	.63	14
Sync and Error CTL	17	110**	2	.31	6.8
Annotation CTL	15	95*	4	.27	6
Roll and Pitch CTL	18	0	0	.33	7.2
FSK Detector, Demod.	25	250	10	.45	10
Interfaces	40	200*	80	.70	16
Memory, 100 KB	1	100*	100	3.5	140
Sync (Int.)	11	96**	5	.09	2.1
Annotation	6	65*	3	.03	4.5
Roll and Pitch	20	160*	8	.15	3.8
TOTALS	188	788	218	6.46	212

\* Power drains that can occur simultaneously

\*\* Error detection power drain approximately 20% of total.



Table 3-11

SL-2 (CM-2H) Integrated Logic Implementation  
Per Unit Parameter Estimates

Unit	Module Count	Peak Power	Avg. Power / Orbit	Wt(lbs.)	Vol(in <sup>3</sup> )
Calculation	175	1600	1200	1.3	43
Sync and Error	58	980	16	.35	11.6
Annotation	60	600	38	.31	11
Roll and Pitch	34	290	15	.19	6.3
FSK Detector, Demod.	25	250	10	.45	10
Interfaces	30	150	60	.54	12
Memory, 25 KB	1	75	75	2.5	100
Delay Line	1	120	84	.65	20
TOTALS	384	2000	1500	6.29	204

Table 3-12

CM-2L Integrated Logic Implementation  
Per Unit Parameter Estimates

Unit	Module Count	Peak Power	Avg. Power/ Orbit	Wt(lbs.)	Vol(in <sup>3</sup> )
Calculation	120	1100	830	.90	30
Sync and Error	58	980	16	.35	11.6
Annotation	60	660	33	.31	11
Roll and Pitch	34	290	15	.19	6.3
FSK Detector, Demod.	25	250	10	.45	10
Interfaces	30	150	60	.54	12
Memory, 25 KB	1	75	75	2.50	100
Core Buffer, 2KB	1	200	8	1.10	50
TOTALS	329	2000	1047	6.34	230.9

Table 3-13

Estimate of Design Parameters for APT Gridding Subsystem

Logical Method	Number of Modules	Peak Power (MW)	Average Power/Orbit (MW)	Weight (lbs.)	Volume (in <sup>3</sup> )	Flight Unit \$ Cost	Engineering \$ Cost
CM-1, CTL (1)	290	1000	200	8.8	260	72 K	210 K
CM-1, Integrated (2)	310	1790	935	6.5	215	71 K	260 K
CM-1, Hybrid (3)	230	925	240	7.1	230	64 K	180 K
SL-2, } CM-2H, }	Integrated (4)	2500	1800	7.1	225	74 K	370 K
CM-2L, Integrated (5)	400	2500	1230	7.1	255	74 K	330 K

(1) Pico-Bit CTL, DI/AN Controls, Inc.  
 (2), (4), (5) Milliwat Micrologic, Fairchild Semiconductor Corp.  
 (3) CTL, and MOS of General Microelectronics, Inc.  
 (4) Magnetostrictive Delay Line, Computer Control Company.  
 (1), (2), (3) 80,000 Bit Serial Memory, DI/AN Controls or UNIVAC.  
 (4), (5) 25,000 Bit Serial Memory, DI/AN Controls or UNIVAC.  
 (5) 2,000 Bit Serial Buffer, DI/AN Controls.

Assumptions:

For CM-1 and CM-2, K = 16 and n = 4.

For SL-2, K = 8.

For the CM-2 system, an extrapolation of the estimates for CM-1 and SL-2 has been performed. The estimate for CM-2H is assumed to be virtually identical to that of SL-2 (Table 3-11). The estimate for CM-2L shown in Table 3-12 is based on the assumption that the CM-2L calculation logic is approximately 2/3 of that needed for SL-2.

The tables include information for two possible additions:

- a. Numeral annotation.
- b. Analog-to-digital conversion in case the roll and pitch errors cannot be made available to the gridding system in digital form.

Table 3-13 summarizes some of the flight system parameters represented in Tables 3-8 through 3-12. A 20% across the board increase in module count, weight, volume, and power over the actual estimates appears in Table 3-13 to offset increases which often occur in translating paper designs to hardware. An exception is taken for the memory estimates where it is assumed the vendor has already inserted this safety factor.

For these estimates it was assumed: 1) that the first flight system is to be delivered in 1966, 2) that the system would be procured in lots of four. Only those components now in production or close to production states were considered in the preliminary design leading to the estimates.

### 3.6.2 Module Parameters

Logic modules assumed in the system estimates are the Fairchild Milliwatt Micrologic flat-pack and the DI/AN CTL Pico-Bit as discussed in Appendix D. Table 3-14 summarizes the per-module parameters of interest.

The values for package weight and volume of logical modules were obtained from actual aerospace and microminiature digital equipments built by DI/AN and others. In the case of CTL Pico-Bit modules, most of the data were obtained on the larger CTL-LSQ module; but it is felt that a fair scaling of parameters has been performed.

### 3.6.3 Reliability of APT On-Board Gridding System

Based on the module count data presented in the previous sections of this report, and the reliability data contained in Appendix E, "Reliability Estimation," one-year reliability figures and MTBF values have been calculated.

Table 3-14

## Per-Module Parameters

Item	Average Power(mw)	Packaged Wt. (lbs.)	Packaged Vol. (in <sup>3</sup> )	Cost, Lots of 1000
913 Flip-Flop	12	0.0057	0.19	\$ 18.55
912 Half Adder	8	0.0057	0.19	10.31
910 Dual Gate	4	0.0057	0.19	7.92
909 Buffer	10	0.0057	0.19	9.07
911 Four Input Gate	4	0.0057	0.19	7.92
CTL-100-24-PB	7x10 <sup>-8</sup> joules per "one" shift	0.018	0.40	40.00

Table 3-15 is a summary of results:

Table 3-15

## Reliability Estimates

<u>Method</u>	<u>MTBF(Hours)</u>	<u>Reliability (1 year)</u>
CM-1, CTL	36,300	.78
CM-1, Integrated Ckts.	69,300	.88
CM-1, Hybrid	50,600	.84
SL-2, Integrated Ckts.	75,900	.89

The supporting data for Table 3-15 is listed in Tables 3-16 through 3-19.

Table 3-16

## CM-1, CTL Reliability Estimate

<u>Logic</u>	<u>Module Count</u>	<u>Failure Rate %/1000 Hours</u>	<u>Total Failure Rate %/1000 Hours</u>
Pico Bit CTL	223	.007	1.561
Integrated Ckt. Flat-Packs	67	.001	.067
Memory (Univac 80,000 Bits)	1	1.13	<u>1.13</u>
TOTAL CM-1, CTL Failure Rate =			2.758

$$MTBF = \frac{1}{\lambda} = \frac{1}{2.758 \times 10^{-5}} = 36,300 \text{ Hours}$$

$$R = .78$$

Table 3-17

## CM-1 Integrated Circuits Reliability Estimate

<u>Logic</u>	<u>Module Count</u>	<u>Failure Rate %/1000 Hours</u>	<u>Total Failure Rate %/1000 Hours</u>
Integrated Ckts.	312	.001	.312
Memory (Univac 80K bit)	1	1.13	<u>1.13</u>

TOTAL CM-1 Integrated Ckt. Failure Rate = 1.442

$$MTBF = \frac{1}{\lambda} = \frac{1}{1.442 \times 10^{-5}} = 69,300 \text{ Hours}$$

$$R = .88$$

Table 3-18

## CM-1 Hybrid Reliability Estimate

<u>Logic</u>	<u>Module Count</u>	<u>Failure Rate %/1000 Hours</u>	<u>Total Failure Rate %/1000 Hours</u>
Pico Bit CTL	103	.007	.721
Integrated Ckts.	123	.001	.123
Memory (Univac 80K bits)	1	1.13	<u>1.13</u>
TOTAL CM-1 Hybrid Failure Rate =			1.974

$$MTBF = \frac{1}{\lambda} = \frac{1}{1.974 \times 10^{-5}} = 50,600 \text{ Hours}$$

$$R = .84$$

Table 3-19

## SL-2 Integrated Ckt. Reliability Estimate

<u>Logic</u>	<u>Module Count</u>	<u>Failure Rate %/1000 Hours</u>	<u>Total Failure Rate %/1000 Hours</u>
Integrated Ckts.	459	.001	.459
Memory (Univac 40K bits)	1	.86	<u>.86</u>
TOTAL SL-2 Integrated Ckt. Failure Rate =			1.319

$$MTBF = \frac{1}{\lambda} = \frac{1}{1.319 \times 10^{-5}} = 75,900 \text{ Hours}$$

$$R = .89$$

## SECTION 4

### ANALOG APPROACHES TO ON-BOARD GRIDDING

#### 4.1 GENERAL

On-board gridding systems which store the latitude-longitude grid as a series of continuous lines rather than discrete points are considered to be "analog" systems in this study. These include systems which project a grid onto the vidicon target (optical mixing) and systems which employ an electronic or electromechanical scan of the grid for subsequent electronic video mixing.

In addition to the weight, power, size, etc., limitations which are to be applied to any type of on-board gridding system, a number of constraints peculiar to electromechanical systems for TIROS and Nimbus type spacecraft should be established. Devices to be used on these spacecraft should not cause changes in the vehicle angular momentum. This requires that the position changes of mechanical parts of the system be compensated to avoid changes in the moments of inertia of the spacecraft. Any "stepped" type of mechanical motion should, in general, be avoided. Rotating devices should possess very small angular moments to avoid interfering with the spacecraft stabilization systems.

A constraint established for the grid storage medium is the use of a transparent type of storage. This permits the grid to be transferred (for optical mixing or electronic scanning) through the use of transmitted light and avoids the problems of background illumination which are inherent in systems employing reflected light.

Another constraint on the design of a gridding system is the unimpaired operation of the APT system in the event of a gridding system failure. This tends to eliminate devices which insert transparencies in the primary optical train of the APT system since the loss of ability to move the grid would result in the mixing of the grid, for the time of failure, into all the subsequent pictures.

Any type of optical mixing which adds light to the pictures to produce grid lines (e. g., mixing through a half-silvered mirror) suffers from a loss of the ability to produce easily discernable lines in any part of the APT picture. A "white" grid line produced by the addition of light would not show up against a background of bright clouds unless part of the dynamic range of the vidicon is reserved for the production of whiter-than-white grid lines. Any reduction of the total range for the cloud picture-data should certainly be avoided.



We might ask what is lost if lines cannot be produced against a bright background. Generally, the user of the picture-data is interested in the position of the edges of cloud systems. The white grid lines would still permit edge positions to be determined although the low contrast between lines and parts of the cloud picture would make this task more difficult. A more serious limitation is the loss of ability to introduce annotation at any part of the picture. Grid maps could have fixed latitude-longitude numerals adjacent to the grid lines only if their appearance in the cloud pictures could be assured. Thus, optical mixing systems will need separate annotation subsystems.

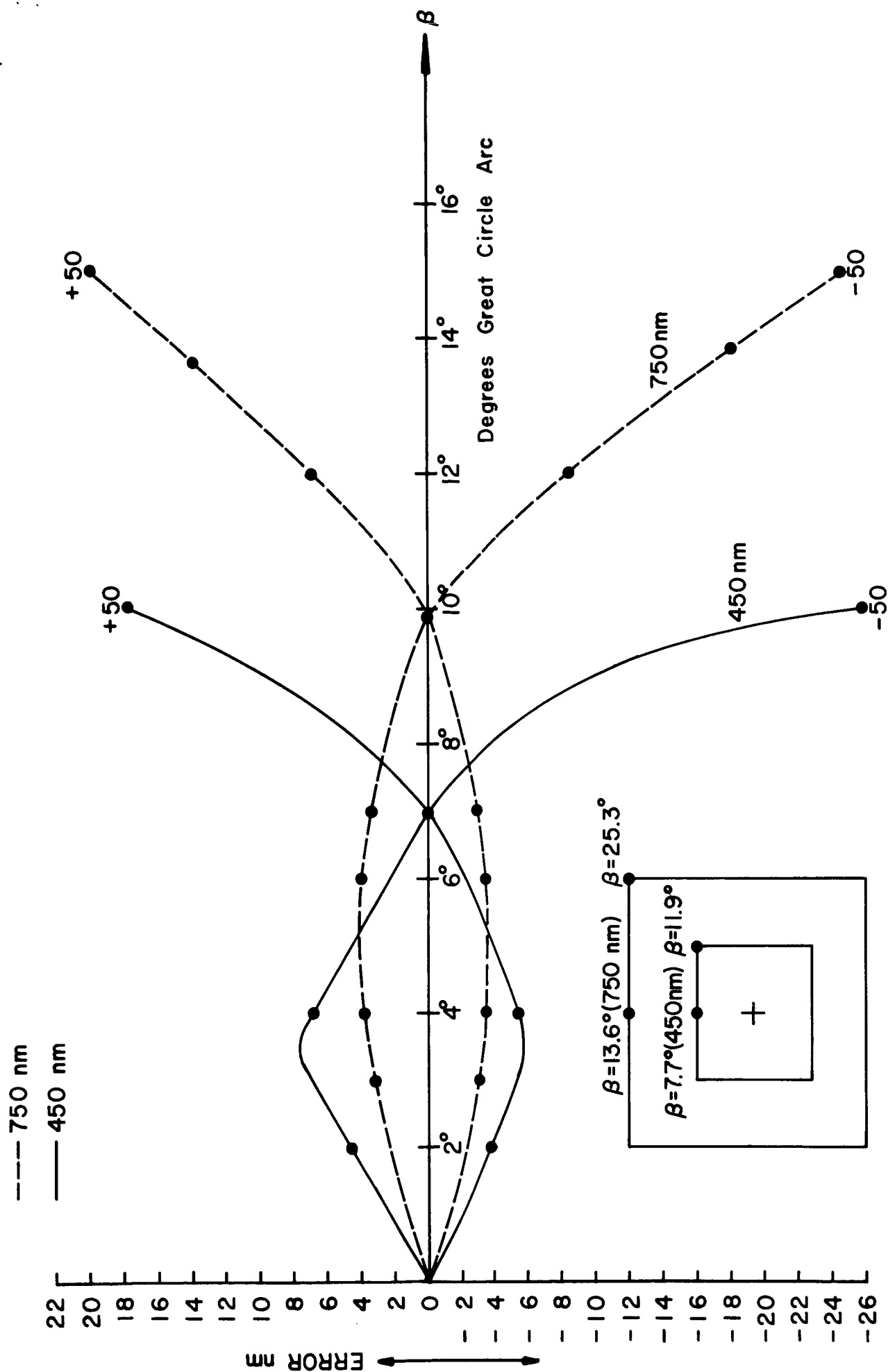
An arbitrary but useful way of classifying some of the approaches considered is the shape of the storage medium. The three shapes considered for grid storage are flat, cylindrical, and spherical. Each of these systems then can be subdivided into systems employing optical mixing or electronic scanning and mixing.

#### 4.2 GRID STORAGE ON A FLAT MEDIUM

The qualities required of the "flat" grid map are macroscopic conformality and constancy of scale. Patently, no global map can have these features. We can first consider mapping the global grid into a number of planes. A projection has been developed by ARACON under an Air Force contract for APT gridding after receipt of the pictures on the ground.

The grid lines are mapped by projecting the surface of the earth from a point 3 earth radii below a potential principal point onto a plane perpendicular to the earth radius and located 0.15 earth radii below the principal point. This projection is not error free but allows a wide area for picture principal points with minimum error combined with a minimum number of planes to obtain global coverage.

The scale of the plane projection is determined by the altitude. Means must be provided on board the satellite for changing the scale of the projection to accommodate elliptical orbits or even slight deviations from programmed altitude for vehicles in circular orbits. Scaling alone is not sufficient to transform the grid projection for one altitude to that of another. In projecting lines from a round earth onto a plane, the spatial relationship of the lines in the plane is not linearly related to the distance between the plane and the sphere. Figure 4-1 shows the relationship between the location error for a point on a grid line as a function of its earth angle departure from the subpoint for 50 mile deviations in altitude from programmed altitudes of 450 and 750 nautical miles. For the programmed altitude it is assumed



LOCATION ERROR (AFTER SCALING CORRECTION)  
FOR A HEIGHT ERROR OF  $\pm 50$  NM

FIG. 4-1

that the grid lines are perfectly mapped on the plane. It can be seen that the error for most of the grid line data in the picture is small with a very rapid increase of error toward the picture corners. For minimum or no error, a separate plane projection would be stored in the satellite for any subpoint which corresponds to a permitted time of picture taking. Since there is no restriction on picture times, a single plane must be used for a range of subpoints.

The use of a single plane projection for a range of satellite subpoints implies that the plane would be continuously moved relative to the projection optics if system complexity is to be avoided. Figure 4-2 illustrates a grid plane. The satellite subpoint track is actually a curved line in the plane. A straight line approximation to the track can be made without encountering serious error only at low altitudes. The slide must move through the focal plane of the projection system in a direction parallel to the subpoint track. If the straight line representations of the subpoint track in the individual frames are aligned parallel to the longitudinal axis of the film strip, the projected image must be rotated so that the heading line would appear as a vertical line in the APT picture. The angle between the heading line and the subpoint track over all the projection planes for a complete orbit would lie in the range of  $\pm 7^\circ$ . Incorporation of an image rotation feature to accommodate this angle also provides the ability to remove the effects of satellite yaw.

A system for projecting grids from flat planes is shown schematically in Figure 4-3. Each film strip contains a series of plane projections. For example, assume that each plane contains the latitude-longitude grid for an earth area which is roughly four times the earth coverage of the APT camera. The planes in each of the two film strips overlap 50%. The film strip from which the grid is projected at picture time is that strip which contains a plane in which the subpoint lies in the mid-50% of the track in the plane (Fig. 4-4). As the satellite progresses in orbit, the strips will advance in the film gates and the strip from which the grid is projected alternates as a function of time.\* Each latitude line on the planes of the film strip corresponds to a specific earth latitude. However, the longitude lines are arbitrary. For a given orbit the longitude position of the subpoint track in the planes is a function of the orbit ascending node. This requires that the film be displaced laterally in the film gate as the film moves through the gate.

---

\* The two series of frames might actually be contained on a single film strip. For purposes of illustrating the method, they are considered to be on separate strips.

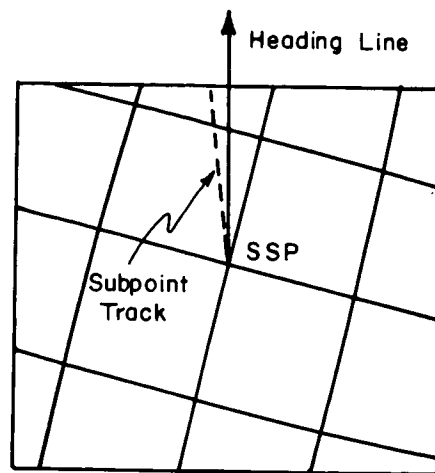


Fig. 4-2 Grid Projection on a Plane

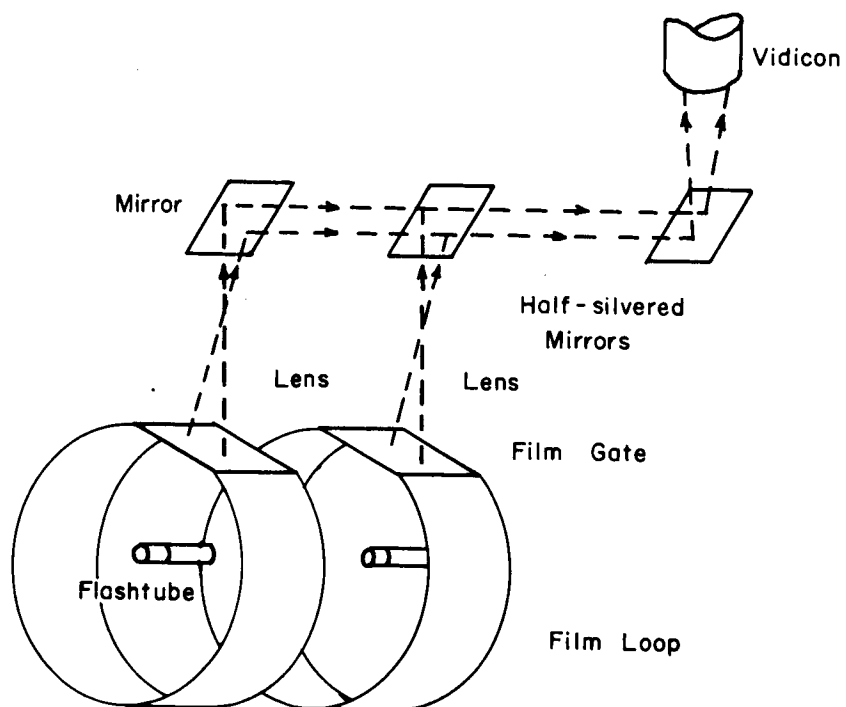


Fig. 4-3 Analog System Using Plane Projections

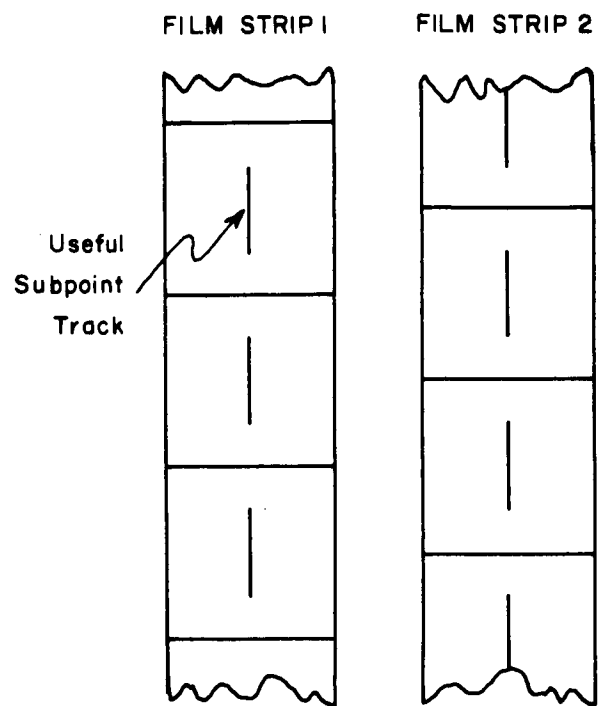


Fig. 4-4 Subpoint Track on the Planes of the Film Strips

Since a two axis frame drive is necessary to employ grid frames with "rubber" longitude lines, the film can be advanced along a curved subpoint track. This eliminates the need for the image rotation feature to obtain the proper heading line direction since the planes would be oriented with the heading line parallel to the longitudinal direction of the film strip. However, the elimination of the capability is attended by a loss of ability to cope with vehicle yaw or errors in orbit inclination.

With the dual optical system illustrated in Figure 4-3, the length of the subpoint track on each frame (grid plane) of a film strip is 50% of the track length on the frame. This represents a departure of  $\pm 25\%$  of the track length on the frame away from the projection point. An examination of the APT grids produced by ARACON showed that the allowable departure from the projection point of the map for a 1% error in grid line location is about  $\pm 5^\circ$  of great circle arc if the camera field of view (side to side) is limited to  $20^\circ$  of great circle arc. This condition where the usable subpoint track length (less than 1% error) of the individual grid frame is 50% of the total track length on the frame, holds for satellite altitudes up to about 600 nautical miles.\* For higher altitudes, the usable length of subpoint track is less than 50% and more than two series of frames (film strips) would be required if the constant speed system is to be retained. Alternatively, a discontinuous stepped typed of film advance could be employed for the higher altitudes although this is not desirable from satellite dynamic considerations. Due to the necessity for a multi-speed drive to handle the entire height range, no further consideration has been given to this approach. The control functions described - scaling, image rotation, two-axis grid plane scan - and the need for a discontinuous drive are generalized parameters common to systems which project or scan latitude-longitude grids stored in the form of a plane projection.

Some of the problems listed above can be avoided if the latitude-longitude grid is mapped in a continuous fashion rather than projected on a series of planes. One approach to continuous mapping on a flat surface is the projection of the earth onto a cylindrical surface which is then "unrolled." Such a projection, the Oblique Equidistant Cylindrical projection, was used for early TIROS hand gridding and backup Nimbus AVCS gridding. The use of the term "projection" may be somewhat

---

\* This assumes the entire tolerable error is obtained from allowing the picture principal point to be anywhere on the mid-50% of the subpoint track in the frame. If we consider that additional errors are present due to lack of perfect registration, height variations, etc., the maximum altitude for the system is probably around 500 nautical miles.

misleading since no unique projection point exists for the developed map. The generating line of the map is a great circle on the earth. Small circles lying in planes parallel to the great circle on the earth become lines parallel to the map generating line. This projection is similar in principle to the conventional equidistant cylindrical projection. However, the cylinder upon which the map is developed is skewed with respect to the poles. The projection is defined by the inclination of the great circle of contact between the cylinder and the earth's sphere.

The use of an OEC map is attractive because the satellite orbit approximates a great circle, at least in inertial space. The rotation of the earth under the satellite orbit makes the actual path of the satellite about the earth different from the great circle. However, for the purposes of mapping, the deviation is not sufficiently great to invalidate the concept. Figure 4-5 is a section of an OEC map with a sample subpoint track.

In obtaining a projection which is useful for a wide range of subpoints and which does not possess discontinuities of the grid lines, we lose the ability to include the effects of the curvature of the earth. Figure 2-2 and 2-3 shows the coverage on the OEC map obtained with the  $107^{\circ}$  lens (perfect attitude) as a function of satellite height. The pincushion distortion, apparent in the figure, can be compensated with a lens possessing the appropriate barrel distortion characteristics. This would unfortunately require a different lens for each altitude at which the satellite may orbit. The range of altitude which could be accommodated with a single lens, assuming altitude variation is the principal contributor to error, can be ascertained from the data of Figure 4-1.

An OEC map of the latitude-longitude grid could be photographed on a continuous film strip which could be run through the exposure (scanning) station in synchronism with the progression of the satellite in orbit. The film would be stretched flat in the exposure gate to keep the portion of the grid to be mixed into the picture in a single plane. The OEC map would always advance through the film gate in such a manner as to permit the heading line of the map to be a vertical line in the APT picture. A translation of the film in a direction perpendicular to the heading line is necessary to keep the subpoint track in the center of the picture. Since this translation is a function of latitude, the translation can be derived from the advance of the film coupled through a cam. Picture scaling as a function of altitude remains the most troublesome of the control functions since scaling calls for a change in the object-image spatial relationship for systems employing optical mixing.

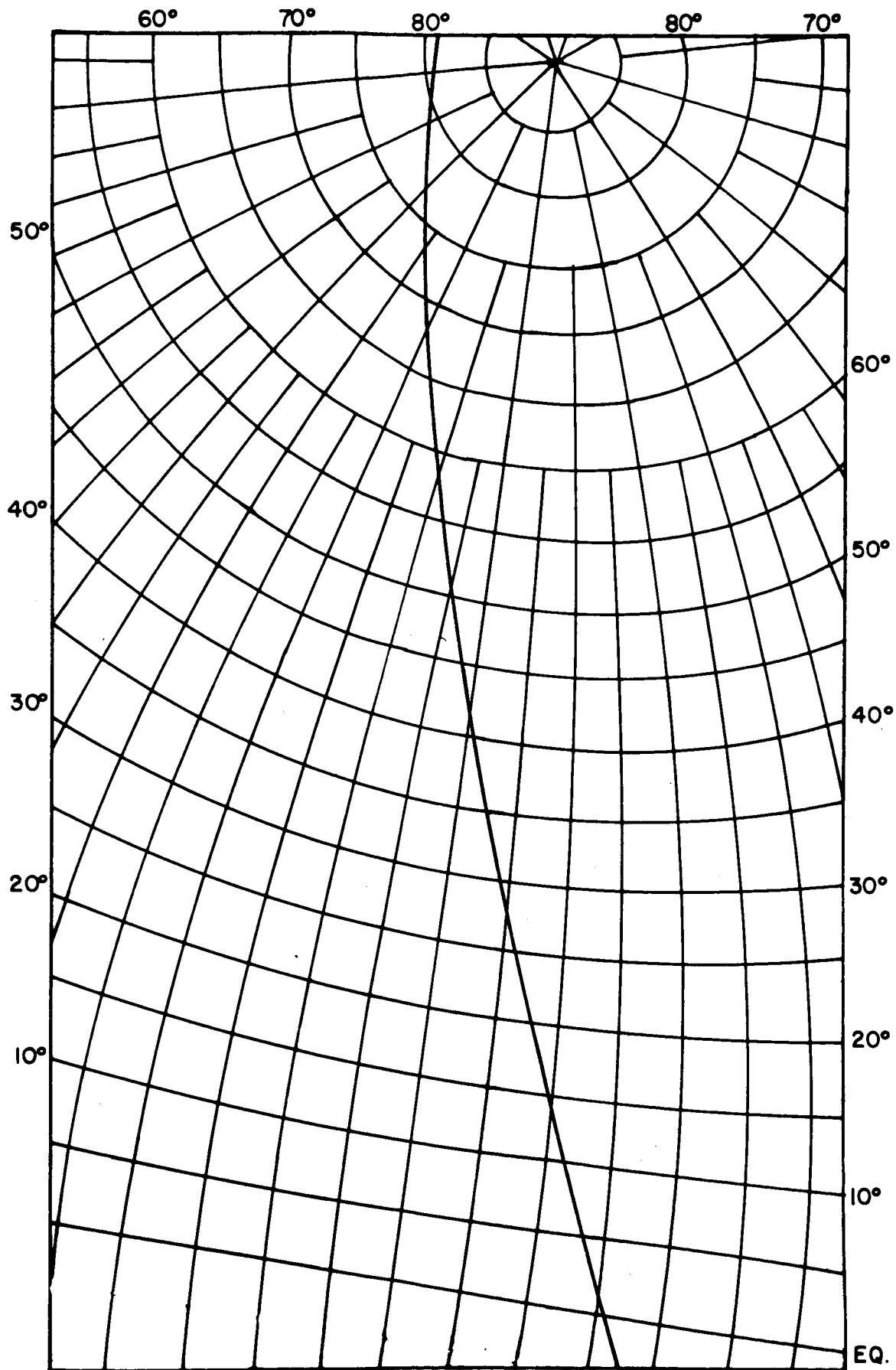


Fig. 4-5 Sample Subpoint Track on OEC Map



The use of an electronic scan of the OEC map offers several advantages. Picture scaling can be accomplished by changing the size of the scanning raster, eliminating the necessity to compensate mechanical motion. Secondly, the detection of a line in the scanner can be used to electronically generate a black-white mark for video mixing, permitting all lines or annotation to be visible independent of the picture background. The film strip could be run directly over the face of the scanner without an intermediate lens (a fiber optic faceplate on a miniaturized vidicon could well be employed). The radially symmetric barrel distortion required to compensate the effects of earth curvature might be obtained through the use of the appropriate magnetic lens in the vidicon.

One drawback to the electronic scan of the grid arises from the rather lengthy time of scan for a single picture. During the 200 second picture scan, the film strip would move several hundred miles past the subpoint for the time of picture taking. This necessitates a shrinking of the scanning raster along the direction of the subpoint track and unfortunately destroys the symmetry of the scan. The situation can be remedied in one of two ways: first, the film could be stopped after a picture is taken, remaining stationary during the scanning process. The film would then be rapidly advanced so that its position is correct for the next picture. This discontinuous type of motion is undesirable from the viewpoint of satellite dynamics. An alternative is the electronic generation of the asymmetrical scan. This is rather complicated since the horizontal and vertical components of the raster must be made a function of departure from the subpoint.

A second disadvantage of the electronic scan is the addition of error which results from position errors, nonlinearities, and magnetically influenced translations of the scanning beam. Since similar errors occur in the APT vidicon, very little of the tolerable 1% error is left for higher order deviations of the grid not corrected by scaling when compensating for height errors.

#### 4.3 GRID STORAGE ON A CYLINDER

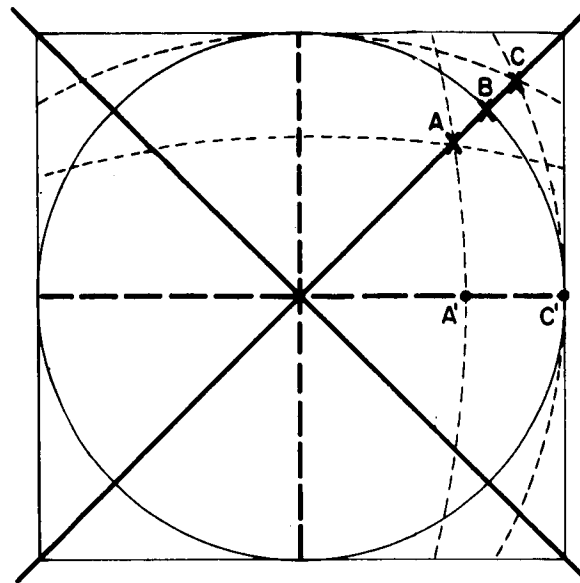
One of the methods of grid storage considered early in the study was the placement of the grid on a continuously rotating cylinder. The cylinder drive was to be a synchronous motor driven from the satellite clock through a digital divider set by ground command to keep the cylinder rotation synchronous with the rotation of the satellite in orbit. The grid stored on the cylinder was to be in the form of an Oblique Equidistant Cylindrical projection.

If an OEC projection is stored on a cylinder, a cylindrical lens must be used to compensate for the cylinder curvature to restore radial symmetry to the projection. However, it might be more attractive to use the curvature of the cylinder to aid in obtaining a picture grid which includes the effects of the curvature of the earth. The cylinder curvature compensates for the earth curvature along the generating line of the cylindrical projection. (The subpoint track departs a small distance from the generating line due to earth rotation; see Fig. 4-5.) A correction for the earth curvature, in a direction perpendicular to the generating line, can be obtained by bringing the edges of the map on the cylinder closer to the generating line an amount proportional to the distance between the edge and the generating line. This results in no error (assuming a linear transfer of cylinder object points to the image plane of the vidicon) for points along the subpoint track or for points in a line perpendicular to the track and lying on a line passing through the subpoint. The maximum error exists for those points which lie on a perpendicular set of lines passing through the subpoint and rotated  $45^{\circ}$  from the lines of zero error (the picture diagonals). The errors encountered as a function of altitude are shown in Figure 4-6. For the 400 nautical mile altitude the errors of a small percentage of the grid points contained in a circle inscribed in the picture and tangent to the borders barely exceed 1%. However, the errors grow rapidly with increasing altitude. Since there does not appear to be any feature of storage of the grid on the cylinder which makes the approach superior to storage of the grid on a film strip as described in the last section, further consideration of this approach was dropped.

#### 4.4 GRID STORAGE ON A SPHERE

Probably the most obvious method of presenting the grid to a scanner or lens is to rotate a sphere bearing inscribed latitude-longitude lines with respect to a scanner or lens aperture. The sphere is rotated with respect to the aperture in accordance with the rotation of the earth sphere relative to a "stationary" satellite. The most obvious advantage of the grid storage on a sphere is the completely distortionless grid projection which may be obtained for any altitude provided the grid is properly scaled as a function of altitude.

One problem is encountered in attempting to use a complete sphere. The axes around which the sphere must rotate to simulate earth rotation and vehicle progression in orbit are not perpendicular. If a perpendicular set of axes is to be used, the rotations must be divided into orthogonal components and a three axis drive employed. This leads to a very general system which can handle any orbit inclination.



$\eta = 20^\circ$  at  $A'$   
 $\eta = 43.5^\circ$  at  $C'$

#### ERROR FIELD

Error 0 along ——— lines  
 Error max along ——— lines

<u>h</u>	<u>A(%)</u>	<u>B(%)</u>	<u>C(%)</u>	(% Field of view)
400	0.17	1.14	2.95	
500	0.22	1.49	3.79	
600	0.26	1.89	4.69	
700	0.31	2.34	5.68	
800	0.36	2.86	6.73	

Fig. 4-6 Error Arising from Cylinder Approximation to Sphere

A digital programming of the drive motor rates allows the compensation of any orbit errors. The digital correction signals would be transmitted to the satellite from the CDA station and stored in memory on board the satellite. An orbit would be segmented in time and each segment would employ an independent set of correction values.

The sphere could be made approximately 4" in diameter and thus is practical from the size viewpoint.

Some rather severe problems arise in trying to optically mix the grid lines on the vidicon focal plane: (1) the extremely wide angular aperture of the lens ( $107^\circ$ ) makes any optical mixing scheme quite awkward; (2) optical mixing would entail a physical modification of the APT camera system.

A more practical mixing approach would involve the use of an electronic scan. However, the requirement for a 200 second scan of the image introduces the same problems listed at the end of Section 4.2 for the scan of the OEC map.

#### 4.5 FEASIBILITY OF ANALOG APPROACHES

The most attractive system appears to be that of Section 4.4 employing an electronic scan of the image. However, this system when compared to the digital systems of Section 3 suffers in several respects. The weight of the system with the sphere, digital memory, communications channel, 4 axis servo and electronic scanner is quite likely to exceed the 6.5 - 9 lbs of the digital systems. The power requirements will also be higher since the servos and some type of illumination draw power in addition to the digital circuitry needed for a flexible system.

Due to these problems and the difficulties associated with optical coupling or electronic scanning previously noted, no further consideration is given to the analog methods.

## SECTION 5

### GROUND COMPUTATION OF THE PICTURE GRID

#### 5.1 GENERAL

This section treats the problems at the ground complex related to preparing the compressed data format that will later be expanded in the satellite to form the grid and annotation. We must distinguish between computer programs and expedients that will be used for simulation, being fed into the breadboard system, and the eventual more sophisticated system that is to be used operationally. In order to cover these points logically, the first paragraphs of this section will be devoted to the general mathematics of gridding. Subsequent paragraphs will cover expedients for simulation, while concluding sections will consider the problems that may be involved in the use of the CDC 924 computer for operational message preparation.

#### 5.2 APPROXIMATION OF GEOGRAPHICAL GRIDS BY STRAIGHT LINES

##### 5.2.1 General Approach

This section describes a method for approximating the projection of a geographical latitude-longitude grid on a square satellite camera screen by a straight line grid network. The ground rules considered are that the satellite camera is at altitudes between 400 and 800 nm., the camera has a  $107^\circ$  field of view on the diagonal ( $87^\circ$  along the sides), and the displacement error of any point on the grid is to be no greater than one percent of the picture side dimension.

The method considered here consists of the replacement of circular arcs on the earth of latitude or longitude lines by straight lines in space and projecting these straight lines onto the camera screen.

##### 5.2.2 Lines of Constant Latitude

Consider first the case of constant latitude lines as indicated in Figure 5-1 by the circular arc ab covering a longitude range  $\psi$  at a latitude  $\phi$ . The best straight-line fit to this curve in this range of longitude is the line a'b', which lies in the plane

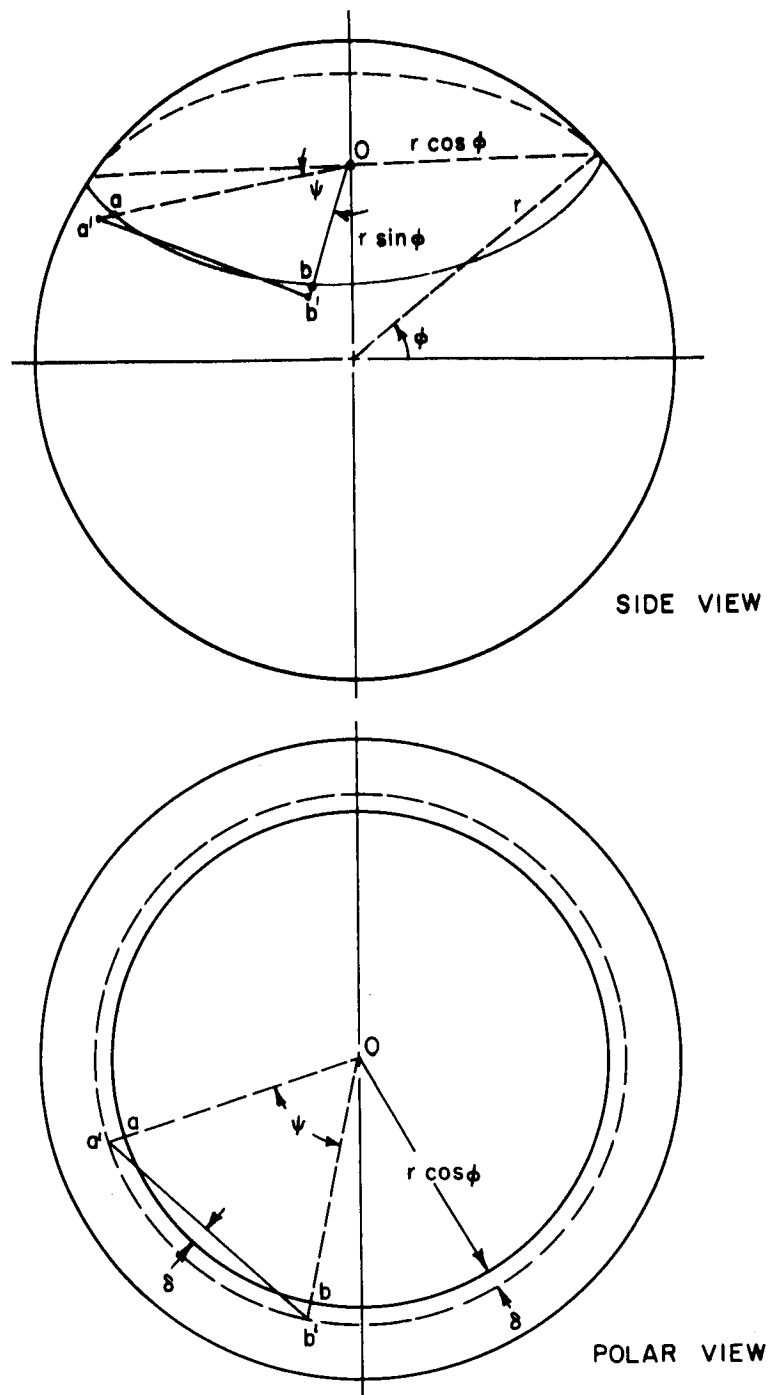


Fig. 5-1 Geometry of Constant Latitude Lines

aOb and which deviates from the curved line ab by not more than the distortion distance  $\delta$  everywhere, where  $\delta$  is given by the equation

$$(r \cos \phi + \delta) \cos (\psi/2) = r \cos \phi - \delta$$

where  $r$  is the radius of the earth, or, in a more convenient form

$$\delta = r \cos \phi \tan^2 (\psi/4) \quad (5.1)$$

For example, for an equatorial longitude range of  $\psi = 15^\circ$ , the distortion  $\delta$  is only 1 nm., and for  $\psi = 30^\circ$  is about 60 nm.

In order to plot the straight line a'b' on a satellite grid it is sufficient to plot the two points  $a'$  and  $b'$  on the grid, since a straight line in space projects onto an undistorted camera screen as a straight line. Plotting of these points is facilitated by noting that the points  $a'$  and  $b'$  can be considered to be points on a sphere of slightly greater radius than the earth and located at a slightly lower latitude, or specifically, the modified sphere properties are related to those of the earth by the equations

$$r \sin \phi = r' \sin \phi'$$

$$r \cos \phi + \delta = r' \cos \phi'$$

where primes designate the modified sphere. For small  $\delta$ , these equations reduce to the form

$$r' = r + \delta \cos \phi \quad (5.2)$$

$$\phi' = \phi - (\delta/r) \sin \phi$$

### 5.2.3 Lines of Constant Longitude

The geometry of lines of constant longitude is identical to that for equatorial ( $\psi = 0$ ) lines of constant latitude, or in other words, for lines of constant longitude the above discussion applies with Equations (5.1) and (5.2) replaced by the equations:

$$\delta = r \tan^2 (\psi/4) \quad (5.1a)$$

$$r' = r + \delta \quad (5.2a)$$

$$\phi' = \phi$$

#### 5.2.4 Error Analysis

The errors involved in the above straight line approximation procedure may be estimated as follows with respect to the allowable angular error ( $e$ ) at the camera. One percent of  $87^\circ$ , or  $0.0190$  radians<sup>†</sup>. The angular error involved in approximating any circular arc on the earth by a straight line may be conveniently estimated by considering the angular error as seen at the satellite along the horizontal centerline of the satellite camera screen (for constant latitude lines) or along the vertical centerline (for constant longitude lines).<sup>\*</sup> Then, in terms of the linear distortion distance, the maximum angular error  $e$  at the satellite corresponding to any point on the earth is

$$e = (\delta/r_1) \sin \tau \quad (5.5)$$

where

$\delta$  is the vector error in the straight line approximation

$r_1$  is the vector distance between the satellite and any point on the earth

$\tau$  is the angle between the  $\delta$  and  $r_1$  vectors

and where expressions for  $\tau$  and  $r_1$  are derived in Section 5.2.6 below. By combining Equation (5.1) with Equations (5.7) through (5.9), the angular error  $e$  seen at the satellite while at latitude  $\phi_s$ , for any straight line approximation covering a longitude angle range of  $\psi$ , is given by the expressions

$$\psi = 4 \tan^{-1} [e \sin \alpha / (\sin \beta \sin (\phi_s \pm \beta) \cos \phi)]^{\frac{1}{2}} \quad (5.6)$$

$$\tan \beta = \sin \alpha / [h/r + 2 \sin^2 (\alpha/2)] \quad (5.7)$$

where

$\phi_s$  is the satellite latitude

$\alpha$  is the great circle angle on the earth between the satellite and the latitude line under consideration (same as  $\phi - \phi_s$  if the north and south poles are not crossed)

$\phi$  is the latitude of the line considered

$\beta$  is the angular distance at the satellite between the satellite vertical centerline and the latitude line considered

Equation (5.4) is plotted in Figure 5-2 for altitudes of 400, 600 and 800 nm. for constant latitude lines at the center of the camera screen ( $\phi_s = \phi$ ;  $\beta, \alpha = 0$ ) and for one of the most distorted lines near the edge of the screen ( $2\beta \approx 87^\circ$ ;  $\phi_s - \alpha = \phi$ )

\* In this analysis, the vertical centerline is assumed to lie approximately in a meridian plane.

† The allowable angular error is  $1\% \times 2 \tan (\frac{1}{2} \times 87^\circ) = 0.0190$  radians



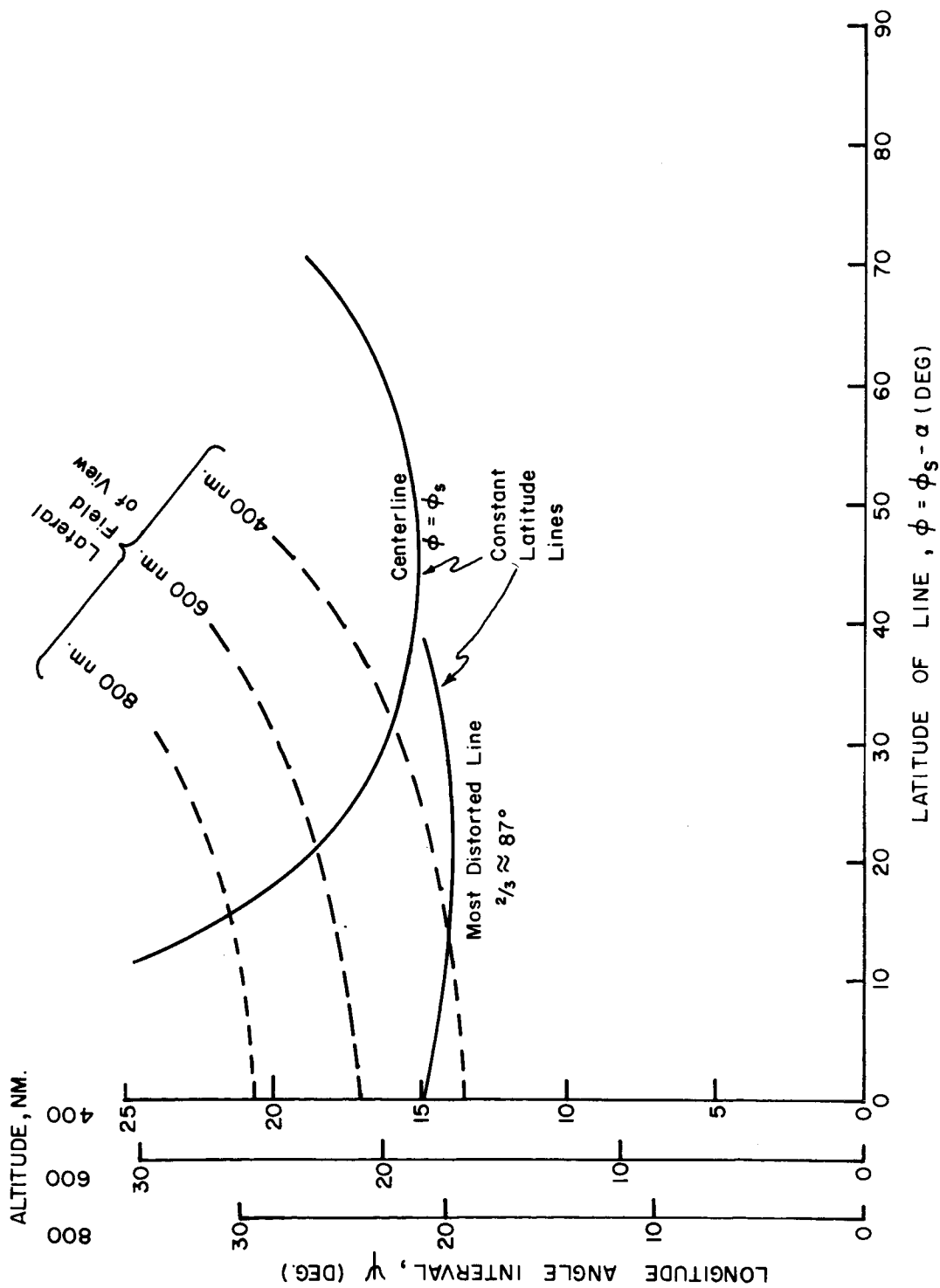


Fig. 5-2 Permitted Arc Length for Straight-Line Approximation

Also shown in Figure 5-2 is the lateral field of view on the camera screen, which is approximately equal to  $2a_{\max}/\cos \phi$  where  $a$  is given by Equation (5.5) with  $2\beta$ , the lateral camera angle, taken as  $87^\circ$ . It may be noted that for a 400 nm. altitude at low latitudes the permitted longitude angle interval exceeds the angular field of view, hence a single straight line approximation is adequate. For most other conditions, a two segment approximation is adequate.

The expression corresponding to Equation (5.4) for lines of constant longitude is (note Eq. (4.10)):

$$\psi = 4 \tan^{-1} [e \sin \alpha / (\sin \beta \sin (\alpha + \beta))]^{\frac{1}{2}} \quad (5.4a)$$

#### 5.2.5 Grid Construction

With the aid of the preceding equations an efficient straight-line latitude longitude grid may be constructed as follows.

Considering first any line of constant latitude ( $\phi_1$ ), it must first be decided what is the range of longitude on the satellite screen ( $\Delta\psi$ ). Next it must be decided how many straight line segments are needed to stay within the specified error on the camera screen. This may be done by solving Equation (5.4) for the maximum allowable range of  $\psi$  for any one straight line segment. Next, having decided the needed number of lines, the distance  $\delta$  is computed from Equation (5.1) at equally spaced values of  $\psi$  and modified earth sphere coordinates for the two endpoints of each straight line segment are computed from Equation (5.2). These endpoints are then subjected to a standard earth-to-camera-screen transformation to locate them on the camera screen and may then be connected by straight lines on the camera screen.

For lines of constant longitude the procedure is the same, except that Equations (5.1), (5.2), and (5.4) are replaced by Equations (5.1a), (5.2a), and (5.4a).

#### 5.2.6 Satellite-Earth Geometry

This section presents various satellite-earth geometrical relationships utilized in the earlier text. Figure 5-3 illustrates a satellite located at the point S at an altitude  $h$  at the latitude  $\phi_s$ . The satellite camera axis is in the plane of the paper, which is taken perpendicular to the north-south axis. The line SP of length  $r_1$  is a ray from the satellite intersecting the earth at the great circle angle  $\alpha$  from the sub-satellite

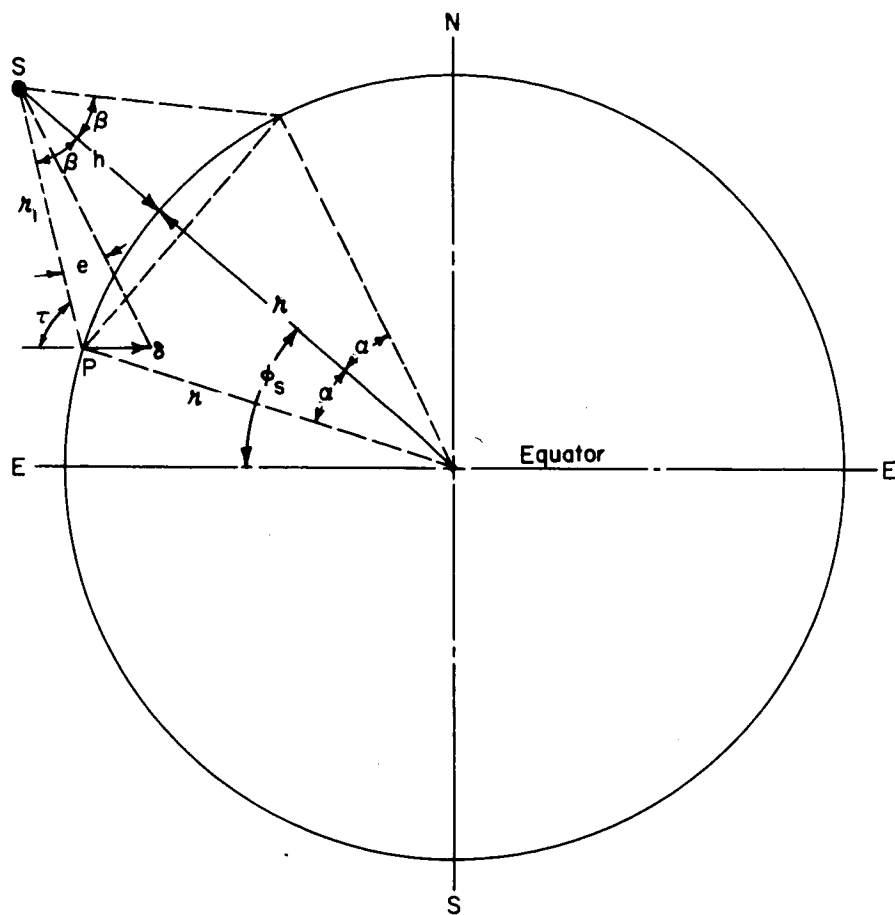


Fig. 5-3 Satellite-Earth Geometry

point. Also of interest is the angular deviation  $\beta$  of the ray from the satellite vertical and the angle  $\tau$  between the ray and a vector  $\delta$  parallel to the equatorial line EE. The following relationships between these variables may be obtained by inspection of Figure 5-3.

$$r \sin \alpha = r_1 \sin \beta \quad (5.6)$$

$$r \sin \alpha = [h + r(1 - \cos \alpha)] \tan \beta \quad (5.7)$$

$$\tau = \phi_s \pm \beta \quad (5.8)$$

where  $r$  is the earth's radius and the  $\pm$  in Equation (5.8) refers to points which are to the south (north) of the sub-satellite point. The angular distance  $e$ , as seen from the satellite, corresponding to the vector  $\delta$ , is

$$e = (\delta/r) \sin \tau$$

which, after application of Equation (5.6), takes the form

$$e = (\delta/r) \sin \tau \sin \beta / \sin \alpha \quad (5.9)$$

If the vector  $\delta$  is taken as vertical (i.e., perpendicular to the surface of the earth) instead of parallel to an equatorial axis, the above equations remain valid except that Equation (5.8) is replaced by the expression

$$\tau = \alpha + \beta \quad (\delta\text{-vertical}) \quad (5.10)$$

### 5.3 CALCULATION OF LATITUDE-LONGITUDE ELLIPSES

#### 5.3.1 Introduction

This section presents basic equations and describes several methods for computing latitude-longitude lines on the image screen of a satellite camera whose axis points to the center of the earth, the image screen being square and perpendicular to the camera axis. Sections 5.3.2 and 5.3.3 present equations and coefficients for computing constant latitude and constant longitude lines, respectively. Section 5.3.4 considers the calculation of intersections of these lines with the edges of the image screen. Sections 5.3.5 and 5.3.6 consider general and specific applications, respectively, of this information to the processing of these data to a form suitable for transmission to a satellite.

### 5.3.2 Constant Latitude Equations

All constant latitude curves will appear on the image screen as ellipses or segments of ellipses, the equations of which are (from Appendix A):

$$x = x_c - B_+ (y - y_c) \pm \sqrt{U_+ [W_+ - (y - y_c)^2]} \quad (5.11)$$

$$y = y_c - B_- (x - x_c) \pm \sqrt{U_- [W_- - (x - x_c)^2]} \quad (5.12)$$

where

$$\begin{aligned} x_c &= -\eta_0 \sin \gamma \\ y_c &= +\eta_0 \cos \gamma \\ B_{\pm} &= Q_{\pm} \sin 2\gamma / R_{\pm} \\ R_{\pm} &= Q_{\pm} \pm Q_{\mp} \cos 2\gamma \\ Q_{\pm} &= a_{\eta}^2 \pm a_{\xi}^2 \\ \bar{U}_{\pm} &= (R_+ R_- - Q_{\pm}^2 \sin^2 2\gamma) / R_{\pm}^2 \\ \bar{W}_{\pm} &= 2 a_{\eta}^2 a_{\xi}^2 / (R_{\pm} U_{\pm}) \end{aligned} \quad (5.13)$$

$$\begin{aligned} \eta_0 &= \zeta_0 \tan \alpha_3 \\ a_{\eta} &= \frac{1}{2} \zeta_0 (A_+ - A_-) \\ a_{\xi} &= \zeta_0 \left( \left[ \cos^2 \phi_1 \sin^2 (\phi_s - \alpha_3) - [(R/r) \sin \alpha_3 - \sin \phi_1 \cos (\phi_s - \alpha_3)]^2 \right] / \right. \\ &\quad \left. [(R/r) \sin \phi_s - \sin \phi_1]^2 \right)^{\frac{1}{2}} \end{aligned}$$

where

$$A_{\pm} = \sin (\phi_1 \pm \phi_s) / [R/r \pm \cos (\phi_1 \pm \phi_s)] \quad (5.14a)$$

$$\tan \alpha_3 = \frac{1}{2} (A_+ + A_-)$$

$$R = r + h \quad (5.15)$$

and

$x$  is the horizontal image screen coordinate  
 $y$  is the vertical image screen coordinate  
 $\phi_s$  is the satellite latitude  
 $\phi_1$  is the latitude of the curve considered  
 $r$  is the radius of the earth  
 $h$  is the satellite altitude  
 $\zeta_o$  is the distance of the camera screen forward of the focal point  
 $\gamma$  is the clockwise angle of the image screen Y-axis from a north-pointing direction

(See Appendix A for the meaning of intermediate symbols not defined above.)

### 5.3.3 Constant Longitude Equations

Constant latitude curves are also described by Equations (5.11), (5.12), (5.13) and (5.15). Equations (5.14a), however, are replaced by the equations (from Appendix A).

$$\begin{aligned}
 \eta_o^* &= \zeta_o \tan \alpha_3^* \\
 a_\eta^* &= \frac{1}{2} \zeta_o (A_+ - A_-) \\
 a_\xi^* &= \zeta_o \left\{ (\sin^2 (\phi_s^* - \alpha_3^*) - [(R/r) \sin \alpha_3^*]^2) / [(R/r) \sin \phi_s^*]^2 \right\}^{\frac{1}{2}} \\
 \tan \alpha_3^* &= \frac{1}{2} (A_+ + A_-) \\
 A_\pm &= \pm \sin \phi_s^* / (R/r \pm \cos \phi_s^*) \\
 \sin \phi_s^* &= \cos \phi_s \sin (\lambda - \lambda_s)
 \end{aligned} \tag{5.14b}$$

where

$\lambda_s$  is the satellite longitude (east)  
 $\lambda$  is the longitude (east) of the curve considered

and where asterisks are used above to distinguish quantities for constant longitude lines from those for constant latitude.

#### 5.3.4 Calculation of Terminal Points of Ellipses

In order to compute practically the latitude-longitude ellipses, it is first necessary to compute the initial and terminal points for each segment of each ellipse appearing on the image screen, plus all minimum and maximum points on each curve appearing on the screen. In addition, these points must be ordered in pairs connecting single valued curve segments with the first point of each pair having the smaller (or larger) value of  $y$ . One procedure for accomplishing this is described below.

There are at most eight possible intersections of an elliptical curve with a square image screen, the coordinates of which may be easily calculated by simultaneous solution of the ellipse Equations (5.11) or (5.12) with the four straight line equations  $x = \pm H$ ,  $y = \pm H$ , where  $H$  is the half-width of the screen. More specifically the equations for the eight numbered point intersections in Figure 5-4 are

$$x = x_c - B_+ (y - y_c) \pm \sqrt{U_+ [W_+ - (y - y_c)^2]} \quad (5.16)$$

$$y = y_c - B_- (x - x_c) \pm \sqrt{U_- [W_- - (x - x_c)^2]} \quad (5.17)$$

where the constants are defined by Equations (5.13). For points 8 and 1 (5 and 4), Equation (5.16) applies with the upper sign for point 1 (6) and with  $y = -H$  (+H); for points 2 and 3 (7 and 6), Equation (5.17) applies with the upper sign for point 3 (6) and with  $x = +H$  (-H). These eight points will not in general all fall on the image screen and may not even exist; e.g., points 1 and 8 do not exist for the dashed curve in Figure 5-4. In the latter case, where there is no intersection of an ellipse with the line for  $y = -H$  (or  $y = +H$ ) the minimum (maximum) point for each ellipse (designated as 8', 1' in Figure 5-4) must be computed, each such point being considered as two separate but identical points. The coordinates of these points and the similar points 4' and 5' are

$$\begin{aligned} y_{8,1} &= y_c - \sqrt{W_+} & ; & & x_{8,1} &= x_c + B_+ \sqrt{W_+} \\ y_{4,5} &= y_c + \sqrt{W_+} & ; & & x_{4,5} &= x_c - B_+ \sqrt{W_+} \end{aligned} \quad (5.18a)$$

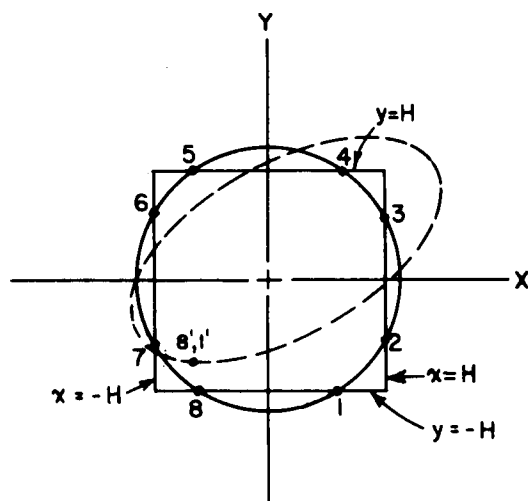


Fig. 5-4 Intersections of Ellipses with Image Screen Edges



ilarly, if points 2 and 3 (or 6 and 7) are not on the line  $x = +H(-H)$ , alternate  
nts are calculated from the equations

$$\begin{aligned} x_{2,3} &= x_c + \sqrt{W_-} \quad ; \quad y_{2,3} = y_c - B_- \sqrt{W_-} \\ x_{6,7} &= x_c - \sqrt{W_-} \quad ; \quad y_{6,7} = y_c + B_- \sqrt{W_-} \end{aligned} \tag{5.18b}$$

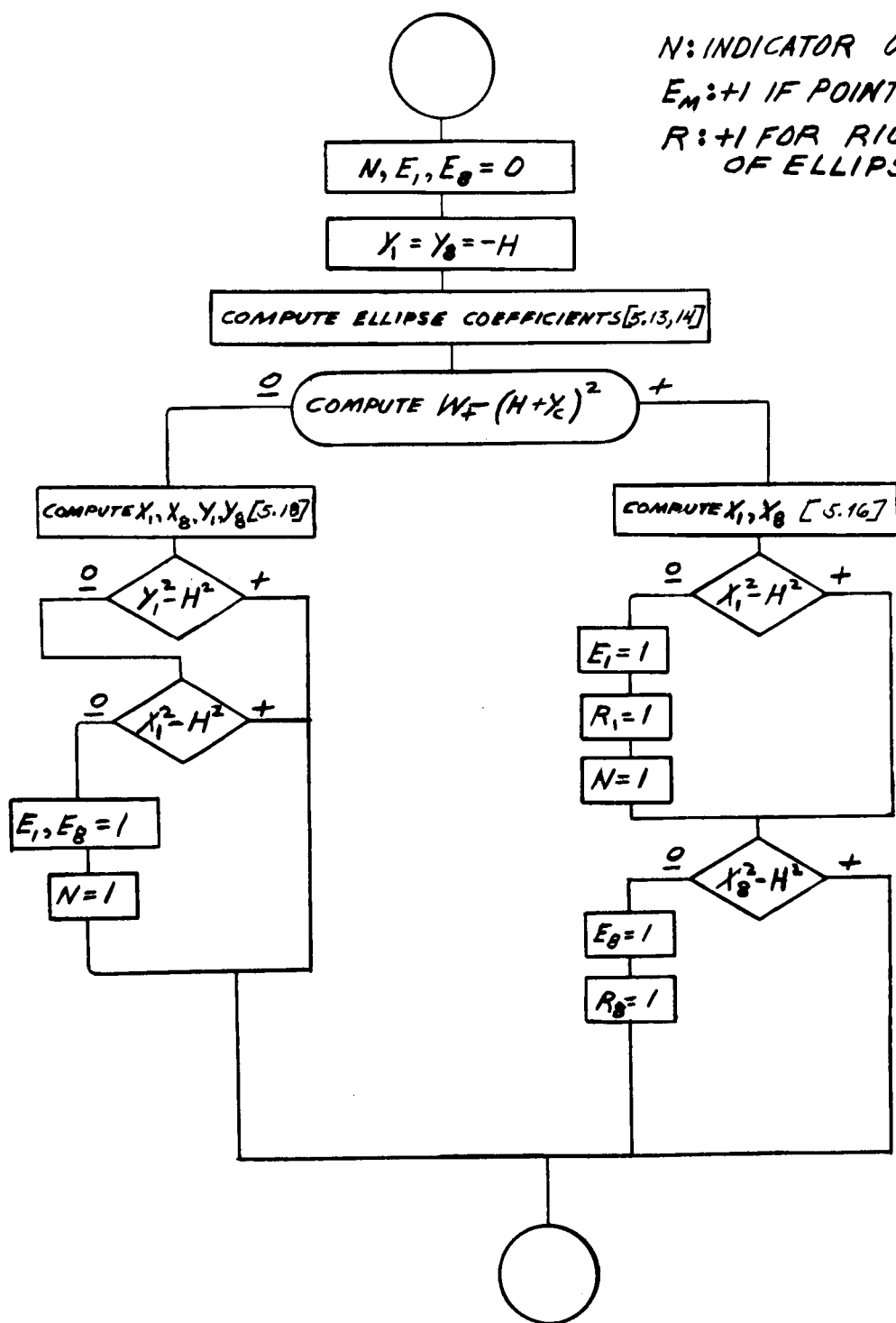
With the aid of the preceding equations, the pairs of real terminal points of  
gments of ellipses may be computed as follows.

1. Compute  $(x_1, y_1)$  and  $(x_8, y_8)$  according to the block diagram in Figure 5-5.  
e right hand side of this diagram refers to the case where the ellipse intersects  
curve  $y = -H$ , and the left hand side to other cases. The parameter  $E_n$  in this  
gram is plus if the point falls on the image screen and zero if off the screen. The  
parameter  $N$ , when positive, indicates the first point computed in the sequence 1-8  
cluding 1', 2', etc., if computed) which appears on the image screen and at which  
ellipse enters the screen, moving counterclockwise around the border of the screen.  
+1 (0 indicates the right (left) hand branch of the ellipse.
2. Compute  $(x_2, y_2)$  and  $(x_3, y_3)$  according to the block diagram in Figure 5-6.  
e symbol  $S_n$  designates a computation of the sign of the slope of the ellipse curve  
/dx) at the point  $n$  (0 if positive and +1 if negative).
3. Compute  $x_4, y_4$  through  $x_7, y_7$  in a similar manner.
4. This process results in a table of the form illustrated below, which may  
used as a point of departure for the subsequent discussion.

Table 5-1  
Screen Edge Intersection Data

$$N = \quad \eta_b = \quad ; \quad Y =$$

Point (n)	$x_n$	$y_n$	$E_n$	$S_n$	$R_n$
1					
2					
.					
.					
8					



$N$ : INDICATOR OF FIRST REAL  
 $E_M$ : +1 IF POINT  $N$  EXISTS  
 $R$ : +1 FOR RIGHT HAND  
 OF ELLIPSE.

FIG. 5-5  
 BLOCK DIAGRAMS FOR INTERSECTIONS AT  $Y = -H$

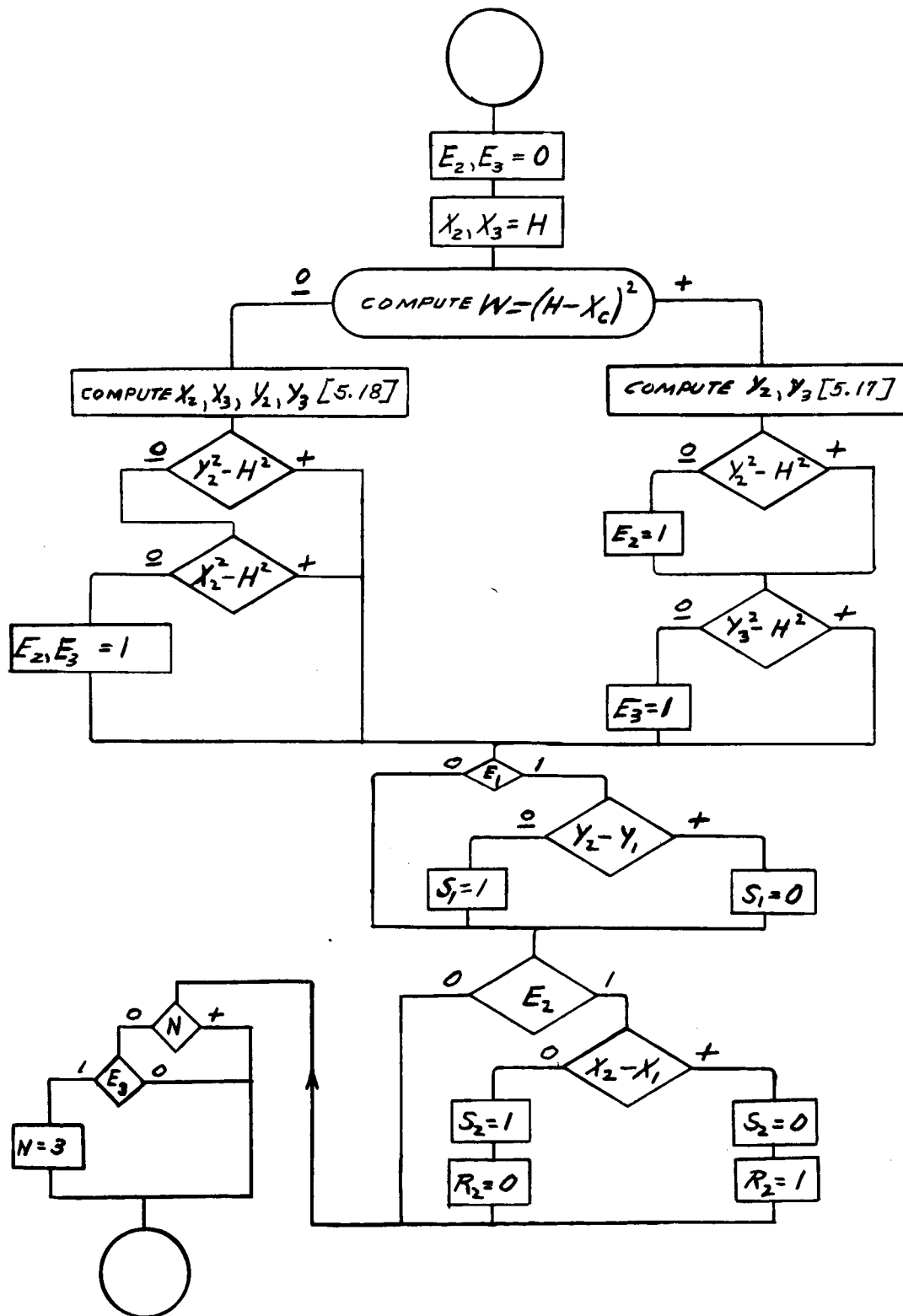


FIG. 5-6  
BLOCK DIAGRAMS FOR INTERSECTIONS AT  $X=H$

5. The resulting points may be ordered in pairs in the manner illustrated by the block diagram in Figure 5-7. This process examines all not already rejected (off screen) points in the sequence 1-8 (for  $v > N$ ), discards points beyond the horizon ( $T$ ,  $a_\eta$  tests; see Appendix A for definition of  $\eta_b$ ), rejects (without further tests) the second point of a pair if the first point is beyond the horizon ( $RJ = 1$ ), pairs points for the two ends of each ellipse segment, and assigns the designations  $y_U, x_U$  ( $y_L, x_L$ ) to the larger (smaller) of the values of  $y, x$  for a point pair.

The preceding illustrates all steps in the image plane latitude-longitude line segment end point and pairing calculations except for the case of meridian lines which are to be terminated in the interior of the image screen at near polar latitudes. (These terminations may be taken into account by computing the  $x, y$  coordinates of such terminal points and modifying Figure 5-7 accordingly to delete or add line segment end points as required by the location of the added points.)

#### 5.3.5 General Approach to Generation of Transmitted Data

This section outlines procedures and presents flow diagrams illustrating the generation of numerical data defining latitude-longitude grid lines through use of the ellipse equations and screen edge intersection data for these lines. This section is restricted to considerations of steps common to several methods of data transmission to the satellite (Methods CM-1A, CM-1R and CM-2L), whereas details of the specific methods are given in Section 5.3.6.

For all of the methods considered in this section for generating latitude-longitude grid line data to transmit to a Nimbus satellite, the procedure outlined in Figure 5-8 is presumed to be followed. That is: (1) the needed ellipse coefficients are generated for each possible ellipse appearing on the satellite screen, using the equations of Sections 5.3.2 and 5.3.3; (2) coordinates of all existing intersection points of these ellipses with the screen edges are evaluated; (3) intersection points are arranged by pairs describing the two endpoints of each grid line segment appearing on the satellite screen; (4) pairs are arranged sequentially in the order of their appearance on the satellite screen; and (5) the preceding information is converted to an appropriate message to be transmitted to the satellite (Sec. 5.3.6). Steps (1) through (4) are almost identical for the various methods considered here and are briefly discussed below. Step 5 depends strongly on the particular satellite computer operation and is discussed in Section 5.3.6 for several of the methods considered in this study.



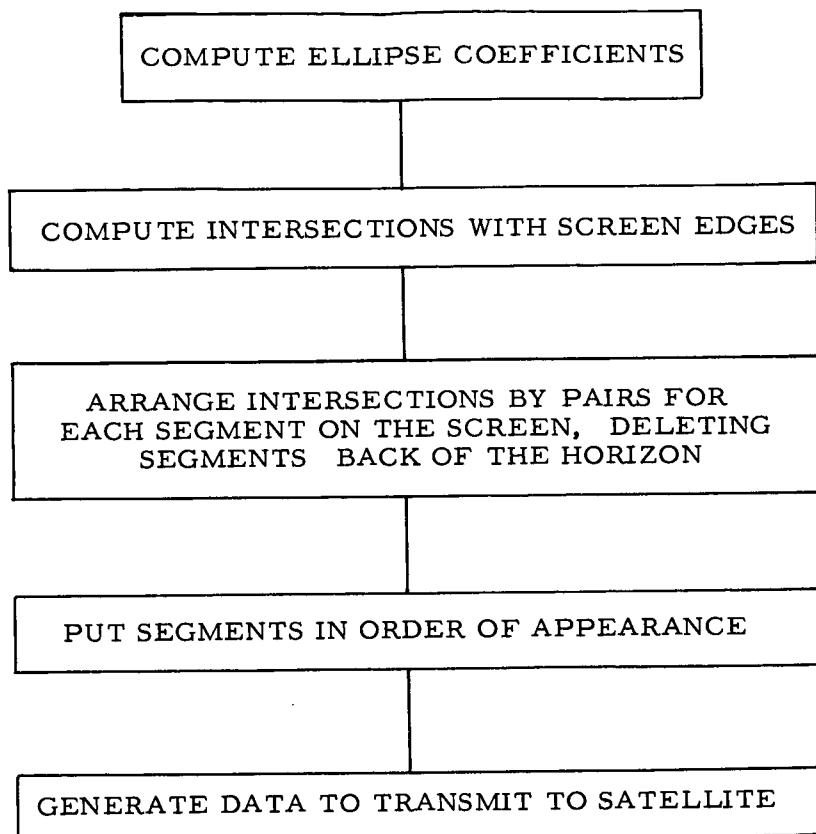


Figure 5-8

General Program for Generating Ellipse  
Data to Transmit to a Satellite

Identification and evaluation of ellipse coefficients for all latitude-longitude line segments appearing on the satellite screen may be accomplished as follows.

1. Determine the satellite subpoint latitude and longitude ( $\phi_s$  and  $\lambda_s$ ) and round these off to the nearest integer values to be plotted ( $\phi_{so}$  and  $\lambda_{so}$ ).
2. Calculate the ellipse coefficients for this constant latitude line (Sec. 5.3.2), and calculate intersections of this ellipse with the screen edges (Sec. 5.3.4).
3. Increase and decrease the initial latitude progressively by the desired latitude interval between grid lines, repeating step 2, until upper limit and lower limit constant latitude lines are reached which do not appear on the satellite screen.
4. For meridian lines follow a procedure similar to steps 2 and 3.
5. For each ellipse, pair off points corresponding to the two ends of all ellipse segments (Sec. 5.3.4), deleting (unseen) segments beyond the horizon and unwanted near-polar sections of meridian lines.
6. The result of the above process is a table in computer storage more or less of the form of Table 5-2 (which applies specifically to Methods CM-1A and CM-1R), with some variations depending on the subsequent desired use of the information. The

Table 5-2

Input Data - Methods CM-1R and CM-1A

$N_i$	$y_U$	$y_L$	$x_U$	$x_L$	S	R	$x_c$	$y_c$	$B_+$	$U_+$	$W'_+^*$	SK	END
1												0	0
2												0	0
3												0	0
.												0	0
.												0	0
.												0	0
NR												0	0

contents of this table consist of NR rows corresponding to the number of grid lines appearing on the camera screen.  $y_U$  ( $y_L$ ) is the y-coordinate of the upper (lower) end of the grid line and  $x_U$  ( $x_L$ ) is the x-coordinate of the right (left) hand end of the grid line. S is an indicator of the grid line slope (0 (1) for dy/dx positive (negative)); R is an indicator of the branch of the ellipse (R = 1 (0) for the right (left) hand branch).

---

\*  $W'_\pm = W_\pm U_\pm$

The remaining coefficients are ellipse equation coefficients (see Sec. 5.3.2), except for the columns SK, END, which are peculiar to Methods CM-1R and CM-1A (see Sec. 5.3.6.1).

7. Further processing of the data now depends strongly on the specific form of the desired message to the satellite and is discussed in Section 5.3.6 for methods CM-1A, CM-1R and CM-2L<sub>B</sub>.

### 5.3.6 Specific Methods of Generating Transmitted Data

This section presents sample flow diagrams illustrating the computation steps for translating the ellipse segment data generated as indicated in Section 5.3.5 into a satellite message for Methods CM-1A, CM-1R and CM-2L<sub>B</sub>.

#### 5.3.6.1 Method CM-1A

The satellite message for method CM-1A is of the form

y x x x x y x x . . .

where each group of y x x x represents a horizontal line on the television sweep where y is the screen vertical coordinate (or line marker) and x x x are the values of the x-coordinate at which grid marks are to be made.

The starting point for generating this message is Table 5-2, whose contents are described in Section 5.3.5. The data in this table is processed as indicated in Figure 5-9 (see also Figs. 5-10 and 5-11 and Table 5-3). For each allowable vertical

Table 5-3

Intermediate Data - Methods CM-1A and CM-1R

x*	1	2	3	.	.	.	200
XR	0	1	1	0	1	0	0

---

\* In this table. values of x refer to rounded off integer values of x on a scale of 200, measured from the left edge of the screen. Equations in the text have values of x and y referenced to the center of the screen.





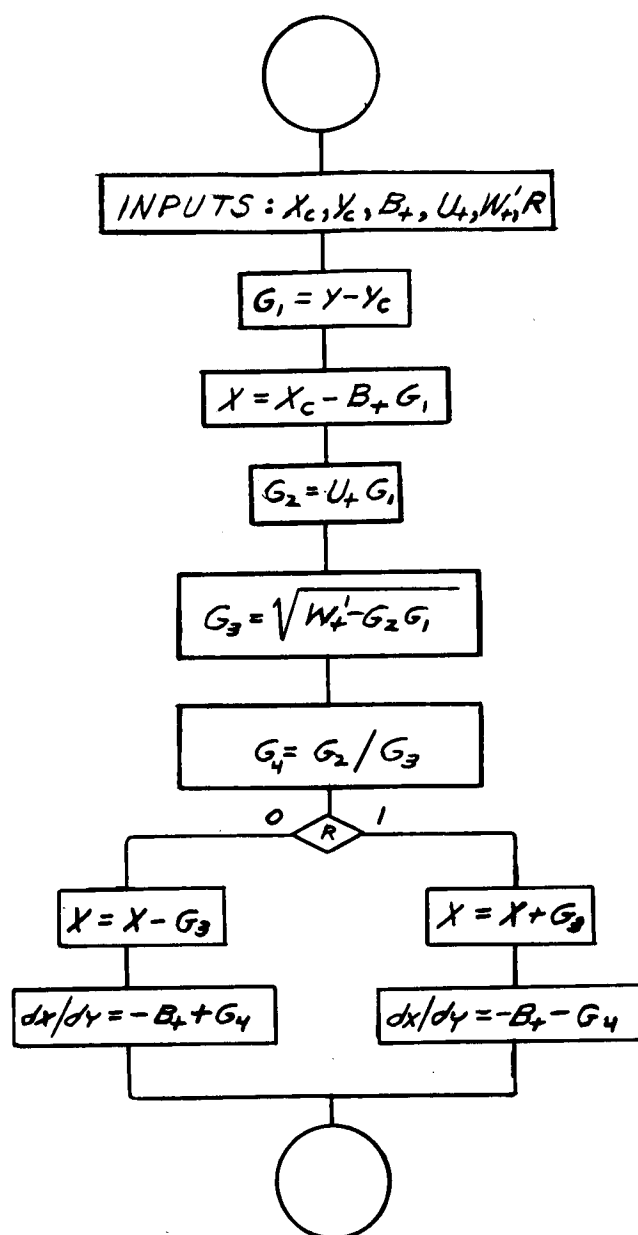


FIG. 5-10  
CALCULATION OF  $X$  AND  $dx/dy$

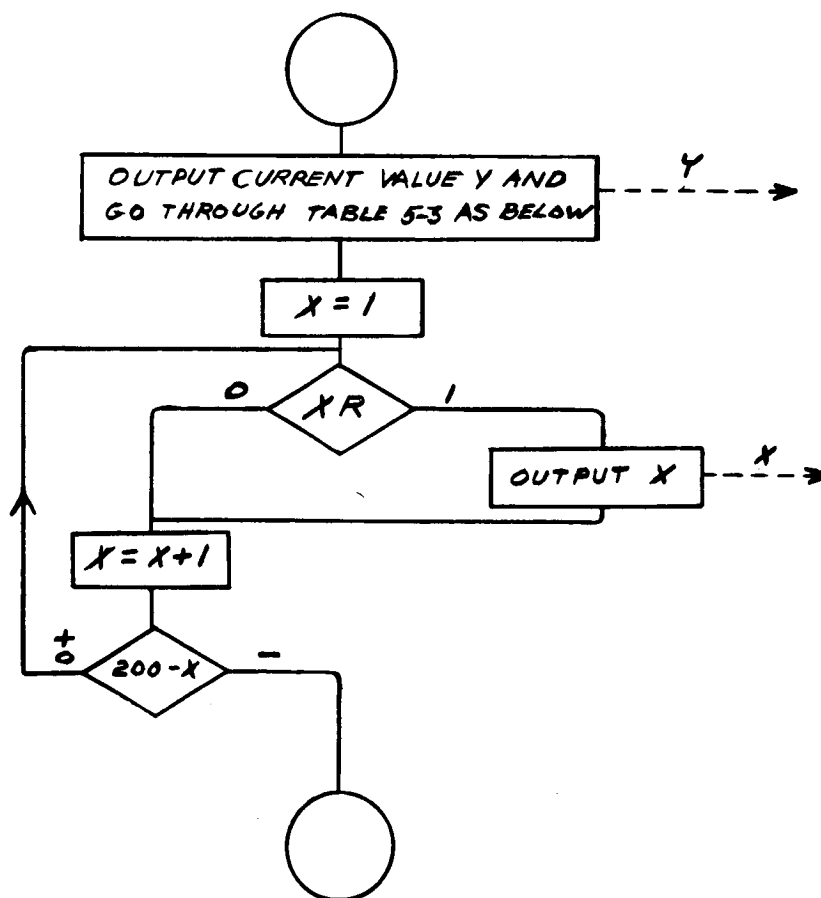


FIG. 5-11  
GENERATION OF TRANSMITTED DATA - METHOD CM-1A  
ADJ ROUTINE

location  $y$  on the image screen the computation in Figure 5-9 proceeds as follows.\* Each grid line is first examined to see if the grid line has already ended at a preceding (larger) value of  $y$  ( $END = 1$ ), to see if the grid line has started yet ( $AN = 1$ ), and if it has started, whether it is desired to put a grid mark on this sweep line ( $SK = 0$ ) or to skip a line ( $SK = 1$ ). If the line is nearly horizontal, more than one point may appear to the right or/and left of the first computed point  $x$ ; values of  $x$  for these points (designated  $x_d$ ) are supplied by the circuits involving  $S_c$  and  $P$ , where the two values of  $S_c$  correspond to points left and right of the first-computed point  $x$  and  $P$  is an indirect counter of the number of allowed multiple points.

Each valid computed grid point location ( $x$  or  $x_d$ ) is entered into Table 5-3 as a +1 in the XR column at the appropriate value of  $x$ . At the conclusion of computations for each value of  $y$ , the information in Table 5-3 is processed as indicated in Figure 5-11, the accumulation of the output of this circuit being the final message to the satellite.

#### 5.3.6.2 Method CM-1R

The satellite message for Method CM-1R is of the form

$$y \ x \ \Delta \ x \ \Delta \ x \ y \ \Delta \ x \ \Delta \ x \ \dots$$

where each group of  $y \ x \ \Delta \ x \ \Delta \ x$  represents a horizontal line on the television sweep, where  $y$  is the screen vertical coordinate,  $x$  is the  $x$ -coordinate for the first grid mark point on the line and the  $\Delta \ x$ 's are the increments in  $x$  to reach the next grid mark point. Generation of this type of message is identical to that described above for Method CM-1A except for the trivial difference that Figure 5-12 replaces Figure 5-11.

#### 5.3.6.3 Sector Coding Method CM-2L<sub>B</sub>

The satellite message for Method CM-2L<sub>B</sub> is of the form (ignoring erase information)

$$y \ x \ SAC \ y \ x \ SAC \ y \ m \ \dots \ m \ x \ SAC \ y \ m \ \dots$$

(see Section 3.2.4.3 and Figures 3-23 and 3-24), where  $y \ x$  are the coordinates of the start of a grid line in a sector designated by the code SAC and the  $m$ 's designate line increment distances in the corresponding sector.

In order to generate the information to be transmitted to the satellite for Method CM-2L<sub>B</sub> the following procedure may be as follows. It is assumed here that (1) the ellipse coefficients have been generated (Sections 5.3.2 and 5.3.3), (2) that

---

\* The operations indicated in Figure 5-9 assume that the grid line data in Table 5-2 have been arranged in order of first appearance of the lines as seen by the television sweep.

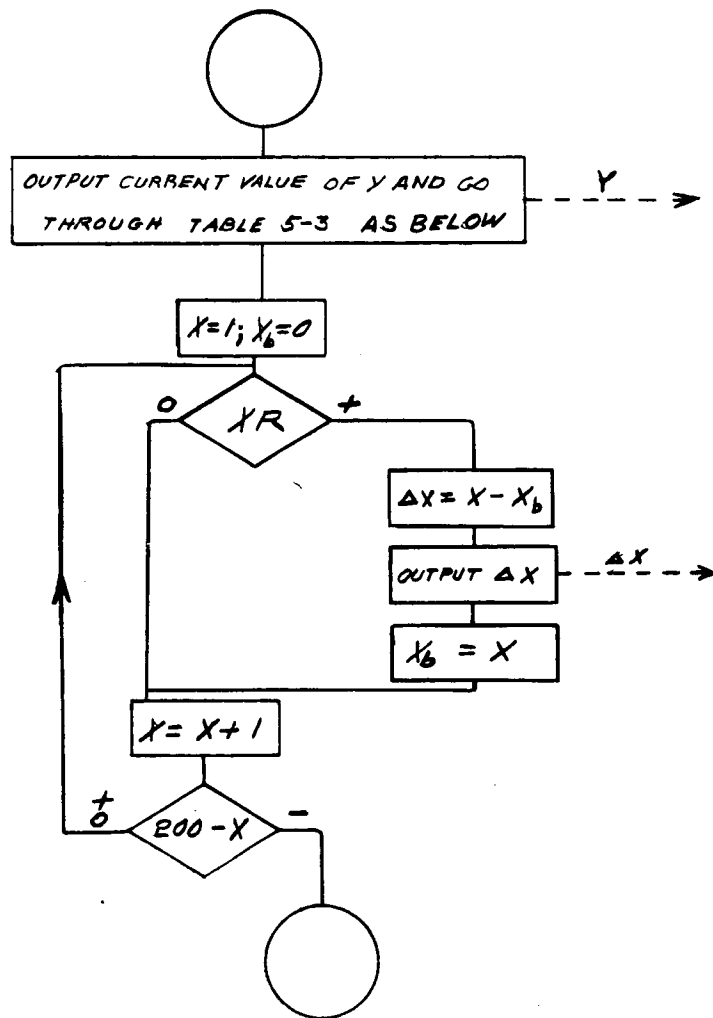


FIG. 5-12

GENERATION OF TRANSMITTED DATA - METHOD CM-1R  
ADJ ROUTINE

intersections with screen edges have been calculated (Sec. 5.3.4) and (3) that intersection points have been paired for each grid line, pairs beyond the horizon deleted, and grid lines placed in order of their encounter by the television sweep (Sec. 5.3.5). These previous steps result in a data table of the form given in Table 5-4 (similar to Table 5-2), which will be used as the starting point for the following discussion.

Table 5-4 contains the following initial information for each grid line ( $N_1$ ):

$y_a, x_a$	integer coordinates of upper end of grid line
S	+1 for initial slope $dy/dx$ negative (0 otherwise)
R	+1 (-1) for right (left) hand branch of ellipse

the remaining parameters being defined in Section 5.3.2 or 5.3.3.

This initial data Table 5-4 is to be used as indicated in Figure 5-13. First, the initial slope of a grid line ( $dx/dy$ ) is evaluated (see Fig. 5-10). From this slope, it may be decided from Figure 5-14 which of the eight possible sectors this grid line first appears in (CT = 1 to 8 clockwise from a horizontal eastward direction), and the required sector coding parameters SAC may be evaluated.

Next, each grid line may be specified by a sequence of numbers of the form (see Sec.3.2.4.3)  $y \ x \ SAC \ L \ m_1 \ m_2 \ m_3 \ . \ . \ . \ m_L \ y \ x \ SAC \ L \ . \ . \ . \dagger$  by following the computation procedure indicated in Figures 5-15 through 5-17, the results being entered into Table 5-5. More specifically, this stage of computation consists of entering the flow diagram of Figure 5-15 at the initial value of CT, proceeding to calculate L and  $m_1, \dots, m_L$  for all points in the sector in the manner illustrated in Figure 5-16 for the typical sector where CT = 3 (see also Figs. 5-17 and 5-10). Next, transfer is made to an adjacent sector as indicated in Figure 5-16 (unless the line ends), giving the new sector starting data  $y \ x \ SAC$ , and so on. (Some details of the block diagram of Fig. 5-16 are indicated in Fig. 5-17).

The end result of this process for all grid lines may conveniently be entered in a storage table of the form of Table 5-5.

It is next desired to process the information in Table 5-5 (for individual grid lines) to mix data for different grid lines and to reassemble the data in Table 5-7 according to the requirements of the satellite transmission message for this method. This process is achieved by first following the block diagram of Figure 5-18\* (see also Fig. 5-19 and Table 5-7), which for each horizontal line on the television camera, generates the data in Table 5-6, which is, after completion of each screen line calculation, transferred to Table 5-7, which is the final message to the satellite. (Dashed line arrows in Fig. 5-18 designate transfer of the indicated quantity to the table indicated at the point of the arrow.)

$\dagger$  L is the number of points in the corresponding sector for a grid line.

\* When reference is made to values of S, A, C and L in this figure, the  $D_L^i$ th group of these quantities appearing in Table 5-5 is meant; values of m correspond to the  $D_m^i$ th value of m in this table.

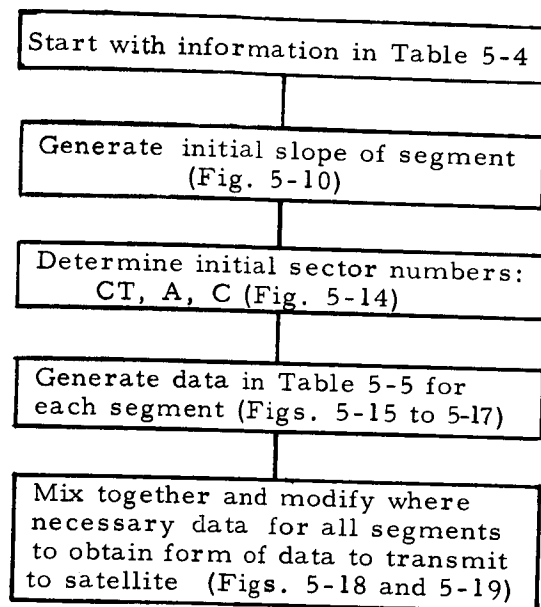


Figure 5-13

Outline of Computations for Method CM-2L<sub>B</sub>

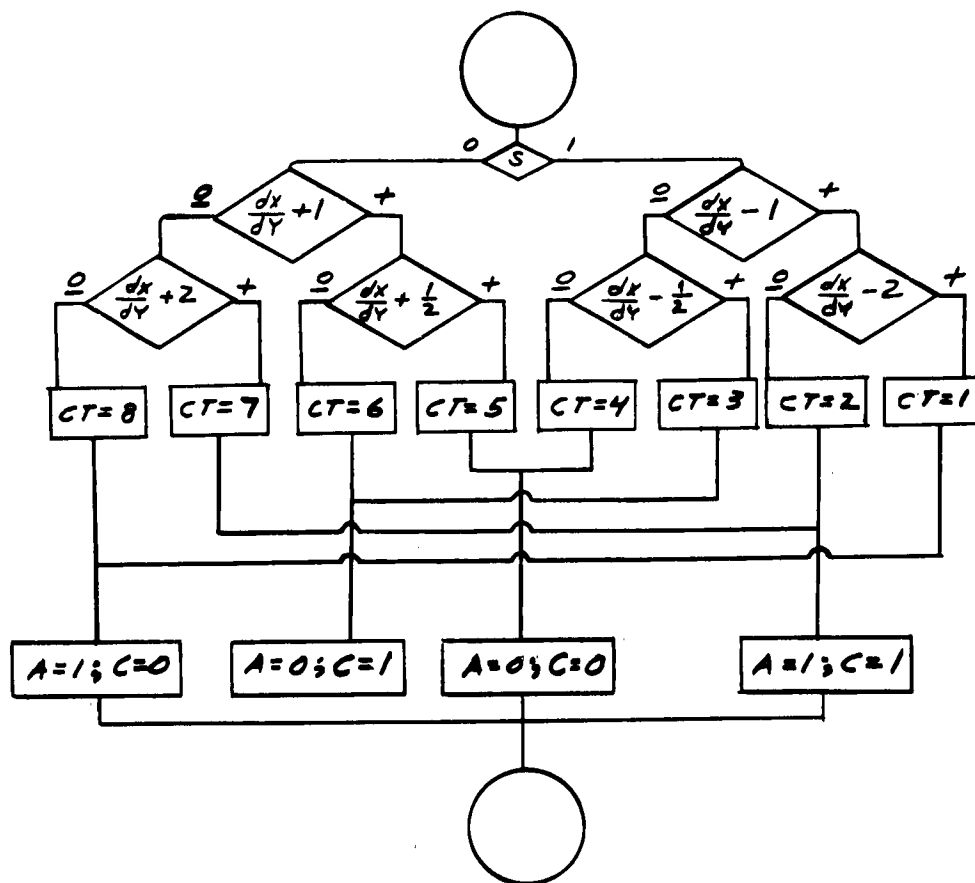


FIG. 5-14

# GENERATION OF CT, A, C COEFFICIENTS

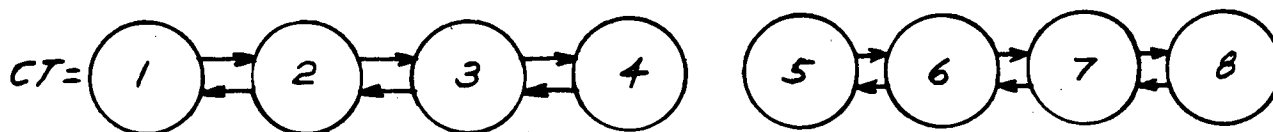


FIG. 5-15

# FLOW DIAGRAM FOR GENERATING SECTOR DATA FOR INDIVIDUAL GRID LINES





1.  $y_a$  and  $x_a$  are the integer coordinates of a grid point under consideration, which are updated after each new point calculation. X and Y are the coordinates of the next point for a given grid line. X is initially calculated exactly and then rounded off to the nearest integer (or truncated). The rounding off process is not indicated in the diagram.
2. The first V test decides if a line has ended yet (+)
3. The second V test decides if the point under consideration is one unit to the right of the last point (0), or to the right (+) or left (-) of this point.
4. The V-1 test decides if the point under consideration is two units to the right of the last point (0) or farther to the right (+).
5. The L tests decide if the point considered is the first point in a sector (0).
6.  $D_m$  is a counter for the number of points in a grid line,  $D_L$  is a counter for the number of sectors traversed by a grid line and  $N_L$  is the total number of sectors traversed by a grid line. m is a coefficient (0 or 1) defining the location of a grid point with respect to the preceding grid point. SAC is a sector code. The Y-distance between adjacent points in this sector is always two units.
7. Dashed-line arrows designate transfer of the indicated quantities to Table 5-5.

Figure 5-17  
Comments on CT Circuit

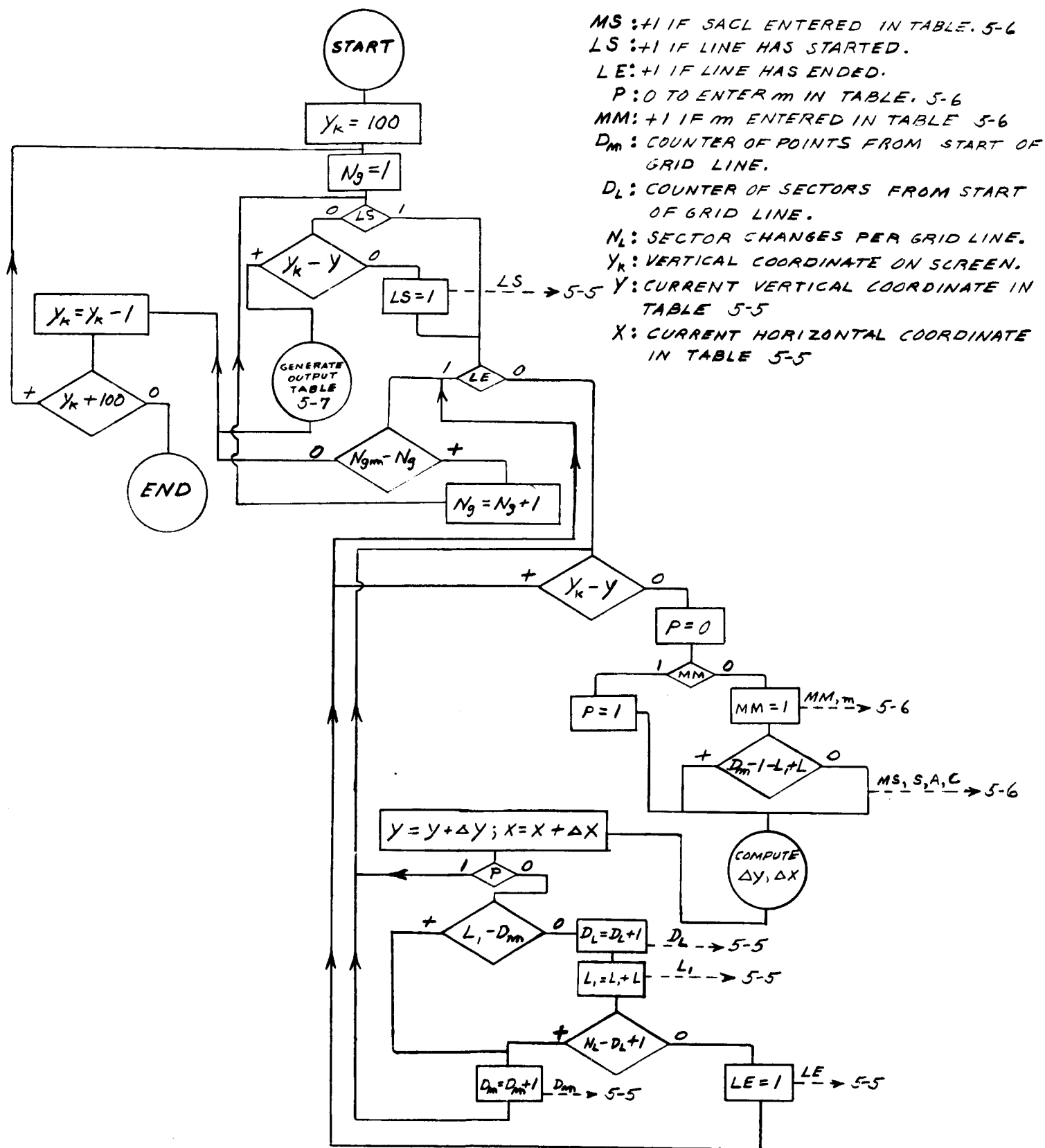


FIG. 5-18

BLOCK DIAGRAM FOR MIXING SECTOR DATA FOR DIFFERENT GRID LINES

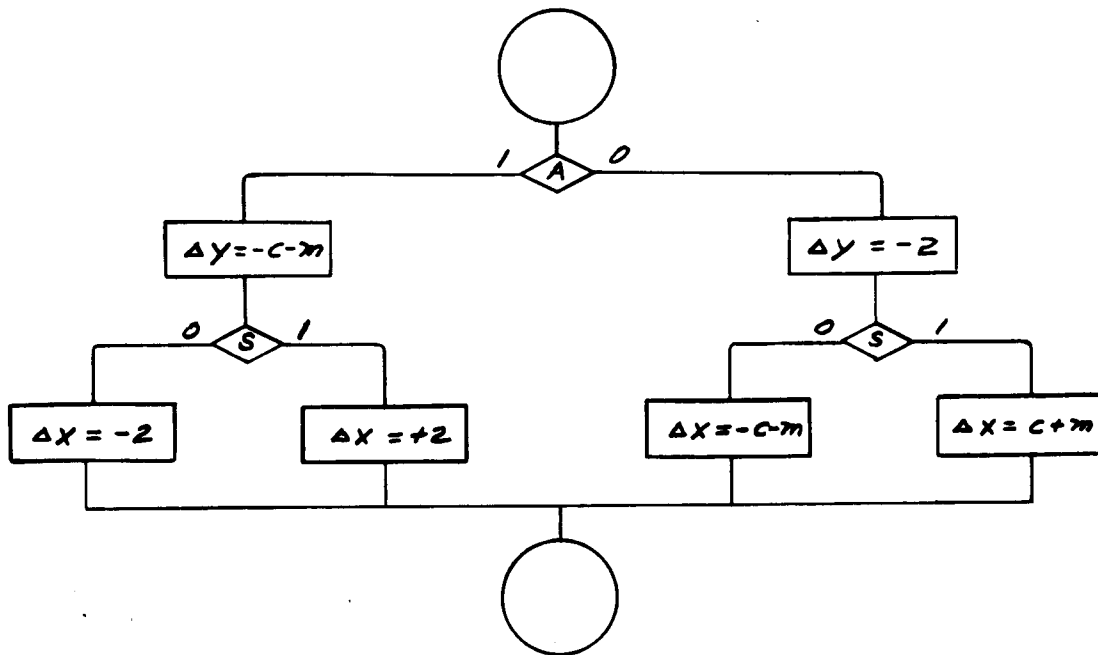


FIG. 5-19  
COMPUTATION OF  $\Delta Y$  AND  $\Delta X$ .

Table 5-4

Input Data - Method CM-2L<sub>B</sub>

$N_1$	$y_a$	$x_a$	$x_U$	S	R	$y_c$	$x_c$	$B_+$	$U_+$	$W'_+$	$B_-$	$U_-$	$W'_-$
1													
2													
3													
.													
.													
.													
NR													

Note:  $y_a, x_a$  are the coordinates of the upper end of each grid line  
 $(y_a \equiv y_U), x_U$  is the x coordinate of the right hand endpoint of each grid line.

Table 5-5

First Intermediate Data Table - Method CM-2L<sub>B</sub>

N <sub>g</sub>	N <sub>L</sub>	D <sub>L</sub> <sup>*</sup>	D <sub>m</sub> <sup>*</sup>	y <sup>*</sup>	x <sup>*</sup>	LS <sup>*</sup>	LE <sup>*</sup>	L <sub>1</sub> <sup>*</sup>	S	A	C	L	S	A	C	L	.	.	m	m	.	.	.
1		1	1			1	0																
2		1	1			1	0																
3		1	1			1	0																
4		1	1			0	0																
.		1	1			0	0																
.		1	1			0	0																
.		1	1			0	0																
NR		1	1			0	0																

Note:  $y, x$  are the coordinates of the upper end of grid lines ( $y_a = y_U$ ). Quantities designated with asterisks change in the course of generating Table 5-6. The initial value of  $L_1$  is the same as the first value of  $L$ .

Table 5-6

Second Intermediate Data Table - Method CM-2L<sub>B</sub>

x*	MM	MS	m	S	A	C
1	0	0				
2	0	0				
3	1	1				
4	1	0				
.	0	0				
.	1	0				
.	0	0				
200	1	0				

Table 5-7

Output Data - Method CM-2L<sub>B</sub>

y	y	x	S	A	C	y	x	S	A	C	.	.	.	.	.	C
1																
	m	m	m	m	m	m	.	.	.	m						
2	*															
	m	m	m	.	.	.	m									
3	*															
	m	m	m	.	.	.	m									
⋮																
⋮																
⋮																

Note: Data is entered in this table sequentially by rows except for locations designated by asterisks.

## 5.4 APPROACHES TO SIMULATION

### 5.4.1 The Simulation Problem

The first step in the development of the on-board gridding system is to build an operating breadboard. The breadboard should be a sufficiently close approximation to space-capable hardware that no fundamental engineering steps remain.

The various methods of gridding presented in this report require a wide variety of content and format of data to be transmitted from ground to satellite, or in the case of the breadboard, from a convenient data source. It is not our purpose here to examine hardware problems of getting data from computer in to breadboard memory, but rather those of organizing an appropriate data stream.

All techniques other than the analog call for quantities of data that discourage manual data preparation, although this possibility should be considered if a limited simulation is sufficient. Use of a computer entails programming, and runaway programming can cost considerably more than the breadboard hardware. This dictates the use of modifications of existing programs where suitable, and the use of FORTRAN or its equivalents where new programming is required.

While it may be premature to consider the computer to be used for simulation, the choice seems to be between the CDC 160A and the CDC 924. The CDC 924 has the advantage of being the computer designated for use in eventual operations, while the 160A has the advantage of greater accessibility (at least to ARACON), a debugged FORTRAN, a large amount of useful software in the form of gridding modules, and an ARACON routine that permits exchanging data between FORTRAN and machine language program sections.

While the 924 has a more powerful command structure than the basic 160A, ARACON uses an internally-developed programming system (ARACOM) for the 160A which gives it equivalent power at a sacrifice in speed.

### 5.4.2 Existing Programs

Two gridding programs are readily available to GSFC. One is the ARACON CDC 160A program, which has been used interchangeably for TIROS and for Nimbus APT gridding. It is organized in modules, permitting ready modification. The basic algorithm involves coordinate transformation from selected latitude-longitude values to the appropriate location on the camera image plane. The program can cope with camera altitudes beyond synchronous height.



The other program is the Nimbus AVCS gridding program for the CDC 924. Its basic algorithm is the same as that of the TIROS program. Input and output are adapted to the on-line operation required by the Nimbus system. The reader is referred to the individual program documentations for greater detail.

The nature of the basic algorithm of these programs is important, as it restricts the degree to which the programs can be profitably altered for preparation of data for simulation. In the following sections we will examine the degree to which the program can be salvaged for simulation for the various digital gridding techniques that have been studied.

#### 5.4.3 Programming Requirements for Simulation

##### 5.4.3.1 Ellipse Technique

As seen in Section 5.3, a whole fresh programming start is required. Because of the on-board complexities, we will not consider the ellipse method further (but see below.)

##### 5.4.3.2 Straight Line Techniques

The straight line technique calls for a number of straightforward modifications to the ARACON gridding program:

1. Elimination of attitude prediction and geography sections.
2. Elimination of TIROS wheel provisions.
3. Addition of false earth provisions outlined in Section 5.2. This should be done anyway in the interest of increased TIROS gridding accuracy.
4. Modification of grid segment originating logic to conform to requirements for limiting the number of line segments. The present program originates a new straight line segment at each latitude-longitude intersection whether it is needed or not. The most effective way of achieving the desired economy of line segments with minimum program complication appears to be a tabular approach, so that the geographic position of all line segment originations is fixed. A more compact approach is semi-tabular; the breaks would occur at longitudes determined by the latitude and longitude of the subpoint.
5. Change of picture boundary from circle to square. This involves introduction of picture azimuth in the picture plane.

6. Output formatting with all required non-data bits added.

7. Output programming to provide a suitable off-line data source for simulation.

We are inclined to retain the present plotter output routine to give a preview of the grid, thereby facilitating debugging of the overall system and avoiding embarrassment at demonstrations.

The programming time required to achieve these changes is about three man-months. It is presumed that the Wallops TIROS computer can be made available for assembly, debugging, and preparation of simulation material. Actual computer time of the present program is about eight seconds per grid with a considerably greater number of coordinate transformations being performed than required for the straight line method. Plotter output (buffered) takes about 25 seconds. Addition of a paper or magnetic tape output for subsequent input to the breadboard should take virtually no time as that output can be achieved on the direct channel during buffered plotter operation.

Computer running time is dictated by the number of coordinate transformations to be performed and by the time required for output formatting. It is estimated that coordinate transforms should take no longer than the time spent by the present TIROS program (about 7 sec per picture). Output formatting would take perhaps another second. Outputting would take 2 sec (magnetic tape) to 10 sec (paper tape). Buffered plotter output would take 25-30 sec during which time all other operations would take place. Thus, the plotter (if used) becomes the pacing item, giving a speed of 30 sec per grid.

#### 5.4.3.3 Coordinate Methods

The coordinate techniques require a different basic algorithm which solves the problem: along a grid line, where is the next point to be gridded? Since this is not determined by definition of the latitude-longitude of the point, it cannot be found by simple coordinate transformation.

This makes necessary the use of the computational algorithm we have described as the ellipse method in which the x-coordinate of a point can be obtained once its y-coordinate is specified. Inspection of Section 5.3 will show that the ellipse method entails a considerable amount of new programming. While this may be done in FORTRAN with relative facility, an alternative procedure may be desirable.

By an increase in density of straight line segments, the 160A TIROS program can be made to approach the computational accuracy of the proper ellipse method. Once the straight lines are established, it will be readily possible to generate gridding coordinates following the logic established in Section 5.3.5.

If a coordinate approach be adopted, we recommend a multi-step programming operation for greatest efficiency:

1. Formatting and output routines plus basic logic to go from straight line parameters to outputted quantities. This will provide immediate outputs for hardware debugging if needed.

2. Grafting (1) onto the basic ARACON grid program. This will involve much the same deletions and additions of the program described for the straight line method. In addition, data ordering will be required which will probably be most easily achieved by a separate pass through the computer.

3. Refinement of the segment origination section of the ARACON program to produce more esthetic and accurate output (a sufficient number of straight line segments so their junctions are not obvious).

4. Addition of annotation routines.

- 5a. If the result of (3) is operationally satisfactory, the program can be tidied up for eventual transcription to 924 language.

- 5b. If not, preliminary programming analysis of the ellipse algorithm is required.

Programming modifications for the coordinate methods are estimated to require five man-months; the additional time is required in special data ordering and formatting. We see no great difference in requirement between CM1 and CM2.

## 5.5 OPERATIONAL PROGRAM

Operational programs are to be written for the CDC 924. It would seem reasonable that the basic 924 monitor programs, functional subroutines, coordinate transformations, and orbit generation routine can be utilized unless they are too convolved with other parts of the program.

In general, substantial modification to existing 924 Nimbus programs would be required, the amount of modification depending on the particular gridding technique adopted for the satellite. New programming can be readily based on 160A programming, as command structure is not dissimilar. The 160-A fixed point arithmetic used by ARACON uses a 27 bit plus sign word. Only occasional rescaling should be required to convert to the 23 bit word of the 924.

Since necessarily the amount of computation to be performed for any orbit is relatively small, there is little reason to strive for extreme operating speed. This should facilitate programming as it will be possible to take advantage of the large internal capacity of the 924 for loose, modular coding.

We estimate that an excellent operational program can be operational in about nine man-months, building on the base of the simulation program. A part of the effort will be involved in integrating this program with other programs to permit operation without upsetting computer routine.

## SECTION 6

### COMPARISON OF APPROACHES TO ON-BOARD GRIDGING

#### 6.1 INTRODUCTION

Preceding sections have eliminated from consideration the analog approaches. Of the digital methods, four approaches show sufficient promise to warrant a detailed comparison. These are:

1. straight-line method SL-2
2. coordinate method CM-1
3. coordinate method CM-2L
4. coordinate method CM-2H

The ground computation of the picture grid should not provide a limitation on any of the three methods although the straight line method is certainly the easiest to implement. Hence, this factor can be eliminated in comparing the relative performance and feasibility of the three systems.

The differences in the flight-system weights are small and although the power differences are appreciable, all are small (less than 2 watts).

The system parameters which are most dependent on the particular approach are:

1. appearance of the picture grid
2. storage requirements
3. error susceptibility

#### 6.2 APPEARANCE OF THE PICTURE GRID

Two characteristics of the superimposed grid line significantly affect system design - mark spacing and smoothness of change in slope. With regard to the latter property, examine the appearance of the grid lines appearing in Figure 6-1 (simulated grid representative of the straight-line method). Although the marks deviate a maximum of 1% from the true grid line, the large slope changes between segments are disturbing (in the opinion of the writer). One solution to this problem is an increase in the number of line segments. The storage requirement for a single orbit with the SL-2 system is 20,000 bits maximum for grid and annotation

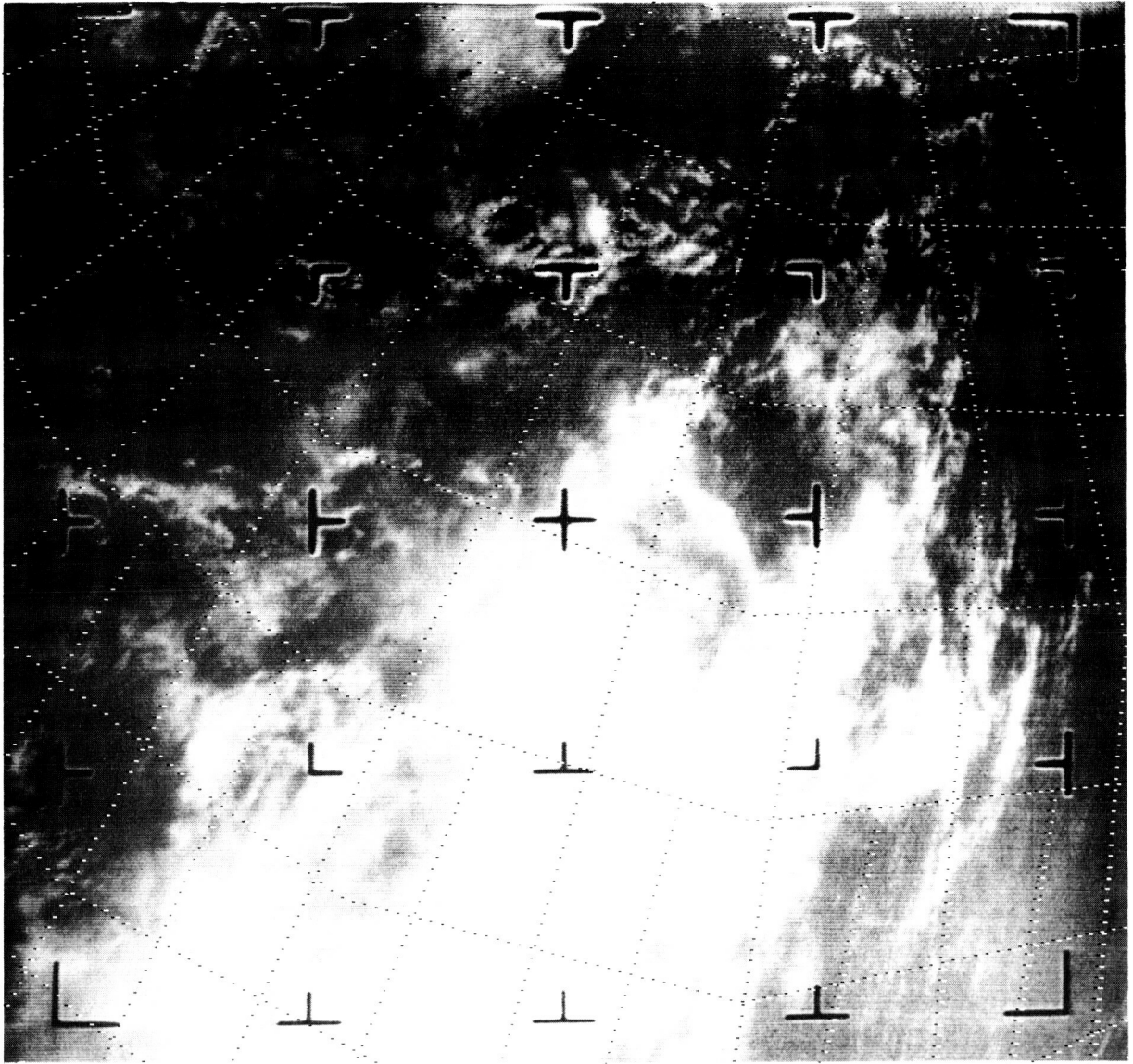


Fig. 6-1 Simulated Grid SL-2

(assuming the more efficient annotation scheme is employed). However, any reasonable increase would bring the storage requirement past that of CM-2H. CM-2H has the additional advantage of a lower logic speed since only one bit is added to Y or X rather than the 10 bit slope added for SL-2. If the appearance of the lines in Figure 6-1 is judged objectionable (compared to the lines typical of a coordinate system, shown in Figures 6-2 to 6-10), the choice between SL-2 and CM-2H is certainly the latter.

With regard to mark spacing, a spacing of eight picture elements provides a very pleasing well-defined line. However, a larger spacing may be adequate. Simulated grids representative of any of the coordinate system approaches with a mesh spacing of two picture elements appear in Figures 6-2 through 6-10. In these figures, grid lines are simulated with mark spacings of 8 (Fig. 6-2, 6-5, 6-8), 12 (Fig. 6-3, 6-6, 6-9), and 16 (Fig. 6-4, 6-7, 6-10) picture elements. Each grid is superimposed on three different cloud pictures to provide a firm basis for evaluation of a satisfactory spacing. Although the mark spacing has no effect on the design of the straight line system, it affects the storage requirement of the coordinate methods. A decrease in mark spacing from 16 to 8 in the CM-1 approach almost doubles the size of the memory. For CM-2 the corresponding increase in memory size is approximately 33%.

### 6.3 SUSCEPTIBILITY TO ERROR

The effects of single-bit errors in the various systems were documented in Section 3. In Section 3 we also saw that operation of the gridding system in any configuration is virtually error free if only thermal noise is considered. The more important considerations are operation with low S/N ratios when operating near antenna pattern nulls and the effects of interference from other spacecraft or ground sources. These factors can only be assessed through experience gained from similar communications channels now in existence.

If interference is judged to be a very serious problem, the CM-1 approach having the lowest error susceptibility is probably the best approach and CM-2L the worst.

Table 6-1  
Comparison of Digital Approaches to On-Board Gridding

Method	Straight-Line SL-2	Coordinate CM-1	Coordinate CM-2L	Coordinate CM-2H
K = 8	Main Store* 20,000 bits Buffer 1,000 bits Weight 7 lbs. Power** 1.8W	Main Store 160,000 bits  Weight 8-9 lbs. Power 1/4 - 1W	Main Store 40,000 bits Buffer 2,000 bits Weight 7 1/4 lbs. Power 1.3W	Main Store 34,000 bits Buffer 1,300 bits Weight 7 1/2 lbs. Power 1.8W
K = 12	Same as above	Main Store 120,000 bits  Weight 7-8 lbs. Power 1/4 - 1W	Main Store 35,000 bits Buffer 2,000 bits Weight 7-7 1/4 lbs. Power 1.3W	Main Store 30,000 bits Buffer 1,300 bits Weight 7-7 1/2 lbs. Power 1.8W
K = 16	Same as above	Main Store 80,000 bits  Weight 6.5 - 7 lbs. Power 1/4 - 1W	Main Store 30,000 bits Buffer 2,000 bits Weight 7 lbs. Power 1.3W	Main Store 25,000 bits Buffer 1,300 bits Weight 7 lbs. Power 1.8W
Comments	1. Poor grid appearance 2. Most complex logic	1. Minimum logic 2. Least vulnerable to error. 3. Largest Memory	1. Most vulnerable to loss of portion of picture grid as a result of bit error.	1. Pleasing grid appearance — Good compromise on all other counts.

\* Storage estimates are for 1 orbit.

\* average



#### 6.4 CONCLUSIONS

Table 6-1 summarizes the storage, weight and power requirements for the four approaches along with comments on characteristics peculiar to the individual approach. Although no severe weight penalty results from the large memory requirement of CM-1, the ability to do multiple orbits and eventually direct-readout infrared (DRIR) is impaired. The multi-orbit/function capability makes the SL-2 and CM-2H approaches attractive. However, the final choice hinges on an assessment of the grid-appearance requirements and the error probability expected in the updata communications channel of the satellite.

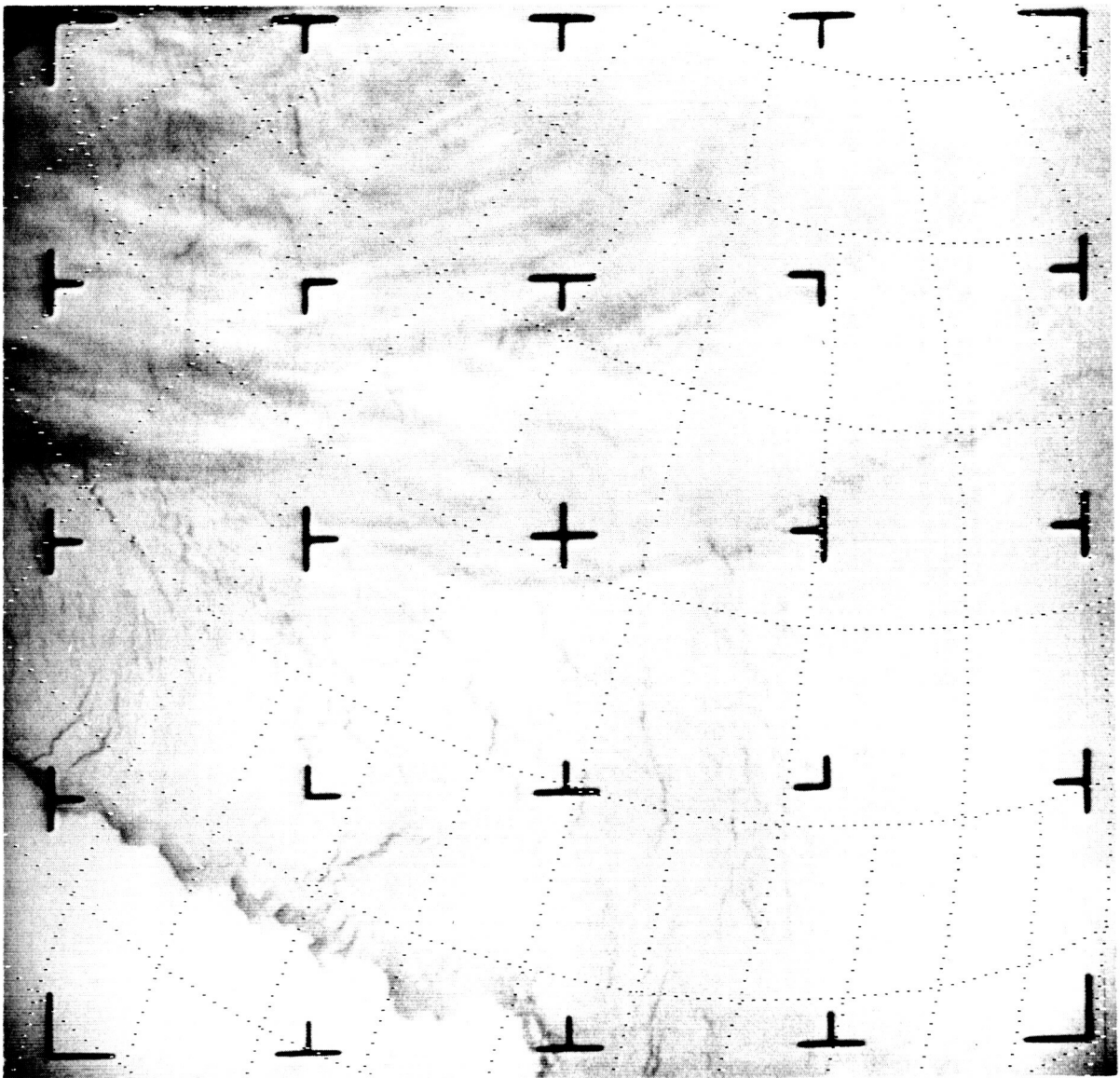


Fig. 6-2 Simulated Grid  $K = 8$

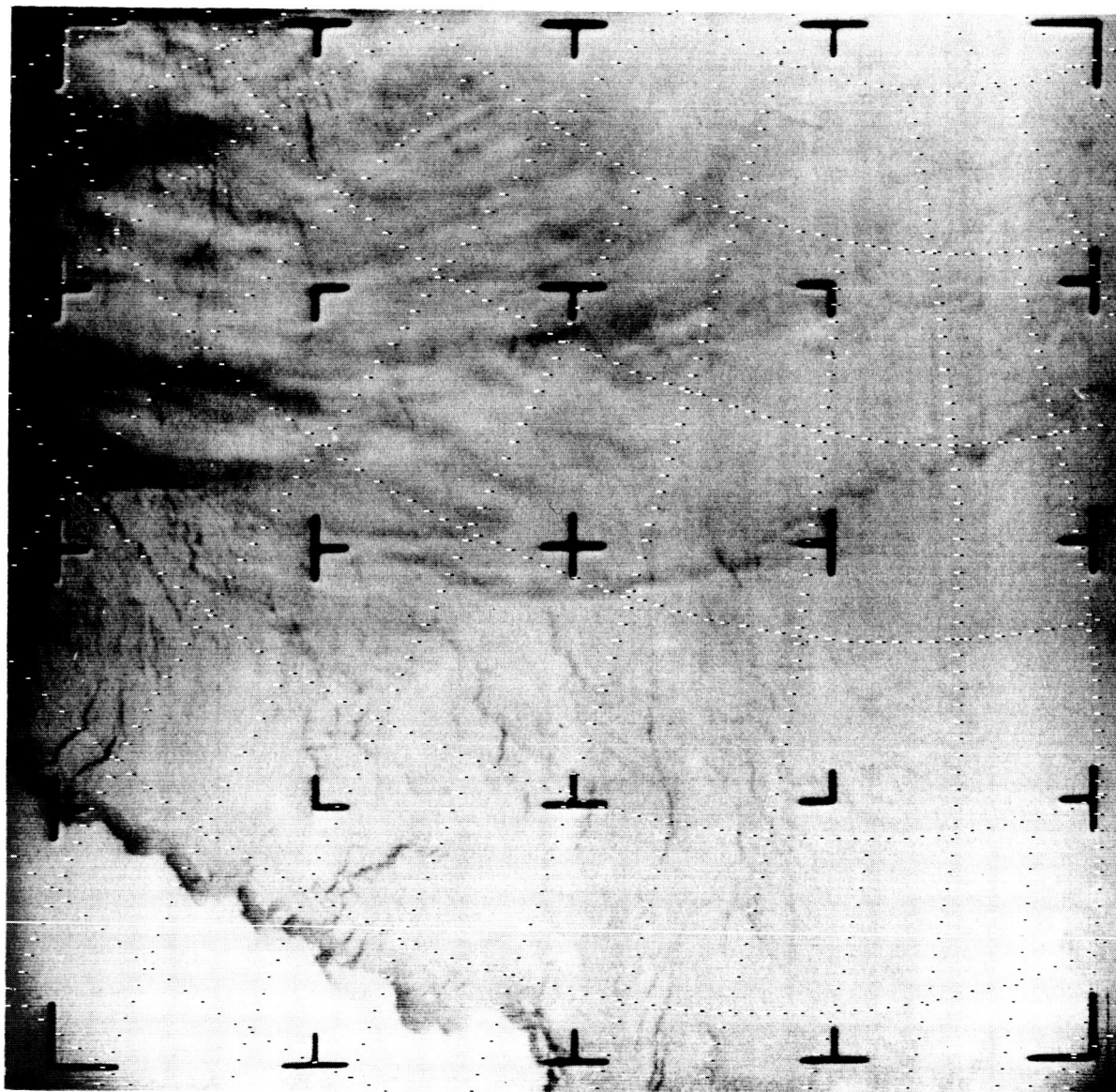


Fig. 6-3 Simulated Grid K =12

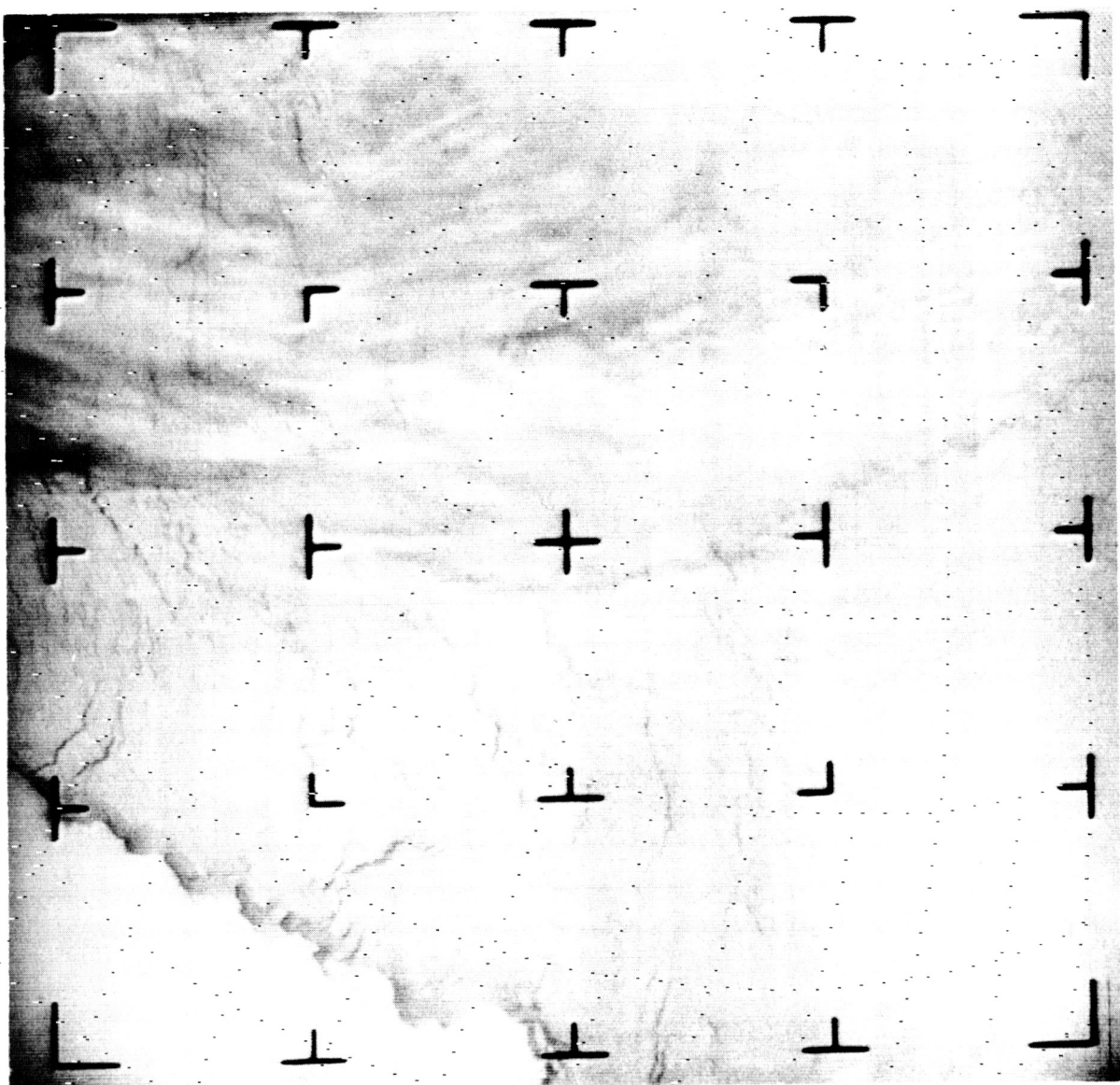


Fig. 6-4 Simulated Grid K = 16

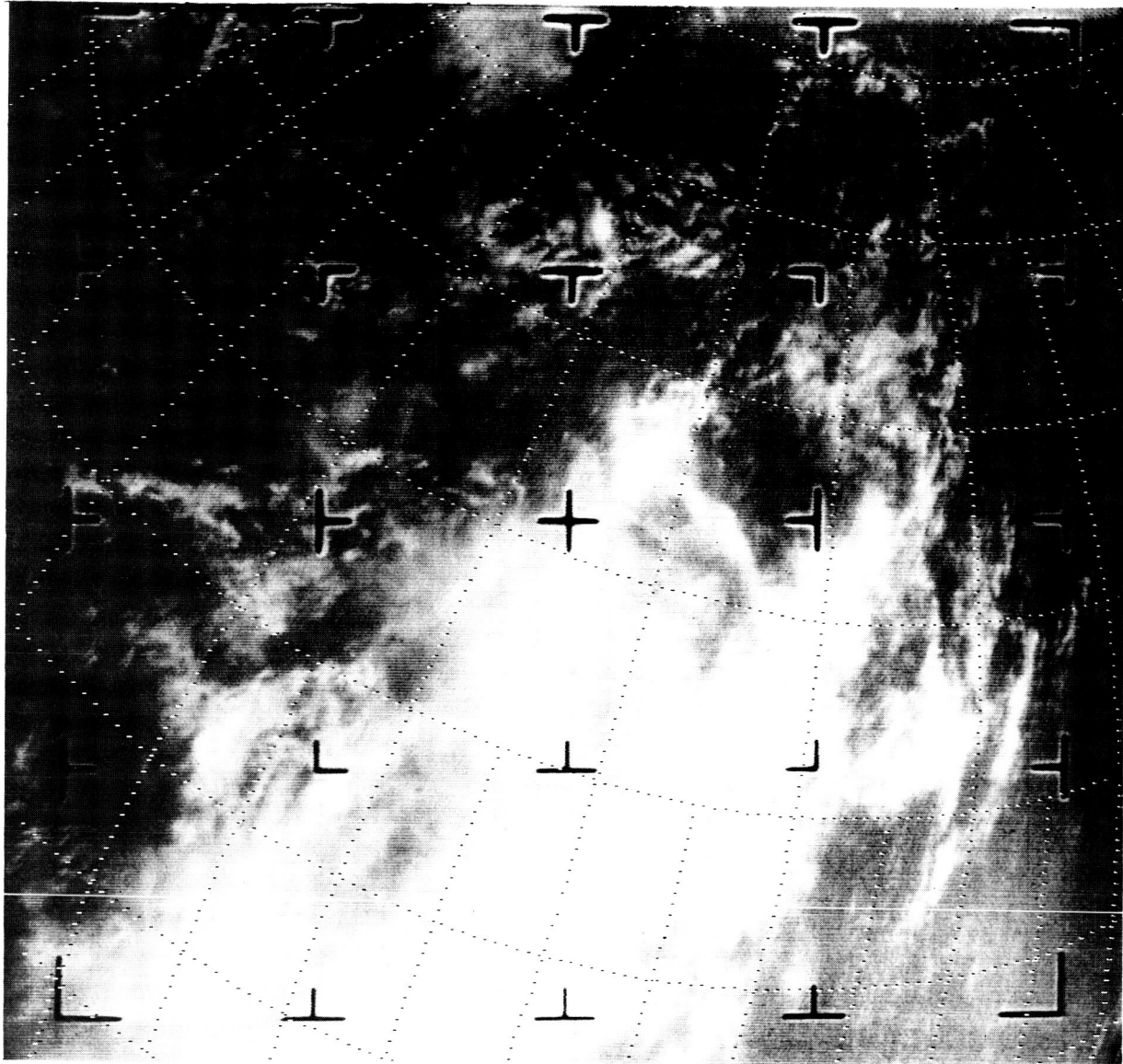


Fig. 6-5 Simulated Grid  $K = 8$

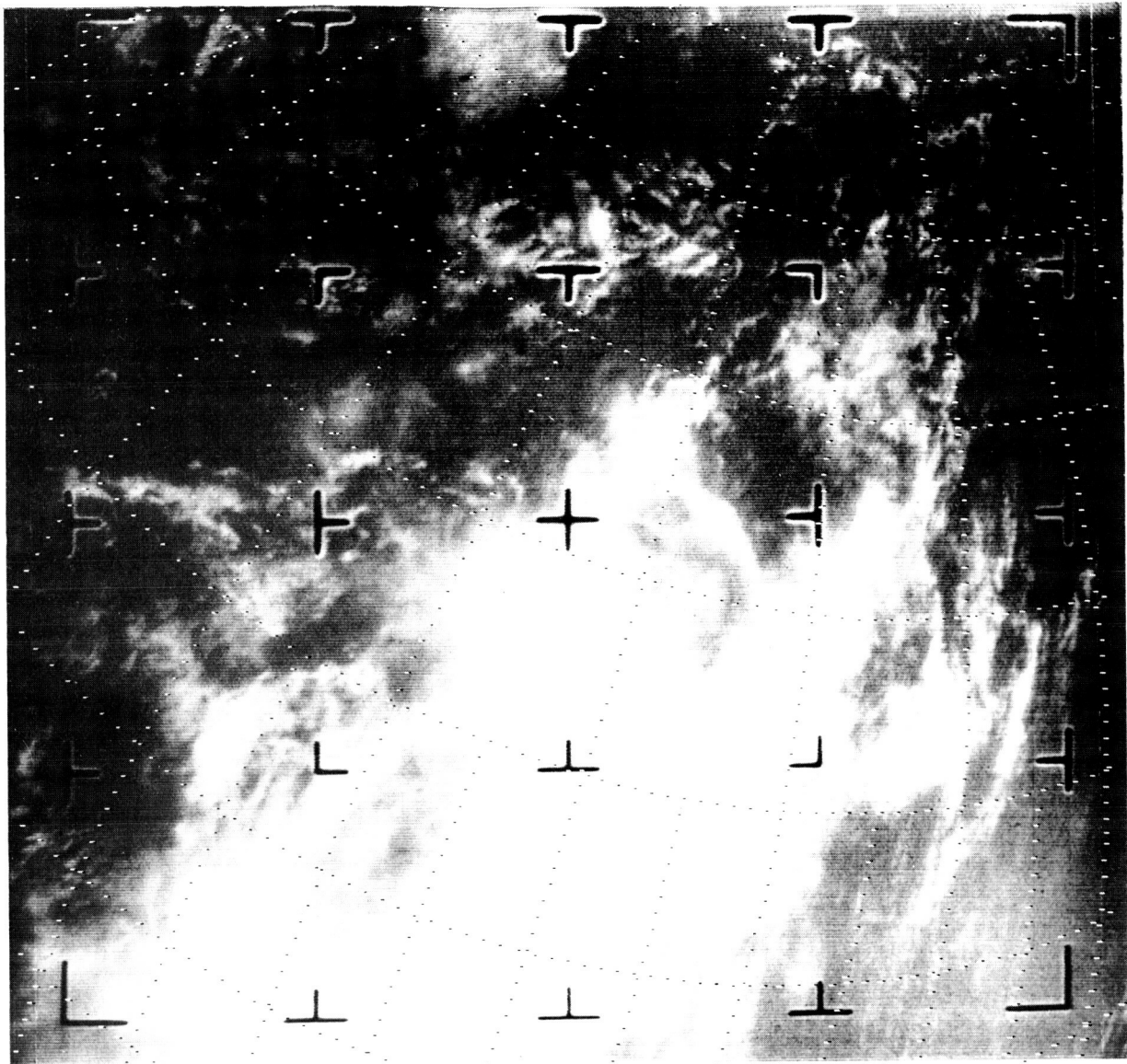


Fig. 6-6 Simulated Grid K = 12



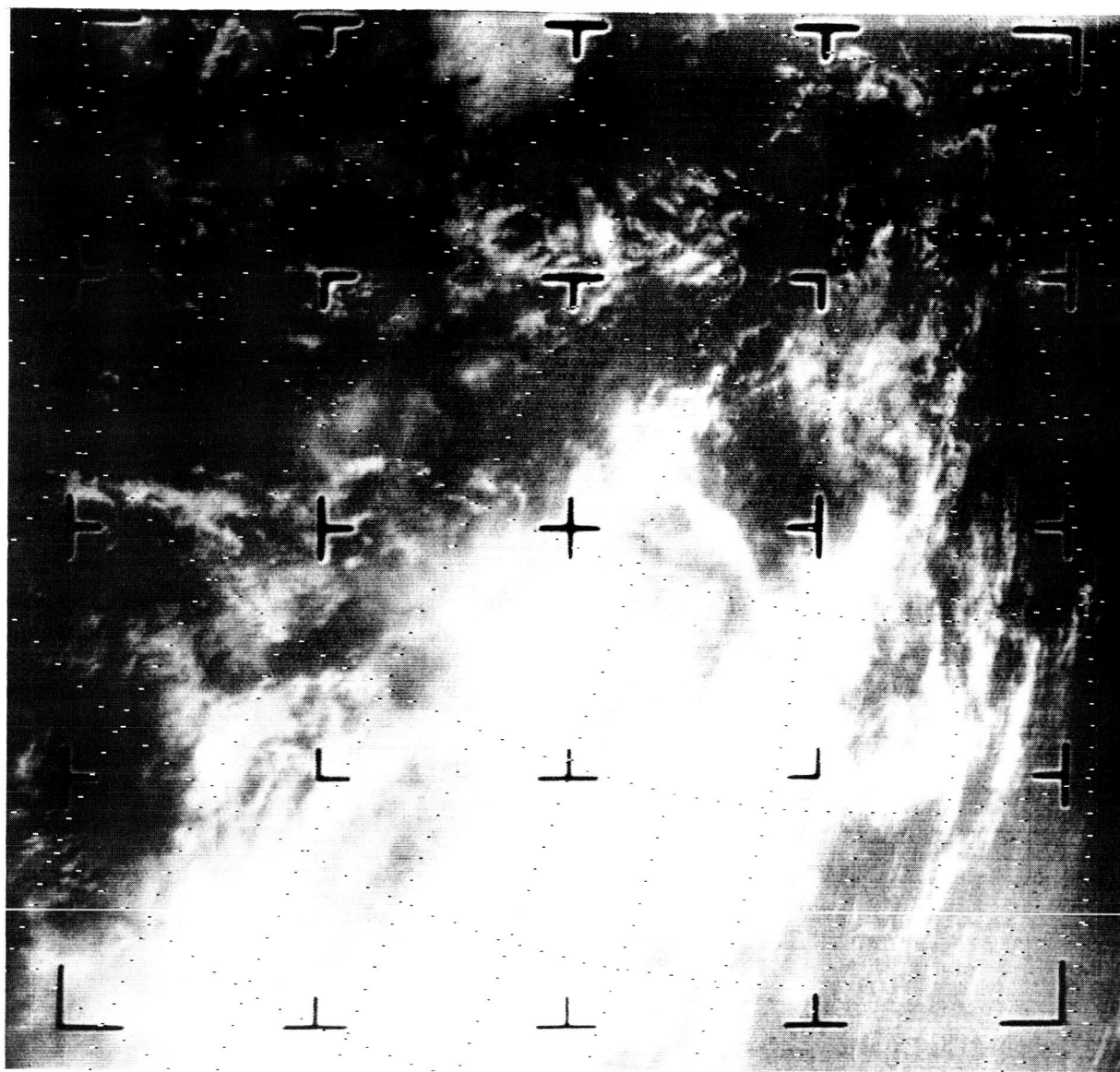


Fig. 6-7 Simulated Grid K = 16

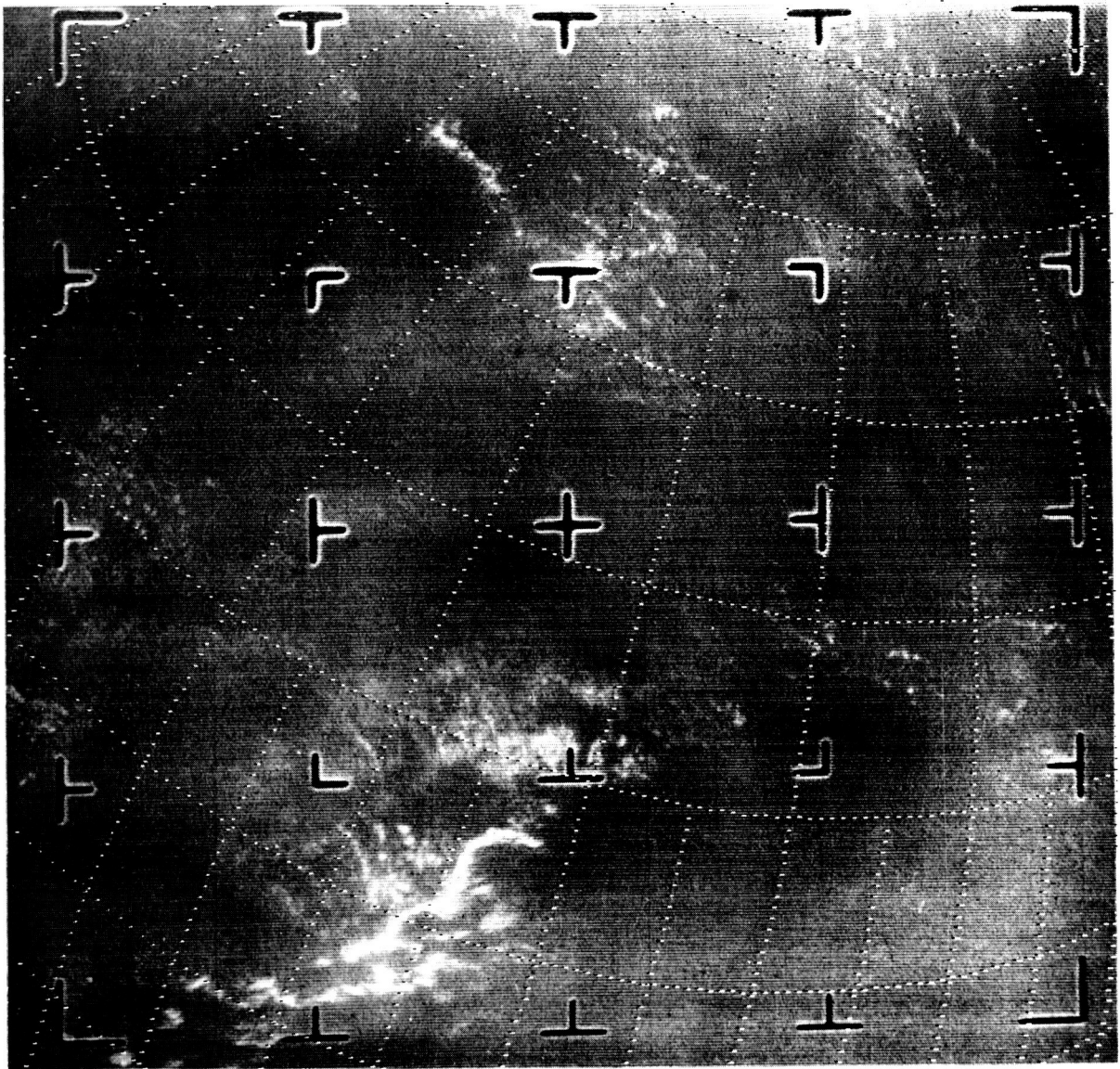


Fig. 6-8 Simulated Grid  $K=8$



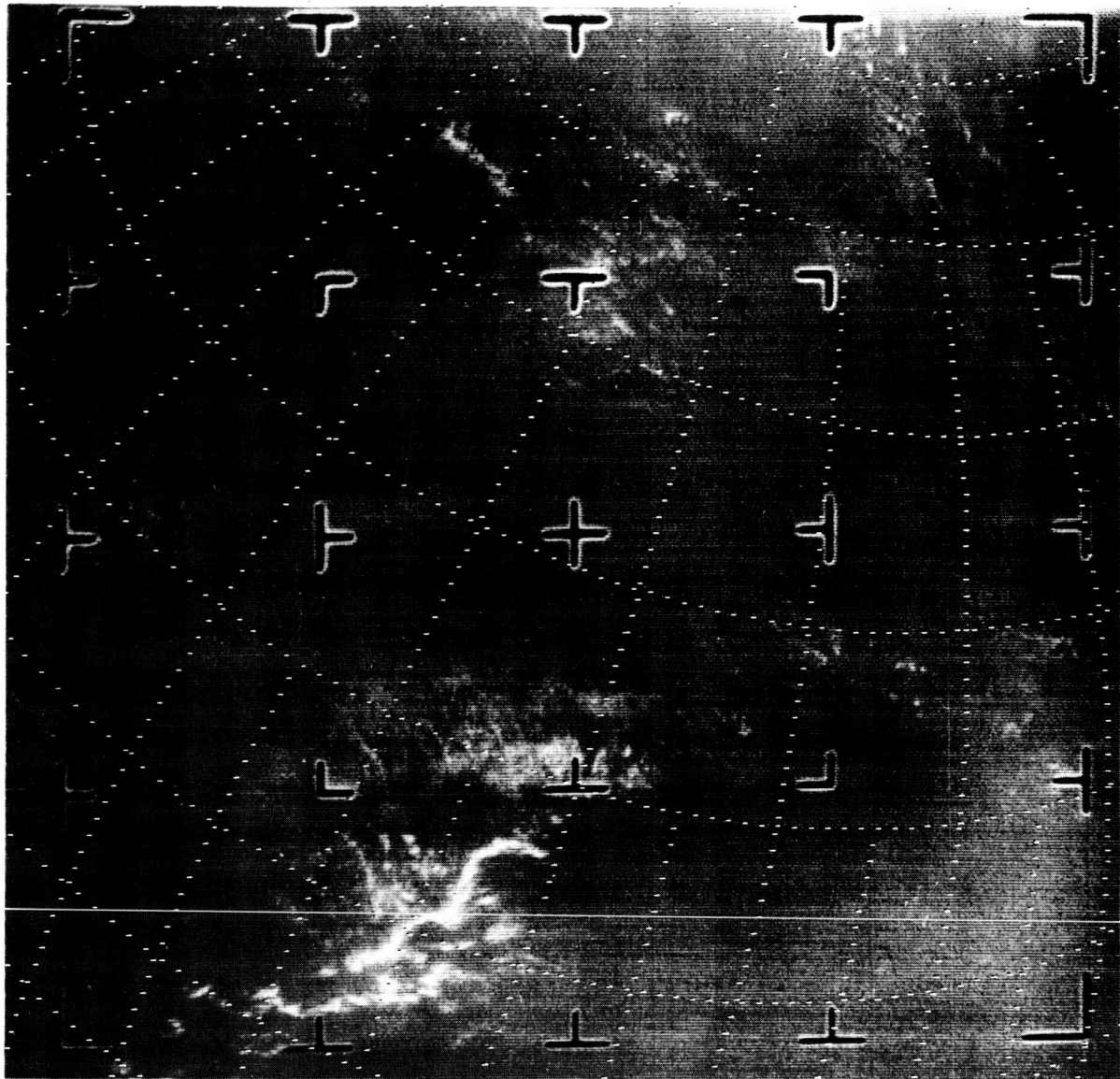


Fig. 6-9 Simulated Grid K = 12

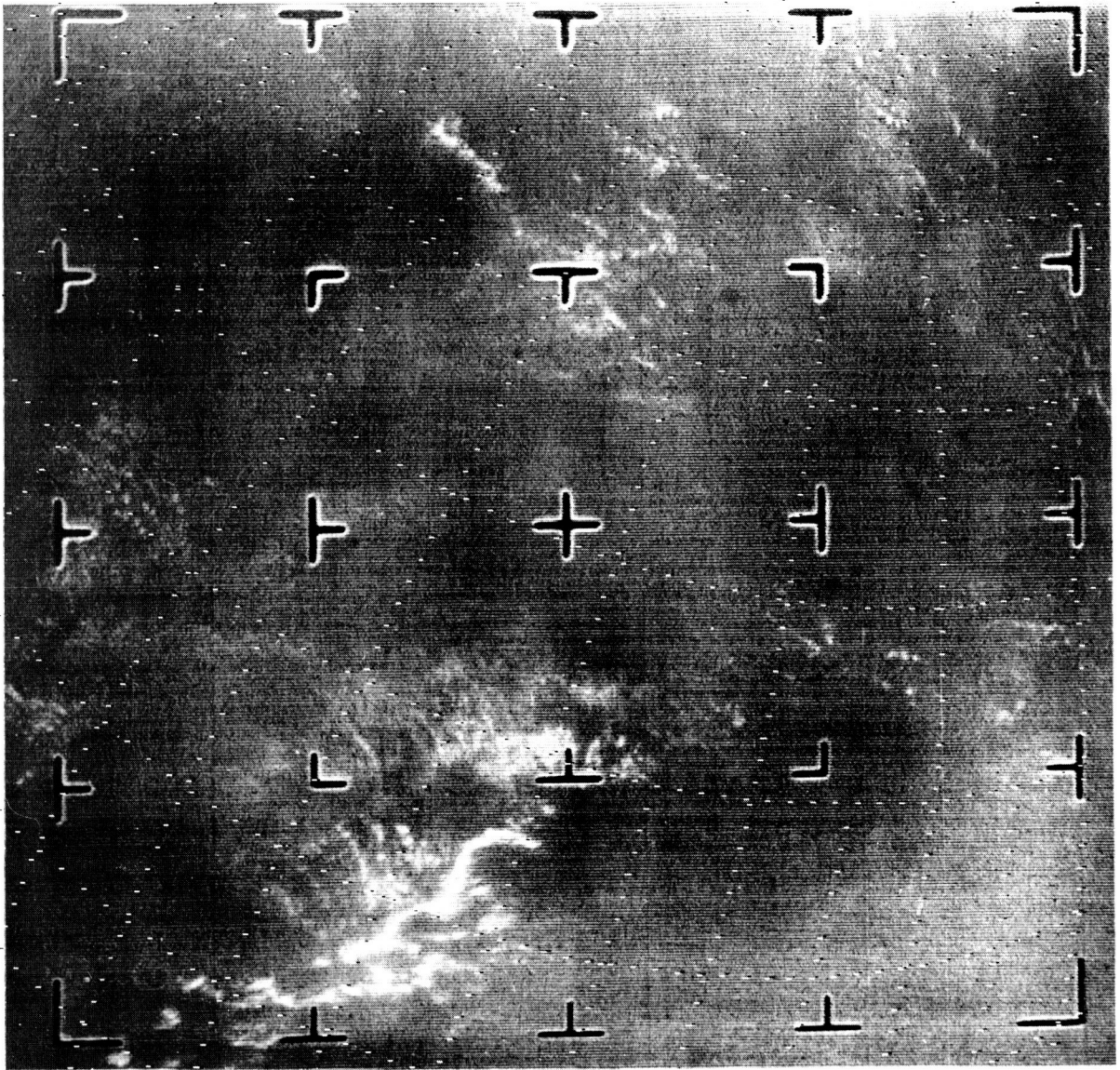


Fig. 6-10 Simulated Grid K = 16

## APPENDIX A

### ELLIPSE CHARACTERISTICS OF LATITUDE-LONGITUDE LINES

This appendix develops equations for the elliptical characteristics of circular latitude or longitude curves as seen on the image plane of a satellite camera. Referring to Figure A-1, the camera axis OT is assumed to pass through the center of the earth, the image plane being perpendicular to the camera axis. The  $\eta$ -axis is perpendicular to the camera axis and is a distance  $\zeta_0$  forward of the camera focal point.

#### A.1 CONSTANT LATITUDE LINES

Consider first the constant latitude circular line QS at the latitude  $\phi_1$  in Figure A-1, as seen by a satellite at the latitude  $\phi_s$ . It is desired to determine the characteristics of the circle QS, as projected on the  $\eta, \xi$  image plane, where the  $\eta$ -axis is a north-south axis and the  $\xi$ -axis is perpendicular to the plane of Figure A-1. This projection is an ellipse whose upper and lower edges correspond to the angles  $\alpha_+$  and  $\alpha_-$  in Figure A-1, respectively, which are given by the expressions:

$$\tan \alpha_{\pm} = (z \cos \phi_s \pm r \cos \phi_1 \sin \phi_s) / (R - z \sin \phi_s \pm r \cos \phi_1 \cos \phi_s) . \quad (\text{A. 1})$$

where

$$R = r + h \quad (\text{A. 2})$$

$$z = r \sin \phi_1 \quad (\text{A. 3})$$

and

$r$  is the radius of the earth

$h$  is the satellite altitude

$\phi_s$  is the satellite latitude

$\phi_1$  is the latitude of the curve considered

A simpler reduced form of Equation (A. 1) is:

$$\tan \alpha_{\pm} = \sin (\phi_1 \pm \phi_s) / [R/r \pm \cos (\phi_1 \pm \phi_s)] \quad (\text{A. 4})$$

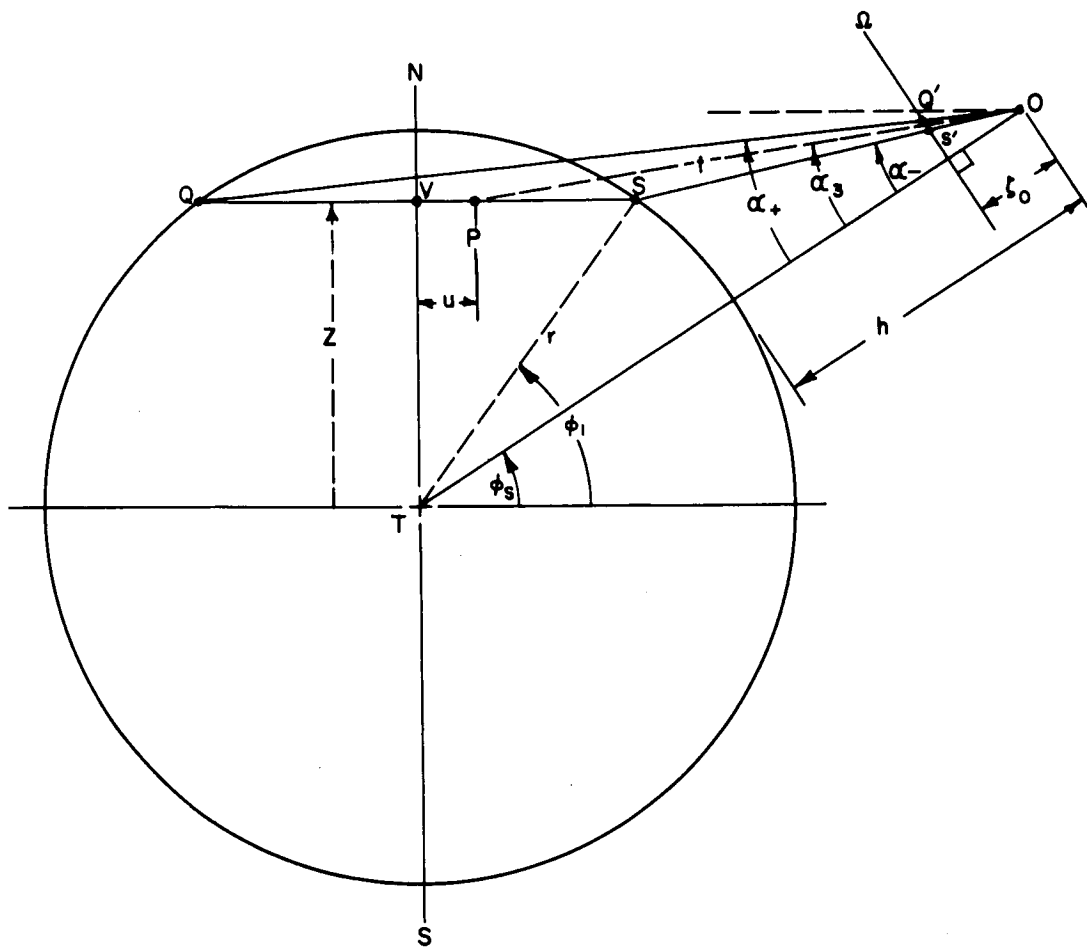


Fig. A-1 Geometrical Relationships for Constant Latitude Lines

The center of the projected ellipse is characterized by the line OP, bisecting the line Q'S, corresponding to the angle  $\alpha_3$ , where

$$\tan \alpha_3 = \frac{1}{2} (\tan \alpha_+ + \tan \alpha_-) \quad (\text{A. 5})$$

In the image plane (Figure A-2), the center of the ellipse has the coordinates ( $\xi = 0$ ;  $\eta = \eta_0$ ), where:

$$\eta_0 = \zeta_0 \tan \alpha_3 \quad (\text{A. 6})$$

and the length of the minor axis of the ellipse ( $a_\eta$ ) is

$$a_\eta = \frac{1}{2} \zeta_0 (\tan \alpha_+ - \tan \alpha_-) \quad (\text{A. 7})$$

The length of the major axis of the ellipse ( $a_\xi$ ) may be obtained by considering the width of the circle QS in Figure A-1 at the location where the plane OP intersects the circle QS. The following geometrical relationships are evident:

$$u = R \cos \phi_s - (R \sin \phi_s - r \sin \phi_1) \cot (\phi_s - \alpha_3) \quad (\text{A. 8})$$

$$t = (R \sin \phi_s - r \sin \phi_1) / \sin (\phi_s - \alpha_3) \quad (\text{A. 9})$$

$$w^2 = r^2 \cos^2 \phi_1 - u^2 \quad (\text{A. 10})$$

$$\tan \alpha_4 = w/t \quad (\text{A. 11})$$

where

$u$  is the distance PV in the plane of Figure A-1

$w$  is the width of the circle QS at the location P (perpendicular to the plane of Figure A-1)

$t$  is the projection of the oblique line OP on the plane of Figure A-1;

this line intersects the circumference of the circle QS at the location P

$\alpha_4$  is the inclination angle of the oblique line OP with respect to the plane of Figure A-1.

The length of the major semi-axis of the ellipse ( $a_\xi$ ) may now be written as:

$$a_\xi = \zeta_0 \tan \alpha_4 \quad (\text{A. 12})$$

The preceding equations give the ellipse characteristics ( $\eta_0$ ,  $a_\eta$ ,  $a_\xi$ ) of the circle QS as projected on a North-South oriented  $\xi\eta$ -axis system in

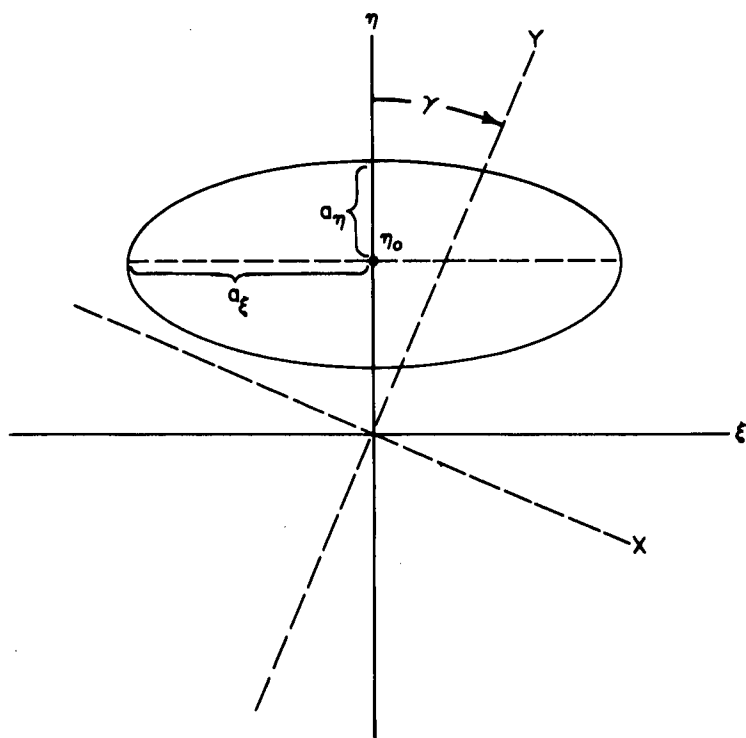


Fig. A-2 Image Plane Relationships for Constant Latitude Lines

the image plane (see Fig. A-2), the equation of this ellipse being:

$$(\eta - \eta_0)^2/a_\eta^2 + \xi^2/a_\xi^2 = 1 \quad (\text{A. 13})$$

The normal image XY-coordinates will be related to the  $\xi\eta$ -coordinates by some rotation angle  $\gamma$  (Fig. A-2) through the transformation:

$$\begin{aligned} \eta &= y \cos \gamma - x \sin \gamma \\ \xi &= x \cos \gamma + y \sin \gamma \end{aligned} \quad (\text{A. 14})$$

Substitution of Equations (A. 14) into (A. 13) gives the following alternate equations describing the constant latitude ellipses in the XY-image plane:

$$\begin{aligned} x &= x_c - B_+(y - y_c) \pm \sqrt{U_+[W_+ - (y - y_c)^2]} \\ y &= y_c - B_-(x - x_c) \pm \sqrt{U_-[W_- - (x - x_c)^2]} \end{aligned} \quad (\text{A. 15})$$

where

$$\begin{aligned} x_c &= -\eta_0 \sin \gamma \\ y_c &= +\eta_0 \cos \gamma \\ B_\pm &= Q_\pm \sin 2\gamma / R_\pm \\ R_\pm &= Q_+ \pm Q_- \cos 2\gamma \\ Q_\pm &= a_\eta^2 \pm a_\xi^2 \\ U_\pm &= (R_+ R_- - Q_-^2 \sin^2 2\gamma) / R_\pm^2 \\ W_\pm &= 2 a_\eta^2 a_\xi^2 / (R_\pm U_\pm) \end{aligned}$$

Another point of interest is the value of  $\eta$  at the horizon ( $\eta_b$ ) for any ellipse, which is given by the equation:

$$\eta_b = \zeta_0(r/h) [(R/r) \sin \phi_1 - \sin \phi_s] / [(1 + R/r) \cos \phi_s] \quad (\text{A. 16})$$

Also of interest is the slope of the ellipse curve at any point, which is given by either of the equations:

$$\begin{aligned} dx/dy &= -B_+ \mp U_+(y - y_c) / \sqrt{U_+[W_+ - (y - y_c)^2]} \\ dy/dx &= -B_- \mp U_-(x - x_c) / \sqrt{U_-[W_- - (x - x_c)^2]} \end{aligned} \quad (A. 17)$$

## A. 2 MERIDIAN LINES

In order to similarly obtain the ellipse characteristics of a meridian (constant longitude) line, it is convenient to refer to the two views in Figure A-3. Consider the meridian line  $Q$  which is located at the longitude  $\lambda$ , while the satellite is in the meridian plane  $Q'$  with the longitude  $\lambda_s$ . In the left hand view, the meridian plane of the satellite ( $Q'$ ) is in the plane of the page; in the right hand view, the meridian line to be drawn ( $Q$ ) is in the plane of the page; the two views are rotated with respect to each other about a polar axis by the angle  $\lambda_e$ , where

$$\lambda_e = \lambda - \lambda_s \quad (A. 18)$$

and

- $\lambda$  is the (east) longitude of the meridian line considered
- $\lambda_s$  is the (east) longitude of the satellite
- $\lambda_e$  is the longitude of the meridian line eastward of the satellite

In the right hand view, the satellite is located at a distance  $R \cos \phi_s \sin \lambda_e$  above the plane of the page, so that the line  $OT$  is inclined from the plane of the page by the angle  $\phi_s^*$ , where

$$\sin \phi_s^* = \cos \phi_s \sin \lambda_e \quad (A. 19)$$

It may now be observed that the geometry of the circle  $Q$  with respect to the point  $O$  in Figure A-3 is the same as the geometry of the circle  $QS$  with respect to the point  $O$  in Figure A-1, provided that  $\phi_s$  is replaced by  $\phi_s^*$  and  $\phi_1$  set equal to zero. Hence, application of Equations (A. 4) through (A. 12) gives:



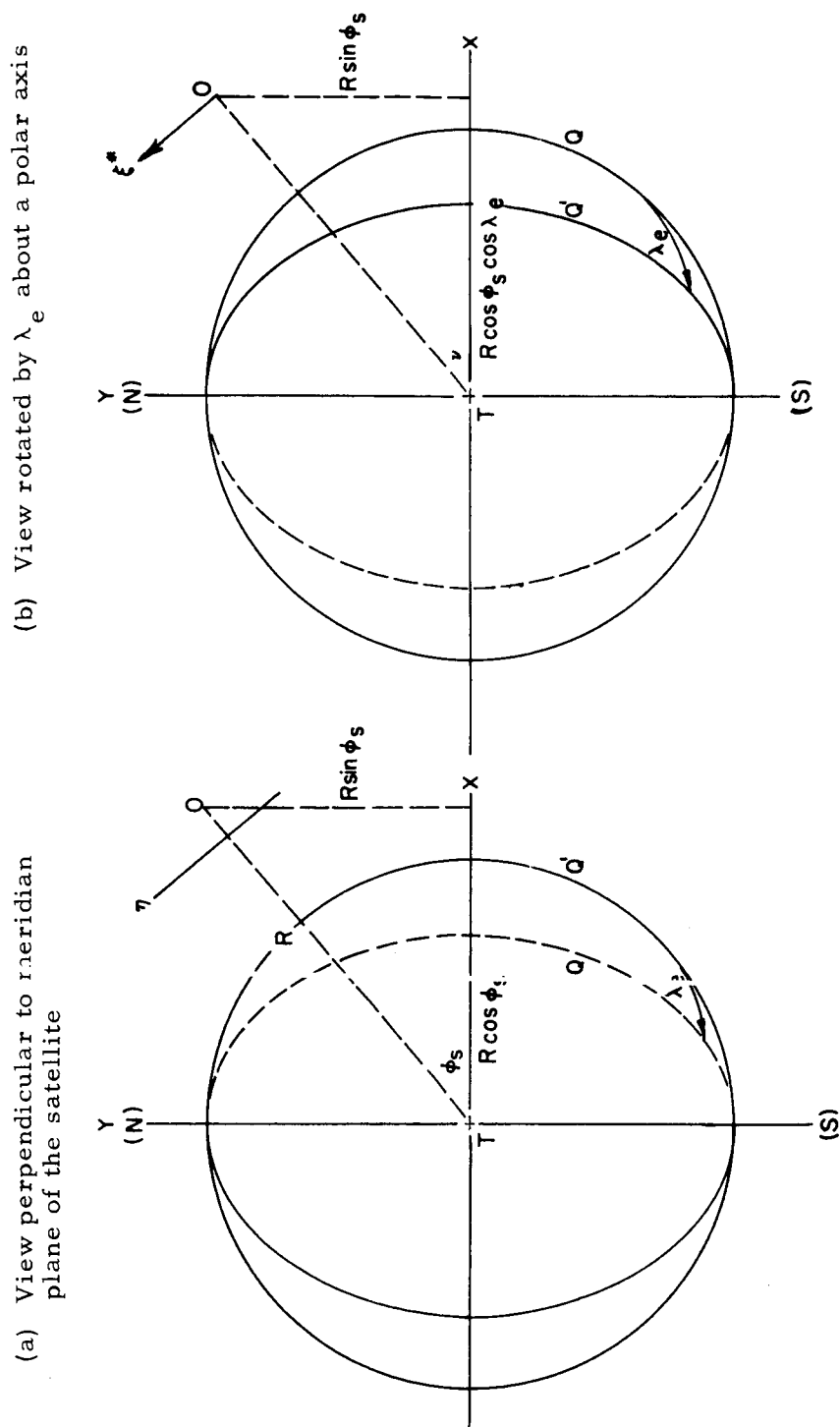


Fig. A-3 Geometrical Relationships for Meridian Lines

$$\begin{aligned}
\tan \alpha_{\pm}^* &= \pm \sin \phi_s^* / (R/r \pm \cos \phi_s^*) \\
\eta_0^* &= \zeta_0 \tan \alpha_3^* \\
\tan \alpha_3^* &= \frac{1}{2} (\tan \alpha_+^* + \tan \alpha_-^*) \\
a_{\eta}^* &= \frac{1}{2} \zeta_0 (\tan \alpha_+^* - \tan \alpha_-^*) \\
a_{\xi}^* &= \zeta_0 \left( \left[ \sin^2 (\phi_s^* - \alpha_3^*) - [(R/r) \sin \alpha_3^*]^2 \right] / [(R/r) \sin \phi_s^*]^2 \right)^{\frac{1}{2}}
\end{aligned} \tag{A. 20}$$

where asterisks are used here to distinguish parameters for meridian lines from analogous parameters for constant latitude lines.

The above equations give the ellipse characteristics with respect to the  $\xi^* \eta^*$ -axis system in the image plane, where the  $\xi^*$ -axis is in the plane of the paper of Figure A-3(b) and the  $\eta^*$ -axis is perpendicular to this plane. It is next desired to relate the  $\xi^* \eta^* \zeta^*$ -axis system to the  $\xi \eta \zeta$ -axis system of Figure A-3(a), which are rotated with respect to each other about a polar axis by the angle  $\lambda_e$ . This requires evaluation of the angle  $\nu$ , which is given by:

$$\tan \nu = \tan \phi_s / \cos \lambda_e \tag{A. 21}$$

In Figure A-3(b), the three components of a unit vector parallel to the  $\xi^*$ -axis, as expressed in a conventional X, Y, Z-axis system, are  $(-\sin \nu, \cos \nu, 0)$ ; in Figure A-2(a) the corresponding components are  $(-\sin \nu \cos \lambda_e, \cos \nu, \sin \nu \sin \lambda_e)$ . It follows that the angle  $\beta$  between the  $\xi^*$ -axis and the  $\eta$ -axis (Fig. A-4) is given by the equations

$$\begin{aligned}
\sin \beta &= \sin \nu \sin \lambda_e \\
\cos \beta &= (\cos \nu) \cos \phi_s + (\sin \nu \cos \lambda_e) \sin \phi_s
\end{aligned} \tag{A. 22}$$

or, reducing these equations with the aid of Equation (A. 21),

$$\tan \beta = \sin \phi_s \tan \lambda_e \tag{A. 23}$$

The angle  $\gamma^*$  between the  $\xi^* \eta^*$ -axis system and the conventional XY-image axis system is then (see Fig. A-4):

$$\gamma^* = 90^\circ + \beta + \gamma \tag{A. 24}$$

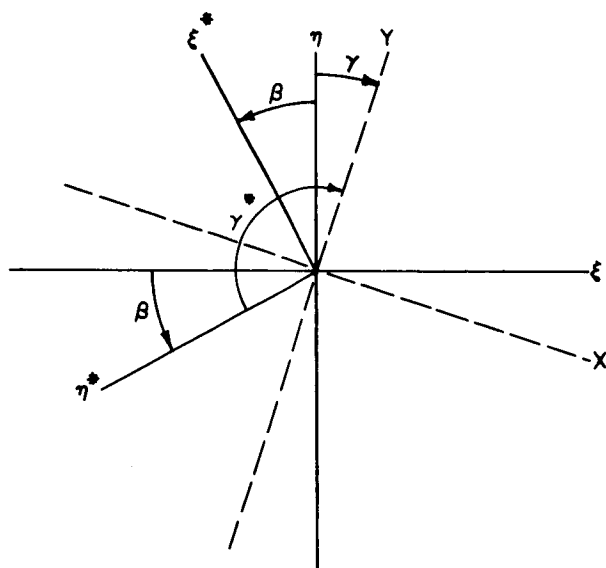


Fig. A-4 Image Plane Coordinate Axes for Meridian Lines

(Some of the above equations apply only for  $|\lambda_e| < 90^\circ$ ; for other angles add multiples of  $\pm 180^\circ$  to  $\lambda_e$  to bring it within this range.)

The final equations of the meridian ellipses in XY image coordinates are given by the same Equations (A.15) as for constant latitude lines, except that asterisks are to be applied to all parameters in these equations.

## APPENDIX B

### ANTENNA PROGRAMMING

The on-board gridding system can be used to facilitate antenna programming at the remote receiving stations. This can be of great importance to military stations cut off from effective communication with NASA or other sources of orbital information. While present techniques permit a resourceful and properly trained individual to construct training programs indefinitely once he has available basic orbital elements and has succeeded in acquiring one or two passes, the requisite talents may not be universally available.

Antenna programming can be simplified by placing the sub-point track or an orbit about 24 hours later on each picture. The track would be marked at 1 or 1/2 minute intervals by grid-type marks. At least one per picture of these should be identified with the actual minute. At a 1/2 minute interval, about 10 dots would cross the picture. It might be necessary to repeat the dots over two or three sweeps to make them conspicuous.

Determination of tomorrow's antenna programs would then be achieved by placing the pictures under an overlay which would be similar to the present gridding overlay with an azimuth-elevation diagram added. In practice, this would be two overlays stapled together to properly locate the azimuth-elevation diagram. The operator need only approximately match latitude-longitude grid lines on picture and overlay. He can then read off required azimuths and elevations against time, giving tomorrow's programs directly.

Accuracy is completely adequate for all current and contemplated APT antennas. Because the overlay height does not correspond exactly to satellite height, some elevation angle error is possible. It goes to zero in the vicinity of the station, where it is most important because of its relation to azimuth slewing.

The addition of this antenna programming feature would vastly simplify ground operations under field conditions.

## APPENDIX C

### MEMORY CONSIDERATIONS

#### C.1 MAIN DATA MEMORIES

##### C.1.1 Magnetic Core Storage

##### C.1.1.1 Background

DI/AN Controls has had experience in designing magnetic core memories, and has here endeavored to supply the basic system principles for the 25,000 or 80,000-bit memories required for the various gridding methods. Each part of the memory system will be given a short discussion. An estimate of engineering parameters is given.

##### C.1.1.2 Operating Modes

The modes necessary for operation of this memory are, (a) repeated serial write to load the memory at the beginning of the orbit, and (b) repeated serial read to unload the memory during the orbit. The data are read out of the memory as required by the calculation logic.

##### C.1.1.3 Power and Weight Estimates

Guides for estimated power consumption and weight are available from DI/AN's experience in building sequential access aerospace core memories. The duty cycle of the memories is so low that the power consumption is essentially equal to the standby power. Peak power during operation is approximately 8 watts for 10 microseconds, but since the read time for a single word is only a few milliseconds, the total energy is inconsequential.

Table C-1 DI/AN Core Memory Estimate

Total Storage	Volume (cu. in.)	Weight (lbs.)	Power at 1KB/sec (mw)	Status
30.1 KB	65	2.9		Developmental Model
30.1	91	3.5	225 Standby + 538mw/KC*	Delivered. No effort on power reduction
4. KB	52	2.5	18 Standby + 14mw/KC*	Delivered
25 KB	80	3.0	41	Estimate for 1966
90 KB	140	5.0	120	Estimate for 1966

\* Read-Write cycle. Read only or Write only would be half the value.

#### C.1.1.4 Design Details

a. Memory Cores and Wiring - Assuming that single-hole ferrite cores are to be used for this memory, balance among the required number of turns, drive power, amount of electronics and system weight and volume leads to the conclusion that 30-mil O.D. cores in a coincident current configuration would be the best to use.

b. Power Gated Sense Amplifier - Because the memory cores produce relatively small output signals, Class A operation of the first stage of the sense amplifier is generally used. In the low-speed applications, the sense amplifier power buss is turned on for only a few microseconds during each read cycle. During the time between read events, the sense amplifier power is turned off, and the standby power of the sense amplifier is reduced to transistor leakage currents, rather than the normal Class A operating power.

The bit rate where this procedure becomes economical from a power standpoint is found by balancing the control circuit power versus the standby power saved by the switching. The crossover is in the vicinity of 100 kc bit rate.

c. Voltage and Current Regulation - Since the Nimbus power supply of 24.5 volts is regulated to  $\pm 2\%$ , little additional voltage regulation is required for proper core memory operation.

Conventional cores receiving drive current compensation with varying temperature generally exhibit a better signal/noise ratio at low power levels than do cores especially designed for stable characteristics over broad temperature ranges. DI/AN has built memories with conventional cores operable from  $-20^{\circ}\text{C}$  to  $+90^{\circ}\text{C}$ , and the specification of temperature required for the APT system ( $0^{\circ}\text{C}$  to  $+60^{\circ}\text{C}$ ) presents no immediate compensation problem. The improved signal/noise ratio allows the use of fewer sense amplifiers and/or wider margins of reliable operation.

d. Read and Load Operations - This memory is to be used in a purely sequential operation; therefore, it is desirable to use four anti-coincident rings for the X and Y driver positions. Rings of  $11 \times 12 \times 13 \times 17 = 28,951$  will serve for the 25,000-bit memory, and of  $14 \times 17 \times 19 \times 23 = 104,006$  for the 90,000-bit memory. In general, the precise number of bits required is less than the product of the four factors. The beginning of up-data reception can be used to reset the memory drive rings back to the first address to receive the data for the forthcoming orbit.

#### C.1.2 Magnetic Thin Film Memories

A number of companies are presently developing various types of thin magnetic film memories for aerospace use. Specific information on memories was obtained from the UNIVAC Division of Sperry Rand Corporation. UNIVAC has delivered to GSFC a laboratory model serial NDRO memory of 98,304 bits which operates at 100 kc/s. Internal organization yields 16-bit words. This is an engineering model of a proposed memory later to be in aerospace packaging. The projected size and weight of the memory in aerospace configuration are less than 140 cubic inches and less than 3.5 lbs. When continuously reading at 100 kc/s, the memory consumes a maximum of 300 milliwatts of power. In addition, a DC/DC converter consumes 130 mw more (72% efficiency) from a 28-volt source, while supplying the 3, 6 and 12 volts required in the memory. Continuous writing at 100 kc/s takes 346 mw. Stand-by power is 85 mw for the memory, and 80-90 mw for the converter. The projected aerospace package, as well as the engineering breadboard, utilizes transistor logic.

UNIVAC had supplied us with information as to engineering parameters for memories expected to be launchable in late 1966.

In Table C-2 are shown characteristics of thin film serial memories already built by UNIVAC and Texas Instruments.



Table C-2 Present Status of Thin Film Memories

<u>Total Storage</u>	<u>Status</u>
4,096 bits	Delivered 1 year ago (TI)
30 KB	Flight model for classified Navy Satellite
98,304 KB	Lab model delivered to GSFC, 434 MW power

In Table C-3 are shown engineering estimates of memories expected to be available in 1966. The final two entries are estimates made by UNIVAC at DI/AN's request.

Table C-3 Engineering Estimates of Thin Film Memories in 1966

<u>Total Storage</u>	<u>Size (cu. in)</u>	<u>Weight (lbs)</u>	<u>Power at 1 KB/sec(MW)</u>	<u>Status</u>
82 KB 10 bits/word, RA	145	3.8	400	Estimate
164 KB	300	10	15,000	Estimate
2.8 MB	624	45	1,500	GSFC contract just awarded
25 KB	70	2.3	75	\$19,000 each in quantities of 4. 1966 projection by UNIVAC at request of DI/AN.
100 KB	100	3.7	100	\$33,000 each in quantities of 4. 1966 projection by UNIVAC at request of DI/AN.

From all indications, it appears that even a memory as large as 100 KB can be held to limits of 100 cu. in., 4 lbs., and 1/2 watt. It should be pointed out that the memories operate on a very low duty cycle and that the power estimates made later in this report are, for all practical purposes, the standby power of the memories.

## C.2 ACTIVE COMPUTATIONAL MEMORY

### C.2.1 Magnetorestrictive Delay Lines

#### C.2.1.1 Delay Line Survey

Both the straight line methods operate in sequential modes. For the purposes of calculation, a delay line is used to store the line segment information applicable to any particular set of sweeps. An engineering survey of the delay line field showed that the magnetorestrictive transducer, wire acoustic delay line served our purposes best.

In connection with the designing of the Nimbus Command System, California Computer Products and the Computer Control Company developed an aerospace-rated delay line very similar to that which would be required by method SL-2. (If this type of line were operated in the NRZ mode, it could also be used on Method SL-1 at 2 mc/s or higher.) A number of other vendors were contacted for information or possible development of a special line. Since CCC has already constructed a line quite similar to that which would be needed for SL-2, most of the information available was on a CCC line.

#### C.2.1.2 SL-2 Requirements

The delay line for use in method SL-2 would have a length of about 2,480  $\mu$  seconds. This time corresponds to the 8 coordinate interval periods between calculation times. Operating frequency would be at least 430 kc/s. No intermediate taps are required.

#### C.2.1.3 Engineering Details

The delay system consists of an acoustic wire delay line driven by a magnetorestrictive transducer along with driver and receiver electronics. The line can be excited to propagate a torsional or longitudinal wave. Due to differences in the wave propagation velocity, the torsional mode line uses about 40% less wire for a given delay than the longitudinal.

Present state-of-the-art puts the product of Bit Rate x Time Delay at 10,000, maximum. In aerospace configuration at 2 mc/s, this would be lowered to about 4,000 and the line loss can be expected to be double (3 db greater) the loss for the same length in commercial design.

Line Modulation - The lines can be driven in three modulation methods:

a. RZ (Return to Zero): In the RZ mode, a "1" pluse is impressed on the line, while a "0" is taken to be the absence of a pulse at strobe time.

b. Bi-Polar: The pulse representing a "1" and "0" are of opposite phase and both are impressed on the line. The output detector is phase sensitive. Detection of the "0" and "1" signals is more reliable than in RZ.

c. NRZ: In Non-Return to Zero, pulses are only impressed when successive bits change. The information rate possible in NRZ is twice that of the other two methods, but noise sensitivity increases. It should be noted that new electronic methods have raised the accuracy of NRZ techniques.

The lines already built by CCC are of length 240 and 660  $\mu$  sec and each requires 120 mw of power when cycling half-ones. The 240  $\mu$  sec line weighs 0.55 lbs; the 660  $\mu$  sec line weighs slightly more. Special driver circuitry was designed for the Nimbus clocks and was built integrally with the wire lines by CCC.

The delay need for SL-2 is considerably longer than the Nimbus clock delay; however, longer lines have been built with aerospace reliability. A delay line built for the Mariner series probe had the following characteristics:

1. Length 5 milliseconds, 500-bit storage.
2. 150 milliwatts power consumption when circulating all "1's".
3. In the receiving, clocking, and recycling stages, power consumption averaged 6 mw (6 volts, 1 ma) per stage. The line driver consumed 30 to 40 mw of power. Output amplifiers, a Schmidt trigger and input/output circuitry consumed the remainder of the power.

The Mariner Mars probe has similar lines on board. On Nimbus, all indications were that the delay lines operated continuously and without error.

At DI/AN's request, the Computer Control Company estimated physical characteristics of a delay line for method SL-2 considering improvements possible by late 1966. The rough characteristics which they projected are as follows:

- a. Size:  $4 \frac{1}{4}'' \times 4 \frac{7}{8}'' \times \frac{3}{4}'' = 15.5 \text{ cu.in.}$
- b. Weight: Approximately 8 oz.
- c. Power Consumption: Approximately 100 mw.
- d. Reliability Specifications: The same or better than those applicable to the Nimbus clock.

### C.2.2 Solid State Storage Elements

Recent developments in microminiature circuitry has made feasible the storage of considerable amounts of data in active flip-flop circuits, with many flip-flops on a single semiconductor chip. The entire circuit is connected as a multiple stage shift register with data input, data output and shift clock input. General Micro-electronics, Inc., (GMI) is marketing and has supplied to DI/AN information on their MOS integrated circuit PL-5000, which is a 20-stage shift register capable of operating at frequencies up to 1 megacycle with power dissipation less than 60 milliwatts. Although neither this nor any other MOS device is as yet aerospace rated, the possibilities for small scale scratch pad storage of these devices by 1966 is extremely good, and DI/AN feels that consideration should be given to this device. The fact that the entire 20-bit shift register fits on a TO5 header, plus the low power consumption, makes this a most promising device for use in the SL-2 synchronizer, and in the numeral generator for use with the coordinate method, if numeral generation on all sweeps is required. (See Section 3.4.1 for numeral generation.) GMI has indicated to DI/AN that they can construct this element to lengths of less than 20 stages and have considered giving intermediate point access to shift register stage outputs. Thus, storage need not be restricted to multiples of 20 bits.

## APPENDIX D

### CHOICE OF LOGIC ELEMENTS FOR SYSTEM MECHANIZATIONS

#### D. 1 GENERAL

One each of two general classes of digital logic elements was chosen for the detailed implementations of the satellite systems. From these implementations the resulting system power, weight, volume, cost and reliability were calculated. The two classes are:

- a. Semiconductor integrated circuits.
- b. Magnetic logic circuits.

Of the integrated circuits, use of the Fairchild Milliwatt Micrologic (MW $\mu$ L) in the "flat pack" package was assumed in the system implementations. Of the magnetic logic, use of the DI/AN Controls CTL-100-24 core transistor logic (CTL) element in the "Pico Bit" package was assumed.

Components now in production or close to production are the only ones considered here. This has been done because components not now in or close to production will not have had sufficient debugging time by early 1966 to assure availability.

The high clock rate (above 400 kc/s for both straight-line methods) requires that integrated circuits be used for mechanization. The low audio (1-20 kc/s) clock rates of the coordinate methods can be handled by either integrated circuits or CTLs.

#### D. 2 AVAILABLE INTEGRATED CIRCUITS

Among the many integrated circuit families that will be available for use in this system, four are especially applicable to our needs because of low power consumption. These are:

- a. Texas Instruments Series 51.
- b. CBS Laboratories Micropower Circuits using high-resistance thin film resistors.
- c. Two families of complementary multichip (NPN/PNP) circuits being developed for NASA by General Instruments Corp. and by J. Sturman at NASA Lewis Research Center.

d. Fairchild Milliwatt Micrologic.

D. 2. 1 Texas Instruments Series 51

The speed of the T. I. Series 51 circuits is marginal at the high clock rates used in the SL methods. In other respects these circuits are satisfactory and they could be used successfully in the integrated circuit CM mechanizations. However, the Fairchild Milliwatt is about as good in power consumption. For simplicity in estimating all system performances, the MW $\mu$ L is preferred over the Series 51, being applicable to all systems considered.

D. 2. 2 CBS Laboratories Micropower Circuits

Equipment using the CBS Micropower circuits is likely to have serious noise sensitivity problems because of the very high circuit impedances. In addition, speed limitations would rule out use in the SL methods. Production availability and reliability are still relatively unknown.

D. 2. 3 Complementary Multichip Circuits

The complementary circuits show great promise for the future but are not yet far enough advanced to be considered with confidence. The G. I. circuits are designed for specialized data conditioning functions, rather than for general purpose logic. NASA-GSFC evaluation of these circuits was begun recently. The NASA-Lewis designs are still in an early stage and performance parameters cannot yet be predicted with confidence.

D. 2. 4 Fairchild Milliwatt Micrologic

The Fairchild Milliwatt Micrologic family was designed for DOD use in applications requiring moderate speed (1-5 mc/s clock, depending on logical complexity) and moderately low power (2-12 mw per circuit, depending on function). These circuits have been in production since 1962 and are lower-power versions of the Fairchild Micrologic family which were first made in 1959. These circuits will meet the speed requirements of both the SL and CM systems. For purposes

of estimating system performance, they are a good compromise among the factors of assured availability and reliability, power, speed, logical functions available, and applicability to all systems considered here. For these reasons their use is assumed in the system estimates.

### D.3 CORE-TRANSISTOR LOGIC (CTL)

CTL elements have been in production since 1954. They have a long record of proven electrical design and operating reliability, including satellite applications. They have the advantage of very low power consumption at low data rates and can be applied to mechanizations of the low clock rate CM systems. The "Pico-Bit" CTL (0.066 in<sup>3</sup>, in production since 1963) has been used for the magnetic logic system mechanizations.

## APPENDIX E

### RELIABILITY ESTIMATION

#### E. 1 INTRODUCTION

The systems described here each make use of logic elements whose reliability is quite high. The practical limitation in the reliability figures given is the number of life test hours actually accumulated. In the case of the integrated circuits considered here, many modules have been tested for a comparatively short time, while in the CTL magnetic logic, tests of a lesser number of modules have continued for more than six years. Since the mathematical reliability parameter is determined on a module-hours basis, the estimates for the two types of logic form a somewhat dubious comparison.

#### E. 2 CTL - MAGNETIC LOGIC

##### E. 2. 1 Life Tests

Supervised field and life tests of DI/AN CTL's have produced no failures attributable to components, circuit design, manufacturing processes or techniques now in use. Except for defects arising from obsolete techniques, two controlled life tests on actual operating systems have accumulated over five million module hours without a failure. In addition, a failure of a CTL element has, to the best of the manufacturer's knowledge, never occurred in a delivered system. In one case, at least 20 million module hours are estimated to have been logged with no reported failures. The total supervised CTL module hours, both field test and life test, is 8.6 million module hours without a known failure. This is equivalent to .018%/1000 hours at a 80% confidence level.

These data apply to the LSQ version of the CTL. Tests made to date on the smaller Pico-Bit version, used in estimates for this report, indicate that it is at least as reliable as the LSQ. The assumed failure rate for the Pico-Bit unit in 1966 is .007%/1000 hours (MTBF of 14.3 million hours). This number is calculated from Minuteman component specifications. Since a great deal more time than this has actually been accumulated in delivered equipment, the number is felt to be excessively low. Component degradations which would constitute "failures" to the



Minuteman specifications do not affect the CTL operation because of the excellence and non-criticality of the circuit design.

#### E. 2. 2 Radiation Tests

For the higher orbits, the satellite can be expected to receive significant doses of radiation in the polar regions. Radiation tests on CTL's have been conducted by Edgerton, Germeshausen and Grier, Inc. and the Naval Research Laboratories.

The experimental dosage levels in these tests are many orders of magnitude higher than those which would be encountered in passage through even the most severe solar flares or through the most intense parts of the Van Allen belt.

a. Radiation Tests by EG&G on DI/AN CTL's - DI/AN CTL's have all been subjected to the following radiation dosage levels:

(1) Exposure to neutrons at energy levels greater than 0.5 Mev for a dosage of  $4.8 \times 10^{12}$  per square centimeter.

(2) Exposure to Gamma Radiation of  $2.3 \times 10^8$  ergs per gram above 1.0 Mev energy level.

In the tests performed after each exposure, there were no noticeable changes in the characteristics of the units.

b. Radiation Tests by U. S. Naval Research Laboratory - The following is a breakdown of the dosages and dose-rates to which each shift register was subjected during testing. All tests were run over a Cobalt source (100 curies) which emits 1 Mev gamma radiation.

<u>Level</u> <u>(R per Hour)</u>	<u>Time</u> <u>(Hours)</u>	<u>Dosage</u> <u>(Roentgens)</u>
3.75	4	15
16.5	4	66
34.8	3	104.4
68.7	6	412.2
137.3	3	411.9
384	2	768
859	2	<u>1,718</u>
	Total Dosage	3,495.5

The counter was checked after each increase in dosage and continued to perform satisfactorily.

### E. 3 FAIRCHILD INTEGRATED MICROLOGIC

#### E. 3. 1 Introduction

Reliability data for the Fairchild integrated circuits has largely been taken on the regular Micrologic series which consumes a good deal more power than the Milliwatt Micrologic presented for the gridding system. However, there is no reason to believe that the data presently being obtained on the MW $\mu$ L series should be any different than for the  $\mu$ L series and we have extrapolated reliability figures into 1966 based on present data.

#### E. 3. 2 Life Test Data

Fairchild logic is possibly under test by the M. I. T. Instrumentation Laboratory for eventual use in the Apollo guidance computer. In the June 1964 issue of Electronic Equipment Engineering, a short article reported on life tests in progress at M. I. T. In this test 13,000 Fairchild Micrologic elements (assumedly of various types) are being operated. As of June 1964, 33 million module hours had been accumulated with no operational failures (one failure occurred in the lot before the test started). A later published report (Electronic News, 23 November 1964) indicated that 71 million module hours had been accumulated. These data reveal a combined failure rate of .0032%/1000 hours at a 90% confidence level.

As with the CTL module, these data are extrapolated to 1966. At that time, present indications predict a failure rate of 0.001%/1000 hours at 90% confidence level. These data have been used in the calculations of Section 3.6.3.

### E. 3. 3 Radiation Data

The integrated circuits are basically solid state devices and react to radiation differently depending on their design basis; i. e. , bipolar devices, planar epitaxially constructed devices, field effect transistors.

With regard to the Fairchild circuits, these circuits were exposed to an integrated dosage of  $10^{15}$  minutes/cm<sup>2</sup>, about two orders of magnitude higher than might be achieved in one year in the center of the Van Allen belt. The Fairchild circuits continued to operate throughout the test but did show deterioration in the waveshape. A similar circuit in discrete components showed no deterioration. The data here is only for neutron flux. Data for gamma radiation are of more concern. The multiplicity of transistors in all integrated circuits causes them to be more susceptible to gamma radiation than their discrete counterparts. In this vein, the use of high frequency devices (such as the Fairchild series) is better since the base region offers a smaller collection area for gammas than in low-frequency devices.

6 July 1965

9G9-11

ERRATA AND ADDENDA SHEET

FOR

APPROACHES TO ON-BOARD GRIDDING OF  
APT PICTURES

(Phase I Final Report)

Contract No. NAS 5-9012

765-21466

Page 3-4, Figure 3-2

Change "APT SWEEP" to "APT SWEEPS."

Page 3-5, third paragraph, line 12

Change "(m = k for this case)" to "(n = K for this case)."

Page 3-5, third paragraph, line 15

Insert the word "maximum" after the word "elements."

Page 3-15, item I, line 1

Omit comma after "40 bits."

Page 3-17, line 1 of the footnote

Change "adapted" to "adopted."

Page 3-22, first paragraph

Change "...described in Section 3.2.4.2" to "...described in Section 3.2.4.1"

Page 3-32, item c, line 4

Change "pluses" to "pulses."

Page 3-32a, Figure 3-14

Replace this illustration with attached revised illustration.

Page 3-32, item e, line 2

Change "...made in S solid state..." to "...made in 8 solid state..."

Page 3-37, second paragraph, line 7

Change "...is composed to two bits..." to "...is composed of two bits..."

6 July 1965

9G9-11

Page 3-40, second paragraph, line 19

The word "vounters" should read "counters."

Page 3-43, after the first paragraph, insert the following (see attached revision of Figure 3-22):

"The output of gate 13 sets a flip-flop which inhibits the clock signals, shifting the contents of registers A and B back to the memory through the 4- word delay."

Page 3-43, after the second paragraph, insert the following:

"The contents of registers A and B are returned to memory only if  $\Delta Y$  is non-zero, which allows the flip flop, inhibiting gate 14, to be reset. For a horizontal line segment, the line segment data will remain in A and B, permitting the generation of mark commands, until a non-zero mark word is withdrawn from memory. After each mark word is withdrawn from the main store following a mark command, it is added to the segment word coming from the delay line. However these words will always be zero while a segment word is in the A and B registers due to the organization of segments into  $45^\circ$  angular bands."

Page 3-44, Figure 3-22

Replace this illustration with attached revised illustration.

Page 3-45

Commentary after Sweep 2 should be interchanged with commentary after Sweep 3.

Page 3-49, Figure 3-26

Change figure title from "... Cycle 2..." to "... Cycle 1..."

Page 3-58, second paragraph, line 2

Change "...the location mark S..." to "...the mark locations..."

Page 3-62, Figure 3-30

The equation: 
$$\frac{E}{N_o} = \frac{\text{Audio B.M.}}{\text{Data Rate}} \times \frac{S}{N} \text{ Audio}$$

Should read: 
$$\frac{E}{N_o} = \frac{\text{Audio BW}}{\text{Data Rate}} \times \frac{S}{N} \text{ Audio}$$

Page 3-66, Section 3.5.3.1, item g, line 3

Change "...on which the above interim..." to "...on which the above condition..."

6 July 1965

9G9-11

Page 3-79, 3-80, 3-81

Change column title "Module Power" to "Module Count."

Page 3-79, 3-80, 3-81, 3-82, 3-83

The column title "Peak Power" is expressed in milliwatts.

Page 3-86, Table 3-14, first column

Change " $7 \times 10^{-8}$  joules" to " $7 \times 10^{-7}$  joules."

Page 3-86, Table 3-15

The MTBF (Hours) and Reliability (1 year) for the SL-2, Integrated Ckts. should read, respectively, 52,400 and .85

Page 3-88, Table 3-19

Below the item "Integrated Ckts." add the item "Delay Line" and insert in each respective column for this item the following: 1, .585, .585. Change Total SL-2 Integrated Ckt. Failure Rate from 1.319 to 1.904. Change MTBF from 75,900 Hours to 52,400 Hours. Change "R = .89" to "R = .85"

Page 5-40 - As the second paragraph of this page, insert the following:

" While no precise estimates of computer running time were made for an operational program, a rough evaluation of the time required to execute the program steps described in the previous sections lead us to believe that a maximum running time per picture would not exceed the time presently required for the 924 computation of an AVCS picture grid."